MECHANICS OF WHOLE-BODY BALANCE AND MOMENTA CONTROL DURING STRAIGHT-LINE GAIT AND 90° TURNS

by

Mitchell Tillman

A DISSERTATION

Submitted to the Faculty of the Stevens Institute of Technology
in partial fulfillment of the requirements for the degree of

DOCTOR OF PHILOSOPHY

Mitchell Tillman, Candidate

ADVISORY COMMITTEE

Antonia Zaferiou, Chairperson Date

Philippe Dixon Date

George McConnell Date

Raviraj Nataraj Date

Damiano Zanotto Date

STEVENS INSTITUTE OF TECHNOLOGY
Castle Point on Hudson
Hoboken, NJ 07030
2024

MECHANICS OF WHOLE-BODY BALANCE AND MOMENTA CONTROL DURING STRAIGHT-LINE GAIT AND 90° TURNS

ABSTRACT

Turning while walking consists of up to 50% of our daily steps, and compared to walking straight, is more likely to result in grievous fall-related injury. This dissertation reveals momentum and balance control during 90° turns to inform future diagnostic and therapeutic solutions to reduce fall-related injuries.

Healthy young and older adults performed three tasks: straight-line gait, pre-planned turns, and turning suddenly after being cued ("late-cued"). Participants' whole-body balance and momenta control in the frontal and transverse (horizontal) planes were quantified using mechanics-based metrics: linear momentum, angular momentum, and center of mass position relative to the foot or feet in contact with the ground ("base of support"). This dissertation shares how turning task, stepping strategy, biological sex, age, and gait speed influence balance and momentum control.

In the frontal plane, pre-planned turns' trajectories resembled circular walking, and the center of mass shifted near or beyond the outside edge of the base of support. The sharper late-cued turns performed by young adults showed the largest range of frontal-plane angular momentum, as participants changed direction suddenly. All metrics indicated that turns challenge balance more than straight-line gait.

In all tasks, though most strongly in late-cued turns, linear momentum in the new direction of travel was generated primarily during right single support (when only the right foot contacts the ground). Leftward transverse-plane rotation was generated primarily after left foot ground contact, during left double support, before the right foot departs the ground. Both young and older adults exhibited these gait phase-specific generation of the most linear or angular momentum. However, young adults generated more linear momentum during both single support phases, while older adults generated more transverse-plane angular momentum during all gait phases.

In faster speed pre-planned turns, young adults' momenta showed minimal differences in either plane vs. preferred-speed turns. However, the faster vs. preferred speed late-cued turns increased frontal- and transverse-plane momenta, also shifting the center of mass nearer to the base of support's edge.

In summary, these findings describe how different turn types affected the mechanics-based balance states during turns and revealed common momenta control strategies between turns and straight-line gait.

Author: Mitchell Tillman

Advisor: Antonia Zaferiou

Date: Oct 28, 2024

Department: Biomedical Engineering

Degree: Doctor of Philosophy

This dissertation is dedicated to my parents. My father Doug Tillman inspired me, and I miss him every day. My mother Cathy Tillman supported me throughout every step of this journey. Thank you both.

Acknowledgments

I'd like to thank Sam Liu for his insights over the years and for listening to my constant sharing of ideas. I also thank Sensei Scott Gave for indirectly giving me the idea to pursue this area of study in the first place - his pursuit of athletic training sparked the idea that I could study movement for a living.

Thank you to Dr. Zaferiou for all of your support and guidance over the last five years. It's been a long road, and I'm a better researcher at the end of it thanks to your mentorship and support.

I'd also like to thank the National Science Foundation and Stevens' Stanley Fellowship and Doctoral Excellence Awards for funding me during my Ph.D. program.

Table of Contents

List of Tables

List of Figures

Acronyms

AP anterior-posterior

ART available response time

BOS base of support

BSIP body segment inertial parameters

CM center of mass

$\overrightarrow{COP}$ center of pressure

ΔH_z change in horizontal-plane H_z

Δp_x change in X-axis TBCM linear momentum

$\overrightarrow{F}$ force (N)

$F_{x,avg}$ X-axis average force (N) ($\overrightarrow{F}$)

g gravitational constant

$\overrightarrow{GRF}$ ground reaction force

$\overrightarrow{H}$ whole-body angular momentum about the TBCM

H_f frontal-plane $\overrightarrow{H}$

$H_{f,min}$ frontal-plane H_f minima

$H_{f,range}$ range of frontal-plane H_f

H_z horizontal-plane $\overrightarrow{H}$

$\overrightarrow{I}$ tensor of inertia

LC late-cued

LD lateral distance

LD_{min} lateral distance minima

LDS left double support

LSS left single support

M_f frontal-plane whole-body moment about the TBCM ($\overrightarrow{M}$)

ML medial-lateral

$\overrightarrow{M}$ whole-body moment about the TBCM

MOS margin of stability

MOS_{min} margin of stability minima

M_z horizontal-plane $\overrightarrow{M}$

$M_{z,avg}$ average horizontal-plane $\overrightarrow{M}$ (M_z)

$\overrightarrow{GRF}_{net}$ net ground reaction force

$\overrightarrow{p}$ TBCM linear momentum vector

PP pre-planned

p_x X-axis TBCM linear momentum

RDS right double support

RSS right single support

SLG straight-line gait

horizontal gait speed horizontal gait speed (m/s)

TBCM total body center of mass

$\overrightarrow{v_{TBCM}}$ TBCM velocity

$\vec{\theta}$ angle

$\vec{v}$ velocity vector

XCOM extrapolated center of mass

Chapter 1

Introduction

1.1 Introduction

This dissertation focuses on understanding momenta and balance control strategies in 90° left turns in healthy young and older adults. This work focuses on overground walking in two common contexts: straight-line gait (SLG), and changing direction by 90° (turning 90°) while walking in both pre-planned (PP) and late-cued (LC) contexts. My work aims to help address the risk of older adults falling down and injuring themselves due to improper momentum control. That is, falling due to loss of balance. Although there are also other reasons that people fall, such as slips, trips, or pushes, balance control during these and other environmentally-induced perturbations are outside the scope of this dissertation. This dissertation is devoted to improving our understanding of balance control during linear and nonlinear gait. This understanding may lead to more specific diagnostics, through better understanding normative values, as well as more targeted training to decrease the chance of falls during locomotion.

In this dissertation, healthy adults across the lifespan performed SLG and 90° left turns as their kinematics were measured to yield information about their balance and momentum control. This information provides a reference for future studies, and may be useful to develop prosthetic devices or physical therapy treatments, with applications likely extending to other nonlinear gait beyond 90° left turns while walking. For example, detailed descriptions of momenta control patterns during typical nonlinear gait may assist in targeting muscles more specifically for physical therapy in response to motor control deficits in nonlinear gait.

1.2 Falls

Falling is a serious societal problem, accounting for $50 billion USD in medical costs in 2015 (1). People of all ages fall, including young (2), middle age (3), and older adults (4). While falls in young adults tend to be caused more by slips and trips (2), in older adults the most common cause is improperly shifting their weight (5), such as during transitional movements including turns while walking. Although all age groups fall, older adults tend to sustain the most grievous fall-induced injuries, such as hip fractures. Impact-related hip fractures likely occur in older adults specifically due to a variety of factors such as decreased reaction times, bone density, and cushioning in the form of protective fat (6). One of every three older adults will fall during a given year (4), of which another one of three (11% of overall population) will sustain an injury that causes the person "to limit your regular activities for at least a day or to go see a doctor" (4).

One of the most common activities of daily life that can result in an injurious fall is turning while walking. A study by Robinovitch et al., (5) recorded video of hundreds of older adults' falls. They reported "improper weight shifting" to be a leading cause of falls in this group (41% of all observed falls). While they did not report specifically whether this improper weight shifting occurred during turns, watching their supplemental videos it is clear that nonlinear gait is frequently involved in the falls. Falls from a standing height or lower cause a majority of hip fractures (7) and hip fractures are 7.9x more likely to occur during falls while turning than in straight-line gait (8). Hip fractures are especially dangerous injuries, with 12-month mortality after the injury reaching approximately 25% (9). Unlike environmental risks of falling such as moving obstacles, uneven terrain, slippery or unstable surfaces, etc., turns while walking are an unavoidable component of daily life. One study by Leach et al. showed that the quality and number of turns performed by healthy older adults negatively correlated with whether someone would fall in a 12 month period (the more turns performed, the less likely to fall), whereas overall activity level did not (10). Therefore, due to the prevalence, difficulty, and functional importance of turns, in this dissertation, I focus on understanding balance during walking and turning, as they are among the most challenging movements to balance that older adults perform routinely (11). By understanding both normative and dysfunctional momentum control, we can develop better diagnostic and rehabilitative technologies to help improve people's balance and reduce the frequency and level of injury of falls.

1.3 Clinical Balance Measurement

There are many balance tests currently used in physical therapy and other clinical settings. Generally, these tests consist of several tasks across multiple domains of balance that are evaluated by the clinician. For example, the BESTest (12) and shorter miniBEST (13) include tasks that are stationary (e.g. stand on one leg), compensatory (catch your balance after leaning into the physical therapist and they let go), and nonlinear gait (e.g. walk and quickly turn and stop). The Dynamic Gait Index (DGI) is similar (14). Several clinical tests such as the 6 Minute Walk Test and Turn In Place Test, The Timed Up and Go (TUG) (15) - an adaptation of which is included in the miniBEST and DGI - include turning components. However, it is only scored as a binary value as to whether the total completion time is above or below the threshold value. Generally, if the person scores worse than a certain cutoff value (e.g. more than 12 seconds completion time for the TUG, less than 19 / 24 score on the DGI, etc.) then they are considered a "fall risk".

These tests provide quick (generally 10-15 minutes), simple, multi-factorial, and relatively objective measures of a person's balance and fall risk across a range of balance conditions. However, they rely on functional outcomes - yielding primarily a "OK/not OK" result - and can be susceptible to "ceiling" effects (16). As a result they cannot provide the much-needed insight into more fundamental biomechanical measures such as momentum control that underpin balance during locomotion, specifically turns (17). For that, mechanics-based laboratory measures are helpful.

1.4 Mechanics-Based Laboratory Balance Measurement

Broadly, two domains have been identified as contributing to the mechanics of balance control: whole-body angular momentum about the TBCM, and foot placement relative to the TBCM position (18). The total body center of mass (TBCM) is important for both domains of whole-body balance control, as it is the point representing the average position of all the body's mass. Whole-body angular momentum about the TBCM ($\vec{H}$) characterizes the whole body's rotation about its TBCM, where faster rotation is a larger $\vec{H}$ absolute value, and no rotation is $\vec{H} = \vec{0}$.

The margin of stability (MOS) is a mechanics-based measure of balance state is the margin of stability (MOS), originally proposed by Hof et al. (19) (see 2.7.5 for details). This metric attempts to account for both the placement of the feet (base of support (BOS)) relative to the TBCM and predict where the TBCM is headed in the near future by imposing the constraints of the inverted pendulum model. It is one of the most commonly used mechanics-based balance metrics during gait due to the inclusion of the velocity term in its calculation. However, this predictive component is only as accurate insofar as the inverted pendulum model accurately represents the person's movement. The inverted pendulum model has been validated in quiet standing (20) and straight-line gait (21), but not during turns.

Therefore, during turns a similar metric called the lateral distance (LD) is useful, as it quantifies the distance between the TBCM - without a velocity term - and the BOS edges, and therefore does not rely on this inverted pendulum assumption, has been used in previous studies of turns (22). When this distance becomes negative, it means that the TBCM is lateral of the lateral edge of the BOS and a lateral fall can occur unless a step is taken to generate a corrective ground reaction force ($\overrightarrow{GRF}$) to place the TBCM back within the boundaries of the BOS and maintain upright posture. Note that removing the inverted pendulum-based velocity component removes the context of the person's dynamics from this metric.

Note that these measures reflect a person's current mechanical state. There is as yet no consensus on the relationship between a person's current mechanical state and their overall balance state (23). For example, a large $\vec{H}$ (fast rotation about the TBCM) could indicate that the person's balance state, and perhaps balance abilities, are worse because large $\vec{H}$ is known to occur during falls. However, if a large $\vec{H}$ and small LD is observed without a resulting fall, then one could argue that while the current balance state may be "poor", this person has sufficient balance abilities that a "poor" balance state does not impose as severe of a threat to balance. A large $\vec{H}$ could be interpreted as a "poor" balance state, but a simultaneous large LD would indicate a "good" balance state, with the feet positioned to adequately control the large $\vec{H}$. Therefore, individual balance metrics do not capture the entirety of the balance state, and throughout this dissertation I will refrain from making overly broad claims about balance itself, and focus instead on people's mechanical states and momentum control.

1.5 Straight-Line Gait

Straight-line (linear) gait occurs when walking in an approximately straight line. Mechanically, this means that the person's TBCM trajectory (velocity vector) is in a consistent direction on average, and their body is also generally facing in that direction. This has been the primary form of locomotion studied, in both treadmill and overground settings.

Gait is a cyclical movement as steps occur repeatedly, alternating with the left and right feet. Phases of gait can be delineated by identifying specific events within the gait cycle. This is important to do because each phase of gait exhibits a distinct context in terms of the BOS geometry, TBCM velocity, muscle activations, and more. Often, four events per gait cycle is used (24), delineating four non-overlapping phases of gait. Starting with the left foot's heel strike, 1. left double support begins with both feet on the ground, and the left foot in front. 2. Left single support occurs when the right foot's toe leaves the ground, and the left foot is the only one on the ground. 3. At approximately 50% of the gait cycle, the right double support phase begins when the right heel strikes the ground in front of the left foot. 4. Finally, right single support occurs when the left foot leaves the ground, and the cycle completes at the next left heel strike. Note that many different ways of categorizing these events exist. For example, prior work has used seven (25), 12 (26), or even up up to 16 events (27) per gait cycle.

This gait cycle accomplishes the goal of TBCM translation through space in a consistent direction. Despite this consistency, the body's facing direction oscillates back and forth slightly with each step, and the TBCM trajectory exhibits small medial-lateral (ML) deviations in all three planes. These small ML deviations necessitate active control of balance (28), whereas the anterior-posterior (AP) control of balance is largely passively controlled by step length and the body's inertia (29). In healthy people, these fluctuations are well controlled by the body's central nervous system to accomplish SLG to avoid losing balance and falling.

Spatiotemporal metrics such as step/stride length and width (spatial) and step/stride duration (temporal) are often computed to provide balance-related information, though they are not direct measures of balance. For example, young adults' narrower step width (30; 31) and decreased double support time (32) vs. older adults is cited as a evidence of young adults' better balance abilities compared to older adults, as the older adults attempt to keep a larger BOS for a greater portion of the gait cycle, potentially to adapt for reduced control of ML TBCM movement (33). Note that these spatiotemporal parameters are indirect measures of the varying components of balance. More direct metrics for quantifying each aspect are more fundamentally mechanics-based.

1.5.1 Whole-Body Angular Momentum

$\vec{H}$ is a measure of how quickly the whole body is rotating about the TBCM. $\vec{H}$ is used to quantify balance in the angular velocity domain rather than velocity vector ($\vec{v}$) because our bodies consist of a system of segments that interact via rotation. That is, when people fall, they tend to fall by rotating towards the ground rather than collapse linearly downward. $\vec{H}$ has the advantage that it is not constrained to rely on a particular type of motion (e.g. to act as an inverted pendulum, see 1.5.2) - the only assumptions are that each segment is a rigid body, and that the segments' mass properties are known.

During SLG, $\vec{H}$ has been found to oscillate about zero in all three planes (34) with a period of one gait cycle in the frontal and transverse planes, and a period of one step (one half of a gait cycle) in the sagittal plane. $\vec{H}$ is typically summarized by its maxima, minima, and range, e.g. (34; 17). Larger $\vec{H}$ range during a task is typically thought to be associated with worse balance, e.g. (17). The earliest studies of balance were on quiet standing, during which any $\vec{H}$ is viewed as a balance perturbation despite the fact that no one stands perfectly still. This line of thought has been extended to dynamic movements - some of the first studies of $\vec{H}$ in SLG concluded that $\vec{H}$ is "tightly controlled" about zero, potentially leading to the idea that excess $\vec{H}$ indicates poorer balance (34; 35). Although, Herr et al. documented that not all movements exhibit this tight regulation, such as hula-hooping (34). Of note, Gu et al. (36) found that the largest segmental angular momenta during SLG occurred in the frontal plane, supporting others' findings that the ML direction requires the most active control of balance (37; 28). This large segmental frontal-plane $\vec{H}$ is surprising given that $\vec{H}$ extrema is largest in the sagittal plane (34).

$\vec{H}$ range is known to be responsive to several factors. It increases with increasing age in the frontal plane (38) and body mass index (BMI) (39). It appears to be agnostic to changes in step length, but adding weights to segment(s) increases $\vec{H}$ (40), as does use of a prosthetic limb (41). However, its relationship with gait speed is unclear (40), either slightly decreasing (42), increasing (40; 43) or showing no change (44; 45; 46).

As $\vec{H}$ is a whole-body measure, to reduce the magnitude of $\vec{H}$ during SLG, any or all segments' $\vec{H}$ can be reduced. This largely occurs through increasing "intersegmental cancellation", whereby the angular momentum of one segment cancels out the angular momentum of another segment (42). This cancellation is most visible in the sagittal plane, as the angular momenta of the left and right legs are quite large, but anti-phase to one another, largely cancelling out (41; 42).

$\vec{H}$ provides important information about the body's rotation, crucial to determine the current balance state (47; 48). However, it lacks the context of where the

TBCM is located relative to the BOS boundary. For example, if the $\overrightarrow{H}$ is rotating the body clockwise (viewed from behind), the threat to balance from a leftward perturbation during the left foot's stance phase is much larger if the TBCM is already positioned near the leftward edge of the BOS.

1.5.2 Margin of Stability

Although step width and length are indirect measures of balance as they don't account for TBCM position, foot placement relative to the TBCM directly affects the current balance state in both the AP and ML directions (49). Leveraging this concept, Hof in 2005 formalized the MOS (19) as a measure of someone's current balance state. The value of the MOS is directly correlated with the momentum required for that person to fall (19). The MOS relies on the inverted pendulum model to predict the TBCM location, which yields the "extrapolated center of mass" (XCOM) position. The MOS is the distance between the XCOM and the center of pressure ($\overrightarrow{COP}$). By accounting for velocity, the classic inverted pendulum model of balance is extended for dynamic situations such as SLG.

A traditional (non-inverted) pendulum consists of a point mass rigidly suspended from a fixed point of rotation. When the mass is raised to a height above its natural resting point, it swings back and forth due to gravity. An inverted pendulum is a traditional pendulum oriented upside down such that the point mass is above the point of rotation, oscillating about a single point. When the point mass of the inverted pendulum is given an initial velocity, as during gait at the start of the single support phase, completing one oscillation (reaching the other end of the pendulum's arc) is considered to require no additional input of energy (50). This point is often taken to be the ankle joint center during standing, (20; 51; 52), though Hof uses the $\overrightarrow{COP}$ during standing and gait, and others use the motion-capture derived edges of the feet to continuously quantify the BOS position during gait (26). The MOS relies on a linearized inverted pendulum model, and according to (53; 49; 52), there are four assumptions in the linearized inverted pendulum model: 1. The body moves as if all of its mass is at the TBCM, meaning the net ground reaction force ($\overrightarrow{GRF}_{net}$) points directly at the TBCM, 2. The $\overrightarrow{COP}$ is stationary during single support and changes instantaneously to the other foot during stepping, 3. The leg during single support behaves rigidly, not changing its length, 4. The TBCM velocity is horizontal, using a small angle approximation of the angle between the vector from the $\overrightarrow{COP}$ to the TBCM and the vertical axis.

The inverted pendulum model has been shown to function well during quiet standing and SLG (21; 20). To validate that a person behaves as an inverted pendulum during a given movement there must be a high correlation between the horizontal TBCM acceleration and the horizontal distance between the $\overrightarrow{COP}$ and TBCM (52; 54). Although the inverted pendulum model was originally formulated for use in the AP direction during quiet standing because of the single axis of rotation intersecting both ankle joint centers (the hips and knees are assumed not to bend), it has often been used to measure balance in the ML direction because that is the direction in which gait must be actively stabilized (28; 37), and is most valid in the ML direction during single leg stance because of the single axis of rotation provided by the single foot's ground contact during that phase (55). With both feet on the ground during SLG, the BOS is wide enough that the body generally does not act as if it were rotating about a single axis of rotation through the ankle joint centers or the $\overrightarrow{COP}$ in either the AP or ML directions. Instead, double support may act as the transition period between pendular swings during single support, providing the additional input of energy needed to continue translating the pendulum (50).

During SLG, the AP MOS is consistently negative, indicating that the XCOM is anterior to the BOS, which means that the person would fall if they didn't continue walking forward (26; 54). In the ML direction, the XCOM tends be positive, staying within the bounds of the BOS, except for late in the single leg stance phase when it becomes negative (26). This moment just before the contralateral foot touches down is crucial for balance as it is when the person is most at risk of falling due to a low or negative lateral MOS (26; 56) and a high H_f (34). They are relying on proper foot placement of the next step to maintain ML balance (18; 21). If the placement of this subsequent step is perturbed too late in the gait cycle to compensate for (>25% of swing phase), then the step after that will need to adjust to maintain balance (57).

Note that step placement and MOS must be controlled on a step-by-step basis (58; 59; 56; 60; 61) . For example, one study of treadmill walking found that long or wide steps were immediately preceded by a smaller MOS (60), and another observed that the MOS of two neighboring steps are well correlated (59). If balance is perturbed laterally, then adjusted foot placement typically corrects the deviation within one to two steps (18; 62).

ML MOS has been shown to be responsive to several factors. First, walking on a treadmill may exhibit larger ML MOS compared to overground walking (63), or at least larger step widths (64). There are conflicting reports as to the effect of aging on the MOS. Arvin et al. in 2016 reported no difference in step width or MOS (33) between young and older adults, but others have reported increases in ML MOS in older vs. young adults (65; 66) potentially indicating older adults' efforts at increasing their ML stability. Note that a larger distance between the feet and the TBCM increases the moment arm, theoretically increasing the ability to generate $\vec{H}$ from the foot's $\overrightarrow{GRF}$. At least one group has posed that the wider steps and larger MOS that older adults tend to exhibit may actually be potentially dangerous for balance (67). Finally, changing gait speed does not appear to affect ML MOS

(68; 69; 70) , however it induces a larger negative AP MOS due to the larger forward velocity (65; 26).

Some of the contrasting observations in the literature may be partially explained by differences in how the MOS is calculated and reported. Curtze and Hof in 2023 provided some reporting guidelines for the MOS (23). Important areas include how the BOS is computed, and how the MOS is summarized (e.g. min, mean, etc.). See section 2.7.5 for how I compute MOS.

1.6 Turning Gait

Turning is believed to be more challenging to balance than SLG for several reasons. First, the addition of a mechanical objective to change direction while translating in the transverse plane intuitively seems to be a more demanding mechanical task than linear translation alone due to the added requirement of changing direction, and there is evidence that the maneuver increases metabolic expenditure, with "sharper" (fewer steps and/or larger angle) turns expending more energy (71; 72). There is also evidence to suggest that turns require more cognitive resources than SLG (73). Second, studies in balance-impaired populations have consistently discovered worse balance performance in these populations during turns than during straight-line gait (74), and decreasing turn performance with worsening disease. For example, Son et al. found that the degree of freezing of gait in people with Parkinson's disease correlates with several kinematic measures of turning gait, but not straight-line gait (75). Similarly, turns take longer to complete for people with more vs. less advanced Parkinson's disease (76; 77).

Humans often walk in relatively short bouts (78), and depending on the setting, up to 50% of those steps can be nonlinear gait (11). Most broadly, nonlinear gait is any type of gait other than straight-line gait where there is a discernible gait cycle and a change in the TBCM velocity direction. While this can take many forms, such as circular walking, side steps, spins, etc. in this dissertation I focus on one of the most common forms of nonlinear gait, "turns while walking" (a.k.a. "turns"). These types of turns are common in the modern carpentered environment as we turn frequently around 90° corners. Interestingly, other forms of nonlinear gait may be more common in outdoor environments as humans have shown a natural propensity for walking in circles in certain conditions such as when placed in an unfamiliar outdoor environment on a cloudy day or at night (and therefore unable to use the sun as a reference point) (79; 80).

While walking in a circle and other types of nonlinear gait can be maintained for long durations, in this dissertation I focus on turning while walking as a transient movement. Therefore, the term "turning while walking" is used here to indicate a *transient* change in direction, beginning with walking straight, then turning, and then walking straight in a new direction. Performing this movement requires meeting the mechanical objectives of braking and accelerating in the initial and final directions of travel, respectively, and rotating the body's facing direction in the transverse plane. Typically, the body's direction of travel $\vec{v}$ and body-facing direction angle ($\vec{\theta}$) change orientation from before to after the turn by similar amounts to maintain the intended destination within the field of view (81; 82; 83). Note that this coupling is not a biomechanical imperative, as decoupling is readily observed in sports movements such as transitioning to a sideways cut while running in football. In that case, the body-facing direction is largely preserved while the direction of travel changes. However, during most activities of daily living, including turns, the direction of travel and the body-facing direction are coupled over the course of the movement. Note that each phase of gait affords a different BOS context for generating the $\overrightarrow{GRF}$ to control linear and angular momentum.

During turns, the various body segments do not rotate at exactly the same time. In young healthy adults there is a "top-down" sequence whereby first the head rotates in the direction of the turn, then the torso, followed by the pelvis and legs (84; 85; 86). However, this sequence can become more "en bloc" - where all segments rotate together - when walking at slower speeds (87) or in some balance-impaired populations such as people with Parkinson's disease (84).

Much less is known about the control of balance during turning gait, at least partially due to the additional methodological and analytical challenges beyond those of SLG due to the continuously changing body-facing and TBCM velocity direction. It is more difficult to ensure that footfalls land within force plates, for example, or even to define concepts as "basic" as step length and width during turns (88; 89), which is trivial and universally agreed upon during SLG. Much of the focus of the study of ecological nonlinear gait has been in the area of continuously monitoring people with balance deficits in the home - such as people with Parkinson's disease - in an attempt to understand and improve their typical ambulation patterns, such as (74; 90). Laboratory studies of 90° turning movements are often restricted to examining a consistent three steps nearest the intersection, e.g. (41; 91; 22; 92; 93) . However, turns can occur with any number of steps (11; 94). People with balance deficits such as older adults or people with Parkinson's disease have been shown to use more steps to complete a turn (95). This could be an indicator of reduced balance confidence or abilities to control their linear and angular momentum during the movement, and a compensatory strategy to minimize mechanical demands of redirecting velocity and body-facing direction in each footfall.

1.6.1 Whole-Body Angular Momentum

$\vec{H}$ magnitude has been shown to increase and become "highly unregulated" during turns (96) relative to SLG. $\vec{H}$ expressed in the body's coordinate system is still maintained near zero both before and after the turn, but during the turn it tends to reach an extrema value near the start which is corrected for at the end of the turn (41; 97). Nolasco et al. have performed some of the most extensive analyses to date of $\vec{H}$ during PP turns (41; 97), describing $\vec{H}$ in all three planes over three turn steps - "initiation", "continuation", and "termination". They found that in the frontal and sagittal planes, during the initiation step, average $\vec{H}$ was more extreme than during the same phase of SLG (frontal plane, viewed from behind: counter-clockwise rotation rotates the head towards the inside of the turn, sagittal plane: body above the TBCM (e.g. head and upper trunk) rotate posteriorly). In the frontal plane, the continuation phase exhibited no differences relative to SLG; however, continuation phase sagittal-plane $\vec{H}$ results in a smaller anteriorly-directed rotation of the body above the TBCM than SLG. Finally the termination step showed a larger average frontal and sagittal-plane average $\vec{H}$ (frontal plane, viewed from behind: clockwise rotation rotates the head towards the outside of the turn, sagittal plane: body above the TBCM rotate anteriorly) vs. SLG. This progression shows how frontal- and sagittal-plane $\vec{H}$ are regulated over the course of several steps. The transverse plane was more positive (in the direction of the turn) in all three steps, generating the change in body-facing direction.

To summarize the frontal and sagittal planes, in healthy young adults, there is an initial self-induced rotation towards the inside of the turn and posteriorly, which is not corrected for until two gait cycles later. Finally, in the transverse plane, because the goal is to transiently generate additional transverse-plane angular momentum, the larger transverse-plane $\vec{H}$ generated during the initiation phase is not counteracted during the turn, instead returning to near zero only at the end of the turn.

1.6.2 Margin of Stability and Lateral Distance

During pre-planned turns, the TBCM trajectory relative to the feet deviates significantly from that observed during SLG, causing deviations in MOS from that observed in SLG. In preparation to perform a lateral maneuver (98) or turn 90° (92), people tend to shift their XCOM nearer to the edge of their foot (exhibit smaller positive MOS) towards the direction of the turn (i.e. left edge of the left foot for a left turn), relative to SLG. This asymmetry of the XCOM relative to the lateral edges of the BOS continues during the turn as well (99; 92). Similar to MOS, LD aims to capture a positional component of ML balance by encompassing the position of the TBCM relative to the BOS in the frontal plane. This metric is preferred when studying turns over the more widely used MOS because the inverted pendulum model on which MOS relies (see 1.5.2) has not been validated in turns. This LD metric has been used only once previously by Dixon et al. (22). They defined the LD in the ML direction as the signed distance from the TBCM to the lateral edge of the BOS. This has the advantage of not relying on the inverted pendulum model, but therefore does not provide context on the person's dynamics, i.e. in which direction the TBCM velocity vector was oriented. In that study, average LD during the first stance phase of the turn increases during turns vs. SLG, and the MOS is much larger than the LD, meaning that there is a relatively large component of the TBCM velocity in the ML direction during the turn (22).

1.7 Turn Strategies

To perform a turn of a given angle, the body's facing direction and TBCM velocity vector both rotate in the transverse plane by approximately that angle (100). Since 1999, using nomenclature originally derived from turning while running literature (101), the strategies used to accomplish these objectives during turns while walking have been categorized as either a "step" or a "spin" turn. These classifications derived from observations in 180° turns - cued by electrical stimulation to the superficial peroneal nerve - that turns either utilized one (spin) or two (step) axes of rotation, corresponding to when the turn was performed by spinning over the inside foot only or when both feet were used, respectively (27). Classifying turns in this fashion has the benefit of providing an at-a-glance overview of how the turn was performed. However, since its inception, it has not applied to all turns performed by all people. The original paper by Hase & Stein (27) describes that only seven of 10 people obeyed the step vs. spin turn strategies classifications. Another seminal paper from Taylor et al. showed that only eight of 10 participants followed this dichotomy (102), with the remaining two participants each doing something unique. Both of these studies omitted the outlier subjects from their analyses.

There is no consensus on how to define a turn strategy, and several methods have been used previously. First, visual observations of foot placement were used in 180° (27), 90° (102), and freeform turns (11), and continue to be used, e.g. (41). Several studies have used algorithmic methods to objectively classify step or spin turn strategies based on whether the outside or inside foot, respectively, was selected by the algorithm at a specific point in time. Akram et al. (103) used the foot whose toe trajectory first deviated mediolaterally. Golyski & Hendershot (104) defined turn strategies by which foot was nearest the intersection of the extrapolated approach and departure TBCM trajectories. Dixon et al. (105) used the foot whose stance phase experienced the maximum pelvis transverse rotation. Olivier et al. (106) proposed using the foot in stance phase at the time of the TBCM trajectory's maximum curvature. Aside from what constitutes a step or spin turn, there are other basic components of turn strategies that the literature does not agree on, including contrasting findings as to whether step or spin turns are more prevalent in various contexts (107; 108; 109; 22), and it is unclear whether a step or spin turn is necessarily safer (110) or more energetically efficient (103).

In addition, many of these turn strategy classification methods, whether visual or algorithmic, require rigidly defined turn phases, most typically enforcing a three step turn phase with "initiation, continuation (or apex), and termination" steps, e.g. (111; 41). This may be due to interpretations of the findings of Glaister et al. (11) which defines and utilizes these three steps during a turn, but does not explicitly constrain turns to only one continuation step. In fact, in that paper the authors describe that three of four turning environments resulted in more continuation steps than initiation or termination, and the fourth environment contained fewer continuation steps (11), rebutting the now-traditional fixed three step turn methodology in the study of 90° turns.

1.8 Late Cueing

Turns are performed in a variety of contexts during daily life. One important yet uncontrollable factor that affects turn performance is the available response time (ART) to turn. This is the length of time between when the cue to turn is perceived and the time by which the turn must be executed. With decreasing ART, the turn becomes more "late-cued" (LC). A "cue" is simply a stimulus indicating to turn. In laboratory settings, these cues have been auditory (112; 110), visual (113; 114; 115; 116; 117), or even administered via electrical stimulation (27). Late cues are common during daily life as well. For example, if a person is attempting to cross a street but the light suddenly turns red, then the ART to stop walking is the time between when the person realizes that the light is now red, and when they would reach the end of the sidewalk if they did not stop. One of the most important evolutionary uses of late-cued turns in both humans and other animals is in predator-prey-environment interactions. Prey must respond to dangers and opportunities in their environment in order to escape the predator and survive, while predators must also respond to the environment and the prey in order to eat. These goals are often accomplished through turning suddenly, as the environment or prey changes suddenly.

The exact delineation between PP and LC in terms of ART is not known, and is likely specific to the movement context. Late cues during gait have been studied not only in turns, but also in sudden stopping while walking (118; 119), in both young and older healthy adults, as well as in people with Parkinson's disease (93). These studies have primarily focused on the context surrounding the capability to execute these sudden movements and the factors that affect them such as aging, walking speed, and phase of gait when the cue is received. Older adults require a longer duration to plan and execute their movements due to systemic age-related changes (120). During gait, the faster a given person is walking, the longer it takes to respond to a cue to change direction (108) or stop (118), though young adults are capable of stopping (119) or turning (115) more quickly at a given speed than older adults. Perhaps the slower gait speed typically observed in older adults is a protective mechanism, providing a longer duration for older adults to execute their movements.

The phase of gait when the cue is provided affects the preferred turn strategy. When the cue to turn is provided in the left foot's stance phase, after the right foot has nearly or already passed the left, then a step turn is more often used. By contrast, if the cue to turn left is received when the right foot is on the ground, then the next left footfall is more typically a spin turn for healthy young adults (27), Also, Patla et al. showed that young adults are unable to turn during the same stance phase as when they are cued to do so. However, more than 70% of the participants were able to do so during the following step, and everyone could do so two steps after the cue (108). This was in the context of performing a 60° turn. Other studies have examined turns of as little as 20° (113), up to 90° (117). Turns of a smaller angle require less ART to successfully execute due to the smaller change in momentum (and therefore energy expenditure) required vs. larger angle turns (108), although Hase & Stein show examples of successful LC 180° turn execution in just one step when the cue to turn is provided at the beginning of the step (27).

Prior work has also shown that the response time to a late cue depends in part on the person's level of preparation. When the person does not expect a cue at all, the central nervous system will be much slower to respond than when a cue is expected in the near future. When a cue to terminate walking is less likely to be presented, gait termination takes longer when cued to do so (119). As another example, Patla et al. found that when participants were cued to suddenly perform up to 60° turns, they were slower to reorient their body-facing direction in the new direction of travel than when they were cued at the start of walking (113).

Comparatively little research has focused on the effects on balance of LC turns. Prior work has observed increased maximum TBCM acceleration (112) and changing foot placement (113). Trunk frontal-plane rotation seems to be more prevalent with more sudden turns, such as LC turns (113; 116). In people with Parkinson's disease, the speed of LC turns is approximately half that of pre-planned (93). More research is needed to understand how LC turns affect balance metrics such as $\vec{H}$, MOS, and

LD.

1.9 Specific Aims

Straight-line gait has been studied extensively, but much less is known about nonlinear gait such as turns while walking despite comprising up to 50% of all steps depending on the environment (11). Falls during turns are especially injurious, being 7.9x more likely to result in hip fracture in older adults than falls during straight-line gait (8). As 90° turns are prevalent in modern carpentered environments, in this dissertation the focus is on 90° turns. Therefore, the overall aim of my dissertation is to describe some of the mechanics of turning during different 90° turns. This will help uncover the mechanisms by which turns are controlled so as to maintain balance while executing the turn, and thereby provide targets to improve physical therapies.

This dissertation has three primary specific aims. First, I aimed to quantify the frontal-plane balance characteristics of young healthy adults during straight-line gait and pre-planned and late-cued turns. Second, I aimed to quantify the linear and angular momentum generation characteristics of young and older healthy adults during those same tasks (late-cued for young adults only).

1.9.1 Aim 1: Identify frontal-plane balance control strategies used during 90° turning while walking, and modifications due to late cueing.

When balance is challenged in the frontal-plane (side to side, ML direction) it can be difficult to avoid a fall as a stepping strategy is not as readily available as it is in the forward-backward (AP) direction. This aim examines how healthy young adults control their momentum and center of mass in the frontal plane at a whole-body level, and preliminarily explores whether this differs between males and females.

Young adults were asked to walk overground in three contexts: straight-line gait (SLG), pre-planned 90° turns while walking (PP turns), and late-cued 90° turns while walking (LC turns). I hypothesized that the range of H_f ($H_{f,range}$) would be smallest during straight-line gait, larger during pre-planned turns, and largest during late-cued turns. I also hypothesized that the minimum lateral distance would be largest during straight-line gait, smaller during pre-planned turns, and smallest during late-cued turns. Finally, I hypothesized that males would show larger values of $H_{f,range}$ and LD_{min} than females in each task.

1.9.2 Aim 2: Identify momenta generation strategies used during 90° turning while walking, and modifications due to late cueing and aging.

The mechanical objectives to execute a turn are in the transverse plane: changing the body-facing direction and the TBCM velocity direction. Young and older adults were asked to walk in the same three contexts as in Aim 1, except that older adults did not perform late-cued turns for timing and/or safety reasons. I hypothesized that the largest change in linear momentum in the new direction of travel would occur during right single support. I also hypothesized that the largest change in angular momentum about the vertical axis through the TBCM would occur during left double support phase. Finally, given that faster gait speeds and response times from young adults are expected, I hypothesized that young adults would generate larger magnitude changes in momentum than the older adults.

1.9.3 Aim 3: Examining momentum and balance control during turns performed at straight-line gait speeds

Gait speed during turning while walking typically decreases relative to straight-line gait. Therefore, in this aim I asked young adults to turn 90° at their preferred speed, matching my prior aims, as well as at the same speed that they walked during straight-line gait. By walking at the same gait speed during both movements, gait speed is removed as a confounding variable, which simplifies the interpreting any changes in momentum between tasks as due only to the differing mechanical contexts of the movement. I hypothesize that, when turning at the same speed as in SLG, LD_{min} will decrease and $H_{f,range}$ will increase compared to turning at preferred speed. Within each phase of gait, similar to aim 2, I also hypothesize that the most transverse-plane linear and angular momentum to turn will be generated during right single support (RSS) and left double support (LDS), respectively, and that this pattern will be exacerbated at SLG vs. preferred speed.

Chapter 2

Methods

2.1 Introduction

In this dissertation, I used optical motion capture to record healthy young and older adults walking straight and turning in a variety of contexts, such as pre-planned or late-cued (chapters 3, 4, and 5) or varying gait speed (chapter 5). I placed the reflective motion capture markers either on top of bony landmarks directly (10 young adult participants in chapter 3), or each body segment had affixed to it a contoured plastic piece with 4-5 markers anchored to it (a "rigid body") and a calibration procedure then identified the position of the segment's bony landmarks (chapter 4 older adults, 5).

The mechanical balance state is quantified using whole-body angular momentum about the TBCM ($\vec{H}$), margin of stability (MOS), and lateral distance (LD). Spatiotemporal gait parameters provide additional context on the movement.

2.2 Equipment

2.2.1 Markered Motion Capture

Passive markered infrared motion capture (Optitrack, NaturalPoint, Eugene, OR USA) is often used in biomechanics to measure movement kinematics, and is currently considered the "gold standard" of position tracking with measurement error $<$ 3mm (121) or less (122). This technology functions by setting up an array of cameras around the entire perimeter of a space (in our case 20 infrared and two high-speed color video cameras) and calibrating them with a rigid body with precision-machined known dimensions so that the relations of the cameras with one another are known. Finally, a ground plane is defined by placing three markers on the horizontal plane. One of the markers defines the origin position, and the other two define the basis vectors of the horizontal plane. With the global coordinate system established, 3D marker positions can be obtained as follows.

Each camera emits infrared light and records any reflections, typically from the infrared-reflective passive markers. The camera generates a 2D image of where the infrared-reflective markers are positioned within its field of view - white pixels indicate a surface with a reflectivity above a certain threshold, while the rest of the visual field is black. Circular clusters of white pixels are interpreted as marker positions. Combining each camera's 2D images and their known 3D positions relative to one another, the marker's 3D positions can be computed using a method called Direct Linear Transformation.

2.2.2 Force Plates

Force plates were installed flush with a floor surface to measure the forces that occur when someone is in contact with them. Often, these are used to quantify the $\overrightarrow{GRF}$ during walking. Despite our lab having five force plates, this $\overrightarrow{GRF}$ data is not available in my studies due to a lack of "clean" steps on the force plates (steps where the entire surface of only one foot is contacting a given force plate), as I did not want to prescribe step placements to our participants. Therefore, in my research force plates are used primarily to measure the participant's mass. The force from the person standing on the plate is transferred to each of three orthogonally-oriented strain gauges inside of the force plates, changing their electrical resistance (Bertec, Columbus, OH). The manufacturer calibrated the plates such that the relationship between resistance and force is known.

2.2.3 Software

All analyses were conducted in MATLAB R2024a Version 24.1 (Mathworks, Natick, MA) utilizing the Curve Fitting Toolbox (for `csaps` cubic spline) and Image Processing Toolbox (for plotting footfall images). R (123) version 4.4.1 was used for all statistical analysis, including the *lme4* package (124) version 3.1-3.

2.2.4 Walkway

A 90° T-intersection with walkways 36 inches wide (125) was defined using tape placed on the ground to mimic a grocery store setting. A monitor at the end of the intersecting walkway provided signage indicating whether or not to turn (broccoli or red "NO" symbol, Figure 3.1) during LC turns. Poles were placed at the corners of the intersection, just outside of the walkway, to prevent people from cutting the corner and better mimic a grocery store setting. For the first young adult cohort, the pole was a camera tripod with a relatively large BOS, meaning that the upright portion of the pole was positioned slightly further from the walkway itself. By contrast, for the second and third cohorts (older adult and second young adult, Figure 2.3) I used thinner plastic poles with a smaller BOS, which allowed the upright portions to be located closer to the corners of the intersection, potentially further constraining people's TBCM trajectory or torso lean more than the camera tripods did.

2.3 Motion Capture Marker Placement

Biomechanical motion capture operates under the assumption that each individual segment is a perfect rigid body, and rotate about the joint center that connects them. Intuitively, this assumption of rigidity seems reasonable for the limb segments, given the long bones providing structure throughout each segment and the relatively small amount of soft tissue surrounding them. This is rigid body assumption may be a larger one for the trunk, as it is quite large, possessing lots of soft tissue and degrees of freedom (126). The hands and feet are also known to break their rigid body model in practice, due to movement of the metatarsophalangeal and metacarpophalangeal joints.

To know the 3D orientation of any rigid body from individual points on the body, a minimum of three points is required. Together, they form a coordinate system that is fixed to that rigid body. That is, from the rigid body's perspective, the coordinate system never moves. This is foundational for studying human motion using motion capture because each individual body segment needs a three-dimensional coordinate system affixed to it, providing anatomically meaningful segment-level position and orientation information. To understand movement kinematics at the whole-body level, I affixed markers to each body segment (head, pelvis, torso, and left and right upper arm, forearm, thigh, shank, and foot).

In this dissertation, two different full body markersets are employed, using two different markering methods as the lab's data collection procedures evolved: what I will call "skeleton markers" and "rigid body clusters". Skeleton markersets consist of individual markers placed onto the skin directly at the site of bony anatomic landmarks (Figure 2.1). While there are various ways of adhering the markers to the skin, I used Velcro™. For the skeleton markerset, markers were placed at the following locations: sternum jugular notch; sternum xiphoid process; C7, T2, and T7 vertebrae; as well as left and right: anterior and posterior head; glenohumeral joint; clavicleacromion joint; humerus lateral epicondyle; posterior aspect of the upper arm; radial and ulnar styloid processes; second and fourth metacarpal; anterior and posterior superior iliac spines; femoral greater trochanter; anterior aspect of the thigh; femoral lateral epicondyle; fibular attachment to the tibia; tibial tuberosity; anterior aspect of the shank; lateral malleolus; first and fifth metatarsal; first distal phalanx; calcaneus.

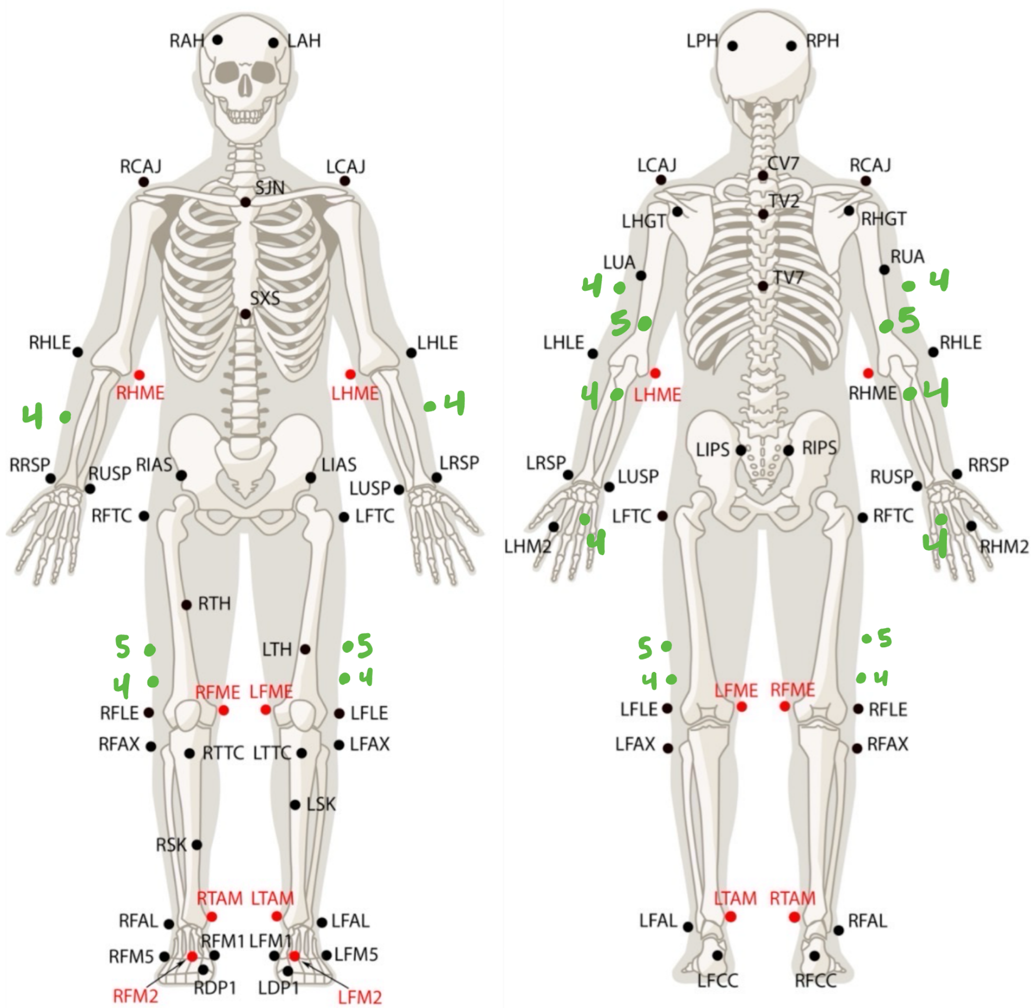

Figure 2.1: A graphic of the skeleton markerset, whereby markers were placed directly on the skin of the anatomic bony landmarks (figure adapted from Optitrack's documentation https://docs.optitrack.com/movement-sciences/movement-sciences-markersets/biomech-57)). The black and red dots are the standard markers in this markerset - black are tracking markers, and the red markers are for the static calibration only and are removed during movement trials. As a minimum of three markers per segment are mathematically required to compute 3D segment orientation, it is advisable to have at least four markers per segment in case one marker is occluded. Therefore, the green points labeled "4" or "5" are additional markers I placed on each segment to provide a fourth or fifth marker, respectively, on that segment.

Rigid body cluster markersets consist of a contoured set of rectangular plastic pieces (the "rigid bodies") that fit the various body segments. Each has at least three markers - typically four - (a "cluster") rigidly affixed via screws to the plastic rigid body. The rigid body cluster is affixed to the skin by wrapping athletic wrap around the body segment (Figure 2.2). This method is used for all segments except the pelvis, head, and torso. For the pelvis, no rigid plastic piece is used, and instead a "rigid body" is constructed from individual skeleton markers placed on the left and right ASIS and PSIS landmarks, in the same fashion that markers are placed on the pelvis for the "skeleton" markerset. For the head, a headband with markers embedded in it is securely attached. For the torso, the markers are affixed to a harness that the participant wears around their chest.

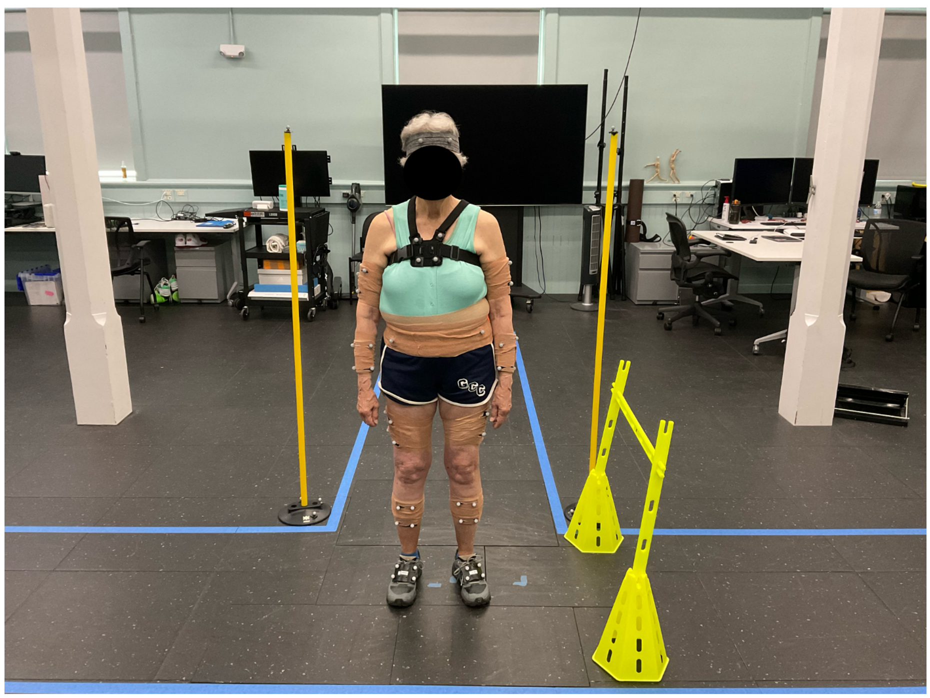

Figure 2.2: The markers were screwed in to plastic plates contoured to fit the body segments. Athletic wrap around each segment held the rigid body marker clusters in place.

The skeleton markerset (Figure 2.1) was used only for the first cohort of 10 young adults (see timeline in Figure 2.3), as that was more directly supported by the motion capture software. As I continued developing our methods, I switched to the rigid body method for the older adult and second young adult cohorts, which eased data collections as individual markers were no longer falling off of the person during trials. In Aims 1 and 2, as both young adults cohorts performed SLG, PP turns, and LC turns at preferred speed, I combine the young adult cohorts with skeleton and rigid body markersets for a larger and more gender-balanced sample than was reported in my published work (127). In Aim 3, as only the second cohort of seven females performed faster turns, only those seven females are included for analysis.

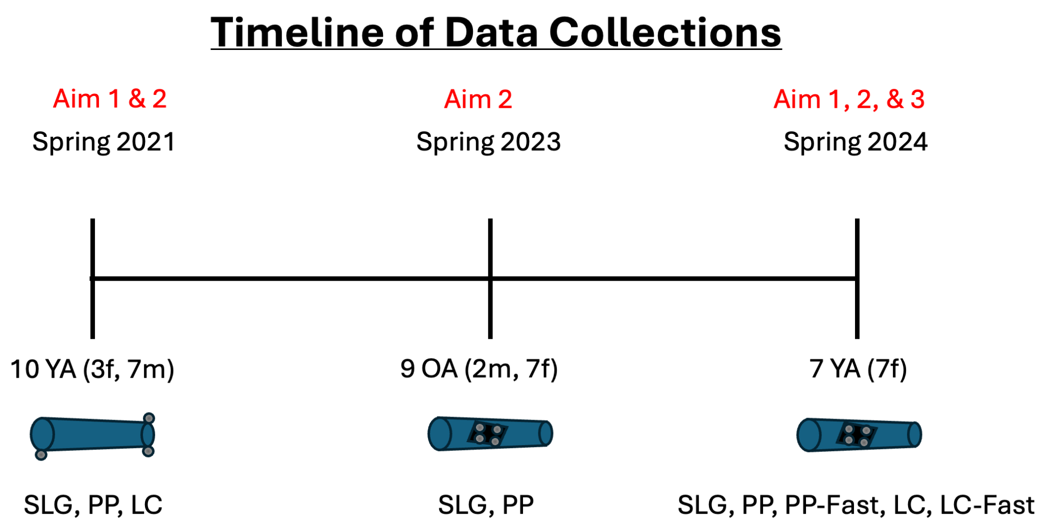

Figure 2.3: Timeline of data collection cohorts and methods, including gender composition and tasks performed (straight-line gait, pre-planned turns, late-cued turns). The red text at the top indicates which aim the dataset was used in. For example, aims 1 and 2 both combined the first and second young adult cohorts into one larger young adult cohort. The blue forearm segment cartoons depict the marker sets used. The skeleton marker set was used only for the first young adult cohort. The rigid body marker clusters were used for the final two collections. Older adults did not perform LC turns. Finally, only the last group of young adults walked faster than preferred speed.

For both markersets, the goal is the same: track the position and orientation of each segment over time. While the skeleton markers are carefully placed directly over the bony landmarks on each segment, the rigid body clusters' placement on each segment is arbitrary, and does not represent the anatomical orientation of a segment. Therefore, for rigid body markers, to relate the "tracking" coordinate system derived from the marker cluster to the "anatomical" coordinate system derived from bony landmarks, a calibration procedure is performed after affixing the marker clusters to each segment. This calibration procedure need only be performed once, assuming no markers fall off of the person or change position relative to the segment they're attached to, as the relation theoretically remains constant.

2.4 Pre-Processing

2.4.1 Data Cleaning

Optical motion capture data yields a wealth of information. However, first it must be "cleaned" to ensure that the data is accurate. In our lab, this process consists of first correcting any missing or incorrect marker labels as possible, either when the data is present but the software's auto-label feature has failed or has mislabeled a marker. Missing or incorrectly labelled marker data will skew the relationship between the tracking and anatomic axes.

2.4.2 Signal Processing

Next, the position data of each marker needs to have any gaps filled, and the data smoothed to reduce noise in the signal. I used a cubic spline (MATLAB `csaps` command) with the smoothing value `p = 0.0005`. This value was chosen through visual inspection of the resulting $\vec{H}$ timeseries, so as to balance amplitude loss with noise minimization. $\vec{H}$ was selected as the reference signal as opposed to any of the other balance-related outcome measures because its computation involves linear and angular velocities, which includes two potential sources of noise: computing angles, and computing velocities (differentiating). The `csaps` smoothing is applied only over the range of data of interest. In our studies the participant began and ended at the edges of the capture volume, so some markers were out of view, and therefore the `csaps` algorithm is applied only over the range of frames in which all markers are in view.

2.5 Biomechanical Modelling

2.5.1 Segment Orientation (Best Marker Names)

Throughout my dissertation I used primarily two methods to generate coordinate systems that were designed to provide the best estimates of the body segments' orientations, given the inherent limitations in motion capture. First I tried a purely distance based method, and later switched to a projected-distance based method. One limitation during motion capture is that the 3D marker positions may experience some jitter due to the process of resolving multiple cameras' 2D estimates into a 3D position, which I have observed to be up to $\pm 1cm$. This error propagates to any computed angles involving that marker - the magnitude of the error in the angle is dependent on the distance of the marker from the vertex of the angle (assuming constant marker jitter magnitude) (Figure 2.4).

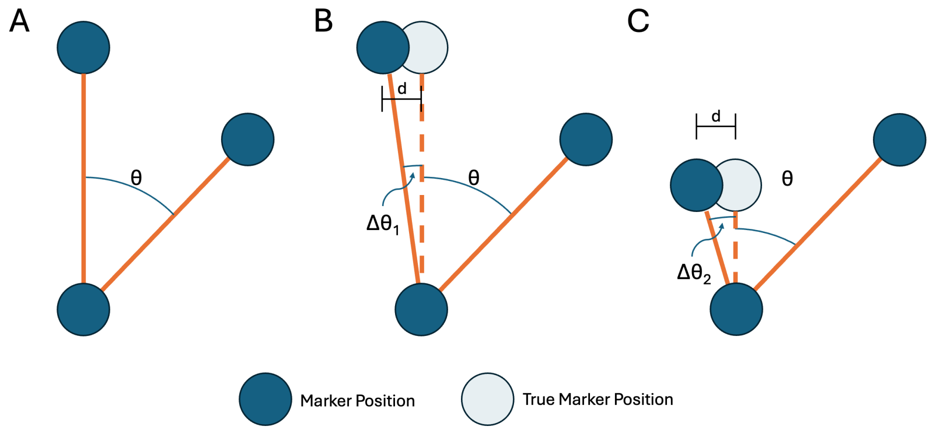

Figure 2.4: Computing angles between three markers' reconstructed 3D positions. (A) the angle computed from marker positions with no jitter, matching their true positions, (B) one of the marker positions is reconstructed erroneously a distance d from its true marker position, changing the computed angle by $\Delta\theta_1$, (C) a different scenario in which the marker is reconstructed a distance d from its true position, but is closer to the vertex of the angle being computed. This jitter causes a change in the angle of $\Delta\theta_2$, which is larger than $\Delta\theta_1$ because it is nearer to the vertex. Therefore, scenario B is more desirable for constructing local coordinate systems from marker positions.

Therefore, in both methods, I must identify the three markers that construct a coordinate system that maximizes the signal-to-noise ratio of true marker position (signal) to marker jitter (error). First, I identify as the first axis of the coordinate system the line between the two markers that are the farthest distance away from one another (markers 1 and 2). At this point, it is not known which of them is marker 1 or 2. Next, in the distance based method that I initially used, the marker farthest from one of the first two markers was selected as the third marker. However, this presented an issue when the three markers were too collinear to one another, as error perpendicular to the first axis in the third marker's position would yield a large angular velocity. As one example, markers placed on the humeral lateral epicondyle, deltoid tuberosity, and acromion-clavicular joint - three common bony landmarks for the upper arm - are actually very collinear, greatly increasing computed segment angular velocities about the long axis.

To minimize that issue, in the projected-distance based method the third marker was selected as the marker that was the farthest perpendicular distance from the line between the first two markers (marker 3). Then, of the first two markers, the one farthest away from the third was deemed the origin marker for that segment (marker 2), and the remaining marker is marker 1. This algorithm's pseudocode is in appendix B.1.

We believe that - better than the solely distance based method or a random selection - the projected-distance based algorithm yields three markers from a list of markers on a segment that are well suited for creating a coordinate system for the study of human movement. The performance of this method was crucial when markers were applied individually to bony landmarks on all body segments because of the increased collinearity and asymmetric placement between markers due to the segments' cylindrical shapes, but is also used when I secured clusters of markers on a rigid piece of plastic to each segment. The only segment that I chose not to use the projected-distance based method for was the pelvis, for two reasons. First, the marker placements on it are fairly symmetric, non-collinear, and each marker has a relatively large distance between the others, mitigating error in angles due to jitter. Second, many of our calculations rely on the pelvis axis as the "body-fixed" axes. Therefore, for the pelvis segment I chose the three markers that resulted in the fewest gaps in the marker data needing to be filled.

This procedure yielded an ordered list of three marker names for each segment. To consistently compute a coordinate system for the rigid bodies, I started with the origin marker (always marker 2). I created a unit vector pointing from marker 1 to 2. This is the X-axis. Next, I create a unit vector pointing from marker 2 to 3. This is used to define the Z-axis as the cross-product of the X-axis unit vector and the vector from marker 2 to 3. Finally, the Y-axis is the cross product of the Z-axis and X-axis, following the right-hand rule. Taken together, these axes form an orthonormal coordinate system that is invariant from the perspective of that segment's skeletal anatomy and its markers. However, it is not aligned in a meaningful way with the segments' skeletal anatomy.

2.5.2 Constructing the Model

Whether the reflective markers are placed carefully on bony landmarks or arbitrarily on the segment as part of a cluster, I still need more information to be able to relate the segments' position and orientation data to an anatomically meaningful model. Several studies have provided careful information about body segment inertial parameters (BSIP) in populations including young healthy adults (128), young healthy athletic adults (129), and healthy older adults (130). They each provide information about how to calculate basic physical quantitities of each body segment such as its mass, center of mass (CM) position, tensor of inertia ($\vec{I}$), segment length, etc. They also define anatomically meaningful coordinate systems relative to bony landmarks for each segment. In this dissertation I rely on (128) because it uses healthy young adults and builds on prior work (131), (132) to take into account asymmetries of mass distribution to provide a CM position and $\vec{I}$ for each segment. This model also has the advantage that the BSIP are provided in three dimensions and are not required to be symmetric about the long axis of the segment, in contrast to other popular models such as (129; 130).

To compute the segments' physical quantities such as CM position, first I need to express their orientation in an anatomically meaningful way. In other words, I need to define a relationship between the coordinate system generated from the markers, and the anatomic axes defined by (128). Therefore, I apply the "tracking to anatomic" rotation matrix to obtain the orientation of the segments' anatomic axes.

Tracking Axes to Anatomic Axes Rotation Matrix

Consider the right forearm segment (Figure 2.5). During static calibration, using a skeleton markerset, the markers are placed on the bony landmarks of the right radial and ulnar styloid processes, and the medial and lateral humeral epicondyles. Thus, I can compute the wrist and elbow joint centers as the mean positions of the radial and ulnar styloid processes and medial and lateral humeral epicondyles, respectively, and then use established segment definitions such as (128) to quantify the orientation of the segment's anatomy. However, some of the markers must be removed for the movement trials, as they would impede participants' movement or be frequently occluded. For example, the medial humeral epicondyle marker would contact the person's torso, or the medial femoral epicondyle markers touching one another, leading to changes in gait to attempt to avoid that contact. Thus, with these markers removed, the segment's orientation can no longer be computed during the movement trials using the mean position of the two markers on either side of the elbow joint to define the joint center. To overcome this limitation, during the static trial, a set of three markers per segment meeting specific criteria (see section 2.5.1) are selected as "tracking markers", and a rotation matrix is defined between each segment's anatomic orientation and the orientation of those three markers during the static trial as follows:

$$^{G}[R]_{tracking}^{anatomic} = {}^{G}[R]_{\vec{I}}^{anatomic}({}^{G}[R]_{\vec{I}}^{tracking})^{T} \tag{2.5.1}$$

where all rotation matrices are expressed in global coordinates, as denoted by superscript G. This rotation matrix between the "tracking axes" and "anatomic axes"

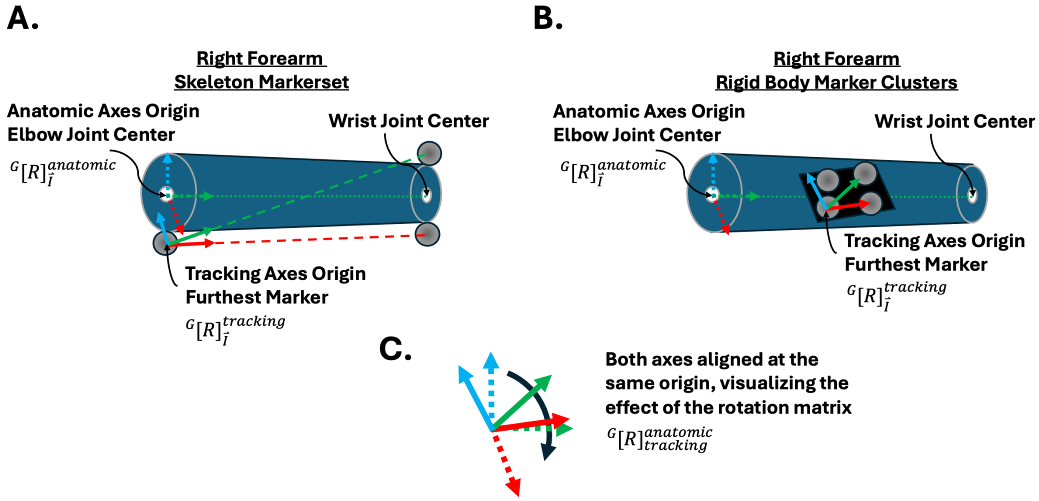

Figure 2.5: Cartoon showing the tracking to anatomic calculation for the right forearm segment. (A) The tracking axes defined by the skeleton marker set, and the anatomic axes aligned with the segment's anatomy. Note that the anatomic axes are dotted, while the tracking axes arrows are solid, as they more closely derive from real measurements. (B) The tracking axes defined by the rigid body marker clusters, and the dotted anatomic axes aligned with the segment's anatomy. (C) A visualization of the effect of the rotation matrix with both axes' origin at the same point.

is theoretically constant. Then, during the movement trials, the rotation matrix is used to rotate the tracking axes into the orientation of the anatomic axes as follows:

$$^{G}[R]_{\vec{I}}^{anatomic} = {}^{G}[R]_{tracking}^{anatomic}\, {}^{G}[R]_{\vec{I}}^{tracking} \tag{2.5.2}$$

This provides a way to compute the joint center locations without requiring markers placed at the joint during movement trials. This method unlocks the ability to place markers freely on the segment, such as placing rigid body marker clusters in the middle of the segment, provided that you perform an additional step during the static calibration to locate the segment anatomic landmarks relative to the segments' markers on the rigid body.

Static Calibration: Digitizing Anatomic Landmarks

The calibration procedure to determine the anatomically meaningful orientation of each body segment when using rigid body marker clusters must be performed at the start of each data collection session after the markers have been placed on the participant. While the participant is standing still (static), I touch the tip of a "digitizing probe" (Optitrack, NaturalPoint, Corvallis, OR) to the bony landmarks on each segment to ascertain the positions of these landmarks, and therefore the joint centers of each segment, relative to the arbitrarily placed "tracking" axes defined by the markers on each cluster. With skeleton markersets, these bony landmarks are already available from the marker positions and no probing process is necessary.

Therefore, for both markerset types, I use these bony landmarks during the static calibration trial to define a rotation matrix from the tracking axes - which are available in all movement trials - to the anatomically meaningful axes used to model the segment orientations through time.

2.5.3 Population-Specific Models

BSIP determination is difficult work involving either cadaveric dismemberment and careful measurement on a scale, or expensive equipment such as DEXA scanners or hydrostatic underwater weighing, which requires submission in water. Therefore, although not ideal, due to the scarcity of these studies and the limitations in the information they provide, it is common in the literature (especially in studies of older adult populations) to use biomechanical models not intended for that population, e.g. (133; 134). In this dissertation, due to differences in the marker set required by the older adult-specific model defined by Dempster (130), I use the model from Dumas et al. (128) - intended for healthy young adults - even in my study of older adults.

Given the potentially limited availability of an appropriate model for the population of interest and the data collected, one of the possible ways to expand the utility of these models is to use them as a starting point for person-specific BSIP estimation, e.g. (135). That study had participants stand on a force plate while motion capture recorded them moving their body pseudorandomly, in a manner that used as many degrees of freedom as possible. Then, they ran an optimization algorithm starting from literature-derived "general" BSIP to match the expected forces from the TBCM acceleration with the forces measured by the force plate.

2.6 Other

2.6.1 Anatomic Planes

There are three anatomic planes for the body. First, the transverse plane is the horizontal plane that divides the upper and lower regions of the body. Next, the frontal plane is the vertical plane that divides the front and back halves of the body. In contrast to straight-line gait, during turns the orientation of the frontal plane changes during the movement, and it is often important to express our variables in this "body-fixed" frontal plane (111). During turns this frontal plane has been previously defined in primarily two ways: the horizontal-plane projection of the vector normal to the TBCM trajectory (111), and the pelvis' anatomic axes projected into the horizontal plane (22). In my work I use the latter method as it decouples how the body-facing direction and the TBCM velocity vector are quantified. Finally, the sagittal plane is now fully defined by the first two planes as being orthogonal to both planes. It is the plane that divides the left and right halves of the body.

2.6.2 Body-Fixed vs. Global Coordinate System

During turns there is no agreed upon method of identifying the body-fixed AP and ML directions. It is necessary to define these directions to express biomechanical variables in a more meaningful reference frame than simply the world-fixed frame (111). During a 90° turn, for example, what was forward in the world-fixed frame becomes sideways in the body-fixed reference frame at the end of the turn. This cross-talk between functional axes can only be resolved with a body-fixed reference frame. However, during SLG, this cross-talk does not exist, as the "body-fixed" reference frame is assumed to always be coincident with the world's. Several methods have been used to define this body-fixed reference frame, that all tend to enforce that the body-fixed vertical axis is parallel with the world's vertical axis. AP can be defined as the tangent to the center of mass trajectory in the horizontal plane, and ML is normal to it.

Another option that has been used is to use the anatomic reference frame of the pelvis as the body-fixed reference frame. Reasons to prefer a pelvis-fixed coordinate system include the fact that it is already included in our model, anatomically connects the upper and lower body, and itself does not rotate much during straight-line gait relative to other segments, and therefore may be the single segment that most accurately reflects the concept of a "whole-body facing direction". It has been shown to be a relatively robust coordinate system as the TBCM changes direction during turns (136). By contrast, other potential candidate segments such as the head or torso seem to be erroneous choices. The head and torso rotate first during a turn, with the head rotating most extensively relative to the other segments (103). However, due to the segments rotating relative to one another, this is not a perfect representation.

2.6.3 Gait Events and Gait Phases

Gait events are detected following the method from (24) modified for nonlinear gait (137). This method consists of identifying peaks and valleys in the anterior-posterior positions of the heels and toes relative to the sacrum, which correspond to heel strike and toe off events, respectively. The modification for turning gait from (137) is to express the heel and toe positions relative to the sacrum in the body-fixed coordinate system. To elaborate on how I implemented this method: First, I isolated the markers corresponding to the heel, toe, and pelvis landmarks (left and right anterior and posterior superior iliac spines (L/R ASIS/PSIS)) positions. Using the pelvis's anatomic axes, I constructed a body-fixed axes where the ML and AP axes are forced to lie in the horizontal plane, and the third axis is vertical. I then expressed foot markers' positions in this body-fixed coordinate system, accounting for arbitrary body-facing directions (Eq. 2.6.1).

$$\vec{r}_{\text{body-fixed}} = {}^{G}[R]_{\vec{I}}^{\text{body-fixed axes}} \, \vec{r}_{\text{global}}^{\,T} \tag{2.6.1}$$

where R is the 3×3 body-fixed coordinate system and $\vec{r}_{global}$ is the 1×3 column vector of the marker positions in global coordinates. Finally, in the body-fixed coordinate system, the peaks and valleys in the AP position of the heel and toe markers corresponded to heel strikes and toe offs, respectively. The phases of gait are then defined as the intervals between the corresponding gait phases. LDS is the period between left heel strike and right toe off, and left single support (LSS) is the period between right toe off and right heel strike, and vice versa for the right gait phases.

2.6.4 Phases of Interest

For each trial, the person started near the edges of the motion capture volume. Thus, they were not visible to the cameras at the start and end of most trials, especially during SLG. Additionally, I wanted to isolate only the time period when the participants were performing the tasks of interest - steady-state SLG, or turning. Therefore, I isolated the phase of interest in each trial based on specific criteria. For SLG, this was the middle 6 m of the walkway, to omit the gait initiation and termination phases. By contrast, the turn phase was defined by the onset and termination of rotation of the pelvis' anteriorly directed anatomic axis (the pelvis' heading angle) in the transverse plane. The onset of rotation was defined by the pelvis' heading angle exceeding three times the standard deviation of the pelvis heading angle during SLG. Rotation termination was defined in the same fashion, but when the heading angle decreased below three times the standard deviation relative to the new (perpendicular) direction of travel. The turn phase was then defined by the heel strike just before rotation onset, and just after rotation termination so that each turn began and ended with similar BOS contexts.

2.7 Balance Metrics

2.7.1 Linear Momentum

Linear momentum, $\vec{p}$, is computed as

$$\vec{p} = m * \vec{v} \tag{2.7.1}$$

where m is the person's mass (kg) and $\vec{v}$ is the velocity of the TBCM (m/s).

2.7.2 Angular Momentum

Whole-body angular momentum about the TBCM, $\vec{H}$, is computed from each segment's $\vec{H}$ as

$$\vec{H} = \sum_{i=1}^{n} [(\overrightarrow{r_{CM_i}} - \overrightarrow{r_{TBCM}}) \times m_i(\overrightarrow{v_{CM_i}} - \overrightarrow{v_{TBCM}}) + \overrightarrow{I_{CM_i}} * \overrightarrow{w_{CM_i}}] \tag{2.7.2}$$

where n is the number of segments, $\vec{r}_{CM_i}$ is the i'th segment's CM position vector, $\overrightarrow{r_{TBCM}}$ is the TBCM position vector, m_i is the i'th segment's mass (kg), $\vec{v}_{CM_i}$ is the i'th segment's CM velocity vector, $\overrightarrow{v_{tbcm}}$ is the TBCM velocity vector, $\vec{I}_{CM_i}$ is the i'th segment's 3×3 tensor of inertia about its own CM, and $\vec{w}_{CM_i}$ is the i'th segment's angular velocity vector about its own CM. All variables are expressed in global coordinates.

Motion capture and the biomechanical models from the literature provide all of the information needed to compute each of these parameters. It is important to express each of these parameters in the same coordinate system that $\vec{H}$ will be expressed in, typically global (lab-fixed) coordinates. The $\vec{I}_{CM_i}$ parameter is provided by the literature as a constant in the segment-fixed coordinate system. Therefore, it must be rotated into the global coordinate system, which will account for the segment's changing orientation relative to the global coordinate system. Summing all of the segments' $\vec{H}$ then yields the whole-body angular momentum. Finally, to express the $\vec{H}$ in an anatomically meaningful way during turns, it is rotated into the pelvis-fixed coordinate system in a similar fashion as done with the motion capture data during gait event detection (see section 2.6.3)

2.7.3 Base of Support Detection

Throughout the evolution of my dissertation, I used a number of different methods for computing the BOS. Generally, the methods all followed the following steps: 1. Identify which markers are in contact with the ground, 2. Compute the BOS as the 2D convex hull of those markers' horizontal-plane positions with MATLAB's `boundary` command. A convex hull is a polygon encompassing a set of points such that all points lie in or on the polygon, and all interior angles are less than 180 degrees. The third argument of `boundary` was set to 0 so that it yields the smallest possible convex hull that encompasses all points. This means that the points on the interior of the foot markers will be *inside* of the BOS, not part of its boundary.

During quiet standing, the markers of both feet are in contact with the ground. The BOS then is approximately constant throughout the trial, encompassing both feet and all of the space between them.

During our gait studies, the BOS changed dynamically. This required detecting when the various markers of the feet were in contact with the ground, and when they were not. The method that I developed to accomplish this was based on the marker heights relative to their height during a quiet standing trial. If the marker was at or below its quiet standing height, then it was deemed to be in contact with the ground. When applying this method to walking it correctly detects when the feet are in contact with the ground, however it also falsely detects the swing foot's midswing position as being on the ground as well. This is because the swing foot's toe marker gets nearer to the ground during midswing than that same marker does during stance phase. To counteract this issue, I instituted gait phase-specific behavior. If the foot is in swing phase, then no marker on that foot is allowed to be deemed to be in contact with the ground. If it is not in swing phase, then it is able to be in contact with the ground if it is below the quiet standing height threshold.

This method works well for walking straight and even 90° turns. However, for the more complicated 180° turns and for movements that don't result in a gait cycle such as standing still, stepping sideways, etc., the gait phase-based method fails due to a lack of typical phases of gait. Fortunately during this study the participants are always walking during the trials.

2.7.4 Lateral Distance

Lateral distance (LD) has been computed in prior works (22) as the ML distance between the TBCM and the nearest lateral edge of the BOS. Prior work defined the lateral edge of the foot using the fifth metatarsal and lateral calcaneus (22). Here, I use the lateral edges of the virtual markers that were defined in the previous section as the lateral edge of the foot:

$$BOS_{ML\ edges} = [min(BOS_{ML}),\ max(BOS_{ML}] \tag{2.7.3}$$

where BOS_{ML} is the ML position of each marker within the BOS, expressed in pelvis-fixed coordinates where the TBCM is at the origin.

Then, in double support, the lateral edge of whichever foot had the most recent heel strike event (i.e. is the foot in front) is selected. In single support, there is only one lateral edge of the BOS. Next, depending on whether the left or right foot's lateral edge is used, in combination with the sign of the lateral edge coordinate, dictates the sign of the LD. For example, if the left foot's lateral edge is used, and its lateral edge coordinate is negative, this becomes a positive LD as the TBCM is medial to the lateral edge of the BOS. However, if the left foot's lateral edge is used and the lateral edge coordinate is positive, this results in a negative LD because the TBCM is lateral

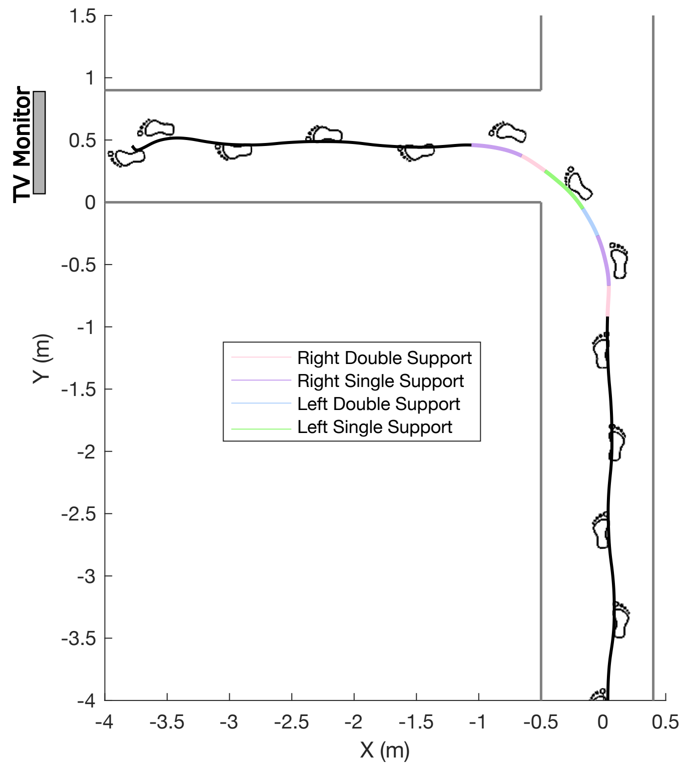

Figure 2.6: Example young adult TBCM trajectory & footfalls during PP turn. During the turn phase, the TBCM trajectory is colored by phase of gait, elsewhere it is black. Left and right foot outlines are shown at midstance.

(left) of the lateral edge of the left foot (e.g. TBCM trajectory lateral to left footfall, Figure 2.6).

2.7.5 Margin of Stability

Margin of stability, MOS, in its original form (19) is computed as the 2D horizontal-plane distance between the XCOM and nearest edge of the BOS. The XCOM position in the global coordinate system is computed as:

$$\vec{r}_{XCOM} = \overrightarrow{r_{TBCM}} + \frac{\overrightarrow{v_{TBCM}}}{\sqrt{\frac{g}{l}}} \tag{2.7.4}$$

where gravitational constant (g) is gravitational acceleration and l is a fixed percentage of leg length. The BOS is a polygon defined by the convex hull around the horizontal-plane positions of the support surfaces that are in contact with the ground. It defines a BOS vector of 2D positions, each of which is one vertex of the BOS boundary. Then, MOS is defined as

$$MOS = min(dist(BOS - \overrightarrow{XCOM})) \tag{2.7.5}$$

Note that Curtze and Hof in 2023 (23) suggest that the BOS during gait should be approximated "using the combined $\overrightarrow{COP}$", quoting prior work that the "effective BOS" is generally approximately one third of the BOS surface area (138). However, given that during turns, $\overrightarrow{COP}$ data is frequently missing or unusable due to footfall issues on the force plates, and that Hof and Curtze state that more theory is needed before applying "effective BOS" to walking, in this dissertation I define the BOS by the outline of the foot marker positions, as done previously by others during SLG (e.g. (26; 65).

In (19) multiple different values of l were provided based on the movement of interest. In this dissertation, I use $l = 1.34 * leg\ length$ as suggested for investigations of frontal-plane movements. Multiple potential values are provided for the proportionality constant, depending on the plane of interest and the body's configuration (19).

This formula for MOS suggests that the XCOM is computed as the sum of the current TBCM position and where the TBCM is about to be based on its velocity and the constraints of the inverted pendulum model.

However, most recent uses of the MOS isolates ML component (22; 26; 60). To accomplish this, in my data analyses I first needed to express the BOS in the pelvis-fixed coordinate system where the XCOM is at the origin. Then, using equation 2.7.3 the ML edges of the BOS are obtained. Finally, modifying equation 2.7.5 to isolate the ML direction:

$$MOS_{ML} = min(|BOS_{ML}|) \tag{2.7.6}$$

If the TBCM is within the BOS medial and lateral edges, then the MOS is positive, otherwise it is negative. Note that this is a different use of the BOS as compared to the LD, for which being medial to the medial edge of the BOS during single stance resulted in a positive value.

Chapter 3

Aim 1: Young Adult Frontal-Plane Balance

3.1 Introduction

Turning while walking is a common component of walking every day. Prior work has shown that depending on the environment, up to 50% of steps during walking are turns (11). 90° turns are ubiquitous, especially while navigating the modern indoor carpentered environment. To successfully accomplish a turn, balance must be maintained while the body changes its facing direction and total body center of mass velocity direction in the horizontal (transverse) plane (139). Balance maintenance necessitates control of the body's TBCM to avoid falling in the frontal or sagittal planes. This TBCM control is accomplished by regulating the body's rotation about the TBCM, as well as the placement of the feet relative to the TBCM (18). Prior work in passive walkers has shown that balance in the sagittal plane can be regulated via natural changes in step length derived largely from the body's own inertia (28). By contrast, balance in the frontal plane must be more actively controlled (37). This combined with the high incidence of injuries in older adults such as hip fractures occurring from falling sideways during turns (8) motivates the current study of the mechanics of frontal-plane balance during naturalistic 90° turns in young adults. By understanding young adults' behavior, we can better understand age-related deficits in turning. Relatedly, given that older adult women are at a higher risk for osteoporosis (140) and therefore fall-related injuries than men, but men are at greater risk of post-fracture mortality (141) this study also aims to stratify these findings by biological sex.

In daily life, turns typically occur in response to a stimulus that informs a person walking that they need to change direction. This stimulus can occur well in advance of the turn itself, which would result in a pre-planned (PP) turn, or it can occur just before the turn needs to happen, which is then deemed a late-cued (LC) turn. Turning behavior changes depending on whether the turn is performed in a PP or LC fashion. Relative to PP turns, LC turns have been shown in older adults to result in increased TBCM acceleration (142) and a larger percentage of spin turns (110). Therefore, LC turns are thought to challenge balance more than PP turns.

A commonly used metric to quantify the rotational component of balance is whole-body angular momentum about the TBCM ($\vec{H}$). $\vec{H}$ quantifies how each segment rotates about the whole body's CM and also includes the segments' rotations about their own CM. Herr and Popovic showed that during SLG, $\vec{H}$ tightly regulated about zero (34) in all three planes. During turns, $\vec{H}$ becomes larger, more asymmetrical, and overall more "unregulated" (96). These changes occur over multiple steps throughout the course of the turn (41). Because $\vec{H}$ oscillates about zero during the gait cycle, the range of $\vec{H}$ as well as its maxima and minima are used to quantify rotational balance control (34; 67; 143; 38). Late-cues will likely increase the rotational demands of the turn, as the same 90° rotation in the horizontal plane must occur within a shorter time frame compared to PP turns. However, to our knowledge, no study has directly investigated the effect of LC turns on $\vec{H}$. In the frontal plane, Patla et al. observed that the trunk rotates more to initiate LC vs. PP turns (113). Additionally, the cognitive load of attending to the LC stimulus may result in a "posture-second" strategy similar to that observed during dual-task walking (144).

To quantify balance via foot placement relative to the TBCM (49), the margin of stability (MOS) is often used (53). The MOS quantifies the position of the XCOM relative to the boundaries of the BOS. The XCOM term is comprised of the TBCM position plus a velocity-based component utilizing the inverted pendulum model (53) to extrapolate where the TBCM is about to be (see section 2.7.5), which is needed to account for the dynamics of the movement. Another similar metric, the lateral distance (LD) has been used in two prior studies (22; 145). LD quantifies the horizontal distance between the TBCM and the BOS boundaries. While this does not account for the movement's dynamics, it has the advantage of not relying on the inverted pendulum model, which has been validated primarily for quiet standing (20) and SLG (21), but not yet in turns. Foot placement has been observed to initiate the turn during PP turns, in contrast to the trunk roll strategy more commonly employed by late-cued turns (113), likely due to the increased available response time (ART) in pre-planned turns. With increasing ART, LC turns are more likely to be able to be performed, and may be performed more like pre-planned turns, utilizing foot placement over trunk roll to initiate the turn.

Therefore, the purpose of this study is to understand how healthy young adults modulate foot placement and rotation relative to the TBCM to maintain balance in the frontal-plane during SLG and 90° turns in two contexts: pre-planned (PP) and late-cued (LC). I hypothesize that 1. the range of frontal-plane $\vec{H}$ ($H_{f,range}$) will increase in LC vs. PP turns, and also be larger in PP turns than in SLG, and 2. Minimum LD (LD_{min}) and MOS (MOS_{min}) will be largest in SLG, smaller in PP turns, and smallest in LC turns.

3.2 Methods

3.2.1 Participants

Participants were included if they were over the age of 18 and under 65, and were conveniently selected from amongst the student body at Stevens. They were ineligible if they had any diagnoses, surgeries, or pain that affected the lower body and their ability to walk. Seventeen participants elected to participate in this study (10 females, 7 males; 25.2 ± 4.2 yrs; 73.9 ± 14.8 kg; 1.79 ± 0.1 m). See Tables A.1 and A.3 for characteristics of each participant.

3.2.2 Experiment Protocol

We placed tape on the floor in a T-shape to simulate two grocery store aisles 0.91 m wide (125) forming a perpendicular intersection. I placed a 2.03 m (85 in) TV screen placed at the end of the intersecting aisle to act as the aisle's signage (Figure 2.6). For 10 participants, I placed 61 retroreflective markers on each participant to record their movements with optical motion capture (200 fps, Motive 2.2, NaturalPoint, Corvallis, OR USA) at the following locations: sternum jugular notch; sternum xiphoid process; C7, T2, and T7 vertebrae; as well as left and right: anterior and posterior head; glenohumeral joint; clavicle-acromion joint; humerus lateral epicondyle; posterior aspect of the upper arm; radial and ulnar styloid processes; second and fourth metacarpal; anterior and posterior superior iliac spines; femoral greater trochanter; anterior aspect of the thigh; femoral lateral epicondyle; fibular attachment to the tibia; tibial tuberosity; anterior aspect of the shank; lateral malleolus; first and fifth metatarsal; first distal phalanx; calcaneus.

The remaining 7 participants were outfitted with one contoured rigid plastic piece for each body segment, each containing clusters of four markers. The plastic pieces were secured to each distal segment with athletic wrap. Markers on the head were secured by headband, a harness for the torso, and the pelvis was tracked in the same way as the first 10 participants with individual markers on bony landmarks. These two cohorts performed the same tasks, and therefore I combine them

Participants were instructed to pretend that they were walking at a comfortable

Figure 3.1: The three possible figures shown on the monitor. (A) A photo of broccoli on a black background, indicating that the person should turn. (B) A red circle with a line through it, a "NO" symbol, on a black background, indicating that the person should continue walking straight. (C) A blank black background, shown before the person reaches the intersection to prevent the participant from knowing whether or not to turn before reaching the intersection.

speed in a grocery store in three scenarios: walking straight, pre-planned turns, and late-cued turns. Other instructions included to pretend that there was no one in front of them but someone was behind them, so that they shouldn't stop but they're not in a rush. For the SLG task, they performed five repetitions walking straight down the 10 m aisle. Next, in the PP task, they were instructed ahead of time that they should turn 90° left to walk down the intersecting aisle because it contained the grocery item of interest as indicated by the monitor displaying a large image of green broccoli, the grocery item of interest. They repeated this 10 times. In the LC task, participants were instructed that there was a 50% chance of needing to turn left 90° or continuing to walk straight. The choice was determined by whether they observed the green broccoli symbol indicating to turn, or a red "NO" symbol (circle with a line through it) indicating to continue walking straight (Figure 3.1). To obtain 10 late-cued turns, 20 trials were performed, with 10 catch trials.

For all tasks, participants were given 15 second rests between each trial and five-minute instructional periods prior to each condition. For PP and LC conditions, the participants were instructed which foot they should begin walking with, in order to encourage a variety of turning behaviors. Each turn condition therefore included five trials starting with each foot.

3.2.3 Kinematic Data Analysis

All marker data were smoothed with a cubic spline filter (MATLAB `csaps` function with the smoothing parameter set to 0.0005) which also filled in all of the gaps in the data due to marker occlusion. Four trials from two subjects were excluded from analysis due to marker occlusion causing missing data. Each participant was modelled using a 15-segment model (128; 146). Joint centers of the wrist, elbow, ankle, and knee were computed by averaging the positions of the two markers placed on opposite sides of the joint. Hip joint centers were determined from Reed et al. (147), and the shoulder joint center was computed following the method from (148). For the torso, the cervical and lumbar joint centers were computed following the method used by Dumas et al. (128) adapted from Reed et al. (147). $\vec{H}$, LD, and MOS were computed at every time point, as well as spatiotemporal gait parameters such as step and stride width, length, and duration following the method of (89).

Phase of Interest

Analyses were conducted during the steady-state phase of SLG (the middle six meters of the walkway), and the turning phase of the PP and LC turning tasks. The turning phase is defined by pelvis rotation and onset three standard deviations beyond the mean pelvis orientation during SLG. The heel strike before the pelvis heading angle exceeds three standard deviations beyond SLG relative to the initial direction of travel begins the turn phase. The heel strike after the pelvis heading angle goes below the three standard deviations threshold relative to the new direction of travel ends the turn phase.

Angular Momentum

$\vec{H}$ was computed following the method described in section 2.7.2. When viewed from behind, positive $\vec{H}$ is clockwise frontal-plane rotation. Max, min, and range of H_f were computed for each trial over the phase of interest.

Base of Support (BOS)

The BOS was computed as described in section 2.7.3. Briefly, the BOS is comprised of virtual markers that define a circle for the forefoot and hindfoot. When any of these markers' vertical position went below the height threshold established during quiet standing (plus a 1cm height tolerance, included to avoid situations where the BOS was incorrect due only to change in shape of the footwear during heel-strike and toe-off subphases.), and that foot is in stance phase, then they were deemed to be in contact with the ground. The BOS is the horizontal-plane convex hull encompassing all of the points of the markers in contact with the ground. The phases of gait were determined via heel strike and toe-off gait events using the relative positioning of the foot markers and pelvis (24) modified for turning gait (137).

Lateral Distance

Lateral distance (LD) is defined as the projection of the distance between the TBCM and the lateral edges of the BOS onto the pelvis-fixed horizontal ML axis. LD was normalized to leg length (hip joint center height) for between-participant comparisons. LD is positive when the TBCM is medial to the lateral edge of the front foot's BOS, and negative when the LD is lateral of the lateral edge of the BOS. In each trial, the maximum and minimum for both feet combined, as well as left and right steps individually were compared.

Margin of Stability

The margin of stability (MOS) (53) is computed similarly to the LD, but instead quantifies the distance between the XCOM (see section 2.7.4 and the medial or lateral edges of the BOS. MOS is positive when the XCOM is between the medial and lateral edges of the BOS, and it is negative if the XCOM is medial of the medial edge or lateral of the lateral edge of the BOS. In each trial, the maximum and minimum for both feet combined, as well as left and right steps individually were compared.

Turn Strategy

Turn strategy is quantified as either "step" or "spin" following the method from Golyski et al. (104). Briefly, this algorithm determines turn strategy based on which foot is nearest to the intersection of the TBCM trajectory before and after the turn during midstance. If it is the inside foot, it is deemed a "spin" turn, and vice versa for a "step" turn.

3.2.4 Statistical Analyses

Linear mixed models were used to assess differences in H_f, LD, ML MOS, and spatiotemporal parameters across SLG and turn conditions. The models included random intercepts for study participant nested within condition, and fixed effects for study condition (*lmer* function in R version 4.4.1) (123). Mixed models were used to handle repeated measurements within study participants. The model was of the form $Response \sim Task + (1|Participant)$, indicating that $Task$ is a fixed effect and participant is a random effect with random intercepts, allowing each participant to have their own baseline for the response. Pairwise comparisons between study tasks were estimated using the `pairs()` function in R. The Holm adjustment for multiple comparisons was used, after excluding interaction effects (comparisons where levels of two or more factors changed simultaneously). Holm-adjusted p-value < 0.05 was used to determine statistical significance.

To stratify the results by Sex, a new model of the form $Response \sim Task * Sex + (1|Participant)$ was used, and the corresponding emmeans formula $Response \sim Task * Sex$. To stratify by $TurnStrategy$, the model $Response \sim Task * TurnStrategy + (1|Participant)$ was used, with emmeans formula $Response \sim Task * TurnStrategy$.

3.3 Results

3.3.1 Spatiotemporal Parameters

Spatiotemporal results and p-values are included in Table 3.1. Significant decreases were observed from SLG to PP turns in gait speed minima, maxima , and median values (all p<0.0001), as well as in LC vs. PP turns (all p<0.0001) (Figure 3.2).

Parameter		Marginal means (95% CL)			Post-hoc pairwise comparisons		
		SLG	**PP**	**LC**	**SLG vs. PP**	**SLG vs. LC**	**PP vs. LC**
Gait Speed (m per s)	Maximum	1.510 (1.431, 1.589)	1.406 (1.327, 1.485)	1.227 (1.148, 1.305)	**<0.0001**	**<0.0001**	**<0.0001**
	Median	1.264 (1.201, 1.327)	1.139 (1.077, 1.202)	0.922 (0.859, 0.984)	**<0.0001**	**<0.0001**	**<0.0001**
	Minimum	1.136 (1.087, 1.184)	0.982 (0.935, 1.030)	0.549 (0.502, 0.597)	**<0.0001**	**<0.0001**	**<0.0001**
Number of Footfalls	Count	8.059 (7.879, 8.240)	3.916 (3.741, 4.092)	3.381 (3.205, 3.557)	**<0.0001**	**<0.0001**	**<0.0001**
Phase Duration (s)	Median	3.988 (3.851, 4.126)	1.683 (1.548, 1.818)	1.416 (1.281, 1.552)	**<0.0001**	**<0.0001**	**<0.0001**
Median Step Duration (s)	Median	0.566 (0.552, 0.580)	0.575 (0.561, 0.589)	0.601 (0.587, 0.615)	**0.0144**	**<0.0001**	**<0.0001**
Median Step Length (m)	Median	0.730 (0.693, 0.767)	0.687 (0.650, 0.724)	0.548 (0.512, 0.585)	**<0.0001**	**<0.0001**	**<0.0001**
Step Width (m)	Maximum	0.132 (0.105, 0.159)	0.298 (0.272, 0.323)	0.223 (0.198, 0.249)	**<0.0001**	**<0.0001**	**<0.0001**
	Median	0.109 (0.089, 0.128)	0.209 (0.190, 0.227)	0.170 (0.151, 0.188)	**<0.0001**	**<0.0001**	**<0.0001**
	Minimum	0.087 (0.066, 0.109)	0.120 (0.101, 0.140)	0.119 (0.099, 0.139)	**0.0059**	**0.0072**	0.8908
Median Stride Duration (s)	Median	1.133 (1.101, 1.165)	1.150 (1.119, 1.181)	1.196 (1.165, 1.227)	0.0819	**<0.0001**	**<0.0001**
Median Stride Length (m)	Median	1.464 (1.383, 1.546)	1.345 (1.264, 1.426)	1.107 (1.027, 1.188)	**<0.0001**	**<0.0001**	**<0.0001**

Table 3.1: Young adults' spatiotemporal metrics per task

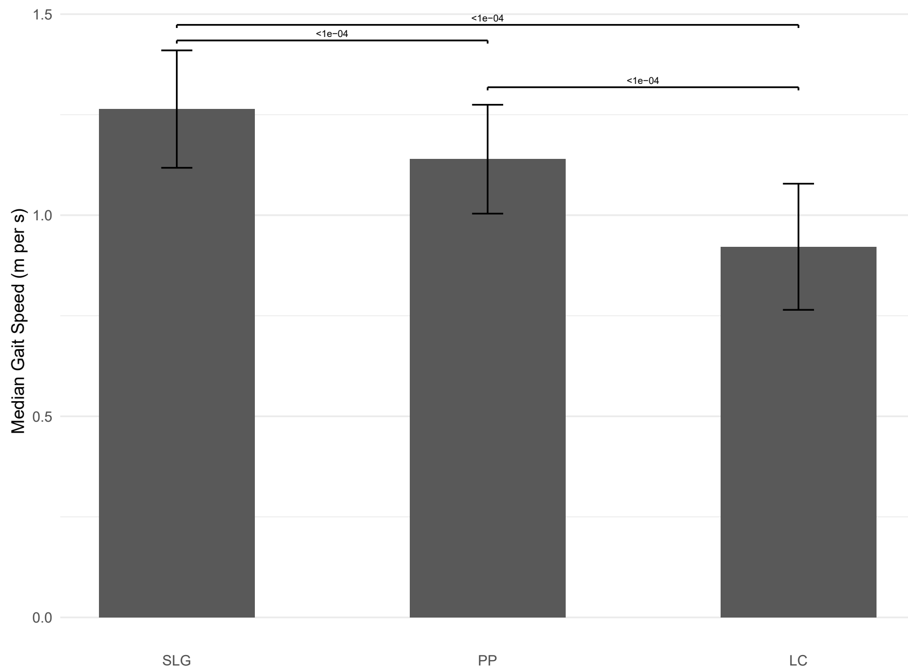

Figure 3.2: Marginal mean of median gait speed for each task for this cohort of 17 young adults. People walked fastest in SLG, and slowest in LC turns.

3.3.2 Frontal Plane Angular Momentum

The range of H_f was significantly smaller during SLG vs. PP turns (p<0.0001) and LC turns (p<0.0001) and during PP vs. LC turns (p<0.0001) (Table 3.2, Figure 3.3). These changes in H_f range were associated with significantly smaller minima from SLG to PP turns and PP turns vs. LC turns (Figure 3.4, $p < 0.0001$), while maxima were only significantly greater during SLG vs. PP turns ($p < 0.0001$) and LC turns ($p < 0.0001$, Table 3.2). There was no difference in H_f maxima in PP vs. LC turns (Table 3.2; $p = 0.2904$).

Parameter		Marginal means (95% CL)			Post-hoc pairwise comparisons		
		SLG	**PP**	**LC**	**SLG vs. PP**	**SLG vs. LC**	**PP vs. LC**
Frontal H (unitless)	Maximum	0.003 (0.003, 0.004)	0.004 (0.004, 0.005)	0.004 (0.004, 0.005)	$<$**0.0001**	$<$**0.0001**	0.5034
	Minimum	-0.004 (-0.004, -0.003)	-0.005 (-0.005, -0.004)	-0.006 (-0.007, -0.005)	$<$**0.0001**	$<$**0.0001**	$<$**0.0001**
	Range	0.007 (0.006, 0.008)	0.009 (0.007, 0.010)	0.010 (0.009, 0.011)	$<$**0.0001**	$<$**0.0001**	$<$**0.0001**
LD (m)	Maximum	0.187 (0.169, 0.204)	0.255 (0.238, 0.272)	0.293 (0.275, 0.310)	$<$**0.0001**	$<$**0.0001**	$<$**0.0001**
	Minimum	0.095 (0.085, 0.105)	0.000 (-0.009, 0.010)	0.058 (0.048, 0.068)	$<$**0.0001**	$<$**0.0001**	$<$**0.0001**
MOS (m)	Maximum	0.099 (0.087, 0.111)	0.149 (0.137, 0.161)	0.166 (0.154, 0.178)	$<$**0.0001**	$<$**0.0001**	$<$**0.0001**
	Minimum	-0.109 (-0.143, -0.076)	-0.132 (-0.165, -0.099)	-0.196 (-0.229, -0.163)	**0.0012**	$<$**0.0001**	$<$**0.0001**

Table 3.2: Frontal-plane balance metrics for 17 young adults during SLG, PP turns, and LC turns. All comparisons between tasks are significant except $H_{f,max}$ in PP vs. LC turns.

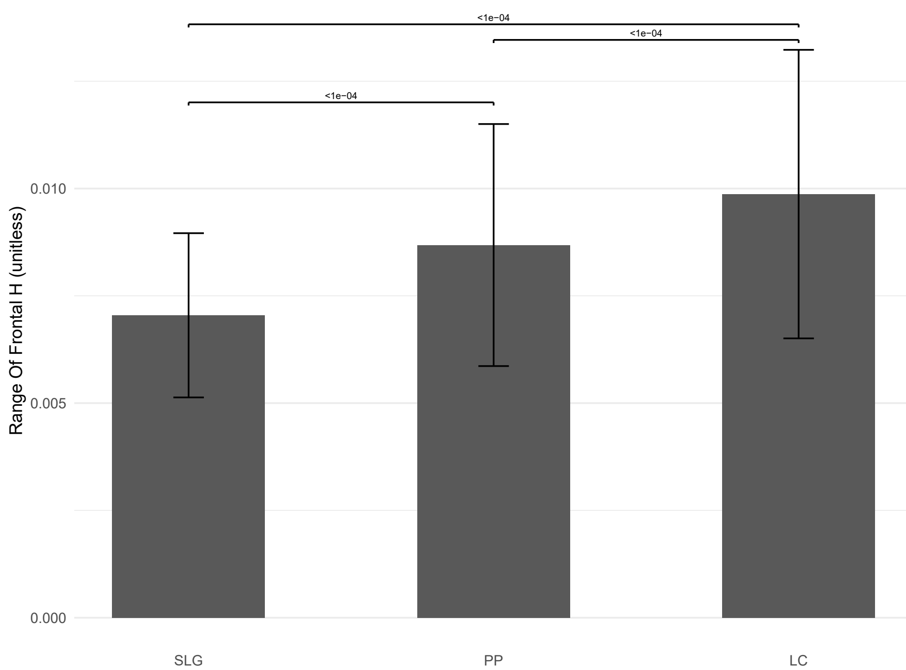

Figure 3.3: Marginal mean $H_{f,range}$ for each task for this cohort of 17 young adults.

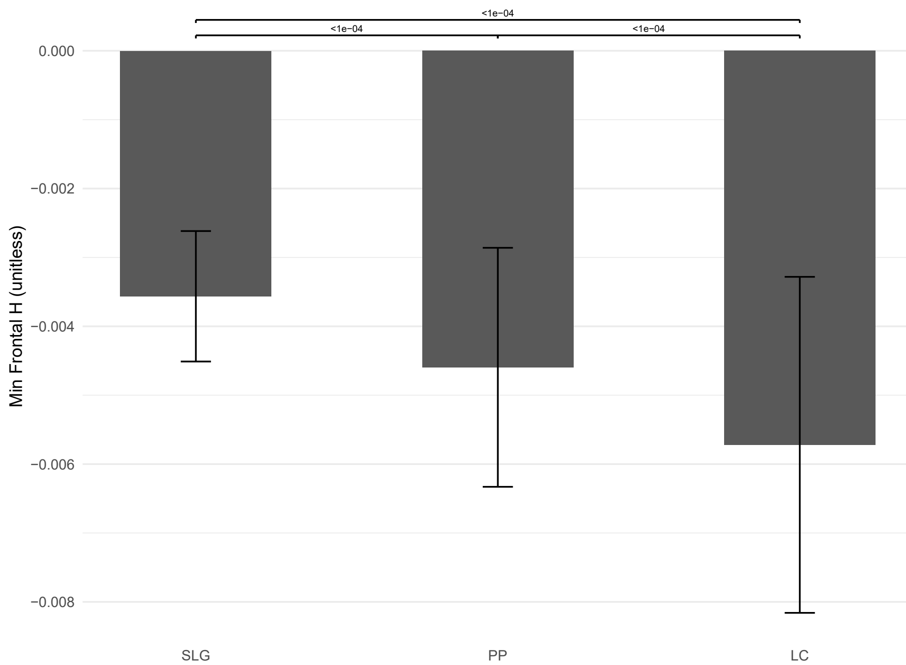

Figure 3.4: Marginal mean $H_{f,min}$ for each task for this cohort of 17 young adults. More negative values correspond to a larger magnitude of frontal-plane rotation acting to rotate the head and torso leftward.

3.3.3 Lateral Distance

The LD_{min} were significantly larger during SLG vs. PP ($p < 0.0001$) and LC turns ($p < 0.0001$), as well as during LC vs. PP turns ($p < 0.0001$) (Figure 3.5, Table 3.2).

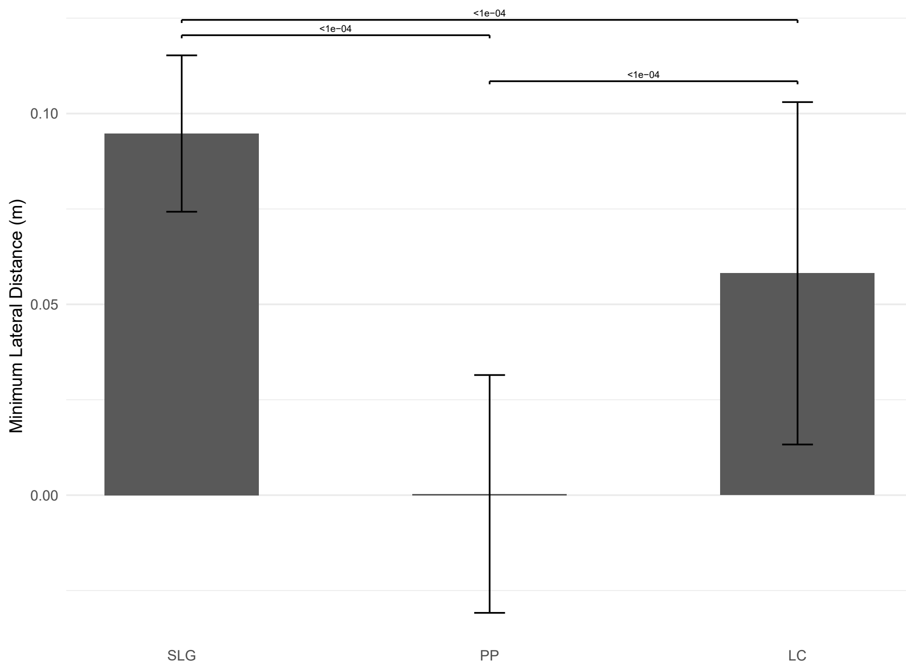

Figure 3.5: Marginal mean LD_{min} for each task for this cohort of 17 young adults. Positive values indicate that the TBCM is within the BOS, while negative values indicate that the TBCM is left of the left edge of the BOS, interpreted as an unstable state.

3.3.4 Mediolateral Margin of Stability

The MOS_{min} were significantly less negative during SLG vs. PP (p=0.0012) and LC turns ($p < 0.0001$) and during PP vs. LC turns ($p < 0.0001$) (Table 3.2, Figure 3.6).

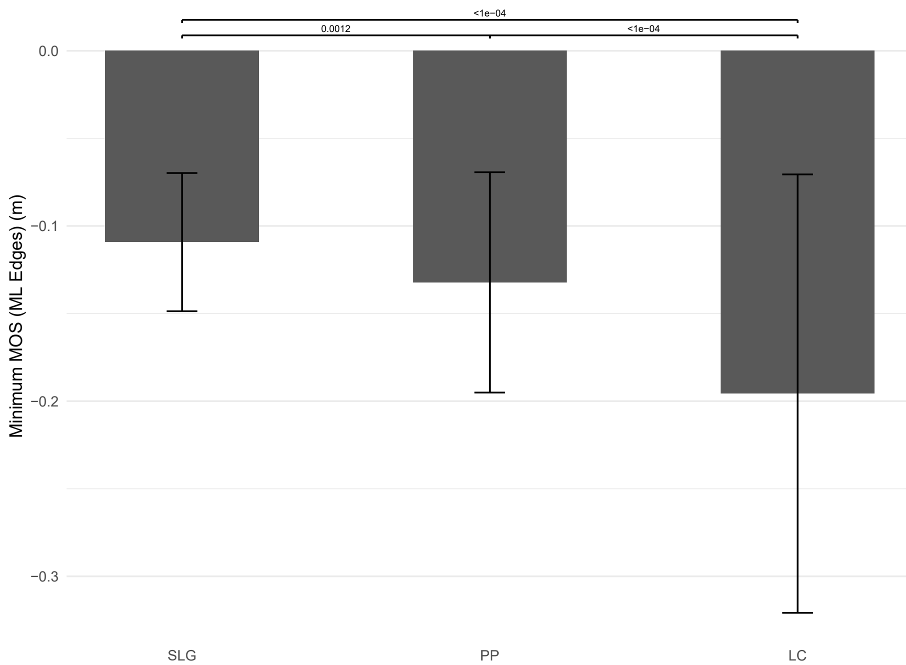

Figure 3.6: Marginal mean MOS_{min} for each task for this cohort of 17 young adults. More negative values mean that the XCOM was further outside of the BOS boundaries, in either the medial or lateral directions.

3.3.5 Turn Strategy

We observed approximately 40% spin turns and 60% step turns across all participants in both PP and LC turns (turn strategy prevalence for all participants in Figure 4.16). In PP turns, participants used as few as 8% spin turns, or as many as 70%. During LC turns, spin turns were as few as 17% , or as many as 67%. No significant differences were observed between turn strategies in any metric besides LD_{min} during LC turns, where spin turns were significantly lower (see representative timeseries in Figure 3.8).

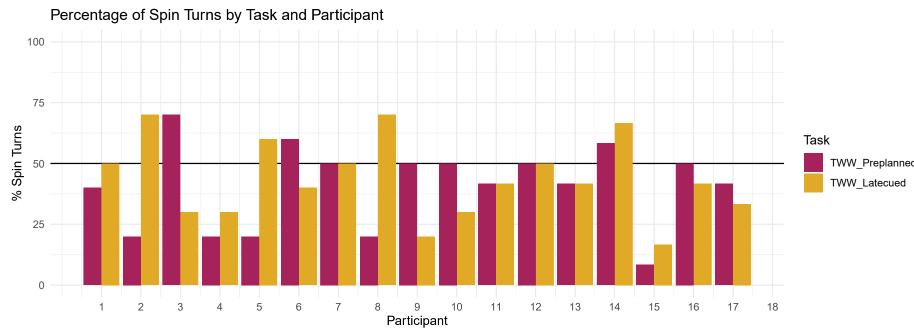

Figure 3.7: Bar graph of young adults' turn strategy prevalence in PP and LC turns. The horizontal black line indicates 50% - below that line more step turns are performed, above it are more spin turns. Prevalence of step vs. spin turn strategy varied between participants in response to turning context (PP vs. LC).

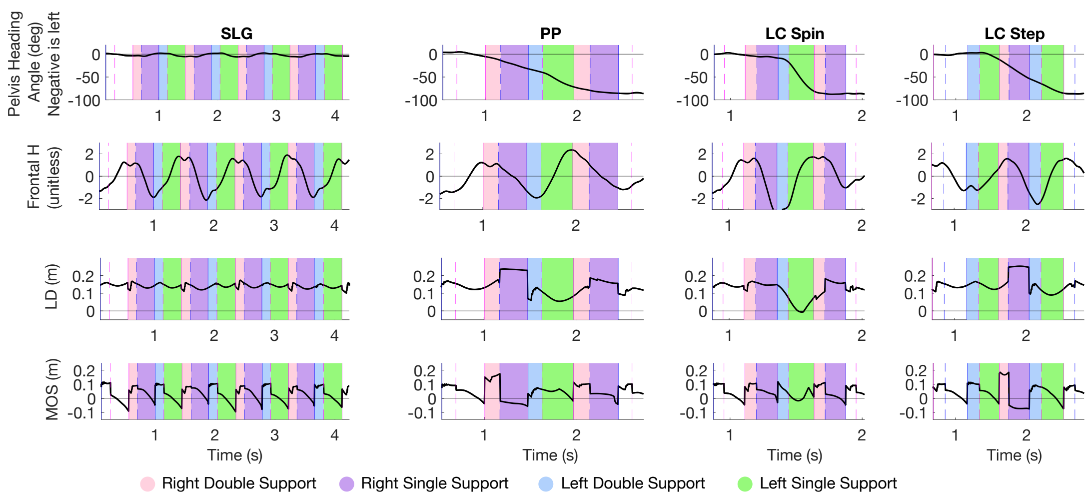

Figure 3.8: Timeseries showing, from top to bottom, the transverse-plane pelvis heading angle, and frontal-plane metrics H_f and LD. From left to right are the different tasks, including an example of a step and spin LC turn. The phases of gait within the phase of interest are color coded. Note that leftward transverse-plane pelvis heading angle (top) is towards the turn. In the second panel, negative H_f acts to rotate the head and trunk leftward towards the inside of the turn, and postive H_f is rightward rotation. In the third panel, negative LD means that the TBCM is outside of the BOS, left of the left edge. In the bottom panel, negative MOS means that the XCOM is outside of the BOS, in either the medial or lateral directions.

3.3.6 Stratification by Biological Sex

No significant differences were observed between males and females for any of the spatiotemporal measures listed in Table 3.1, nor for MOS_{min}. However, in all three tasks, males displayed a larger $H_{f,range}$ than females (max. p=0.0002) (Figure 3.9), driven by both a more extreme $H_{f,min}$ (max p=0.0029) and H_f maxima (max p=0.0243).

Additionally, females exhibited a significantly smaller LD_{min} in all three tasks compared to males (max p=0.0004; Figure 3.10). Finally, MOS minima were not different between males and females for any of the three tasks (p $\geq$ 0.5716; Figure 3.11).

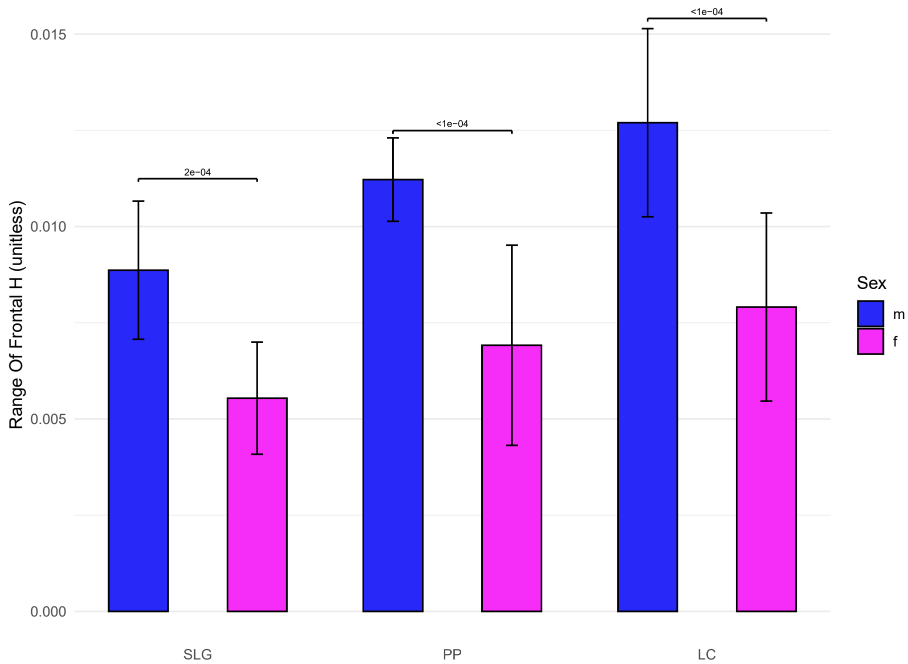

Figure 3.9: Marginal mean $H_{f,range}$ for males and females. Significant differences between tasks are omitted here for clarity. Males exhibited larger $H_{f,range}$ than females in each task.

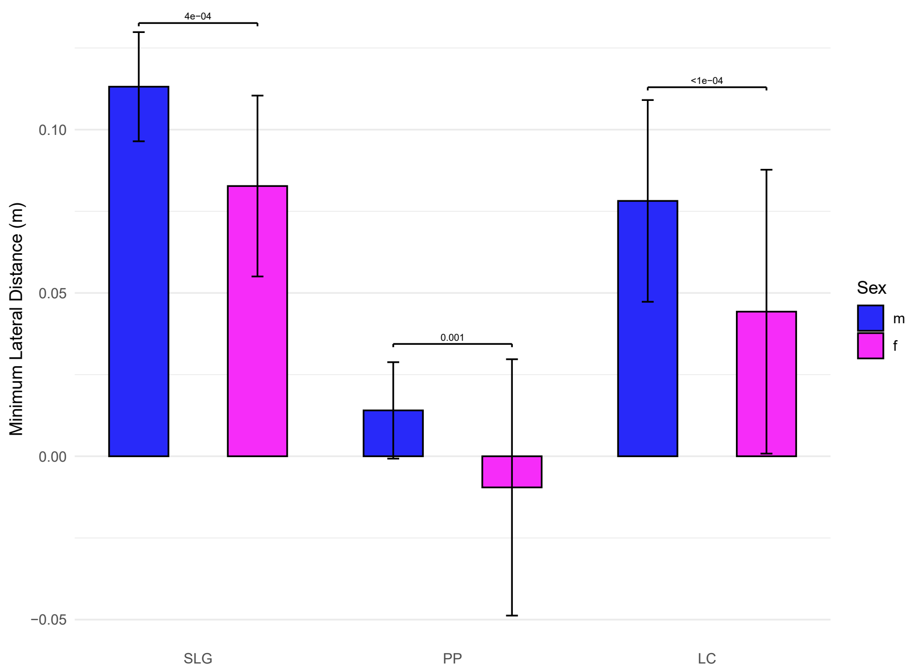

Figure 3.10: Marginal mean LD_{min} for males and females. Significant differences between tasks are omitted here for clarity. Females exhibited lower LD_{min} vs. males in each task, meaning that their TBCM is more lateral to their BOS vs. males.

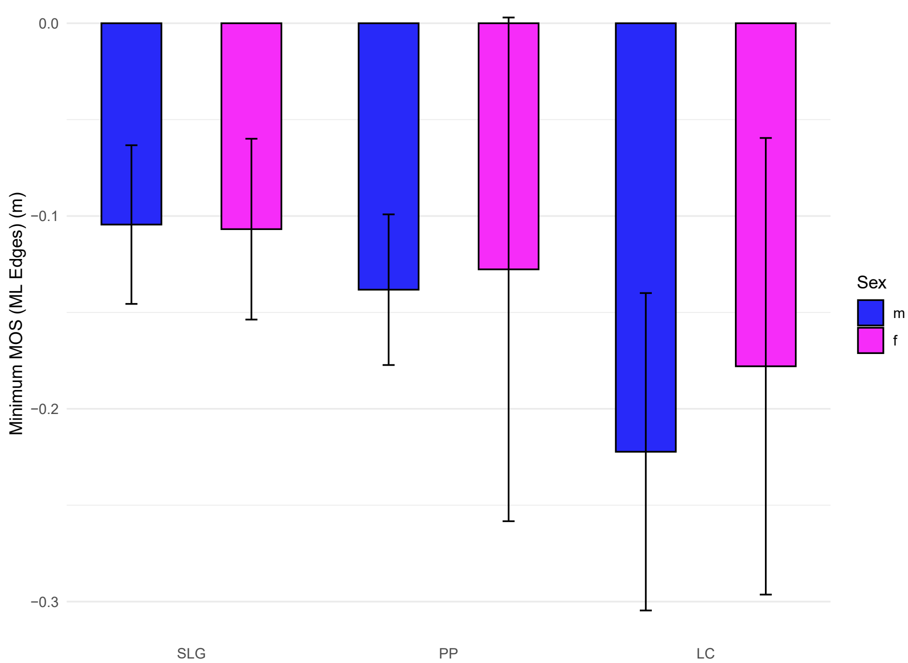

Figure 3.11: Marginal mean MOS_{min} for males and females. Significant differences between task are omitted here for clarity. There were no gender differences within any task for MOS_{min}

.

3.4 Discussion

The purpose of this study is to understand the mechanics of frontal-plane balance during three tasks: SLG, and PP and LC 90° left turns. I hypothesized that the $H_{f,range}$ would be largest during LC turns, smaller in PP turns, and smallest during SLG. This hypothesis was supported. Secondly, I hypothesized that LD and MOS minima would be smallest in LC turns, larger in PP turns, and largest in SLG. Partially supporting this hypothesis, LD_{min} was largest in SLG compared to PP and LC turns. Contrary to our hypothesis, LD_{min} was larger in LC than PP turns. For MOS_{min}, the hypothesis was supported that SLG > PP turns, and PP > LC turns. A summary of the main findings of this Aim is provided in Table 3.3.

Cohort	Factor 1	Factor 2	Metric	Finding
17 YA	Task		Hf Range	LC > PP PP > SLG
			LD Min	PP < SLG PP < LC SLG = LC
			MOS Min	SLG > PP PP > LC
		Sex	Hf Range	M > F all tasks
			LD Min	F < M all tasks
			MOS Min	F = M all tasks
		Turn Strategy	Hf Range	Step = Spin all tasks
			LD Min	PP Spin = Step LC Spin < Step
			MOS Min	Step = Spin all tasks

Table 3.3: Main findings in this cohort of 17 YA for Aim 1 for each Task (top), stratified by Sex (middle) or Turn Strategy (bottom).

The $H_{f,range}$ findings are supported by prior literature that average H_f during turns vs. SLG becomes larger (41) and more "unregulated" (96). Additionally, LC turns have been shown to be initiated with frontal-plane trunk rotation, which can be done quickly and at any time in the gait cycle, whereas PP turns are initiated by adjusting step placement, which requires waiting for the proper phase of the gait cycle to execute (113). With shorter turn durations and fewer footfalls during the turn, the angular momentum to rotate the body in the transverse plane must be generated more quickly, which likely also exacerbates H_f (149). I also observed a slower gait speed during LC turns vs. PP turns, which some studies have reported to increase $H_{f,range}$ (40; 150), while others have reported decreases in $H_{f,range}$ with increased gait speed (42). Further work should expand on the effect of gait speed on H_f (see chapter 5).

During PP and LC turns, both LD_{min} and MOS_{min} were both smaller than during SLG, as the TBCM or XCOM, respectively, translated leftward during the turn, as found previously (151; 92; 102; 152). PP turns afford preparation time that results in a TBCM trajectory that exhibits side to side oscillations but appears more like circular gait, with the TBCM near the lateral (left) edge of the BOS (left foot). This agrees with a study by Orendurff et al. on circular gait of 1 m radius which also observed the TBCM near the lateral edge of the BOS in the direction of the turn (left edge for left turns) (99) at walking speeds similar to those observed in this cohort's PP turns (1.0 - 1.2 m/s). The LC turns, with their lower gait speed and dearth of preparation time before the turn, showed a TBCM trajectory further from the lateral edges of the BOS, which is visually more similar to the slow speeds reported by Orendurff et al (0.6 m/s), which are similar to the speeds during LC turns in this study.

Spatiotemporal parameters and turn strategies may provide additional context for the observation of greater LD_{min} and smaller MOS_{min} in LC vs. PP turns. In PP turns, gait speed was faster, the turns took longer, and more footfalls were used to execute the turn vs. LC turns. Additionally, sharper turns (smaller TBCM trajectory radius) were empirically observed in LC turns, though not explicitly compared in this study. Prior work has shown that the percent duration that the XCOM and TBCM spent outside of the lateral edge of the BOS increased in turns with increasing gait speed (145), which agrees with our findings. One difference in this vs. prior studies is that the LC turns in this study exhibited small turn radii, as they were constrained to decide whether to turn within a very short period within the intersection. Larger turn radii allows for faster gait speeds (71; 153).

The quantification of turn strategy using the method from (104) is slightly muddied during LC turns as some participants performed a "half-step", setting the left foot down directly next to the right foot. This may have inflated the number of spin turns, as the left foot is planted where it otherwise would not have been so as to quickly perform the turn with the right foot. Some prior work shows that PP turn strategies are balanced (93) and LC favor step turns (113). However, other findings show a preference for spin turns during LC turns (93; 110). These findings are specific to the population of interest, and likely the experimental conditions and turn strategy quantification method as well. During LC step turns, where the right foot is more responsible for executing the turn, the left foot's LD_{min} was larger than when a spin turn is performed. In agreement with these findings of larger LD_{min} in LC step turns, other studies have interpreted step turns to also be more "stable" (27; 102). During LC spin turns, often the LD_{min} was actually smaller than during LC step turns (Figure 3.8). By contrast, $H_{f,range}$ seems to be not as affected, if at all, by turn strategy (though not empirically tested here).

The analysis of sex differences is preliminary due to the different markerset (skeleton vs. rigid bodies) and pole placements at the intersection (larger BOS camera tripod vs. smaller BOS plastic poles) used between the predominantly male first cohort vs. the all female second young adult cohort (section 2.2.4). I observed larger $H_{f,range}$ in males than females, a pattern typically interpreted as more "dangerous" or "unstable". However, the lower LD_{min} in females than males indicates that in the positional domain of balance, females' posture is more "dangerous". This difference was also observed in non-normalized $H_{f,range}$. The literature on the existence of sex differences during gait is contrasting (154), with the most persistent kinematic frontal-plane difference being that males and females show larger ranges of motion in the torso and hips, respectively (155), in agreement with the larger $H_{f,range}$ in males found here.

The study has several limitations. First, despite our best efforts to replicate the environment of a grocery store, the motion capture cameras required line of sight that prevented us from having people turn around shelves as they would do in a typical grocery store. Next, the lab space may have been insufficient to elicit steady state SLG after the turn. There was only 4 m of walkway after the turn, which may have resulted in a "turn and slow down"-style task. Next, I did not randomize the order of the tasks. Everyone first performed SLG followed by PP turns followed by LC turns in the first young adult cohort, therefore there may be an order effect, though the second young adult cohort randomized this order. Finally, our choice of turn phase was selected so as to encompass the entirety of the turning movement. However, this novel method precludes comparisons with prior work that used different turn phases. It is also possible that there are earlier preparatory adjustments than pelvis rotation that were missed with this turn phase definition. Our findings are specific to this cohort and analytical selection.

In the future, I aim to understand how behavior in the sagittal and transverse planes may affect frontal plane balance control, and how balance control in all three planes changes in different populations. For example, taking longer steps may influence side to side balance differently in healthy young vs. older adults. Next, I want to further investigate the effect of gait speed on frontal-plane balance control by asking participants to walk at their preferred, faster, or slower speed. Finally, I want to understand how balance control and turn strategies change depending on the phase of gait when the cue is provided to turn, as in (27).

Chapter 4

Aim 2: Effects of Aging on Transverse-Plane Momenta Generation in Four Phases of Gait

4.1 Introduction

Turning can be performed in a variety of ways, such as PP or LC, and using a varying number of footfalls. No matter how the turn is performed, to accomplish the turn, linear momentum and the body's facing direction must be redirected towards the new direction of travel. Often, analyses rely on a three step turn phase (e.g. (41; 92)). However, to compare momentum control across different types of turns, I isolate each of the four phases of gait: left and right single and double support. Each of these phases of gait provide a different BOS context for generating the transverse-plane linear and angular momentum needed to turn.

Aging is also known to change how turns are performed (156). Older adults experience declines in reaction time, muscle strength, and confidence in their balance abilities (120; 157), and often take longer and more steps to complete a turn (158). By comparing the linear and angular momenta generation strategies of young vs. older adults, I can determine if momentum generation is a limiting factor in older adult turning performance.

The purpose of this study is to examine how linear and angular momentum are generated within each phase of gait during SLG and PP turns in young and older healthy adults, and LC turns for young adults only (for safety reasons). I hypothesize that (1) the largest change in linear momentum in the new direction of travel (leftward) will be generated during right single support vs. each other gait phase, (2) transverse-plane angular momentum in the direction of the left turn will be generated during left double support vs. each other gait phase, during each of the three tasks, and (3) during RSS and LDS the magnitude of linear and angular momenta, respectively, in LC will be larger than PP, and PP larger than SLG. I also hypothesize that (4) young adults will generate larger changes in linear and angular momenta than older adults in right single support and left double support, respectively.

4.2 Methods

4.2.1 Participant Recruitment

An older adult and young adult cohort participated in this study. The young adult cohort is the same as that in chapter 3 (see section 3.2.1. The older adult cohort consisted of nine healthy older adults (2 m, 7 f; 71 $\pm$ 6 yrs; 73.6 $\pm$ 15.4 kg; 1.65 $\pm$ 0.06 m). The following eligibility criteria needed to be met in order for older adults to participate: age of 65 years or more, no falls within the prior six months, ability to walk at least one fourth of a mile unassisted in the community, scored 23 or higher on the Montreal Cognitive Assessment (159) and 19 or higher on the Dynamic Gait Index (14) and reported no injuries or pain in the lower extremities. See Tables A.1 and A.3 for characteristics of each young adult participant, and Table A.2 for characteristics of the older adult participants.

4.2.2 Experiment Protocol

We instructed participants to imagine that they were walking down the aisle of a grocery store. To mimic that environment, I placed tape on the floor to form two aisles (each 0.91 m wide) and a 90° intersection (Figure 2.6). Retroreflective motion capture markers were placed on participants to quantify their kinematics using optical motion capture (200/250 fps for young/older adults, Motive 2.2/3.0 for young/older adults, NaturalPoint, Corvallis, OR, USA). For young adults, markers were placed using the same procedure as in section 3.2.2.

For older adults, markers were rigidly affixed to plastic pieces that were contoured to fit the various body segments (using the same method as the young adults, see section 3.2.2). For each segment except for the head, pelvis, and torso, the plastic pieces were secured to each body segment using athletic wrap. Markers attached to a headband captured the head segment. Markers were affixed to the torso using a chest harness. For the pelvis, markers were placed directly on the bony landmarks (left and right anterior and posterior superior iliac spines) and secured with athletic wrap around the waist.

Participants were instructed to pretend that they were in a grocery store "walking at a comfortable pace" in three contexts: walking straight, pre-planned turns, and late-cued turns (older adults did not perform late-cued turns due to safety concerns). See Supplemental videos in (127) for first-person view of the tasks. Participants were instructed to walk as if they were walking with people behind them (so that they should not stop suddenly), but they were not in a rush.

First, they performed at least five trials of straight-line gait down the 10 m aisle. Older adults performed at least 10 trials, so that there would be at least five trials for each of the left and right starting foot. Next, both groups performed 10 pre-planned turns, and finally the young adults performed 10 late-cued turns to the left. Only leftward turns were performed so as to keep the duration of the visit to less than two hours. Between trials, 15 second rest periods were provided, as well as an instructional and practice period between each condition that lasted approximately five minutes. For each condition (except for the young adults SLG) I instructed the participants to begin with the left or right foot, as instructed, the order of which was randomized. When turning in a pre-planned fashion, the participant knew before the trials began that they should perform a 90° left turn in each trial, as though the upcoming aisle contained the broccoli that they were looking for. A large television monitor (2.03 m diagonal) at the end of the intersecting aisle always showed the large green broccoli image (Figure 3.1; Figure 2.6). In the late-cued turn condition (young adults only) when they reached the intersection, the television monitor would show either the green broccoli image, indicating to turn, or it would show a large red circle with a line through it ("NO" symbol) indicating not to turn because the broccoli was not in that aisle (Figure 3.1). Before they reached the intersection, the screen remained black. There was a 50% chance of needing to turn vs. continue walking straight. Thus, the young adults performed 10 late-cued turns and 10 catch trials (no turn). Only the late-cued turns were analyzed from this condition.

4.2.3 Data Analysis

3D marker data was smoothed using a cubic spline filter (MATLAB `csaps` function; smoothing parameter set to 0.0005), which also filled in any gaps due to occlusion in the marker data. I rejected two trials each in two subjects due to excessive gaps in the data. I constructed a biomechanical model of each participant following the method of Dumas et al. (128; 146). The shoulder joint center was computed using an offset from the acromion position (148), and the hip joint centers were computed as an offset from bony landmarks of the pelvis (160). As I were also interested in examining the effect of step vs. spin turn strategy on momenta control, turn strategy was computed following Golyski et al. (104). Briefly, if the left foot is nearest the middle of the intersection for a left turn, then the turn is classified as a spin turn. If it is the right foot, then the turn is a step turn.

4.2.4 Phases of Interest

During each task, I confined our analysis to the time period (phase) of interest. During SLG trials, this was determined by when the TBCM was within the center 6 m of the 10 m walkway. The heel strike before and after the TBCM entered and exited this region defined the beginning and end, respectively, of the SLG phase of interest. During PP and LC turns, the phase of interest is the "turn phase", determined by pelvis heading angle. The start of the turn phase was the last heel strike before pelvis heading angle rotated beyond the SLG values (exceeded three times standard deviation from the mean heading angle during SLG) relative to the initial direction of travel. The end of the turn phase is defined similarly by when the heel strike occurred after the pelvis heading angle value returned below three times standard deviation from the SLG mean relative to the new direction of travel (-X direction, Figure 2.6).

4.2.5 Gait Phases

Gait phases were determined as the interval between the appropriate gait events, which were computed following the method of Zeni et al. (24), with a modification for turning gait (137). Left double support phase is the interval from left heel strike to the frame before right toe off, and vice versa for right double support. Left single support is the interval from right toe off to the frame before right heel-strike, and vice versa for right single support.

4.2.6 Linear Momentum

The linear momentum was computed in the directions of each of the three global axes. The direction of the turn is the global X-axis (leftward is negative). Therefore, the linear momentum in the direction of the turn is computed as the X-component of the TBCM velocity multiplied by the participant's mass. The Δp_x during each of the four phases of gait was computed. $F_{x,avg}$ was computed as $\Delta p_x / phase\ duration\ (sec)$ for each phase of gait.

4.2.7 Angular Momentum

The whole-body angular momentum about the TBCM is computed as the sum of each segment's $\vec{H}$, following the methods described in section 2.7.2, and elsewhere (34; 41). The ΔH_z was computed as $H_{z,final} - H_{z,initial}$ during each of the four phases of gait. $M_{z,avg}$ was computed as $\Delta H_z / phase\ duration\ (sec)$ for each phase of gait. Positive H_z is defined as rotating the body's facing direction leftward, towards the direction of the turn.

4.2.8 Statistical Analyses

The primary outcome measures (average acceleration, average moment, change in linear velocity, and change in angular momentum) across the four gait phases (right double support, right single support, left double support, left single support) within study task (straight-line gait, pre-planned and late-cued turn conditions) and across task within gait phase were examined using linear mixed models (LMMs). The LMMs included fixed effects for gait phase and study task, resulting in the model $Response \sim Task * GaitPhase + (1|Participant)$. If there were multiple instances of a gait phase within the phase of interest (e.g. Figure 4.17, right single support), the outcome variables were averaged across the multiple instances within that trial. The number of repetitions of gait phases ranged from 3-5 during straight-line gait, 1-2 during pre-planned turns, and 0-2 during late-cued turns. If there were no instances of a particular gait phase within a trial, the gait phase outcome variable was assigned a missing value for that trial and was excluded from analyses.

Selected descriptive measures such as gait speed were also examined over the entire phase of interest within the trial, leveraging the model $Response \sim Task + (1|Participant$, yielding one scalar value per trial for each variable.

Mixed models were chosen because they appropriately model the nested nature of the dataset, where Gait Phase is nested within Trial, Trial nested within Task, etc. handling repeated measurements within study participants and missing data well. Pairwise comparisons of the study outcome measures between gait phases within each study task and between tasks within each gait phase were conducted using the `pairs()` command with no adjustment for multiple comparisons. The Holm adjustment for multiple comparisons was used, after excluding interaction effects (comparisons where levels of two or more factors changed simultaneously). A Holm-adjusted p-value < 0.05 was used to determine statistical significance.

A secondary analysis explored whether turn strategy ("spin" versus "step" turn) moderated the relationship between gait phase and study outcomes within each study condition. To do this, a three-way interaction term between gait phase, study task, and turn strategy was included in a linear mixed model, $Response \sim GaitPhase * Task * TurnStrategy + (1|Participant)$. Since straight-line gait has no associated turn strategy, this analysis was limited to the subset of observations from pre-planned and late-cued turns.

4.2.9 Comparison of Older vs. Younger Adults

In contrast to the earlier analyses which were within-participant (and task) and between gait-phase, a between-age group comparison is a between-participant comparison. Therefore, to better compare between participants, the data is normalized to unitless form for $\vec{H}$ (17) and TBCM linear momentum vector ($\vec{p}$) is divided by participant mass (leaving units of m/s). The linear mixed model to examine across age groups, task, and gait phase was $Response \sim AgeGroup * Task * GaitPhase + (1|Participant)$.

4.3 Results

4.3.1 Young Adults

Gait Speed

Gait speed was larger during each double support phase than either single support phase for SLG and PP turns (max $p<0.0001$). Similar to chapter 3, within each phase of gait horizontal gait speed is larger in SLG than PP turns, and PP > LC turns (Figure 4.1). During both turning tasks, gait speed during LSS was greater than during RSS ($p<0.0001$), in contrast to SLG which showed no such asymmetry.

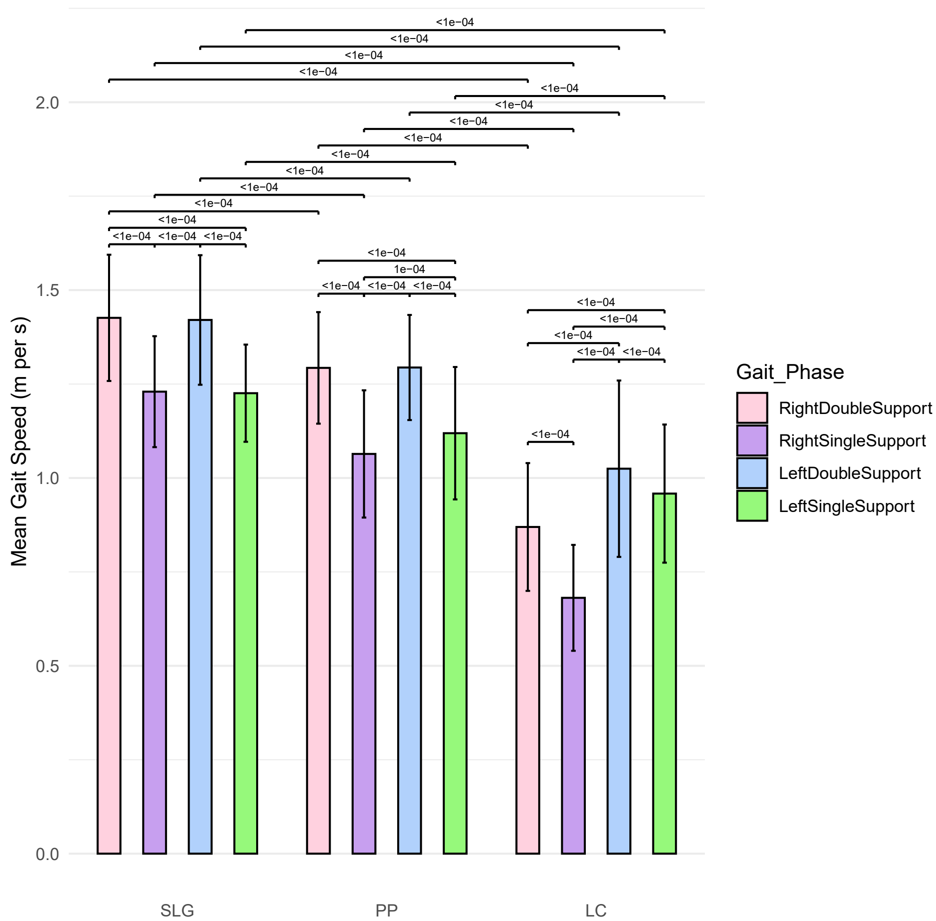

Figure 4.1: Young adults' marginal mean horizontal gait speed for each task & gait phase. Black bars indicate pairs of task and gait phase combinations that are significantly different from one another. Double support phases are faster than single support phases for all tasks. SLG is faster than PP, which in turn is faster than LC within each phase of gait. During SLG, speeds during left and right single support phases are matched, but during turns LSS is faster than RSS.

Linear Momentum

During all three tasks, leftward Δp_x and $F_{x,avg}$ were significantly greater during the right single support phase vs. any other phase ($p < 0.0001$; Table 4.1; Figures 4.2, 4.3), with the exception of PP turns' RSS vs. LDS being not different for $F_{x,avg}$ (p=1).

Parameter	Gait Phase	Marginal means (95% CL)				Post-hoc pairwise comparisons					
		RDS	**RSS**	**LDS**	**LSS**	**RDS vs. RSS**	**RDS vs. LDS**	**RDS vs. LSS**	**RSS vs. LDS**	**RSS vs. LSS**	**LDS vs. LSS**
Average Fx (N)	SLG	0.608 (-7.826, 9.043)	-29.160 (-37.595, -20.726)	-7.543 (-15.977, 0.891)	24.600 (16.166, 33.034)	**<0.0001**	**0.0170**	**<0.0001**	**<0.0001**	**<0.0001**	**<0.0001**
	PP	-50.050 (-58.256, -41.843)	-60.872 (-69.079, -52.666)	-59.795 (-68.002, -51.588)	-28.259 (-36.466, -20.052)	**<0.0001**	**0.0002**	**<0.0001**	0.6490	**<0.0001**	**<0.0001**
	LC	-43.369 (-51.621, -35.117)	-100.081 (-108.337, -91.825)	-63.454 (-71.657, -55.251)	-25.697 (-33.901, -17.494)	**<0.0001**	**<0.0001**	**<0.0001**	**<0.0001**	**<0.0001**	**<0.0001**
	SLG vs. PP	**<0.0001**	**<0.0001**	**<0.0001**	**<0.0001**	-	-	-	-	-	-
	SLG vs. LC	**<0.0001**	**<0.0001**	**<0.0001**	**<0.0001**	-	-	-	-	-	-
	PP vs. LC	**0.0228**	**<0.0001**	0.3654	0.5572	-	-	-	-	-	-
Average Mz (N*m)	SLG	-12.179 (-12.635, -11.724)	2.865 (2.410, 3.321)	10.970 (10.515, 11.425)	-2.194 (-2.649, -1.739)	**<0.0001**	**<0.0001**	**<0.0001**	**<0.0001**	**<0.0001**	**<0.0001**
	PP	-11.861 (-12.251, -11.472)	2.511 (2.122, 2.901)	12.388 (11.999, 12.778)	-2.575 (-2.964, -2.185)	**<0.0001**	**<0.0001**	**<0.0001**	**<0.0001**	**<0.0001**	**<0.0001**
	LC	-6.669 (-7.072, -6.265)	2.014 (1.610, 2.419)	9.728 (9.339, 10.116)	-3.208 (-3.596, -2.819)	**<0.0001**	**<0.0001**	**<0.0001**	**<0.0001**	**<0.0001**	**<0.0001**
	SLG vs. PP	0.6059	0.6059	**<0.0001**	0.6059	-	-	-	-	-	-
	SLG vs. LC	**<0.0001**	**0.0304**	**0.0003**	**0.0047**	-	-	-	-	-	-
	PP vs. LC	0.2987	**<0.0001**	0.1010	-	-	-	-	-	-	
Delta Hz (kg*m^2 per s)	SLG	-2.176 (-2.279, -2.073)	1.094 (0.991, 1.197)	1.941 (1.838, 2.044)	-0.855 (-0.958, -0.752)	**<0.0001**	**<0.0001**	**<0.0001**	**<0.0001**	**<0.0001**	**<0.0001**
	PP	-2.077 (-2.164, -1.989)	0.986 (0.898, 1.073)	2.233 (2.145, 2.320)	-1.034 (-1.122, -0.947)	**<0.0001**	**<0.0001**	**<0.0001**	**<0.0001**	**<0.0001**	**<0.0001**
	LC	-1.173 (-1.264, -1.082)	0.856 (0.765, 0.947)	1.954 (1.867, 2.042)	-1.272 (-1.360, -1.185)	**<0.0001**	**<0.0001**	0.4575	**<0.0001**	**<0.0001**	**<0.0001**
	SLG vs. PP	0.4575	0.4575	**0.0002**	0.0533	-	-	-	-	-	-
	SLG vs. LC	**<0.0001**	**0.0045**	0.8410	**<0.0001**	-	-	-	-	-	-
	PP vs. LC	**<0.0001**	0.2138	**<0.0001**	**0.0012**	-	-	-	-	-	-
Delta Px (kg*m per s)	SLG	-0.243 (-2.989, 2.503)	-11.086 (-13.831, -8.340)	-1.669 (-4.415, 1.077)	9.844 (7.098, 12.590)	**<0.0001**	0.5001	**<0.0001**	**<0.0001**	**<0.0001**	**<0.0001**
	PP	-8.799 (-11.446, -6.152)	-24.044 (-26.692, -21.397)	-10.840 (-13.487, -8.192)	-11.355 (-14.003, -8.708)	**<0.0001**	0.1009	**0.0254**	**<0.0001**	**<0.0001**	1.0000
	LC	-7.328 (-9.995, -4.662)	-42.570 (-45.238, -39.902)	-13.435 (-16.081, -10.789)	-11.333 (-13.979, -8.688)	**<0.0001**	**<0.0001**	**<0.0001**	**<0.0001**	**<0.0001**	0.0987
	SLG vs. PP	**<0.0001**	**<0.0001**	**<0.0001**	**<0.0001**	-	-	-	-	-	-
	SLG vs. LC	**<0.0001**	**<0.0001**	**<0.0001**	**<0.0001**	-	-	-	-	-	-
	PP vs. LC	0.4021	**<0.0001**	**0.0249**	1.0000	-	-	-	-	-	-

Table 4.1: Young adults' transverse-plane linear and angular momenta generation per task & gait phase

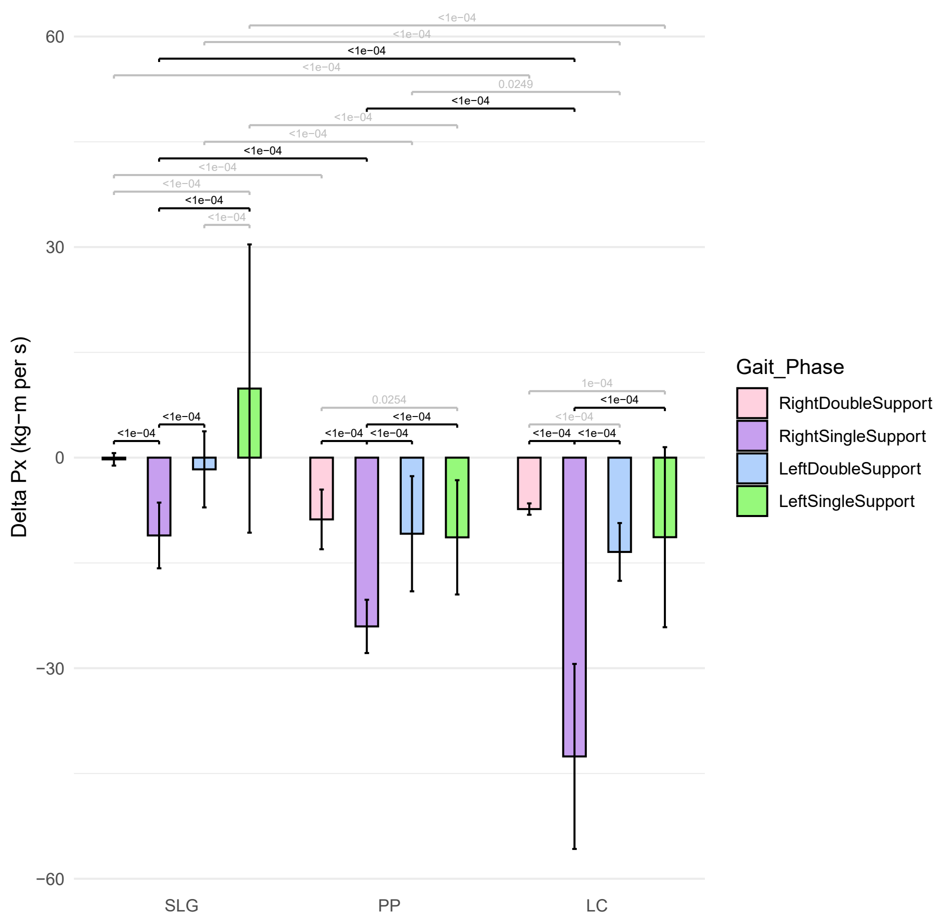

Figure 4.2: Young adults' marginal mean Δp_x for each task & gait phase. Positive values indicate rightward Δp_x, while negative indicates leftward, in the direction of the turn. Horizontal bars indicate significant differences between main effects of Task and Gait Phase (i.e. pairs where only one factor changes levels, such as PP LSS vs. PP RSS). The black bars represent significant comparisons involving the phase of interest, RSS. Leftward RSS is largest in each task, and larger in LC vs. PP turns.

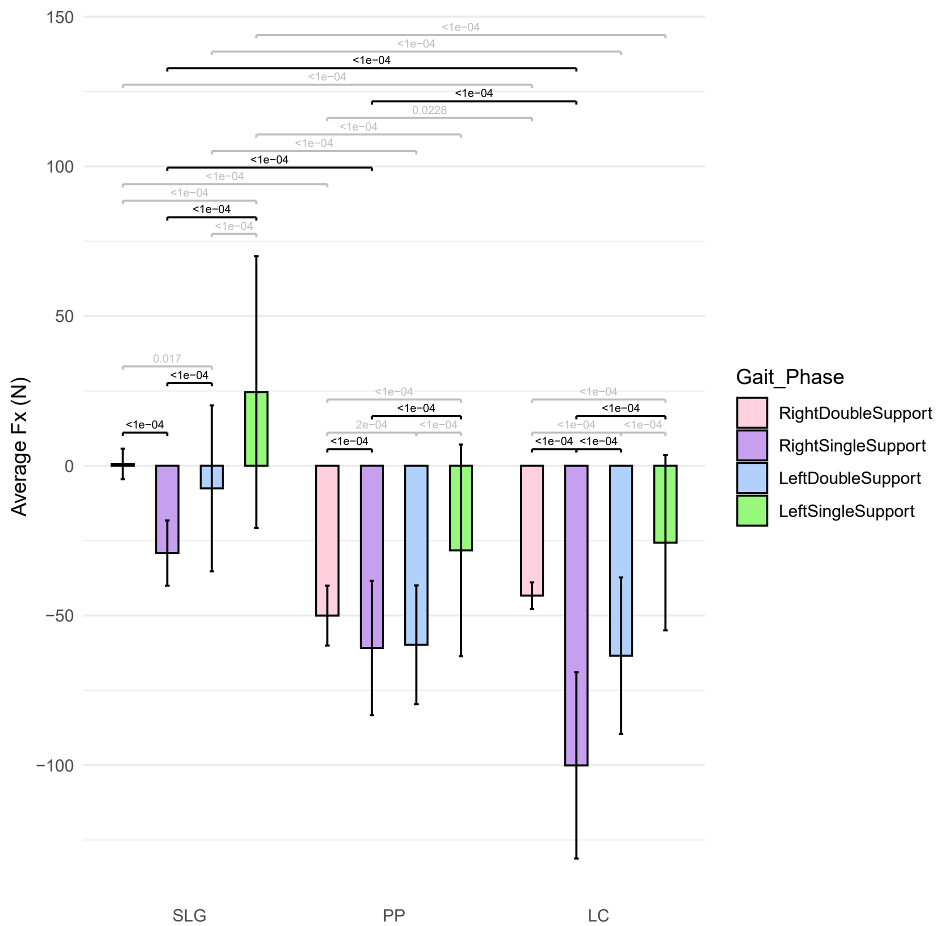

Figure 4.3: Young adults' marginal mean $F_{x,avg}$ for each task & gait phase. Positive values indicate rightward $F_{x,avg}$, while negative indicates leftward, in the direction of the turn. Horizontal bars indicate significant differences between main effects of Task and Gait Phase (i.e. pairs where only one factor changes levels, such as PP LSS vs. PP RSS). The black bars represent significant comparisons involving the phase of interest, RSS. Between gait phases, leftward RSS is largest in SLG and LC turns only in each task, and between tasks, leftward RSS is larger in LC vs. PP turns.

Leftward Δp_x and $F_{x,avg}$ during RSS were significantly larger in LC turns than PP turns. LDS Δp_x was significantly larger in LC vs. PP turns (p=0.0249). Rightward right double support (RDS) $F_{x,avg}$ was larger in PP vs. LC turns (p=0.0228).

Angular Momentum

During SLG, PP, and LC turns, leftward ΔH_z and $M_{z,avg}$ were significantly greater during left double support (when the left leg was forward) vs. any other phase (p-values $<$ 0.0001; Table 4.1, Figures 4.4, 4.5).

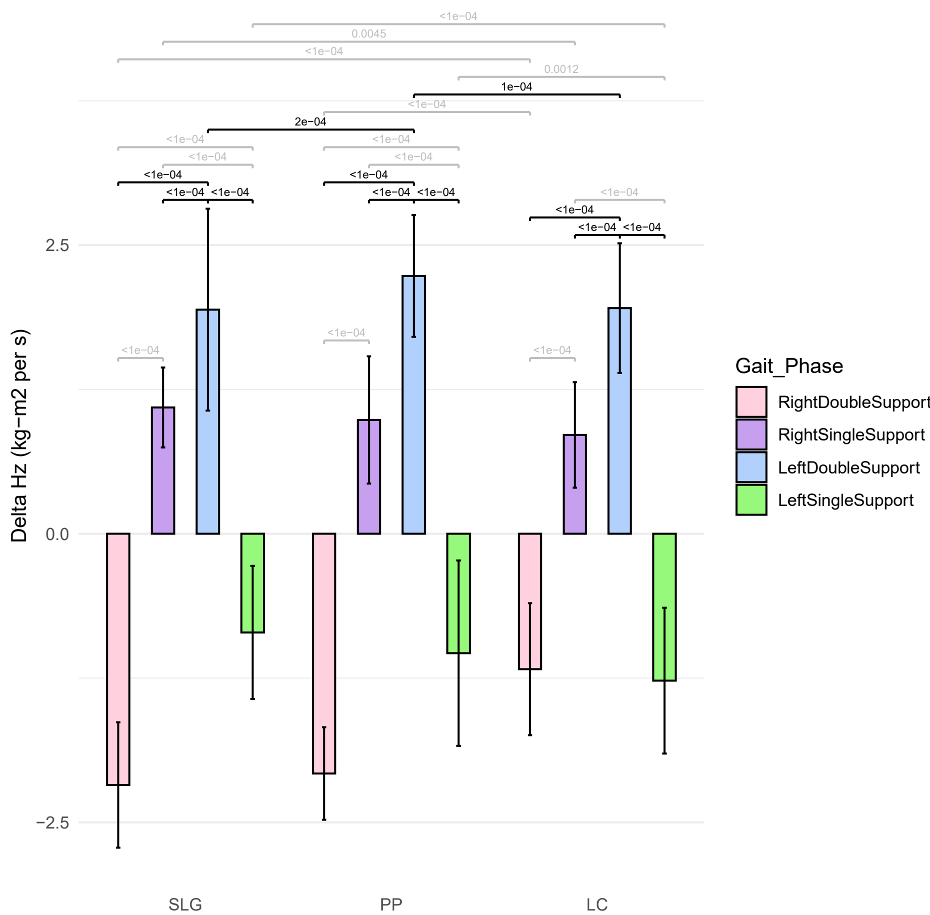

Figure 4.4: The marginal mean ΔH_z for each task & gait phase for the young adult cohort. Positive values indicate leftward transverse-plane rotation of the body-facing direction, in the direction of the turn, while negative values indicate the opposite rotation. Horizontal bars indicate significant differences between main effects of Task and Gait Phase (i.e. pairs where only one factor changes levels, such as PP LSS vs. PP LDS). The black bars represent significant comparisons involving the phase of interest, LDS. In each task, the largest amount of leftward H_z is generated during LDS. More leftward rotation is generated (LDS) and counteracted rightward (RDS) in PP vs. LC turns.

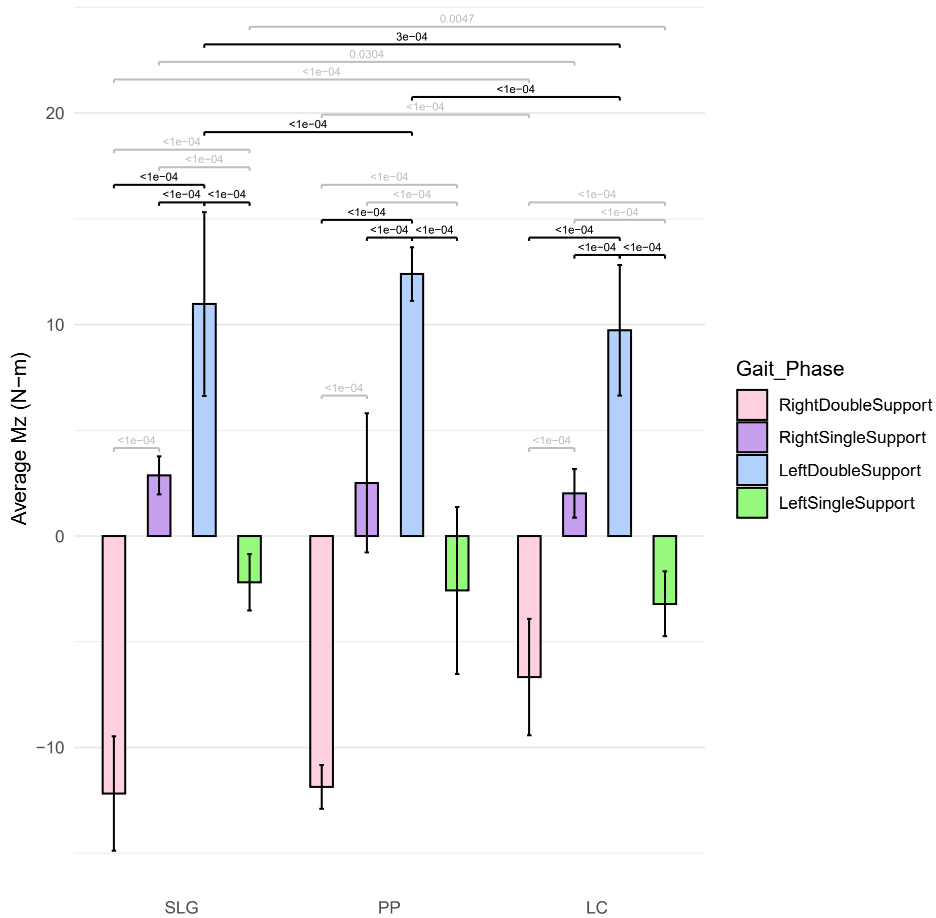

Figure 4.5: Young adults' marginal mean $M_{z,avg}$ for each task & gait phase. Positive values indicate leftward transverse-plane rotation of the body-facing direction, in the direction of the turn, while negative values indicate the opposite rotation. Horizontal bars indicate significant differences between main effects of Task and Gait Phase (i.e. pairs where only one factor changes levels, such as PP LSS vs. PP LDS). The black bars represent significant comparisons involving the phase of interest, LDS. In each task, the largest amount of leftward $M_{z,avg}$ is generated during LDS. There is a larger average leftward moment during (LDS) counteracted by a rightward moment during (RDS) in PP vs. LC turns.

Leftward ΔH_z and $M_{z,avg}$ during LDS were largest in PP turns (p $\leq$ 0.0002). ΔH_z in LDS showed no difference between SLG and LC turns, but $M_{z,avg}$ was larger in SLG vs. LC turns. Rightward ΔH_z in LSS was significantly larger in LC vs. PP turns (p=0.0012), while rightward ΔH_z in RDS was significantly larger in PP vs. LC turns (p<0.0001). For $M_{z,avg}$, only rightward RDS was smaller between PP and LC turns (p<0.0001). Finally, for ΔH_z and $M_{z,avg}$ in SLG I observed larger rightward during RDS (p<0.0001), larger leftward in RSS (p$\leq$0.0304), and smaller rightward

LSS ($p \leq 0.0047$) compared to LC turns.

4.3.2 Older Adults

Older adults' spatiotemporal measures are provided for reference in Table 4.2, and momenta generation values per gait phase in Table 4.3.

Parameter		Marginal means (95% CL)		Post-hoc pairwise comparisons
		SLG	**PP**	**SLG vs. PP**
Gait Speed (m per s)	Maximum	1.453 (1.375, 1.531)	1.288 (1.210, 1.366)	<**0.0001**
	Median	1.210 (1.145, 1.276)	1.018 (0.952, 1.083)	<**0.0001**
	Minimum	1.074 (1.010, 1.138)	0.846 (0.782, 0.910)	<**0.0001**
Number of Footfalls	Count	8.320 (7.792, 8.848)	4.512 (3.985, 5.040)	<**0.0001**
Phase Duration (s)	Median	3.967 (3.657, 4.278)	1.983 (1.673, 2.294)	<**0.0001**
Median Step Duration (s)	Median	0.542 (0.520, 0.564)	0.568 (0.546, 0.590)	<**0.0001**
Median Step Length (m)	Median	0.673 (0.639, 0.707)	0.604 (0.569, 0.638)	<**0.0001**
Step Width (m)	Maximum	0.108 (0.093, 0.123)	0.257 (0.241, 0.272)	<**0.0001**
	Median	0.086 (0.067, 0.106)	0.160 (0.140, 0.179)	<**0.0001**
	Minimum	0.065 (0.044, 0.086)	0.080 (0.059, 0.101)	0.0704
Median Stride Duration (s)	Median	1.084 (1.040, 1.128)	1.132 (1.088, 1.175)	<**0.0001**
Median Stride Length (m)	Median	1.348 (1.281, 1.415)	1.187 (1.120, 1.254)	<**0.0001**

Table 4.2: Spatiotemporal parameters for 9 older adults during SLG, PP turns, and LC turns.

Parameter	Gait$_{phase}$	Marginal means (95% CL)				Post-hoc pairwise comparisons					
		RDS	**RSS**	**LDS**	**LSS**	**RDS vs. RSS**	**RDS vs. LDS**	**RDS vs. LSS**	**RSS vs. LDS**	**RSS vs. LSS**	**LDS vs. LSS**
Average Fx (N)	SLG	8.911 (3.912, 13.909)	-26.981 (-31.979, -21.983)	-10.385 (-15.383, -5.387)	28.251 (23.253, 33.250)	**<0.0001**	**<0.0001**	**<0.0001**	**<0.0001**	**<0.0001**	**<0.0001**
	PP	-43.963 (-48.951, -38.975)	-50.946 (-55.934, -45.958)	-60.960 (-65.948, -55.972)	-16.098 (-21.086, -11.110)	**0.0003**	**<0.0001**	**<0.0001**	**<0.0001**	**<0.0001**	**<0.0001**
	SLG vs. PP	**<0.0001**	**<0.0001**	**<0.0001**	**<0.0001**	-	-	-	-	-	-
Average Mz (N-m)	SLG	-14.535 (-15.101, -13.970)	4.003 (3.438, 4.568)	14.128 (13.563, 14.694)	-3.829 (-4.394, -3.264)	**<0.0001**	**<0.0001**	**<0.0001**	**<0.0001**	**<0.0001**	**<0.0001**
	PP	-13.344 (-13.904, -12.783)	3.766 (3.206, 4.326)	13.505 (12.945, 14.066)	-3.551 (-4.112, -2.991)	**<0.0001**	**<0.0001**	**<0.0001**	**<0.0001**	**<0.0001**	**<0.0001**
	SLG vs. PP	**0.0133**	0.9854	0.3727	0.9854	-	-	-	-	-	-
Delta Hz (kg-m2 per s)	SLG	-2.617 (-2.753, -2.482)	1.427 (1.291, 1.562)	2.564 (2.428, 2.699)	-1.370 (-1.505, -1.234)	**<0.0001**	**<0.0001**	**<0.0001**	**<0.0001**	**<0.0001**	**<0.0001**
	PP	-2.611 (-2.745, -2.477)	1.374 (1.240, 1.508)	2.575 (2.441, 2.709)	-1.326 (-1.460, -1.192)	**<0.0001**	**<0.0001**	**<0.0001**	**<0.0001**	**<0.0001**	**<0.0001**
	SLG vs. PP	1.0000	1.0000	1.0000	1.0000	-	-	-	-	-	-
Delta Px (kg-m per s)	SLG	1.729 (0.399, 3.058)	-9.715 (-11.044, -8.385)	-1.929 (-3.258, -0.599)	10.114 (8.784, 11.443)	**<0.0001**	**<0.0001**	**<0.0001**	**<0.0001**	**<0.0001**	**<0.0001**
	PP	-8.275 (-9.601, -6.949)	-18.974 (-20.300, -17.648)	-11.658 (-12.984, -10.333)	-6.189 (-7.515, -4.863)	**<0.0001**	**<0.0001**	**0.0002**	**<0.0001**	**<0.0001**	**<0.0001**
	SLG vs. PP	**<0.0001**	**<0.0001**	**<0.0001**	**<0.0001**	-	-	-	-	-	-

Table 4.3: Older adults' transverse-plane linear and angular momenta generation per task & gait phase

Gait Speed

During SLG, overall gait speed was larger than in PP turns ($p<0.0001$) over the entire turn (Table 4.2). This also held true for the mean gait speed within each phase of gait (all $p<0.0001$) (Figure 4.6). Between phases of gait, during SLG, gait speed was not different between left and right single ($p=0.8753$) and double support ($p=0.2307$), and the double support phases were faster than the single support phases (all $p<0.0001$). During the leftward turns, gait speed during left and right double support was not different ($p=0.6845$). However, gait speed was significantly larger during LSS vs. RSS ($p<0.0001$) during turns.

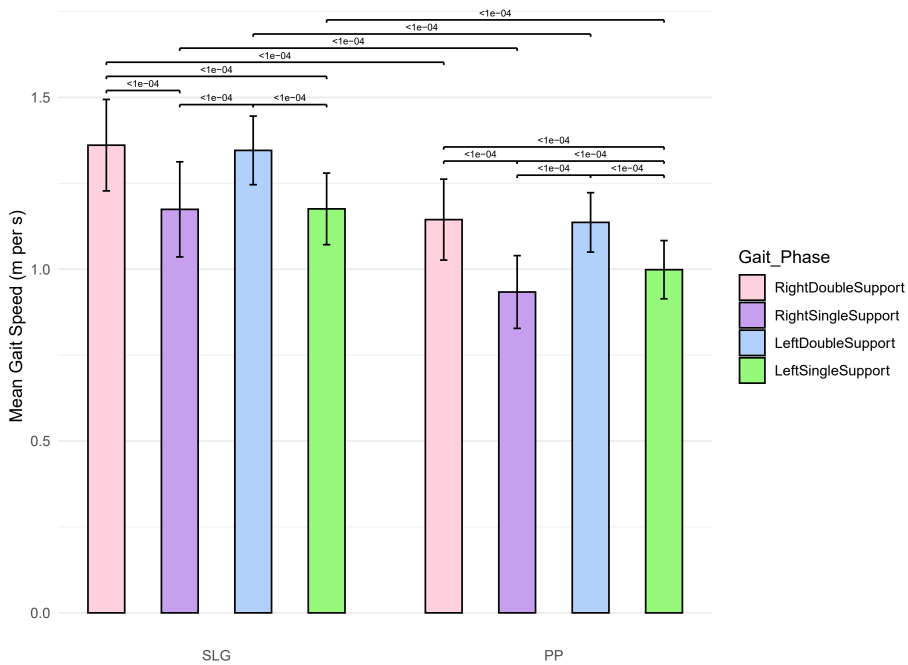

Figure 4.6: Older adults' marginal mean horizontal gait speed for each task & gait phase. During turns, LSS is faster than RSS, but they are not different during SLG. Dobule support phases are significantly faster vs. single support in both tasks.

Linear Momentum

The Δp_x was significantly different for every pairwise comparison between levels of $Task$ and $GaitPhase$. During SLG, it was near zero in LDS and RDS (Figure 4.7), and a large positive (rightward) and negative (leftward) for LSS and RSS, respectively. During PP turns, the Δp_x tended to be negative in each phase of gait for all trials, and were significantly more negative than SLG (p<0.0001) with the largest negative Δp_x in RSS.

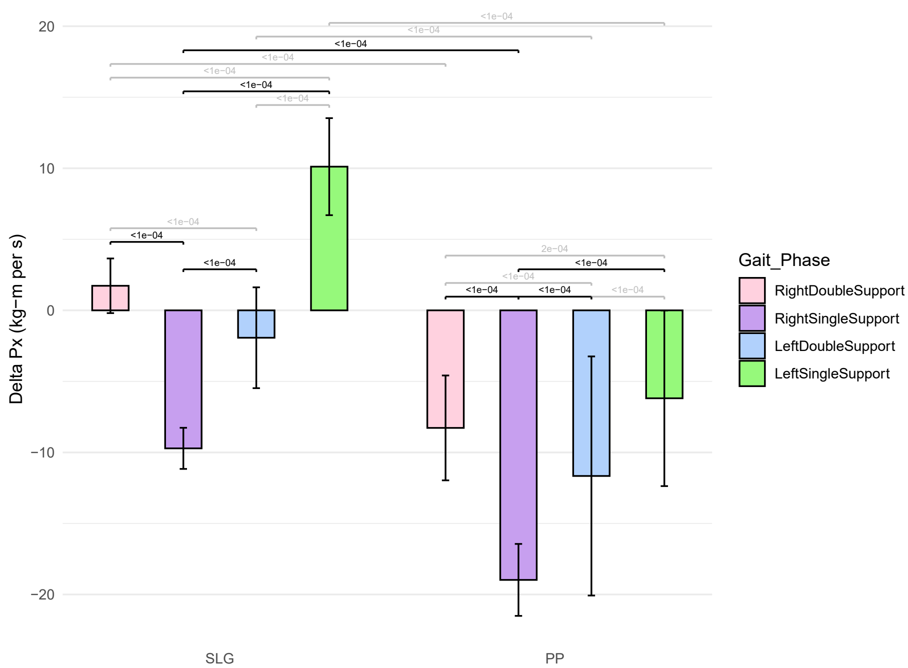

Figure 4.7: Older adults' marginal mean Δp_x for each task & gait phase. ositive values indicate rightward Δp_x, while negative indicates leftward, in the direction of the turn. Horizontal bars indicate significant differences between main effects of Task and Gait Phase (i.e. pairs where only one factor changes levels, such as PP LSS vs. PP RSS). The black bars represent significant comparisons involving the phase of interest, RSS. RSS is largest magnitude in each task, and larger in PP turns vs. SLG.

When accounting for gait phase duration with $F_{x,avg}$, the same trends persisted in SLG as from Δp_x. However, during turns, LDS showed the largest leftward $F_{x,avg}$, followed by RSS, then RDS. LSS exhibited much less leftward $F_{x,avg}$ than the other gait phases.

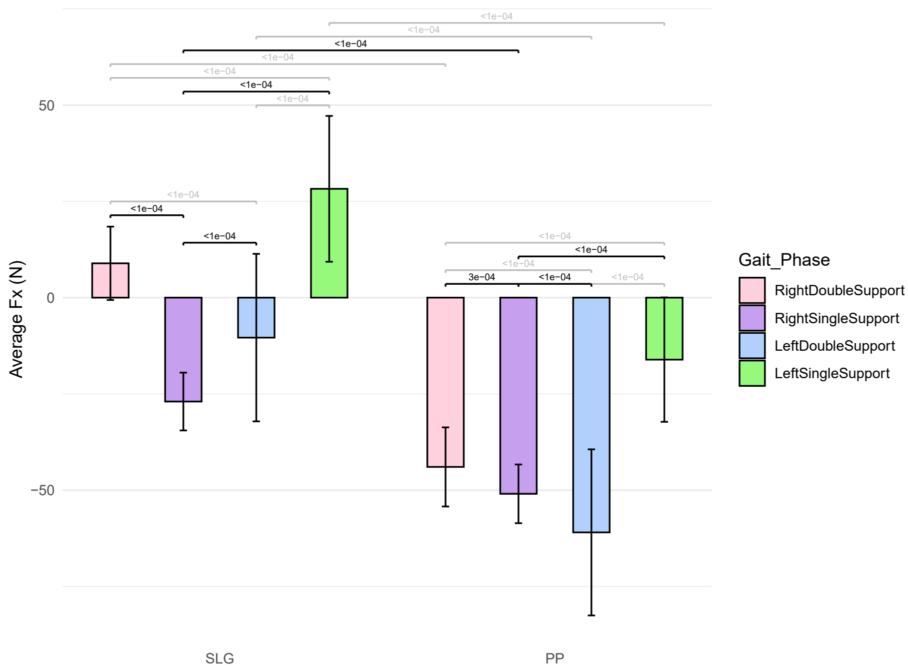

Figure 4.8: Older adults' marginal mean $F_{x,avg}$ for each task & gait phase. Positive values indicate rightward $F_{x,avg}$, while negative indicates leftward, in the direction of the turn. Horizontal bars indicate significant differences between main effects of Task and Gait Phase (i.e. pairs where only one factor changes levels, such as PP LSS vs. PP RSS). The black bars represent significant comparisons involving the phase of interest, RSS. During turns, the largest leftward $F_{x,avg}$ occurs during LDS, in contrast to Δp_x results.

Angular Momentum

In contrast to linear metrics, in the angular domain, with the exception of RDS $M_{z,avg}$ being smaller rightward in PP turns vs. SLG (p=0.0133), ΔH_z and $M_{z,avg}$ did not differ between SLG and PP turns (p≥0.3727). Within each task, each gait phase was different from each other gait phase (all p<0.0001). I observed the largest leftward ΔH_z towards the turn during LDS, followed by RSS (Figure 4.9).

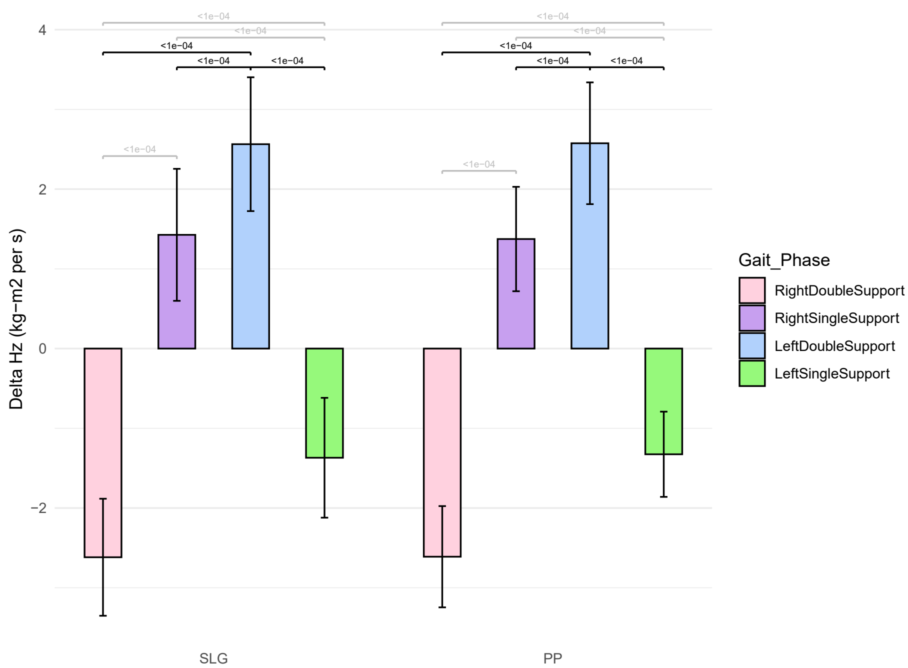

Figure 4.9: Older adults' marginal mean ΔH_z for each task & gait phase. Positive values indicate leftward transverse-plane rotation of the body-facing direction, in the direction of the turn, while negative values indicate the opposite rotation. Horizontal bars indicate significant differences between main effects of Task and Gait Phase (i.e. pairs where only one factor changes levels, such as PP LSS vs. PP LDS). The black bars represent significant comparisons involving the phase of interest, LDS. The largest amount of leftward H_z is generated during LDS, and the magnitude of ΔH_z does not differ between tasks in any gait phase.

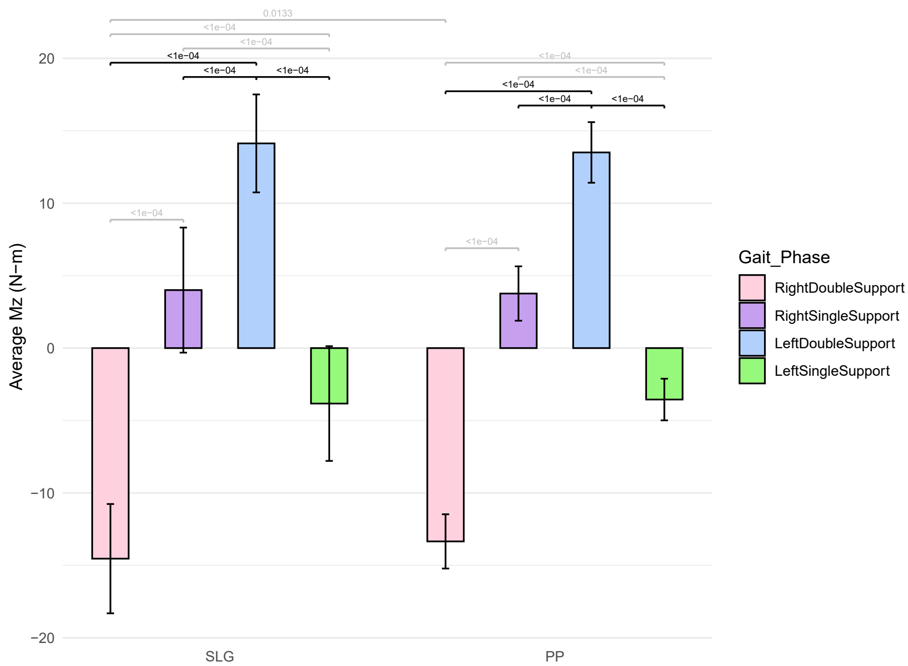

Figure 4.10: Older adults' marginal mean $M_{z,avg}$ for each task & gait phase. Positive values indicate leftward transverse-plane rotation of the body-facing direction, in the direction of the turn, while negative values indicate the opposite rotation. Horizontal bars indicate significant differences between main effects of Task and Gait Phase (i.e. pairs where only one factor changes levels, such as PP LSS vs. PP LDS). The black bars represent significant comparisons involving the phase of interest, LDS. In each task, the largest amount of leftward $M_{z,avg}$ is generated during LDS. SLG and PP turns generate similar leftward H_z during LDS, but less rightward ΔH_z during RDS in PP turns vs. SLG.

4.3.3 Young vs. Older Adults

Gait Speed

Although young adults tended to walk slightly faster during both SLG and PP turns, the young and older adult cohorts' gait speeds did not differ significantly across the whole trial (SLG p=0.3457, PP turn p=0.0517), nor did they differ within any phase of gait (Figure 4.11; p≥0.1338).

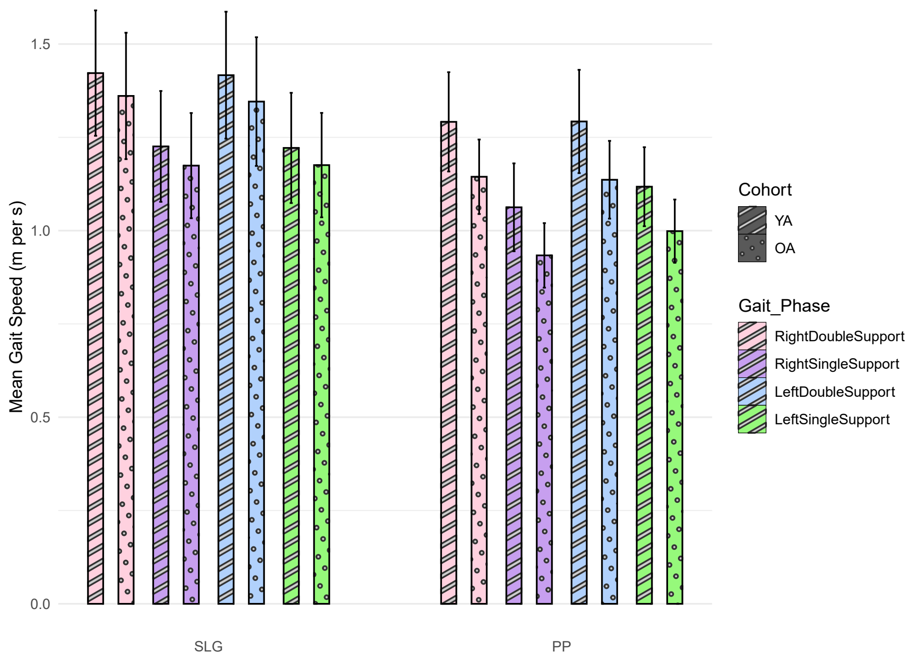

Figure 4.11: Young vs. older adults' marginal mean horizontal gait speed for each task & gait phase. Only significant differences between young and older adults are shown here for clarity. This cohort of young and older adults did not show significant difference in speed during any phase of gait.

Linear Momentum

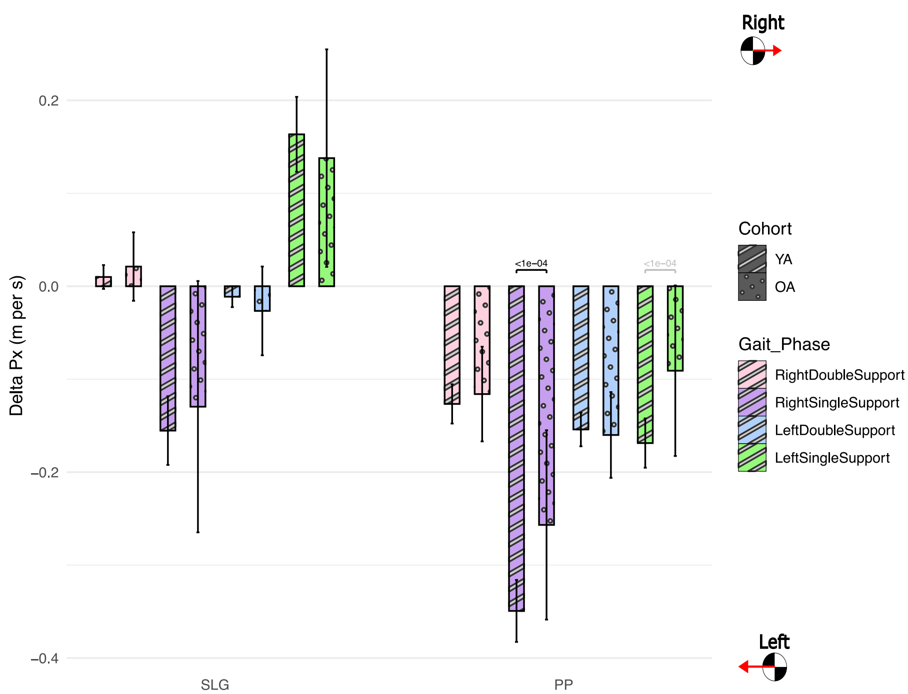

Figure 4.12: Young vs. older adults' marginal mean Δp_x for each task & gait phase. Only significant differences between young and older adults are shown here for clarity. Positive values indicate rightward Δp_x, while negative indicates leftward, in the direction of the turn. Horizontal bars indicate significant differences between between age groups. The black bars represent significant comparisons involving the phase of interest, RSS. Leftward Δp_x is larger in young adults during left and right single support phases.

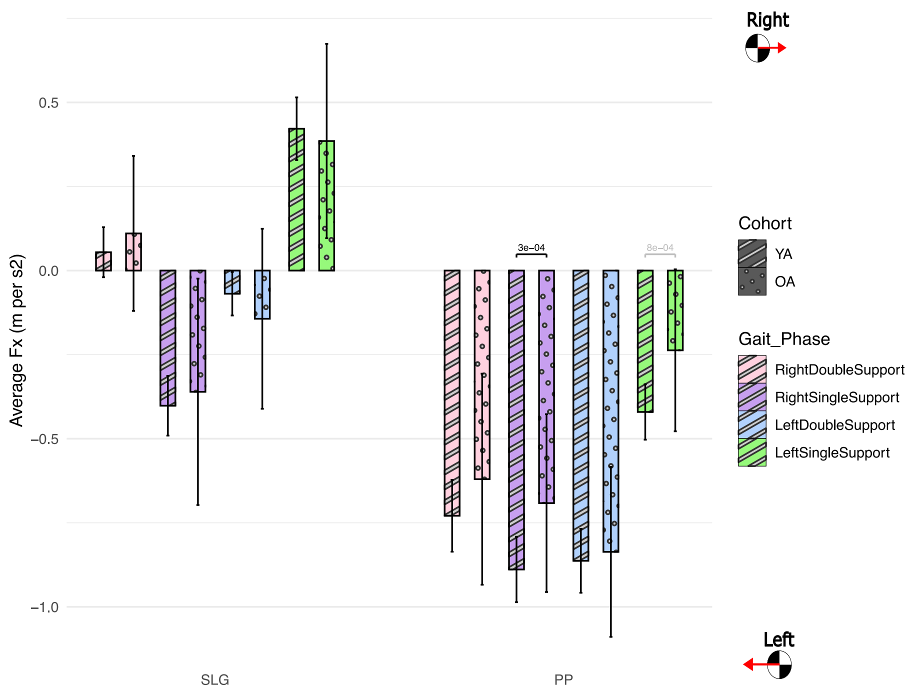

Figure 4.13: Young vs. older adults' marginal mean $F_{x,avg}$ for each task & gait phase. Only significant differences between young and older adults are shown here for clarity. Positive values indicate rightward $F_{x,avg}$, while negative indicates leftward, in the direction of the turn. Horizontal bars indicate significant differences between age groups. The black bars represent significant comparisons involving the phase of interest, RSS. Leftward $F_{x,avg}$ is larger in young adults during left and right single support phases, but no age-related difference is found during LDS.

During SLG, the Δp_x was not different in any phase of gait between the two age groups (Table 4.4, Figure 4.7; p≥0.2603). In PP turns, young adults exhibited significantly greater negative (leftward) Δp_x and $F_{x,avg}$ during LSS (p≤0.0008) and RSS (p≤0.0003) compared to older adults. Also during turns, the difference in Δp_x and $F_{x,avg}$ between age groups was not different from zero during the left and right double support phases (p≥0.1036).

	Task	Estimated marginal mean difference between age groups (p-value) LDS	LSS	RDS	RSS
Δp_x (m/s)	Straight-line gait (SLG)	0.015 (0.9061)	0.026 (0.2603)	-0.011 (1)	-0.026 (0.2603)
	Pre-planned turns (PP)	0.006 (1)	-0.078 (<**0.0001**)	-0.011 (1)	-0.093 (<**0.0001**)
$F_{x,avg}$ (m/s^2)	Straight-line gait (SLG)	0.074 (0.5866)	0.037 (1)	-0.056 (1)	-0.041 (1)
	Pre-planned turns (PP)	-0.027 (1)	-0.183 (**0.0008**)	-0.109 (0.1036)	-0.197 (**0.0003**)
ΔH_z (unitless)	Straight-line gait (SLG)	-0.6232 (<**0.0001**)	0.5142 (<**0.0001**)	0.4411 (<**0.0001**)	-0.333 (**0.0005**)
	Pre-planned turns (PP)	-0.3427 (**0.0001**)	0.2914 (**0.0011**)	0.5342 (<**0.0001**)	-0.3884 (<**0.0001**)
$M_{z,avg}$ (1/s)	Straight-line gait (SLG)	-3.1756 (<**0.0001**)	1.6174 (**0.0001**)	2.3384 (<**0.0001**)	-1.1551 (**0.0107**)
	Pre-planned turns (PP)	-1.1199 (**0.0073**)	0.9741 (**0.0229**)	1.48 (**0.0001**)	-1.2573 (**0.0017**)

Table 4.4: The difference in young vs. older adults' transverse-plane linear and angular momenta generation per task & gait phase. Positive values indicate that the older adult value is more positive (more rightward/less leftward p_x, more leftward/less rightward H_z) than for young adults.

Angular Momentum

During SLG and PP turns, ΔH_z is larger magnitude (leftward or rightward) in older vs. young adults during all four phases of gait (p$\leq$0.0011) compared to young adults (Figure 4.14).

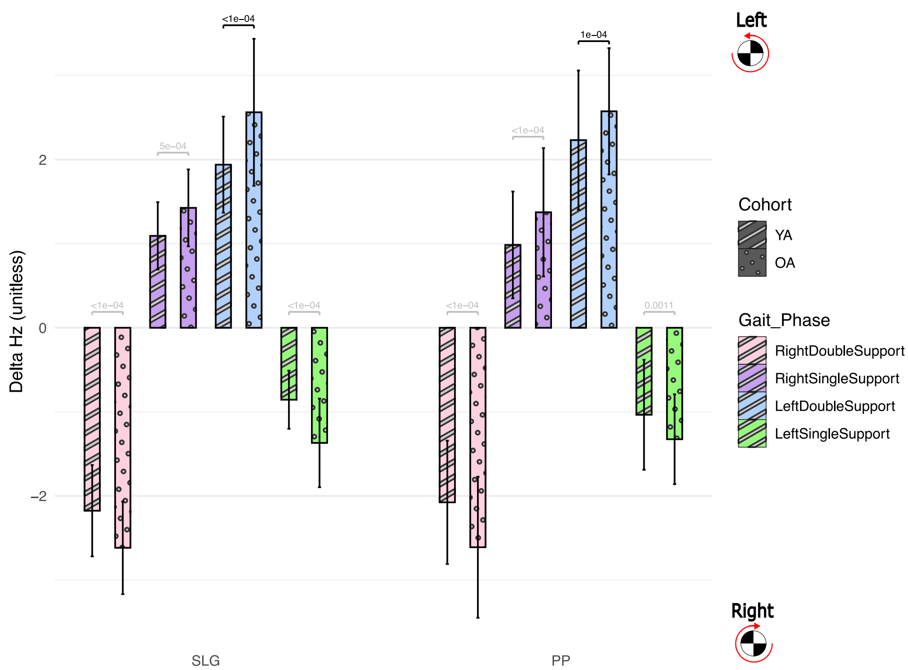

Figure 4.14: Young vs. older adults' marginal mean ΔH_z for each task & gait phase. Only significant differences between young and older adults are shown here for clarity. Positive values indicate leftward transverse-plane rotation of the body-facing direction, in the direction of the turn, while negative values indicate the opposite rotation. Horizontal bars indicate significant differences between age groups. The black bars represent significant comparisons involving the phase of interest, LDS. Older adults exhibit larger magnitude ΔH_z than young adults in each phase of gait, in both SLG and PP turns.

When accounting for gait phase duration with $M_{z,avg}$, older adult $M_{z,avg}$ magnitude is greater than young adults during each phase of gait in both tasks (p$\leq$0.0229).

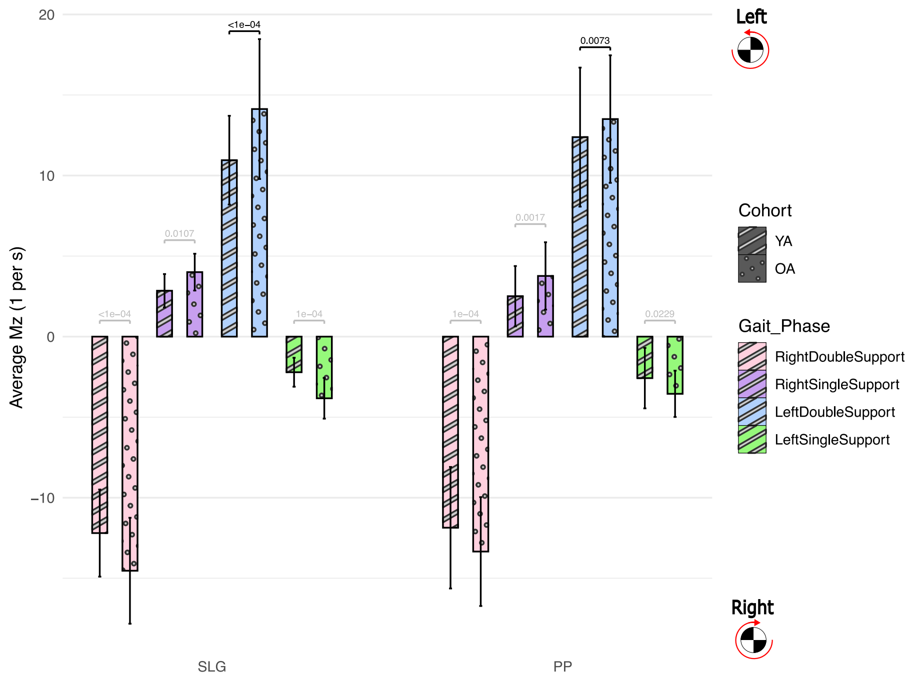

Figure 4.15: Young vs. older adults' marginal mean $M_{z,avg}$ for each task & gait phase. Only significant differences between young and older adults are shown here for clarity. Positive values indicate leftward transverse-plane rotation of the body-facing direction, in the direction of the turn, while negative values indicate the opposite rotation. Horizontal bars indicate significant differences between age groups. The black bars represent significant comparisons involving the phase of interest, LDS. Older adults exhibit larger magnitude $M_{z,avg}$ than young adults in each phase of gait, in both SLG and PP turns.

4.3.4 Turn Strategy

Both age groups showed an overall preference for step (60%) over spin turns (40%). Older adults tended to use spin turns more frequently (43.4%) than young adults (39.8%) (Figure 4.16). Older adults showed smaller LD_{min} in PP spin turns than step turns (p<0.0001), specifically during LSS and LDS phases, but for young adults this trend was not significant during PP turns (p=0.1178). Young adults' LD_{min} was significantly smaller only in LC spin vs. step turns (p=0.0004).

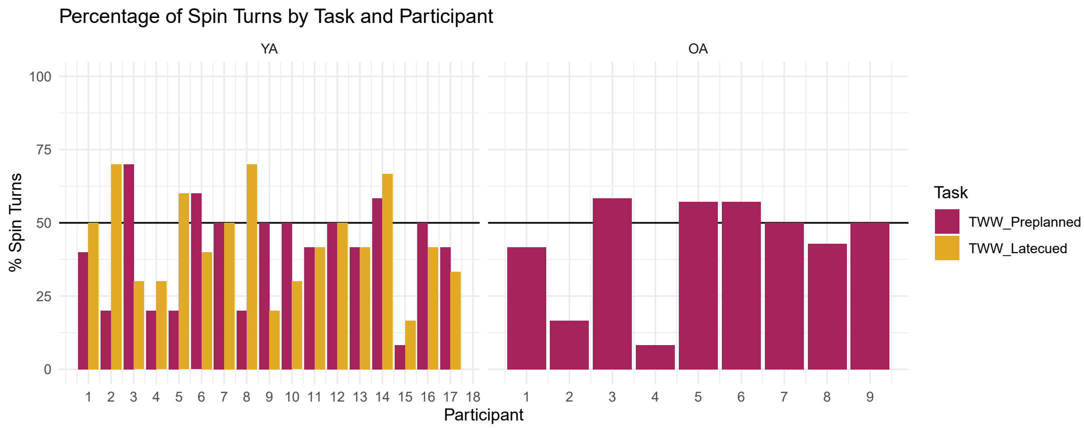

Figure 4.16: Bar graph of young and older adults' turn strategy prevalence. Higher bars indicate that proportionally more spin turns were performed. The black horizontal line marks 50%. Below that line more step turns were performed, above it were more spin turns.

In young adults, no significant turn strategy related differences were observed in PP turns. During young adults' LC turns, LSS showed significantly larger magnitudes of Δp_x and $F_{x,avg}$ in spin turns, and larger magnitude RSS in step turns (similar $F_{x,avg}$ trend not significant). In older adults' PP turns, they also showed larger magnitude Δp_x and $F_{x,avg}$ in LSS during spin vs. step turns, as well as larger magnitude $F_{x,avg}$ in RDS.

4.4 Discussion

The purpose of this analysis was to understand how transverse-plane linear and angular momentum about the TBCM are generated during 90° left turns and SLG in young and older adults, and secondarily to compare the momenta generation across age groups. Our first hypothesis that leftward Δp_x (in the new direction of travel) is largest during RSS phase was partially supported in both young and older adults, as the largest Δp_x was observed in RSS, in agreement with our hypothesis, but for $F_{x,avg}$, LDS often matched (young adult PP turns) or exceeded (older adults PP turns) RSS phase. Our second hypothesis that transverse-plane angular momentum was generated in LDS phase was supported in both age groups. The third hypothesis that young and older adults generate more linear and angular momentum in their respective gait phases of interest during LC (young adults only) vs. PP turns vs. SLG was only supported for Δp_x and $F_{x,avg}$. For young adults, ΔH_z and $M_{z,avg}$ were largest during PP turns. For older adults, there was no difference in ΔH_z or $M_{z,avg}$ between PP turns and SLG. Finally, our hypothesis that young adults would generate larger magnitudes of momenta in each phase of gait than older adults was supported in the linear momentum domain, but unsupported in the angular momentum domain. Young adults exhibited larger Δp_x and $F_{x,avg}$ than older adults during LSS and RSS phase of PP turns, but show no age-related difference in SLG. For angular momentum generation, older adults showed larger magnitude ΔH_z than young adults during each phase of gait in both SLG and PP turns.

Overall, these results suggest that generating the momenta needed to walk straight or to turn occurs within specific phases of gait, and that turns and SLG, as well as young and older adults, all primarily utilize the same phases of gait to accomplish the two tasks' similar yet different mechanical objectives. This converges with other independent lines of evidence that SLG and turns are accomplished by modifying a common motor strategies (161; 111), and are not controlled entirely separately despite the differences in mechanical objectives. The leftward linear momentum needed for a 90° left turn is primarily generated during RSS phase in both young and older healthy adults, while the momenta generation to rotate the body's facing direction primarily occurs during LDS. Finally, older adults appear to generate larger magnitudes of H_z during both SLG and PP turns than young adults. A summary of these main findings is provided in Table 4.5.

Cohort	Factor 1	Factor 2	Factor 3	Metric	Finding
17 YA	Task	Gait Phase		ΔPx	RSS < all other phases RSS LC < PP
				$F_{x,avg}$	RSS < all other phases, except PP RSS = RDS RSS LC < PP
				ΔHz	LDS > all other phases LDS PP > SLG LDS PP > LC LDS SLG > LC RDS SLG = PP RDS PP < LC RDS SLG < LC
				$M_{z,avg}$	LDS > all other phases LDS PP > SLG LDS PP > LC LDS SLG > LC RDS = RDS PP RDS PP < LC RDS SLG < LC
9 OA	Task	Gait Phase		ΔPx	RSS < all other phases
				$F_{x,avg}$	PP LDS < PP RSS, RSS second largest magnitude
				ΔHz	LDS > all other phases LDS PP = SLG RDS PP = SLG
				$M_{z,avg}$	LDS > all other phases LDS PP = SLG RDS SLG < PP
YA vs. OA	Task	Gait Phase		ΔPx	RSS YA < OA
				ΔHz	Magnitude of OA > YA all phases
Both age groups	Task	Gait Phase	Turn Strategy	ΔPx	Step RSS < Spin RSS Spin LSS < Step LSS
				ΔHz	Step = Spin

Table 4.5: Main findings for Aim 2 for each Task and Gait Phase for 17 YA (top section), 9 OA (second section), YA vs. OA (third section), and turn strategy findings across both age groups (bottom section).

4.4.1 Linear Momentum

During SLG, I observed that the Δp_x is small over the course of each single stance phase. During LSS, rightward p_x is generated to arrest the body's leftward momentum, and begin to translate the TBCM rightward, and vice versa during RSS. By contrast, during PP turns, because the goal is to generate leftward p_x, each phase of gait generates leftward p_x, with RSS generating the most in all turn types for both age groups. This likely occurs during RSS vs. any other phase because single stance affords the opportunity for the longest duration for TBCM translation, and doesn't require the TBCM to cross over the left foot as in LSS. During LSS in a left turn, the TBCM can move laterally to the BOS, making it more difficult to maintain balance. When accounting for the gait phase durations, because the double support phases are much shorter than single support, $F_{x,avg}$ during double vs. single support phases are more similar magnitude than Δp_x double vs. single support. This phenomenon occurs more strongly in LDS than RDS, with a larger relative increase in LDS $F_{x,avg}$, which in older adults even surpasses the RSS value. Perhaps this is because LDS directly follows RSS, and so additional p_x may still be being generated (negative slope of p_x in Figure 4.17). Alternatively, this larger $F_{x,avg}$ in LDS finding may be due to our methodology of defining the turn phase by pelvis heading, which resulted in turns being defined more frequently as beginning with the left foot; I have preliminarily observed larger Δp_x earlier in the turn (e.g. Figure 4.17), thus potentially leading to larger $F_{x,avg}$ when more LDS occur earlier in the turn than RDS.

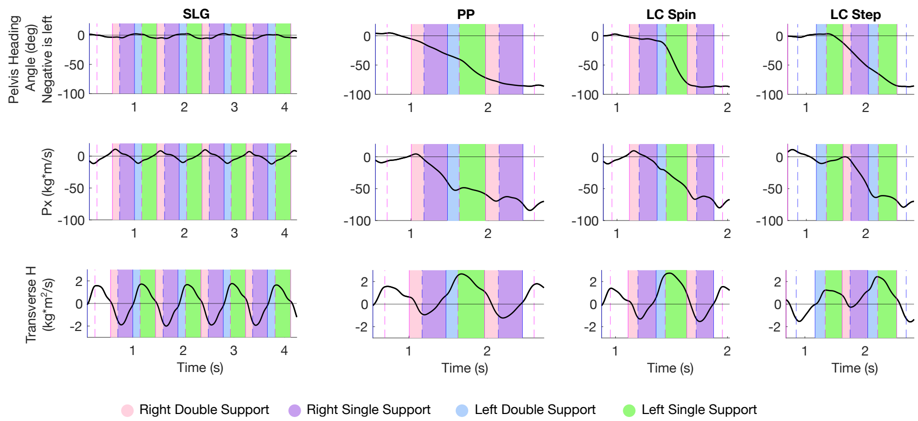

Figure 4.17: Example timeseries of trials from one young adult participant. From top to bottom, transverse-plane heading angle, H_z, and p_x. From left to right are each task, SLG, PP turns, and LC step and spin turns. The shaded regions indicate each phase of gait within the phase of interest in each task. Note that leftward transverse-plane pelvis heading angle (top), and leftward p_x (middle) are both in the direction of the turn. For H_z (bottom), leftward towards the turn is positive.

In young adults, Δp_x in RSS is largest in LC turns, and in both cohorts RSS Δp_x is larger magnitude in PP turns than SLG. The larger RSS Δp_x in LC turns is sensible, as the duration to generate p_x is shorter than in PP turns, while the p_x before ($p_x \sim 0$) and after the turn ($p_x \sim |\vec{p}|$) will be similar in both tasks, despite the slower gait speed while the LC turns are being performed. The $F_{x,avg}$ follows the same trend, being larger in LC than PP turns, and in PP turns vs. SLG.

4.4.2 Angular Momentum

During all tasks, the largest magnitude ΔH_z occurs during LDS and RDS. During double support, rotation away from the front leg (e.g. rightward rotation - positive H_z - during LDS) is arrested, and the body begins to rotate towards the front leg in preparation for the rear leg's swing phase. ΔH_z magnitude is lower during single support phases as the body is rotating more quickly (H_z is higher) during swing phase. With both feet on the ground during double support phases, the body is able to arrest and then generate rotation while still maintaining balance, utilizing the larger BOS and redundant control afforded by the two $\overrightarrow{GRF}$ vectors (139).

During SLG, the left and right phases approximately cancel each other out to walk straight. Interestingly, during turns the left and right phases' ΔH_z also appear to largely cancel each other out, much more than I expected when sustainedly changing the body-facing direction. LDS in young adults is the only phase of gait exhibiting larger ΔH_z between PP turns and SLG, but is not different in older adults. Therefore, in contrast to Δp_x during turns where all gait phases consistently generate net leftward linear momentum, H_z maintains periodicity, continuing to exhibit oscillations even during turns when changing the body-facing direction (Figure 4.17).

LC turns in the young adult cohort exhibit reduced ΔH_z magnitudes during LDS and RDS vs. PP turns, for LDS at the grouped level and during spin turns only. RSS does not change between turn tasks, but LSS ΔH_z is larger magnitude in LC turns. While I theorize that the larger ΔH_z in LSS may be influenced by LC spin turns, in which essentially the entire turning movement occurs during a single LSS phase, including a relatively extreme rotation, there is no statistically significant difference between step and spin turns' LSS ΔH_z in young or older adults (p=1). The smaller negative LC turns' ΔH_z in RDS makes sense relative to PP turns, as perhaps the body limits rightward rotation in an effort to minimize the ΔH_z needed to accomplish the turn, while also satisfying the increased Δp_x objective.

4.4.3 Phase of Interest Bias

The start of the turn phase was defined by the heel strike that occurred just before the pelvis orientation exceeded three times the standard deviation of the headings observed during SLG (section 2.6.4). This Aim's finding that leftward rotation is generated during LDS leads to a bias in the turn phase definition, where for young adults during PP turns more turns were deemed to begin with the left foot more frequently (63.7% across all participants) (Figure 4.18). Note that during young adults' LC turns, this figure drops to 48.6%, as the pelvis does not begin turning until reaching the intersection, and due to the suddenness of the movement, either the left or right foot would begin the turn, in a more balanced fashion.

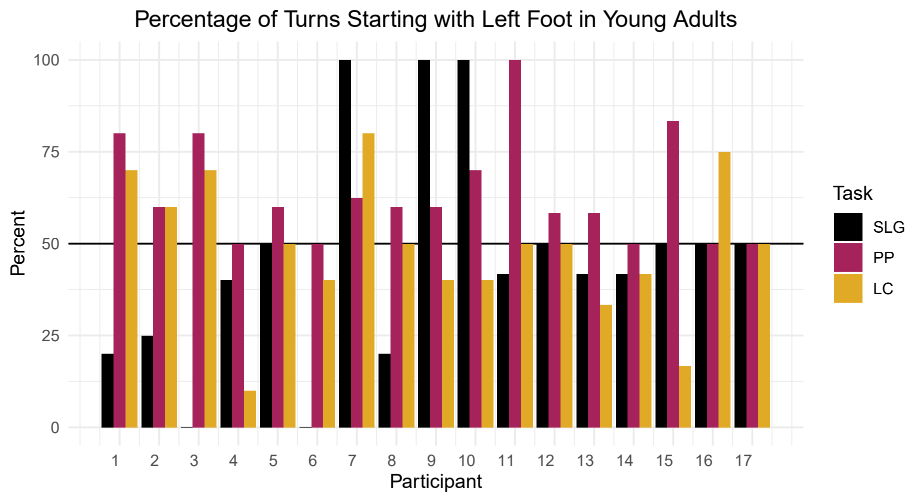

Figure 4.18: Percentage of trials where the phase of interest began with the left foot for each participant and task, in young adults. Note that while participants were instructed which foot to begin walking with, the foot that began the phase of interest was self-determined. In pre-planned turns, there is a >50% prevalence of the left foot beginning the turn, as the turn phase was defined by pelvis rotation, which occurs more during left double support. In late-cued turns, this prevalence diminishes due to the lack of planning and uncertainty regarding the need to turn.

Chapter 5

Aim 3: Frontal and Transverse Plane Effects of Turning at Straight-Line Gait Speeds in Healthy Female Young Adults

5.1 Introduction

Chapters 3 and 4 describe the control of whole-body balance and momenta generation in SLG, PP turns, and LC turns, primarily using momentum-based metrics. Muddying the comparison between tasks is the decrease in gait speed from SLG to PP turns, and PP turns to LC turns. Typically, a confounding variable would be controlled for in the statistical analysis. However, whole-body angular momentum about the TBCM ($\vec{H}$) as well as TBCM linear momentum vector ($\vec{p}$) both contain TBCM velocity ($\overrightarrow{v_{TBCM}}$) in their formula, limiting the ability to interpret the meaning of the resultant values after controlling for gait speed.

Gait speed is an important biomechanical variable, predicting mortality (162) and may predict fall incidence (163) in older adults and clinical populations. Gait speed is known to reduce as a result of aging (119; 164) and in clinical populations compared to young healthy controls. Gait speed during turning while walking also naturally decreases relative to SLG due to the increased metabolic cost of changing direction (71). A sharper turn at a given speed - or a faster speed for a given turn - correspond to larger linear acceleration, and therefore larger forces required to turn. Therefore, decreasing gait speed during turns relative to SLG may be a balance protective strategy, as changing direction further challenges balance beyond the demands of SLG, and falls during turns can be especially injurious (8).

Previous studies have shown mixed changes in $\vec{H}$ in response to changing gait speeds (165). They have found that with increasing gait speed, $\vec{H}$ may increase (40; 43), decrease (42), or show no change (44; 45; 46). Another component of balance is foot placement relative to the TBCM, which I quantify using the LD metric (see section 2.7.4). I am not aware of any studies that have directly investigated how LD changes with gait speed. However, (99) showed that with increasing gait speed the TBCM tends to be positioned nearer to the inside edge of the BOS.

In turns, decreased gait speed may alter the person's movement priorities. For example, there is a speed-turning radius trade-off (71), and minimum frictional requirements to consider (153). Slower speeds may also increase "en-bloc" rotation (when the body's segments tend to rotate together as a unit) (87), which is typically considered a less demanding movement strategy from a control perspective, though is associated with less agile balance control (84; 166).

The purpose of this study is twofold. First, to remove gait speed as a confounding variable when comparing $\vec{H}$ and LD between SLG and turns by asking participants to perform both tasks at the same speed. Second, to examine the effect of walking and turning at this faster gait speed vs. at preferred speed. Using similar analyses as in chapters 3 and 4, I hypothesize the following. First, when comparing between the faster speed turns and SLG, the between-task findings in 3 and between-task and gait-phase findings in 4 will be replicated. Second, when comparing across speeds within PP and LC turns, the frontal- and transverse-plane measures will be more extreme vs. preferred speed (larger $H_{f,range}$, lower LD_{min}, larger Δp_x and ΔH_z during RSS and LDS, respectively).

5.2 Methods

5.2.1 Participant Recruitment

Seven females participated in this study (20.57 ± 1.40 yrs; 57.26 ± 9.66 kg; 1.65 ± 0.08 m) after providing informed consent to a protocol approved by Stevens Institute of Technology's Institutional Review Board (IRB). All participants self-reported no injury, pathology, difficulty walking, or other balance impairment. See Table A.3 for characteristics of each participant.

5.2.2 Experiment Protocol

Participants first completed the same three tasks as in sections 3.2.2 and 4.2.2. During the SLG task, the mean and standard deviation of their horizontal gait speed was computed. Then, they also completed another block of PP and LC turns after being asked to walk at the same mean horizontal gait speed ± two standard deviations of SLG horizontal gait speed. If they walked too fast or slow, they were informed that they needed to modify their speed accordingly and the trial was repeated.

5.2.3 Data Analysis

Frontal-Plane Angular Momentum

H_f was computed following the method described in section 2.7.2. When viewed from behind, positive H_f is clockwise frontal-plane rotation about the TBCM. Max, min, and range of H_f were computed for each trial over the phase of interest.

Lateral Distance

Lateral distance was defined as the horizontal distance between the TBCM and the BOS lateral edge, where lateral was defined by the pelvis mediolateral axis. More detail about the LD and BOS computations can be found in sections 2.7.4 and 2.7.3, respectively. To compare across participants, the lateral distance was normalized to leg length (hip joint center height).

5.2.4 Phases of Interest

The phase of interest for all turning tasks was computed by finding the heel strike before and after the pelvis began and ended rotating, respectively. SLG phase of interest was the middle 6 m of the 10 m walkway. This follows the method defined in 3.2.3.

5.2.5 Turn Strategy

Turn strategies were quantified following the method from Golyski et al. (104) which determines "step" vs. "spin" turn strategy by which foot is nearest to the intersection of the turn. "Spin" turns turn over the inside foot, while "step" turns use the outside foot.

5.2.6 Statistical Analyses

We used R (123) to model the data with a linear mixed model (lme4 in the lmer package) to account for the hierarchical repeated measures within the dataset. The model for analyzing H_f and LD_{min} over the entire phase of interest is *Response* $\sim$ *Task + (1|Participant)*. This means that *Task* is a fixed effect, while *Participant* is a random effect. Pairwise comparisons were conducted between all tasks using `pairs()` and the formula *Response* $\sim$ *Task*. Investigating within each phase of gait requires the model *Response* $\sim$ *Task*Gait Phase + (1|Participant)*, and the emmeans formula *Response* $\sim$ *Task*Gait Phase*. The Holm adjustment for multiple comparisons was used, after excluding interaction effects (comparisons where levels of two or more factors changed simultaneously). A Holm-adjusted p-value < 0.05 was used to determine statistical significance.

5.3 Results

5.3.1 Gait Speed

There was no significant difference in horizontal gait speed between the faster PP turns and SLG ($p=0.0581$). I also observed a slower gait speed in preferred speed PP turns relative to both SLG ($p < 0.0001$) and PP turns at fast speed ($p < 0.0001$). Finally, each LC turn condition was slower than each PP turn condition ($p < 0.0001$) as participants were unable to maintain the same horizontal gait speed in LC turns as in SLG (Figure 5.1, $p < 0.0001$).

Parameter		Marginal means (95% CL)					Post-hoc pairwise comparisons									
		SLG	**PP**	**PP-Fast**	**LC**	**LC-Fast**	**SLG vs. PP**	**SLG vs. PP-Fast**	**SLG vs. LC**	**SLG vs. LC-Fast**	**PP vs. PP-Fast**	**PP vs. LC**	**PP vs. LC-Fast**	**PP-Fast vs. LC**	**PP-Fast vs. LC-Fast**	**LC vs. LC-Fast**
Gait Speed (m per s)	Maximum	1.503 (1.377, 1.629)	1.435 (1.309, 1.561)	1.517 (1.391, 1.643)	1.196 (1.070, 1.322)	1.334 (1.208, 1.460)	**<0.0001**	0.2273	**<0.0001**	**<0.0001**	**<0.0001**	**<0.0001**	**<0.0001**	**<0.0001**	**<0.0001**	**<0.0001**
	Median	1.236 (1.142, 1.330)	1.140 (1.046, 1.233)	1.210 (1.117, 1.304)	0.879 (0.785, 0.973)	1.001 (0.907, 1.094)	**<0.0001**	0.0581	**<0.0001**	**<0.0001**	**<0.0001**	**<0.0001**	**<0.0001**	**<0.0001**	**<0.0001**	**<0.0001**
	Minimum	1.112 (1.043, 1.181)	0.983 (0.914, 1.052)	1.038 (0.969, 1.108)	0.541 (0.471, 0.610)	0.625 (0.555, 0.694)	**<0.0001**	**<0.0001**	**<0.0001**	**<0.0001**	**<0.0001**	**<0.0001**	**<0.0001**	**<0.0001**	**<0.0001**	**<0.0001**
Number of Footfalls	Count	8.071 (7.867, 8.276)	3.786 (3.581, 3.990)	3.756 (3.550, 3.961)	3.227 (3.021, 3.434)	3.241 (3.032, 3.450)	**<0.0001**	**<0.0001**	**<0.0001**	**<0.0001**	1.0000	**<0.0001**	**<0.0001**	**<0.0001**	**<0.0001**	1.0000
Phase Duration (s)	Median	3.971 (3.790, 4.151)	1.581 (1.400, 1.762)	1.554 (1.373, 1.735)	1.310 (1.129, 1.492)	1.225 (1.043, 1.407)	**<0.0001**	**<0.0001**	**<0.0001**	**<0.0001**	0.5172	**<0.0001**	**<0.0001**	**<0.0001**	**<0.0001**	0.1187
Median Step Duration (s)	Median	0.562 (0.530, 0.594)	0.567 (0.535, 0.599)	0.564 (0.532, 0.596)	0.599 (0.567, 0.631)	0.571 (0.539, 0.603)	1.0000	1.0000	**<0.0001**	0.4680	1.0000	**<0.0001**	1.0000	**<0.0001**	1.0000	**<0.0001**
Median Step Length (m)	Median	0.716 (0.677, 0.756)	0.686 (0.646, 0.726)	0.718 (0.679, 0.758)	0.525 (0.485, 0.565)	0.556 (0.517, 0.596)	**<0.0001**	0.7848	**<0.0001**	**<0.0001**	**<0.0001**	**<0.0001**	**<0.0001**	**<0.0001**	**<0.0001**	**<0.0001**
Step Width (m)	Maximum	0.129 (0.091, 0.167)	0.299 (0.261, 0.337)	0.300 (0.261, 0.338)	0.219 (0.180, 0.258)	0.258 (0.218, 0.298)	**<0.0001**	**<0.0001**	**<0.0001**	**<0.0001**	0.9559	**0.0001**	0.1148	**0.0001**	0.1148	0.1148
	Median	0.108 (0.074, 0.142)	0.215 (0.181, 0.249)	0.216 (0.182, 0.250)	0.186 (0.152, 0.221)	0.215 (0.179, 0.250)	**<0.0001**	**<0.0001**	**<0.0001**	**<0.0001**	1.0000	0.3866	1.0000	0.3866	1.0000	0.3866
	Minimum	0.088 (0.048, 0.129)	0.133 (0.093, 0.174)	0.134 (0.093, 0.175)	0.153 (0.111, 0.194)	0.172 (0.129, 0.214)	0.1218	0.1218	**0.0073**	**0.0003**	1.0000	1.0000	0.3172	1.0000	0.3172	1.0000
Median Stride Duration (s)	Median	1.122 (1.055, 1.189)	1.133 (1.067, 1.200)	1.125 (1.058, 1.192)	1.178 (1.111, 1.245)	1.105 (1.038, 1.172)	1.0000	1.0000	**<0.0001**	0.6935	1.0000	**0.0018**	0.1449	**0.0002**	0.5748	**<0.0001**
Median Stride Length (m)	Median	1.432 (1.340, 1.523)	1.336 (1.245, 1.427)	1.410 (1.318, 1.501)	1.034 (0.943, 1.126)	1.079 (0.986, 1.171)	**0.0016**	0.4172	**<0.0001**	**<0.0001**	**0.0206**	**<0.0001**	**<0.0001**	**<0.0001**	**<0.0001**	0.2603

Table 5.1: Spatiotemporal metrics for 7 young adults during SLG, PP turns at preferred and faster speed, and LC turns at preferred and faster speed

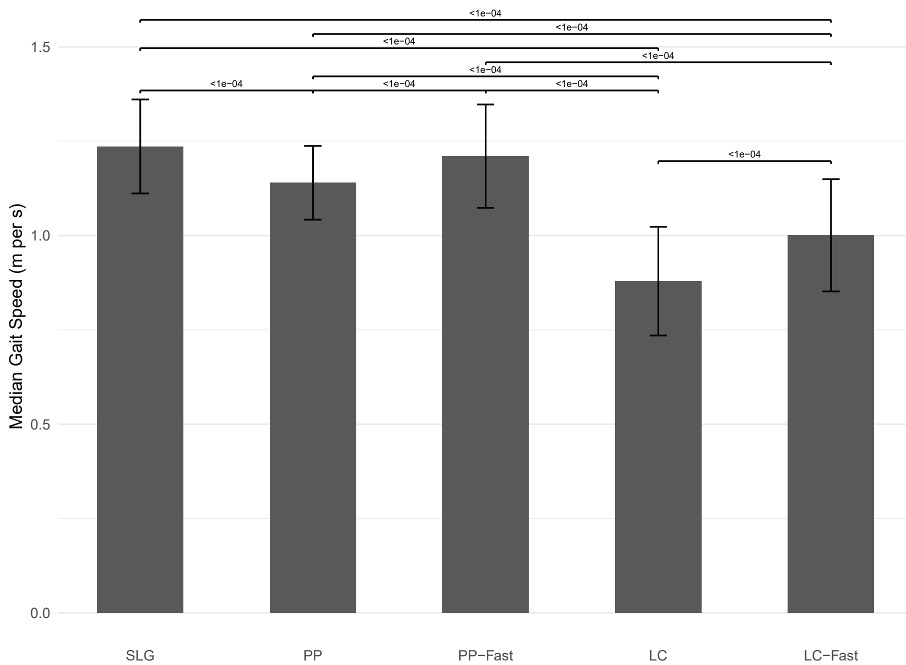

Figure 5.1: The marginal means of the median horizontal gait speed for each task and turn speed. Note that the preferred speed PP turns are significantly slower than both SLG and SLG-speed PP turns, while there is no significant difference in speed between SLG and SLG-speed PP turns. Also, preferred speed LC turns are significantly slower than the faster speed LC turn condition.

5.3.2 SLG vs. Fast speed PP and Fast speed LC turns

In the frontal plane, similar to preferred speed findings in chapter 3, compared to SLG, the faster speed conditions for PP and LC turns resulted in larger $H_{f,range}$ (Figure 5.2, Table 5.2 p $<$ 0.0001), and lower LD_{min} (Figure 5.3; p $<$ 0.0001). In the transverse plane, our primary findings agreed with those at preferred speed. Namely, that compared to SLG, during RSS the faster PP and LC turns exhibited larger magnitude leftward Δp_x (Figure 5.4; p $<$ 0.0001) and $F_{x,avg}$ (Figure 5.5; p $<$ 0.0001). LDS leftward ΔH_z in the faster PP turns was the only task significantly larger than SLG (Figure 5.7; p$<$0.0001).

Parameter		Marginal means (95% CL)			Post-hoc pairwise comparisons	
		SLG	PP-Fast	LC-Fast	SLG vs. PP-Fast	SLG vs. LC-Fast
Frontal H (unitless)	Maximum	0.003 (0.002, 0.003)	0.003 (0.003, 0.004)	0.004 (0.003, 0.005)	**<0.0001**	**<0.0001**
	Minimum	-0.003 (-0.003, -0.002)	-0.004 (-0.005, -0.003)	-0.005 (-0.005, -0.004)	**<0.0001**	**<0.0001**
	Range	0.006 (0.005, 0.007)	0.007 (0.006, 0.008)	0.009 (0.008, 0.010)	**<0.0001**	**<0.0001**
LD (m)	Maximum	0.178 (0.160, 0.196)	0.258 (0.240, 0.276)	0.298 (0.280, 0.316)	**<0.0001**	**<0.0001**
	Minimum	0.079 (0.067, 0.092)	-0.018 (-0.031, -0.006)	0.023 (0.010, 0.036)	**<0.0001**	**<0.0001**
MOS (m)	Maximum	0.085 (0.074, 0.096)	0.138 (0.126, 0.149)	0.158 (0.146, 0.169)	**<0.0001**	**<0.0001**
	Minimum	-0.104 (-0.158, -0.049)	-0.148 (-0.203, -0.093)	-0.202 (-0.256, -0.147)	**<0.0001**	**<0.0001**

Parameter	Task	Marginal means (95% CL)				Post-hoc pairwise comparisons					
		RDS	RSS	LDS	LSS	RDS vs. RSS	RDS vs. LDS	RDS vs. LSS	RSS vs. LDS	RSS vs. LSS	LDS vs. LSS
Average Fx (N)	SLG	2.941 (-2.509, 8.390)	-23.848 (-29.298, -18.399)	-4.617 (-10.067, 0.832)	24.025 (18.575, 29.474)	**<0.0001**	0.0910	**<0.0001**	**<0.0001**	**<0.0001**	**<0.0001**
	PP-Fast	-47.988 (-53.516, -42.459)	-58.729 (-64.258, -53.201)	-55.419 (-60.833, -50.005)	-28.780 (-34.194, -23.366)	**0.0047**	0.0920	**<0.0001**	0.8387	**<0.0001**	**<0.0001**
	LC-Fast	-53.553 (-59.393, -47.714)	-92.474 (-98.313, -86.634)	-57.002 (-62.490, -51.515)	-34.208 (-39.695, -28.721)	**<0.0001**	0.8387	**<0.0001**	**<0.0001**	**<0.0001**	**<0.0001**
	SLG vs. PP-Fast	**<0.0001**	**<0.0001**	**<0.0001**	**<0.0001**	-	-	-	-	-	-
	SLG vs. LC-Fast	**<0.0001**	**<0.0001**	**<0.0001**	**<0.0001**	-	-	-	-	-	-
Average Mz (N-m)	SLG	-12.141 (-12.491, -11.791)	2.576 (2.227, 2.926)	10.646 (10.297, 10.996)	-1.796 (-2.146, -1.446)	**<0.0001**	**<0.0001**	**<0.0001**	**<0.0001**	**<0.0001**	**<0.0001**
	PP-Fast	-11.870 (-12.228, -11.511)	1.851 (1.493, 2.210)	12.819 (12.474, 13.165)	-2.098 (-2.444, -1.752)	**<0.0001**	**<0.0001**	**<0.0001**	**<0.0001**	**<0.0001**	**<0.0001**
	LC-Fast	-7.940 (-8.332, -7.548)	1.475 (1.083, 1.867)	10.694 (10.340, 11.048)	-2.652 (-3.006, -2.298)	**<0.0001**	**<0.0001**	**<0.0001**	**<0.0001**	**<0.0001**	**<0.0001**
	SLG vs. PP-Fast	0.6838	**0.0273**	**<0.0001**	0.6838	-	-	-	-	-	-
	SLG vs. LC-Fast	**<0.0001**	**0.0003**	0.8504	**0.0053**	-	-	-	-	-	-
Delta Hz (kg-m2 per s)	SLG	-2.162 (-2.243, -2.081)	0.986 (0.905, 1.066)	1.873 (1.792, 1.953)	-0.695 (-0.776, -0.614)	**<0.0001**	**<0.0001**	**<0.0001**	**<0.0001**	**<0.0001**	**<0.0001**
	PP-Fast	-1.997 (-2.079, -1.914)	0.715 (0.632, 0.797)	2.154 (2.074, 2.234)	-0.825 (-0.904, -0.745)	**<0.0001**	**<0.0001**	**<0.0001**	**<0.0001**	**<0.0001**	**<0.0001**
	LC-Fast	-1.353 (-1.443, -1.262)	0.576 (0.486, 0.667)	1.917 (1.835, 1.999)	-0.987 (-1.069, -0.905)	**<0.0001**	**<0.0001**	**<0.0001**	**<0.0001**	**<0.0001**	**<0.0001**
	SLG vs. PP-Fast	**0.0253**	**<0.0001**	**<0.0001**	0.0748	-	-	-	-	-	-
	SLG vs. LC-Fast	**<0.0001**	**<0.0001**	0.4491	**<0.0001**	-	-	-	-	-	-
Delta Px (kg-m per s)	SLG	0.501 (-1.100, 2.101)	-9.163 (-10.764, -7.563)	-0.805 (-2.406, 0.795)	9.350 (7.749, 10.950)	**<0.0001**	0.6242	**<0.0001**	**<0.0001**	**<0.0001**	**<0.0001**
	PP-Fast	-8.016 (-9.649, -6.383)	-22.771 (-24.404, -21.138)	-9.263 (-10.848, -7.677)	-11.324 (-12.910, -9.738)	**<0.0001**	0.6242	**0.0113**	**<0.0001**	**<0.0001**	0.2223
	LC-Fast	-8.348 (-10.107, -6.590)	-35.608 (-37.366, -33.849)	-11.062 (-12.678, -9.446)	-14.645 (-16.261, -13.028)	**<0.0001**	0.0866	**<0.0001**	**<0.0001**	**<0.0001**	**0.0060**
	SLG vs. PP-Fast	**<0.0001**	**<0.0001**	**<0.0001**	**<0.0001**	-	-	-	-	-	-
	SLG vs. LC-Fast	**<0.0001**	**<0.0001**	**<0.0001**	**<0.0001**	-	-	-	-	-	-

Table 5.2: Marginal means and p-values for SLG, fast PP turns, and fast LC turns presented for frontal-plane balance metrics per-task (top) and transverse-plane linear and angular momenta generation metrics per task and gait phase (bottom).

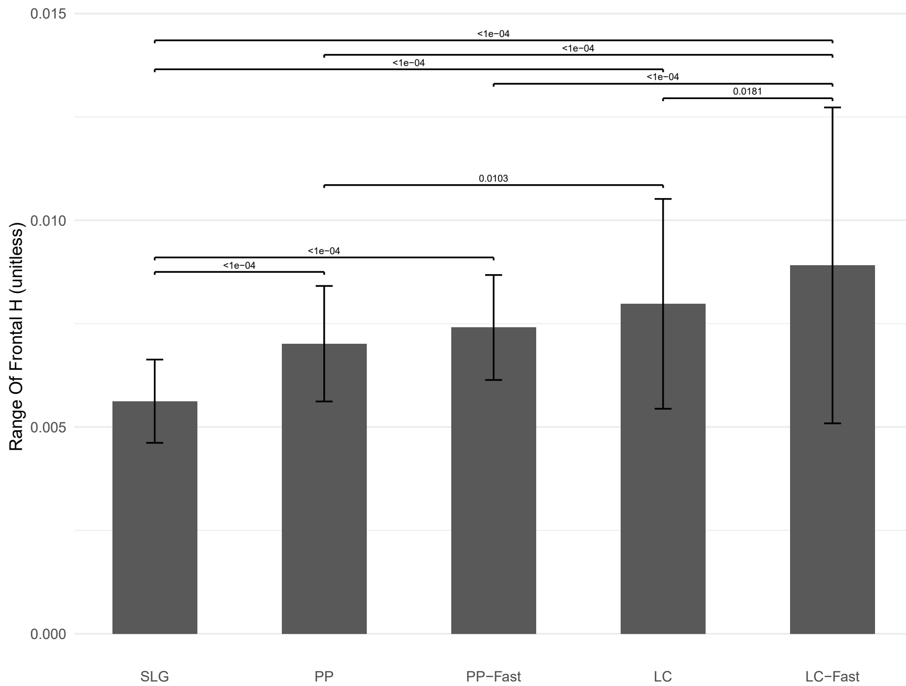

Figure 5.2: The marginal means of the mean $H_{f,range}$ for each task and turn speed.

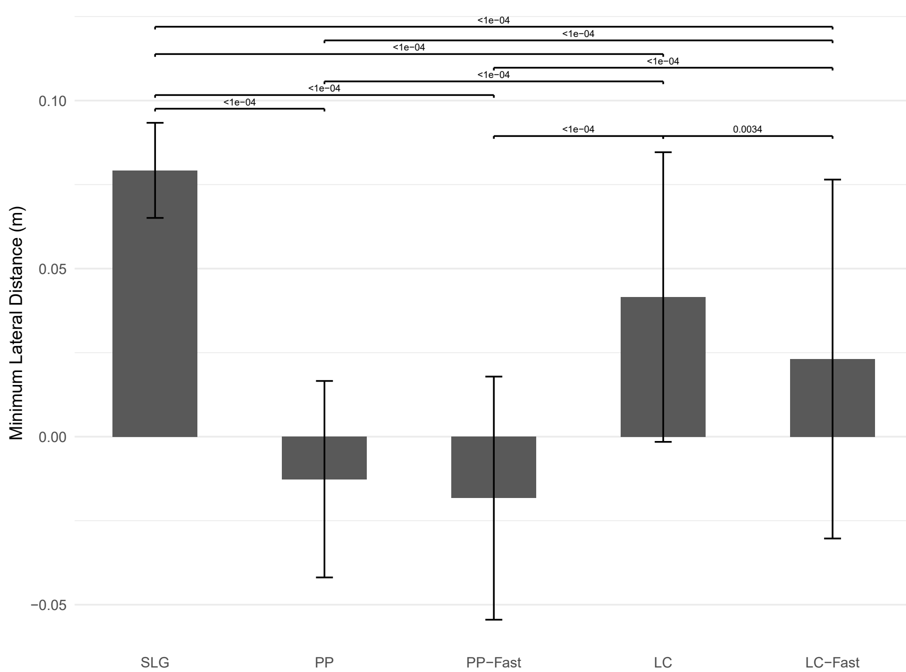

Figure 5.3: The marginal mean LD_{min} for each task and turn speed. Positive values indicate that the TBCM is within the BOS, while negative values indicate that the TBCM is left of the left edge of the BOS, interpreted as an unstable state. Fast speed LC turns showed significantly lower LD_{min} vs. preferred speed LC turns, but still larger than PP turns at either speed. There was no difference in preferred vs. fast speed PP turns.

5.3.3 Fast speed PP vs. Fast speed LC turns

Similar to chapter 3, LC vs. PP turns showed larger LD_{min} (Figure 5.3; p < 0.0001) and a larger $H_{f,range}$ (Figure 5.2, Table 5.3; p < 0.0001). In the transverse-plane, Δp_x and $F_{x,avg}$ during RSS were larger leftward during the fast LC turns (Figures 5.4, 5.5; p < 0.0001). During LDS, leftward ΔH_z and $M_{z,avg}$ are smaller (ΔH_z p=0.0014, $M_{z,avg}$ p<0.0001), and the RDS ΔH_z is smaller rightward (ΔH_z p < 0.0001, $M_{z,avg}$ p<0.0001) during LC vs. PP turns (Figures 5.7, 5.8).

Parameter		Marginal means (95% CL)		Post-hoc pairwise comparisons
		PP-Fast	**LC-Fast**	**PP-Fast vs. LC-Fast**
Frontal H (unitless)	Maximum	0.003 (0.003, 0.004)	0.004 (0.003, 0.005)	**0.0005**
	Minimum	-0.004 (-0.005, -0.003)	-0.005 (-0.006, -0.004)	**0.0042**
	Range	0.007 (0.006, 0.009)	0.009 (0.008, 0.010)	**0.0007**
LD (m)	Maximum	0.259 (0.232, 0.286)	0.299 (0.272, 0.326)	**<0.0001**
	Minimum	-0.018 (-0.036, -0.000)	0.024 (0.006, 0.042)	**<0.0001**
MOS (m)	Maximum	0.138 (0.125, 0.152)	0.158 (0.144, 0.172)	**0.0005**
	Minimum	-0.150 (-0.223, -0.077)	-0.206 (-0.279, -0.133)	**<0.0001**

Parameter	Task	Marginal means (95% CL)				Post-hoc pairwise comparisons					
		RDS	**RSS**	**LDS**	**LSS**	**RDS vs. RSS**	**RDS vs. LDS**	**RDS vs. LSS**	**RSS vs. LDS**	**RSS vs. LSS**	**LDS vs. LSS**
Average Fx (N)	PP-Fast	-48.126 (-55.701, -40.552)	-58.868 (-66.442, -51.294)	-55.355 (-62.816, -47.894)	-28.715 (-36.176, -21.254)	**0.0294**	0.2983	**<0.0001**	1.0000	**<0.0001**	**<0.0001**
	LC-Fast	-53.536 (-61.428, -45.645)	-92.457 (-100.349, -84.565)	-57.016 (-64.549, -49.484)	-34.222 (-41.754, -26.690)	**<0.0001**	1.0000	**<0.0001**	**<0.0001**	**<0.0001**	**<0.0001**
	PP-Fast vs. LC-Fast	0.6726	**<0.0001**	1.0000	0.6593	-	-	-	-	-	-
Average Mz (N-m)	PP-Fast	-11.870 (-12.262, -11.477)	1.851 (1.459, 2.244)	12.819 (12.441, 13.198)	-2.098 (-2.476, -1.719)	**<0.0001**	**<0.0001**	**<0.0001**	**<0.0001**	**<0.0001**	**<0.0001**
	LC-Fast	-7.940 (-8.370, -7.511)	1.475 (1.045, 1.904)	10.694 (10.307, 11.082)	-2.652 (-3.040, -2.265)	**<0.0001**	**<0.0001**	**<0.0001**	**<0.0001**	**<0.0001**	**<0.0001**
	PP-Fast vs. LC-Fast	**<0.0001**	0.2026	**<0.0001**	0.0886	-	-	-	-	-	-
Delta Hz (kg-m2 per s)	PP-Fast	-1.997 (-2.087, -1.906)	0.715 (0.624, 0.805)	2.154 (2.067, 2.241)	-0.825 (-0.912, -0.737)	**<0.0001**	**<0.0001**	**<0.0001**	**<0.0001**	**<0.0001**	**<0.0001**
	LC-Fast	-1.353 (-1.452, -1.254)	0.576 (0.477, 0.675)	1.917 (1.828, 2.006)	-0.987 (-1.076, -0.898)	**<0.0001**	**<0.0001**	**<0.0001**	**<0.0001**	**<0.0001**	**<0.0001**
	PP-Fast vs. LC-Fast	**<0.0001**	**0.0421**	**0.0006**	**0.0211**	-	-	-	-	-	-
Delta Px (kg-m per s)	PP-Fast	-8.043 (-10.146, -5.940)	-22.798 (-24.901, -20.695)	-9.250 (-11.301, -7.199)	-11.312 (-13.363, -9.261)	**<0.0001**	0.6749	0.0574	**<0.0001**	**<0.0001**	0.3805
	LC-Fast	-8.314 (-10.559, -6.070)	-35.574 (-37.819, -33.329)	-11.062 (-13.146, -8.978)	-14.645 (-16.728, -12.561)	**<0.0001**	0.1991	**<0.0001**	**<0.0001**	**<0.0001**	**0.0377**
	PP-Fast vs. LC-Fast	0.8398	**<0.0001**	0.4417	0.0547	-	-	-	-	-	-

Table 5.3: Marginal means and p-values for fast PP and fast LC turns presented for frontal-plane balance metrics per-task (top) and transverse-plane linear and angular momenta generation metrics per task and gait phase (bottom).

5.3.4 Preferred vs. fast speed PP turns

There are no statistically significant differences in the frontal or transverse plane between speeds of PP turns, other than a larger $M_{z,avg}$ during LDS in faster vs. preferred speed turns (Table 5.4; p $<$ 0.0001). Stratifying by turn strategy resulted in only step turns' $M_{z,avg}$ significantly larger in LDS at fast vs. preferred speeds (p $<$ 0.0001), while spin turns were not (p=1).

Parameter		Marginal means (95% CL)		Post-hoc pairwise comparisons
		PP	**PP-Fast**	**PP vs. PP-Fast**
Frontal H (unitless)	Maximum	0.003 (0.003, 0.004)	0.003 (0.003, 0.004)	0.6001
	Minimum	-0.004 (-0.004, -0.003)	-0.004 (-0.004, -0.004)	0.0567
	Range	0.007 (0.007, 0.007)	0.007 (0.007, 0.008)	0.1190
LD (m)	Maximum	0.241 (0.222, 0.260)	0.257 (0.238, 0.276)	**0.0001**
	Minimum	-0.013 (-0.032, 0.007)	-0.019 (-0.038, 0.001)	0.1508
MOS (m)	Maximum	0.135 (0.120, 0.151)	0.138 (0.122, 0.153)	0.4831
	Minimum	-0.130 (-0.165, -0.094)	-0.145 (-0.180, -0.110)	**0.0139**

Parameter	Task	Marginal means (95% CL)				Post-hoc pairwise comparisons					
		RDS	**RSS**	**LDS**	**LSS**	**RDS vs. RSS**	**RDS vs. LDS**	**RDS vs. LSS**	**RSS vs. LDS**	**RSS vs. LSS**	**LDS vs. LSS**
Average Fx (N)	PP	-41.924 (-49.158, -34.690)	-53.183 (-60.417, -45.949)	-49.601 (-56.835, -42.367)	-26.583 (-33.817, -19.349)	**0.0001**	**0.0211**	<**0.0001**	0.4788	<**0.0001**	<**0.0001**
	PP-Fast	-47.831 (-55.098, -40.564)	-58.573 (-65.840, -51.305)	-55.492 (-62.712, -48.273)	-28.853 (-36.072, -21.633)	**0.0004**	**0.0211**	<**0.0001**	0.4788	<**0.0001**	<**0.0001**
	PP vs. PP-Fast	0.1209	0.1474	0.1209	0.4788	-	-	-	-	-	-
Average Mz (N-m)	PP	-11.534 (-11.845, -11.223)	2.029 (1.719, 2.340)	11.470 (11.159, 11.781)	-1.856 (-2.167, -1.546)	<**0.0001**	<**0.0001**	<**0.0001**	<**0.0001**	<**0.0001**	<**0.0001**
	PP-Fast	-11.867 (-12.185, -11.549)	1.854 (1.536, 2.172)	12.818 (12.511, 13.126)	-2.099 (-2.407, -1.791)	<**0.0001**	<**0.0001**	<**0.0001**	<**0.0001**	<**0.0001**	<**0.0001**
	PP vs. PP-Fast	0.3683	0.5041	<**0.0001**	0.5041	-	-	-	-	-	-
Delta Hz (kg-m2 per s)	PP	-2.014 (-2.085, -1.944)	0.784 (0.713, 0.855)	2.044 (1.973, 2.115)	-0.732 (-0.803, -0.662)	<**0.0001**	<**0.0001**	<**0.0001**	<**0.0001**	<**0.0001**	<**0.0001**
	PP-Fast	-1.997 (-2.069, -1.924)	0.715 (0.642, 0.787)	2.154 (2.084, 2.224)	-0.825 (-0.894, -0.755)	<**0.0001**	<**0.0001**	<**0.0001**	<**0.0001**	<**0.0001**	<**0.0001**
	PP vs. PP-Fast	0.7325	0.3554	0.1206	0.2064	-	-	-	-	-	-
Delta Px (kg-m per s)	PP	-7.330 (-9.307, -5.354)	-20.615 (-22.591, -18.639)	-8.905 (-10.881, -6.928)	-10.615 (-12.591, -8.638)	<**0.0001**	0.3355	**0.0013**	<**0.0001**	<**0.0001**	0.2805
	PP-Fast	-7.956 (-9.948, -5.964)	-22.711 (-24.703, -20.719)	-9.290 (-11.260, -7.321)	-11.352 (-13.322, -9.382)	<**0.0001**	0.4940	**0.0010**	<**0.0001**	<**0.0001**	0.1229
	PP vs. PP-Fast	1.0000	0.1229	1.0000	1.0000	-	-	-	-	-	-

Table 5.4: Marginal means and p-values for preferred speed and fast LC turns presented for frontal-plane balance metrics per-task (top) and transverse-plane linear and angular momenta generation metrics per task and gait phase (bottom).

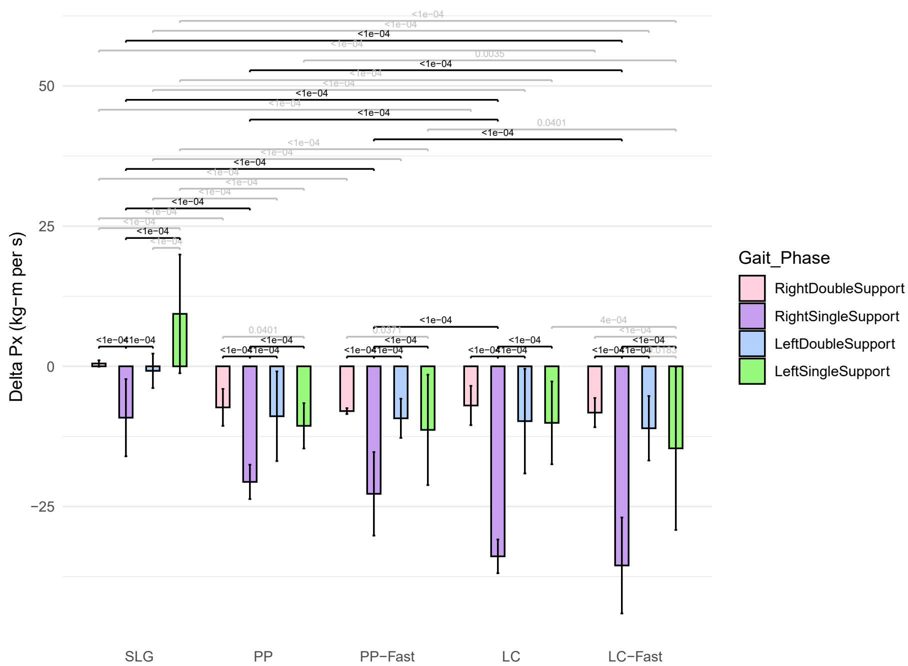

Figure 5.4: The marginal mean Δp_x for each task and gait phase. Positive values indicate rightward Δp_x, while negative indicates leftward, in the direction of the turn. Horizontal bars indicate significant differences between main effects of Task and Gait Phase (i.e. pairs where only one factor changes levels, such as PP LSS vs. PP RSS. The black bars represent significant comparisons involving the phase of interest, RSS). Leftward Δp_x is larger in this cohort during fast speed LC vs. fast PP turns, but is not different between speeds of LC turns or speeds of PP turns.

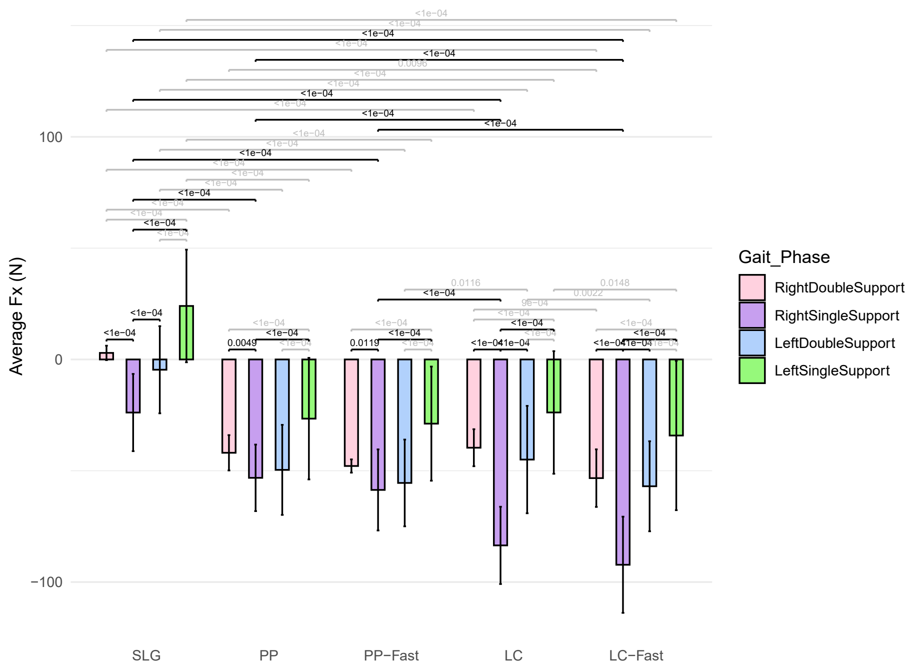

Figure 5.5: The marginal mean $F_{x,avg}$ for each task and gait phase. Positive values indicate rightward $F_{x,avg}$, while negative indicates leftward, in the direction of the turn. Horizontal bars indicate significant differences between main effects of Task and Gait Phase (i.e. pairs where only one factor changes levels, such as PP LSS vs. PP RSS. The black bars represent significant comparisons involving the phase of interest, RSS). Leftward RSS is largest in SLG and LC turns only, and larger in faster & preferred speed LC vs. faster & preferred speed PP turns. Note that during faster vs. preferred speed LC turns, leftward $F_{x,avg}$ increased in each phase of gait other than RSS.

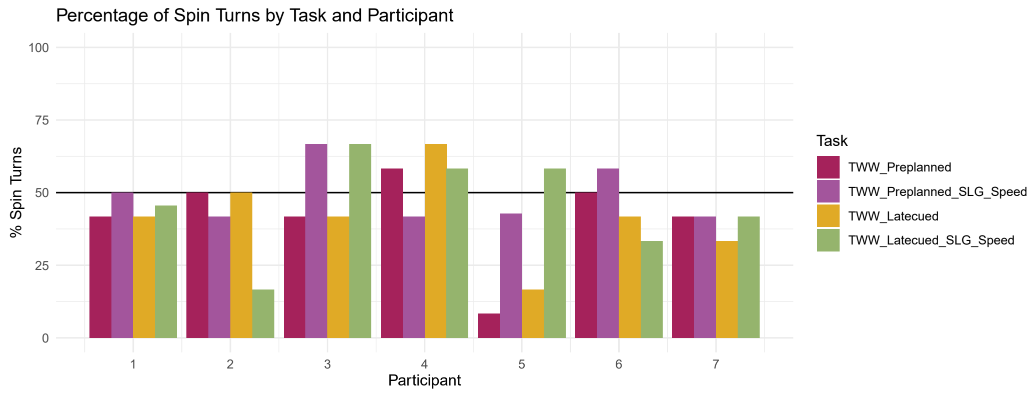

Figure 5.6: Bar graph of young adults' turn strategy prevalence at preferred and faster speeds. Prevalence of step vs. spin turn strategy varied between participants in response to turning context (PP vs. LC) and gait speed.

5.3.5 Preferred vs. fast speed LC turns

Faster speed LC turns result in larger $H_{f,range}$ (Table 5.6; p $=$ 0.0181) and lower LD_{min} (p $=$ 0.0029) vs. preferred speed LC turns. In the transverse plane, RSS leftward Δp_x (p=1) and $F_{x,avg}$ (p=0.3011) are not different between speeds of LC turns. $F_{x,avg}$ is larger leftward in fast vs. preferred speed LC turns for each gait phase besides RSS (Figure 5.5; max p $=$ 0.0022). Δp_x is only larger leftward during fast vs. preferred speed LC turns during LSS phase (p=0.0004). In the angular domain, faster vs. preferred speed LC turns show larger LDS ΔH_z (p $=$ 0.0069) and $M_{z,avg}$ (p $<$ 0.0001). $M_{z,avg}$ is also larger rightward in RDS during the faster turns (p=0.0002), while ΔH_z is not different (Table 5.6; p=0.7946).

Parameter		Marginal means (95% CL) LC	Marginal means (95% CL) LC-Fast	Post-hoc pairwise comparisons LC vs. LC-Fast
Frontal H (unitless)	Maximum	0.004 (0.003, 0.005)	0.004 (0.003, 0.005)	0.1109
	Minimum	-0.004 (-0.005, -0.003)	-0.005 (-0.006, -0.004)	**0.0177**
LD (m)	Range	0.008 (0.006, 0.010)	0.009 (0.007, 0.011)	**0.0183**
	Maximum	0.276 (0.241, 0.311)	0.302 (0.267, 0.337)	**0.0019**
	Minimum	0.041 (0.027, 0.056)	0.023 (0.008, 0.038)	**0.0244**
MOS (m)	Maximum	0.155 (0.145, 0.164)	0.160 (0.150, 0.170)	0.4588
	Minimum	-0.172 (-0.274, -0.070)	-0.215 (-0.317, -0.113)	<**0.0001**

Parameter	Task	Marginal means (95% CL) RDS	RSS	LDS	LSS	Post-hoc pairwise comparisons RDS vs. RSS	RDS vs. LDS	RDS vs. LSS	RSS vs. LDS	RSS vs. LSS	LDS vs. LSS
Average Fx (N)	LC	-39.889 (-46.524, -33.253)	-83.765 (-90.400, -77.129)	-44.933 (-51.357, -38.508)	-23.769 (-30.193, -17.345)	<**0.0001**	0.4248	**0.0005**	<**0.0001**	<**0.0001**	<**0.0001**
	LC-Fast	-53.799 (-60.765, -46.833)	-92.719 (-99.686, -85.753)	-57.032 (-63.484, -50.580)	-34.238 (-40.690, -27.786)	<**0.0001**	0.4412	<**0.0001**	<**0.0001**	<**0.0001**	<**0.0001**
	LC vs. LC-Fast	**0.0071**	0.1089	**0.0117**	**0.0337**	-	-	-	-	-	-
Average Mz (N-m)	LC	-6.746 (-7.180, -6.311)	1.651 (1.217, 2.086)	8.416 (8.000, 8.832)	-2.364 (-2.781, -1.948)	<**0.0001**	<**0.0001**	<**0.0001**	<**0.0001**	<**0.0001**	<**0.0001**
	LC-Fast	-7.939 (-8.401, -7.476)	1.476 (1.014, 1.939)	10.694 (10.276, 11.113)	-2.652 (-3.071, -2.233)	<**0.0001**	<**0.0001**	<**0.0001**	<**0.0001**	<**0.0001**	<**0.0001**
	LC vs. LC-Fast	**0.0006**	0.6590	<**0.0001**	0.6590	-	-	-	-	-	-
Delta Hz (kg-m2 per s)	LC	-1.241 (-1.345, -1.137)	0.672 (0.568, 0.776)	1.701 (1.602, 1.801)	-0.894 (-0.994, -0.795)	<**0.0001**	<**0.0001**	<**0.0001**	<**0.0001**	<**0.0001**	<**0.0001**
	LC-Fast	-1.353 (-1.464, -1.242)	0.576 (0.465, 0.687)	1.917 (1.817, 2.017)	-0.987 (-1.087, -0.887)	<**0.0001**	<**0.0001**	<**0.0001**	<**0.0001**	<**0.0001**	<**0.0001**
	LC vs. LC-Fast	0.4448	0.4448	**0.0109**	0.4448	-	-	-	-	-	-
Delta Px (kg-m per s)	LC	-7.037 (-9.263, -4.811)	-33.939 (-36.165, -31.713)	-9.764 (-11.913, -7.615)	-10.071 (-12.220, -7.922)	<**0.0001**	0.3156	0.2181	<**0.0001**	<**0.0001**	1.0000
	LC-Fast	-8.368 (-10.713, -6.022)	-35.628 (-37.973, -33.282)	-11.065 (-13.224, -8.906)	-14.647 (-16.806, -12.488)	<**0.0001**	0.3241	**0.0002**	<**0.0001**	<**0.0001**	0.0776
	LC vs. LC-Fast	1.0000	1.0000	1.0000	**0.0084**	-	-	-	-	-	-

Table 5.5: Marginal means and p-values for preferred speed and fast LC turns presented for frontal-plane balance metrics per-task (top) and transverse-plane linear and angular momenta generation metrics per task and gait phase (bottom).

Parameter		Marginal means (95% CL) LC	Marginal means (95% CL) LC-Fast	Post-hoc pairwise comparisons LC vs. LC-Fast
Frontal H (unitless)	Maximum	0.004 (0.003, 0.005)	0.004 (0.003, 0.005)	0.1109
	Minimum	-0.004 (-0.005, -0.003)	-0.005 (-0.006, -0.004)	**0.0177**
	Range	0.008 (0.006, 0.010)	0.009 (0.007, 0.011)	**0.0183**
LD (m)	Maximum	0.276 (0.241, 0.311)	0.302 (0.267, 0.337)	**0.0019**
	Minimum	0.041 (0.027, 0.056)	0.023 (0.008, 0.038)	**0.0244**
MOS (m)	Maximum	0.155 (0.145, 0.164)	0.160 (0.150, 0.170)	0.4588
	Minimum	-0.172 (-0.274, -0.070)	-0.215 (-0.317, -0.113)	**<0.0001**

Parameter	Task	Marginal means (95% CL)				Post-hoc pairwise comparisons					
		RDS	RSS	LDS	LSS	RDS vs. RSS	RDS vs. LDS	RDS vs. LSS	RSS vs. LDS	RSS vs. LSS	LDS vs. LSS
Average Fx (N)	LC	-39.889 (-46.524, -33.253)	-83.765 (-90.400, -77.129)	-44.933 (-51.357, -38.508)	-23.769 (-30.193, -17.345)	**<0.0001**	0.4248	**0.0005**	**<0.0001**	**<0.0001**	**<0.0001**
	LC-Fast	-53.799 (-60.765, -46.833)	-92.719 (-99.686, -85.753)	-57.032 (-63.484, -50.580)	-34.238 (-40.690, -27.786)	**<0.0001**	0.4412	**<0.0001**	**<0.0001**	**<0.0001**	**<0.0001**
	LC vs. LC-Fast	**0.0071**	0.1089	**0.0117**	**0.0337**	-	-	-	-	-	-
Average Mz (N-m)	LC	-6.746 (-7.180, -6.311)	1.651 (1.217, 2.086)	8.416 (8.000, 8.832)	-2.364 (-2.781, -1.948)	**<0.0001**	**<0.0001**	**<0.0001**	**<0.0001**	**<0.0001**	**<0.0001**
	LC-Fast	-7.939 (-8.401, -7.476)	1.476 (1.014, 1.939)	10.694 (10.276, 11.113)	-2.652 (-3.071, -2.233)	**<0.0001**	**<0.0001**	**<0.0001**	**<0.0001**	**<0.0001**	**<0.0001**
	LC vs. LC-Fast	**0.0006**	0.6590	**<0.0001**	0.6590	-	-	-	-	-	-
Delta Hz (kg-m2 per s)	LC	-1.241 (-1.345, -1.137)	0.672 (0.568, 0.776)	1.701 (1.602, 1.801)	-0.894 (-0.994, -0.795)	**<0.0001**	**<0.0001**	**<0.0001**	**<0.0001**	**<0.0001**	**<0.0001**
	LC-Fast	-1.353 (-1.464, -1.242)	0.576 (0.465, 0.687)	1.917 (1.817, 2.017)	-0.987 (-1.087, -0.887)	**<0.0001**	**<0.0001**	**<0.0001**	**<0.0001**	**<0.0001**	**<0.0001**
	LC vs. LC-Fast	0.4448	0.4448	**0.0109**	0.4448	-	-	-	-	-	-
Delta Px (kg-m per s)	LC	-7.037 (-9.263, -4.811)	-33.939 (-36.165, -31.713)	-9.764 (-11.913, -7.615)	-10.071 (-12.220, -7.922)	**<0.0001**	0.3156	0.2181	**<0.0001**	**<0.0001**	1.0000
	LC-Fast	-8.368 (-10.713, -6.022)	-35.628 (-37.973, -33.282)	-11.065 (-13.224, -8.906)	-14.647 (-16.806, -12.488)	**<0.0001**	0.3241	**0.0002**	**<0.0001**	**<0.0001**	0.0776
	LC vs. LC-Fast	1.0000	1.0000	1.0000	**0.0084**	-	-	-	-	-	-

Table 5.6: Marginal means and p-values for preferred speed and fast LC turns presented for frontal-plane balance metrics per-task (top) and transverse-plane linear and angular momenta generation metrics per task and gait phase (bottom).

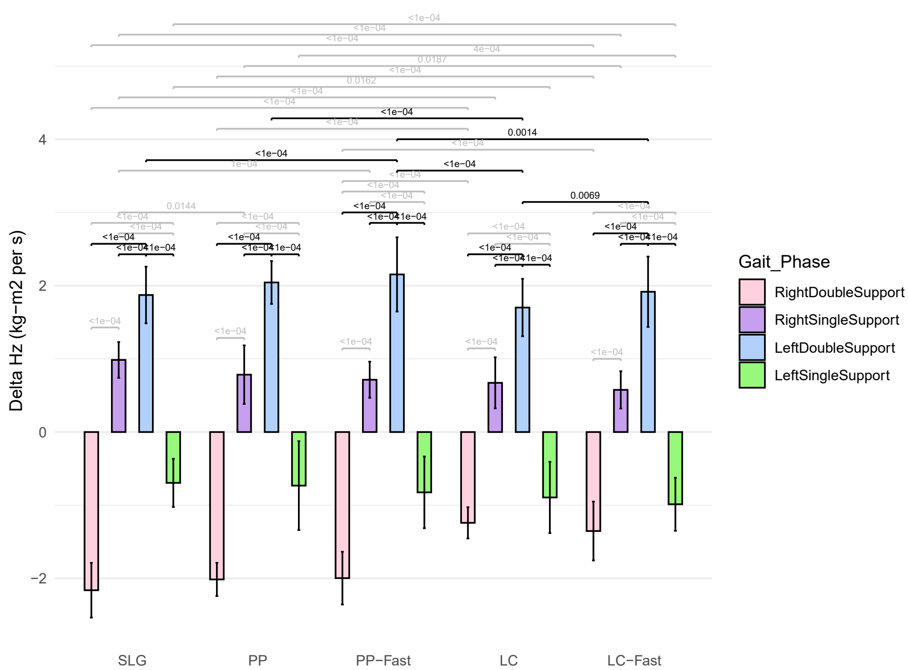

Figure 5.7: The marginal mean ΔH_z for each task and gait phase. Positive values indicate leftward transverse-plane rotation of the body-facing direction, in the direction of the turn, while negative values indicate the opposite rotation. Horizontal bars indicate significant differences between main effects of Task and Gait Phase (i.e. pairs where only one factor changes levels, such as PP LSS vs. PP LDS). The black bars represent significant comparisons involving the phase of interest, LDS. The largest amount of leftward H_z is generated during LDS in fast PP turns vs. any other task. Faster LC turns generated more leftward ΔH_z during LDS vs. preferred speed LC turns, but were not different in RDS. PP turns showed no differences between gait speeds in any gait phase.

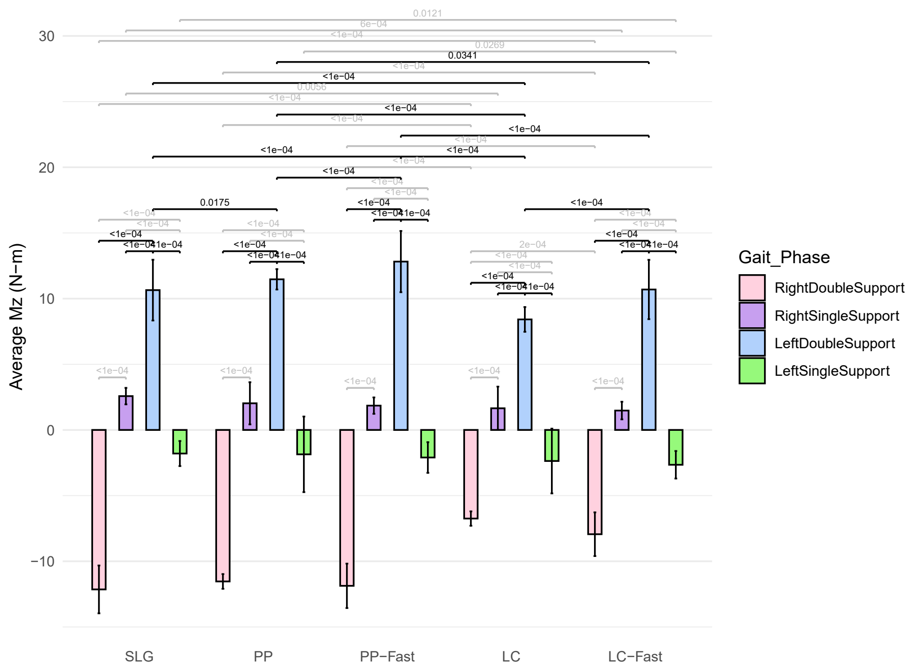

Figure 5.8: The marginal mean $M_{z,avg}$ for each task and gait phase. Positive values indicate leftward transverse-plane rotation of the body-facing direction, in the direction of the turn, while negative values indicate the opposite rotation. Horizontal bars indicate significant differences between main effects of Task and Gait Phase (i.e. pairs where only one factor changes levels, such as PP LSS vs. PP LDS). The black bars represent significant comparisons involving the phase of interest, LDS. The largest amount of leftward $M_{z,avg}$ is generated during LDS. In both PP and LC turns, there is a larger average moment during (LDS) in faster vs preferred speed turns, but no difference in RDS. Faster speed LC turns exhibit reduced leftward and rightward $M_{z,avg}$ in LDS and RDS, respectively, vs. the fast PP turns.

When stratifying by turn strategy, within the faster LC turns, LD_{min} is lower ($p<0.0001$) in spin vs. step turns. In RSS, leftward Δp_x is larger during faster LC step vs. spin turns ($p=0.0074$), but not $F_{x,avg}$ ($p=0.1453$). Between tasks, in LDS, leftward ΔH_z and $M_{z,avg}$ increase in the faster vs. preferred speed LC step turns ($p\leq0.0064$).

5.4 Discussion

This study investigated the effect of attempting to walk at a similar speed as SLG during 90° PP and LC turns on frontal- and transverse-plane balance measures in an attempt to remove horizontal gait speed as a covariate from the comparisons of balance and momenta metrics during turns vs. SLG, as well as to assess the effect of increasing horizontal gait speed on those metrics. When comparing faster speed LC vs. PP turns vs. SLG, I replicated the findings at preferred speeds in chapters 3 and 4. Similar to preferred speed findings in chapter 3, I found that during the faster speed LC vs. PP turns, the largest $H_{f,range}$ occurred during LC turns, while the smallest LD_{min} occurred during PP turns. Similar to preferred speed findings in chapter 4, I found that RSS generates leftward linear momentum to change trajectory while LDS generates leftward angular momentum to rotate the body's facing direction. When comparing preferred speed and faster speed turns of the same turning condition, PP turns did not exhibit any changes in the frontal or transverse plane, except for an increase in LDS leftward $M_{z,avg}$. At faster vs. preferred speeds of LC turns, however, frontal-plane balance measures "worsened" (larger $H_{f,range}$ and lower LD_{min}), while transverse-plane linear momentum generation did not change, and leftward angular momentum generation increased. A summary of this Aim's findings can be found in Table 5.7

This experiment successfully induced gait speeds during PP turns that approximated that of horizontal gait speed during SLG (p=0.0581), and which were significantly larger than speeds during PP turns at preferred speed (p<0.0001). However, those speeds were not attainable by any participant during LC turns at faster speeds, leading to a significantly slower LC turn than PP or SLG horizontal gait speed (p<0.0001). Increasing horizontal gait speed increased the prevalence of spin turns during PP turns (41.7% preferred speed spin turns vs. 46.2% spin turns at SLG speeds). By contrast, the prevalence of step vs. spin turns did not change at all between speeds in LC turns (61.3% preferred speed vs. 61.2% faster speed)

Cohort	Factor 1	Factor 2	Metric	Finding
7 YA	Task	-	Gait speed	PP-Fast=SLG PP-Fast > PP SLG > PP
			Hf Range	PP-Fast = PP LC-Fast > LC LC-Fast > PP-Fast
			LD Min	LC-Fast < LC PP-Fast = PP LC-Fast > PP-Fast
		Gait Phase	ΔPx	RSS < all other phases RSS PP-Fast = PP RSS LC-Fast = LC RSS LC-Fast < PP-Fast
			$F_{x,avg}$	RSS < all other phases RSS PP-Fast = PP RSS LC-Fast = LC RSS LC-Fast < PP-Fast
			ΔHz	LDS > all other phases LDS PP-Fast = PP LDS PP-Fast > LC-Fast LDS LC-Fast > LC RDS PP-Fast = PP RDS PP-Fast < LC-Fast
			$M_{z,avg}$	LDS > all other phases LDS PP-Fast > all other tasks RDS PP-Fast = PP RDS PP-Fast < LC-Fast RDS LC-Fast < LC

Table 5.7: Main findings for Aim 3 for the frontal-plane metrics over the whole phase of interest for each Task (top), and the transverse-plane metrics within each Gait Phase (bottom).

5.4.1 SLG vs. PP turns at preferred and SLG speeds

Between preferred and fast (SLG) speeds of PP turns, I did not observe significant differences in the frontal-plane balance metrics $H_{f,range}$, $H_{f,min}$, $H_{f,max}$, or LD_{min}. Likely, the observed change in gait speed of ∼0.1 m/s from their preferred speed is simply an insufficient stimulus to elicit changes to these metrics in healthy young adults. Reaffirming the preferred speed findings from chapter 3 of the additional challenge to balance posed by turns vs. SLG, PP turns at both speeds showed more extreme values of $H_{f,range}$ and LD_{min} vs. SLG.

In the transverse plane, during RSS, Δp_x and $F_{x,avg}$ exhibited larger magnitudes than during SLG, owing to the need to generate leftward p_x to turn. Preferred speed PP turns' ΔH_z and $M_{z,avg}$ in LDS were not different from SLG, but at the faster speed were significantly larger than SLG LDS, indicating that ΔH_z may increase with speed, in agreement with prior work showing increases in $\vec{H}$ with increasing speed (43), although again other studies have shown decreases in $\vec{H}$ with increasing speed (42).

5.4.2 PP turns at preferred vs. faster speeds

Between speeds of PP turns, during RSS Δp_x and $F_{x,avg}$ were not different. In LDS, ΔH_z was not different, though $M_{z,avg}$ was larger leftward at faster speeds, perhaps due to the (insignificantly) shorter LDS duration at faster speeds. When examining step vs. spin turns, the only significant difference is that $M_{z,avg}$ is larger in faster vs. preferred speed PP turns during step but not spin turns.

5.4.3 LC turns at preferred vs. faster speeds

During LC turns, I observed a larger $H_{f,range}$ in faster vs. preferred speed turns, and lower LD_{min}. The lower LD_{min} occurred due to more turns occurring over the left foot vs. at preferred speeds. Similar to preferred speed turns' H_f and LD timeseries (Figure 3.8), H_f is near zero approximately when LD_{min} occurs in both preferred-speed and faster LC turns, but has a large positive slope (frontal-plane $\overrightarrow{M}$ (M_f)) that facilitates the head and trunk to rotate rightward, away from the left edge of the BOS. Thus, while there is never a single point in time when both metrics suggest a "worse" balance state, both measures manifest more extreme values at faster speed LC turns over the course of the multiple steps during the turn, potentially leading to challenges regulating balance over the multiple steps of the turn.

In the transverse plane, Δp_x and $F_{x,avg}$ during RSS were not different across LC turn speeds. The other gait phases appeared to increase linear momentum generation during faster LC turns, when considering both the increased Δp_x in LSS, and increased $F_{x,avg}$ in LDS and RDS. During LDS, ΔH_z and $M_{z,avg}$ were larger at faster speeds in LC turns, though still smaller than during PP turns' LDS at the same speed due to the significantly smaller magnitude of rightward ΔH_z during RDS in LC turns. This unexpected finding highlights the reduced rightward rotation during LC turns, even relative to PP turns. This reduced rotation in both directions may be an effort to stabilize the head and gaze leftward to attend to the visual cue, stabilizing vestibular information and visual perception of the monitor and new direction of travel (81; 167).

During faster speed LC turns, ΔH_z increases while Δp_x did not. This may be due to the fact that at faster speeds, participants would often overshoot the intersection (Figure 5.9), resulting in a larger ΔH_z to accomplish the sudden turn of more than 90°, which would not cause a corresponding increase in Δp_x.

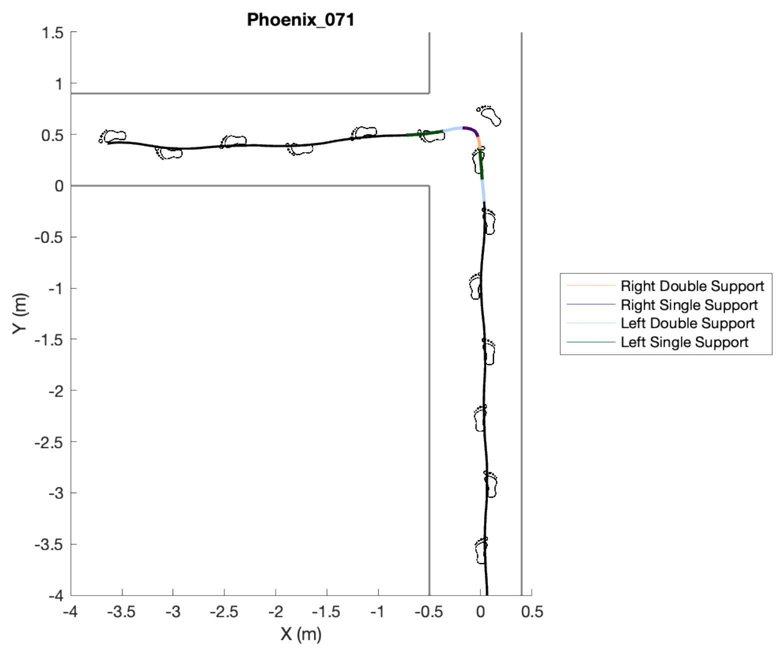

Figure 5.9: Footfalls and TBCM trajectory during a fast LC turn. Note that the TBCM trajectory initially overshoots the intersection, resulting in a turn of more than 90° magnitude as the participant is walking too fast and struggles to turn rapidly enough in response to the cue to turn.

When stratifying by turn strategy, in the frontal plane the only significant change is that faster LC turns exhibit lower LD_{min} in spin vs. step turns, at similar values to those observed in PP turns. In the transverse plane, RSS Δp_x is larger during faster LC step vs. spin turns, which is compensated for by a corresponding increase in LSS Δp_x during spin vs. step turns, highlighting the more prominent role of the LSS in producing force during spin vs. step turns. Finally, in contrast to the findings without turn strategy stratification, ΔH_z during LDS is larger in faster vs. preferred speed LC step turns, while there is no difference in any other phase of gait between the two speeds of PP turn. This increase in ΔH_z during LDS without a corresponding decrease in ΔH_z during another gait phase in step vs. spin turns may reflect the increased rotational demands during faster LC step vs. spin turns, though it is unclear why this occurs in step turns' LDS instead of spin turns LSS, which earlier results suggest is the most rotationally demanding turn strategy and gait phase.

5.4.4 Limitations and Future Work

The major limitation, and one of the major findings, of this study is the inability for any participants to maintain the SLG speed during the LC turns, precluding the ability to compare LC and PP turns at the same horizontal gait speed. This is likely due to the short ART between the visual cue presentation and the turn initiation. I hypothesize that participants anticipated the need to leave enough time to (1) decide whether they needed to turn, (2) initiate the turn. Future work may modify the protocol to facilitate either faster LC turns or slower PP turns.

Chapter 6

Conclusion

Balance and momenta control during turning gait is an understudied area, despite turns' increased risk of injury due to falls and prevalence during daily life. This dissertation reports on studies wherein healthy young and older adults were asked to walk straight, as well as walk and turn 90° to the left. I measured their spatiotemporal parameters and frontal-plane balance metrics, as well as their linear and angular momenta generation in the direction of the turn. While both turning tasks challenged balance more than straight-line gait, late-cued turns were more challenging to balance than pre-planned turns. The late-cued turns also resulted in larger magnitude linear momentum generation than pre-planned turns, despite slower horizontal gait speed. Angular momentum generation in the direction of the turn was largest during pre-planned turns, and late-cued turns exhibited less angular momentum generation away from the turn. Angular momentum generation was not modulated by turn strategy in either age group, but linear momentum generation was. Step turns showed a relatively larger role of right single support in linear momentum generation, while spin turns increased the role of left single support.

Young adults walked and turned in pre-planned and late-cued fashion at preferred speed, as well as speeds matching straight-line gait, which they were unable to maintain during late-cued turns. While I did not observe significant differences during pre-planned turns in frontal- or transverse-plane metrics, likely due to the small difference in gait speed, in the faster late-cued turns I observed significantly worsened balance metrics and increased momenta generation compared to late-cued turns at preferred speeds.

Aim	Cohort	Factor 1	Factor 2	Factor 3	Metric	Finding
Aim 1	17 YA	Task			Hf Range	LC $>$ PP
					LD Min	PP $<$ LC, SLG $=$ LC
					MOS Min	PP $>$ LC
			Sex		Hf Range	M $>$ F all tasks
					LD Min	F $<$ M all tasks
					MOS Min	F $=$ M all tasks
			Turn Strategy		Hf Range	Step $=$ Spin all tasks
					LD Min	Spin $<$ Step LC turns
					MOS Min	Step $=$ Spin all tasks
Aim 2	All Cohorts	Task	Gait Phase		Left ΔPx Left ΔHz	RSS $<$ all other phases LDS $>$ all other phases
	YA vs. OA	Task	Gait Phase		Left ΔPx	RSS YA $<$ OA
					Left ΔHz	Magnitude of OA $>$ YA all phases
Aim 3	7 YA	Task			Gait speed	PP-Fast $=$ SLG, PP-Fast $>$ PP
					Hf Range	LC-Fast $>$ LC, PP-Fast $=$ PP
					LD Min	LC-Fast $<$ LC, PP-Fast $=$ PP
			Gait Phase		ΔPx	RSS LC-Fast $=$ LC RSS PP-Fast $=$ PP
					Left ΔHz	LDS PP-Fast $=$ PP LDS PP-Fast $>$ LC-Fast LDS LC-Fast $<$ LC RDS PP-Fast $=$ PP RDS PP-Fast $<$ LC-Fast
Aims 2 & 3	All Cohorts	Task	Gait Phase	Turn Strategy	Left ΔPx	Step RSS $<$ Spin RSS Spin LSS $<$ Step LSS
					Left ΔHz	Step $=$ Spin for all tasks and cohorts

Table 6.1: Overview of main findings by aim, cohort, and factors. Note that for Δp_x, "$<$" means values are more negative, i.e. larger magnitude leftward $\vec{p}$. For ΔH_z, LDS is positive, and RDS is negative, so "$>$" and "$<$" indicate larger magnitude leftward and rightward, respectively.

Young and older adults both performed preferred-speed PP turns 90° to the left. In this task, compared to young adults, older adults generated larger magnitude change in transverse-plane angular momentum during each phase of gait, while young adults generated larger changes in linear momentum during left and right single support phases.

Additionally, I preliminarily explored the effect of biological sex on these measures, finding that there is no difference between the sexes in spatiotemporal measures during straight-line gait or turns. However, males exhibited larger range of frontal-plane H_f than females, while females exhibited lower lateral distance minima. These contrasting findings may indicate disparate balance control strategies in males and females. More work is needed to understand the effect of biological sex on frontal-plane balance.

In summary, this dissertation provides additional evidence that turning while walking challenges balance and momenta control above and beyond the demands of straight-line gait. Additionally, factors such as environmental context, gait speed, biological sex, and aging each impact balance and momenta control as well.

Appendix A

Participant Characteristics

Data from three cohorts of participants collected over three years are reported in this dissertation. See the timeline for details (Figure 2.3). This appendix contains three tables - one per cohort - listing anthropometric measures of age, biological sex, height, and mass for each participant.

Note that the young adult cohort in Aim 1 consists of two cohorts, Tables A.1 and A.3. Participant characteristics for the older adult cohort in Aim 2 is in Table A.2.

Participant	Sex	Age (yrs)	Height (m)	Mass (kg)
1	f	27	1.75	67.9
2	f	26	1.75	59.5
3	m	30	1.73	78.8
4	m	26	1.73	73.5
5	f	25	1.75	58.5
6	m	30	1.76	74.7
7	m	29	1.68	74.1
8	m	20	2.05	109.9
9	m	20	1.88	92.8
10	m	19	1.81	69.9

Table A.1: Characteristics of the first young adult cohort of three females and seven males.

Participant	Sex	Age (yrs)	Height (m)	Mass (kg)
1	m	66	1.68	67.5
2	f	71	1.70	75.1
3	m	67	1.74	80.6
4	f	68	1.69	91.6
5	f	82	1.65	61.6
6	f	69	1.66	95.0
7	f	78	1.58	75.0
8	f	66	1.57	43.8
9	f	71	1.63	72.8

Table A.2: Characteristics of the nine older adult participants.

Participant	Sex	Age (yrs)	Height (m)	Mass (kg)
1	f	22	1.71	71.2
2	f	20	1.67	68.7
3	f	19	1.67	54.2
4	f	20	1.75	55.3
5	f	23	1.60	46.8
6	f	20	1.51	46.7
7	f	20	1.64	57.7

Table A.3: Participant characteristics of the second young adult cohort, consisting of seven females.

Appendix B

MATLAB Pseudocode

B.1 Best Marker Names

```
function [best_marker_names] = best_marker_names(
   markerData, markerNames)
%% 1. Both methods.
% Find the two markers that are farthest apart on the
   segments.
markerName1, markerName2 = findFarthestMarkers(markerData,
    markerNames);

%% 2a. Distance method.
% Find the marker that is farthest from the specified
   marker
[markerName3_potential1, dist1] =
   findFarthestMarkerFromMarker(markerData, markerName1);
[markerName3_potential2, dist2] =
   findFarthestMarkerFromMarker(markerData, markerName2);
if dist2 > dist1
    markerName3 = markerName3_potential2;
else
    markerName3 = markerName3_potential1;
end
```

```
%% 2b. Projected-distance method
markerName3 = findFarthestPerpendicularMarker(markerData,
   markerName1, markerName2)

%% 3. Both methods. Order markers 1 and 2 by distance from
    marker 3 so that marker 2 is always the origin marker,
    farthest from the other two.
marker1Pos = markerData.(markerName1);
marker2Pos = markerData.(markerName2);
marker3Pos = markerData.(markerName3));
dist_from_marker3_to_marker1 = norm(marker1Pos -
   marker3Pos);
dist_from_marker2_to_marker1 = norm(marker2Pos -
   marker3Pos);
% Swap marker names 1 & 2.
if dist_from_marker3_to_marker1 <
   dist_from_marker3_to_marker1
    markerName1tmp = markerName1;
    markerName1 = markerName2;
    markerName2 = marker1tmp;
end
```

Appendix C

Defense Slides

C.1 Defense Slides

Mechanics of Whole-Body Balance and Momentum Control During Straight-Line Gait and 90° Turns

Oct 28, 2024

Dr. Mitchell Tillman

STEVENS INSTITUTE OF TECHNOLOGY 1870

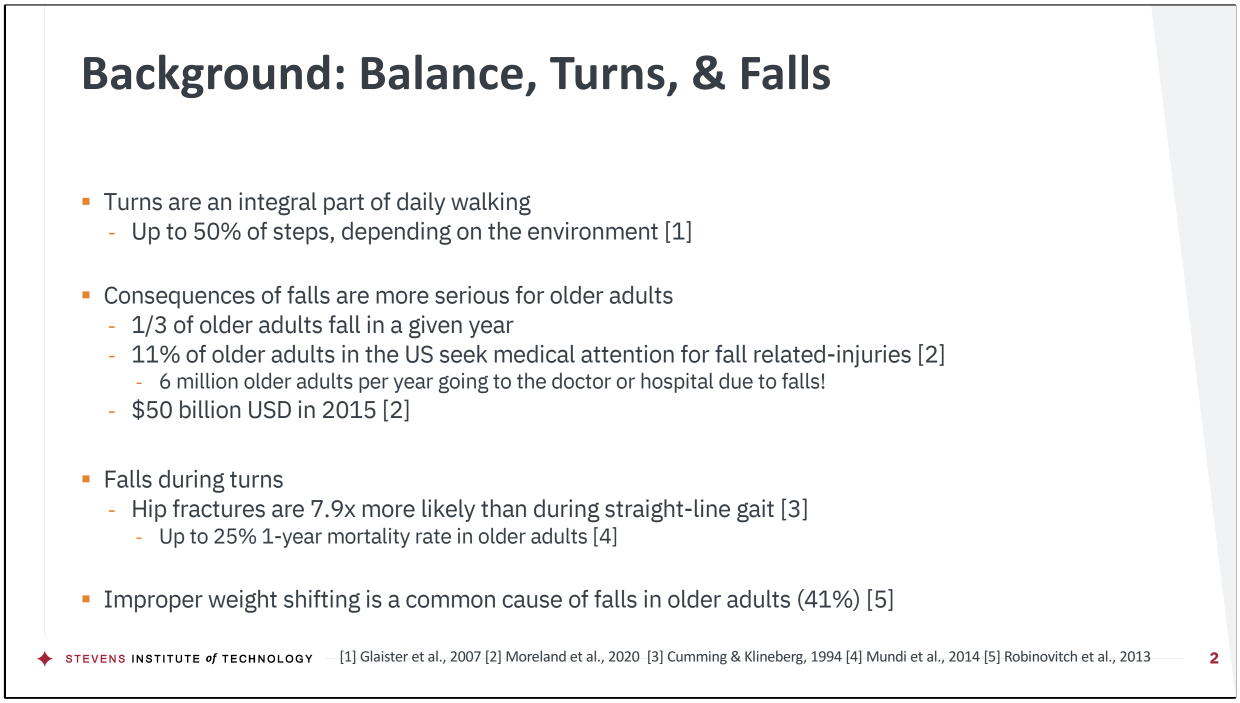

Turns are an integral part of daily walking. Depending on the environment, turns have been shown to comprise up to 50% of all steps taken.

Occasionally, while walking we can lose our balance and fall. While people of all ages fall, the consequences of falls are more serious for older adults. One in three adults over age 65 will fall in a given year, and one in three of those (11% of all older adults) will seek medical attention for fall-related injuries. In 2015 in the US alone, fall-related injuries were responsible for $50 billion USD in medical costs.

Falling during turns can exacerbate the risk of injury. Falls during turns have been reported to be 7.9x as likely to result in a hip fracture, which carry up to a 25% 1 year mortality rate for older adults.

A seminal study by Robinovitch et al. in 2013 aimed to uncover common causes of falls by placing video cameras in the public spaces of a community living center. They found that the most common cause of falls in older adults – 41% - is improper weight shifting. Turns are thought to challenge balance by increasing the demand to properly shift weight. Depending on the turning context, this demand can increase or decrease.

Response Time: Pre-Planned & Late-Cued Turns

One factor that influences the demand for weight shifting is how suddenly the turn must be executed. Depending on the time available to respond, the turn may be performed in a pre-planned or late-cued fashion. To contextualize what pre-planned and late-cued means, think about walking through a grocery store. So, if you're walking down the aisles of a grocery store that you're familiar with, you approach the aisle, and you simply execute the turn down into that aisle, because you know that's the aisle that contains the item that you're interested in.

That's a preplanned turn, whereas during late-cued turns, imagine that you're in a grocery store that you're not familiar with, or they change the layout of your favorite grocery store, and therefore, as you're approaching an aisle, you're not quite sure whether you need to turn. So, you have to come up to the intersection with that aisle, turn and look at the sign and determine whether you need to turn. That is a late-cued turn, because you're only executing the turn after suddenly deciding that you need to do so.

To quantify how each of these turning contexts affects balance, first we need to be able to quantify someone's balance state.

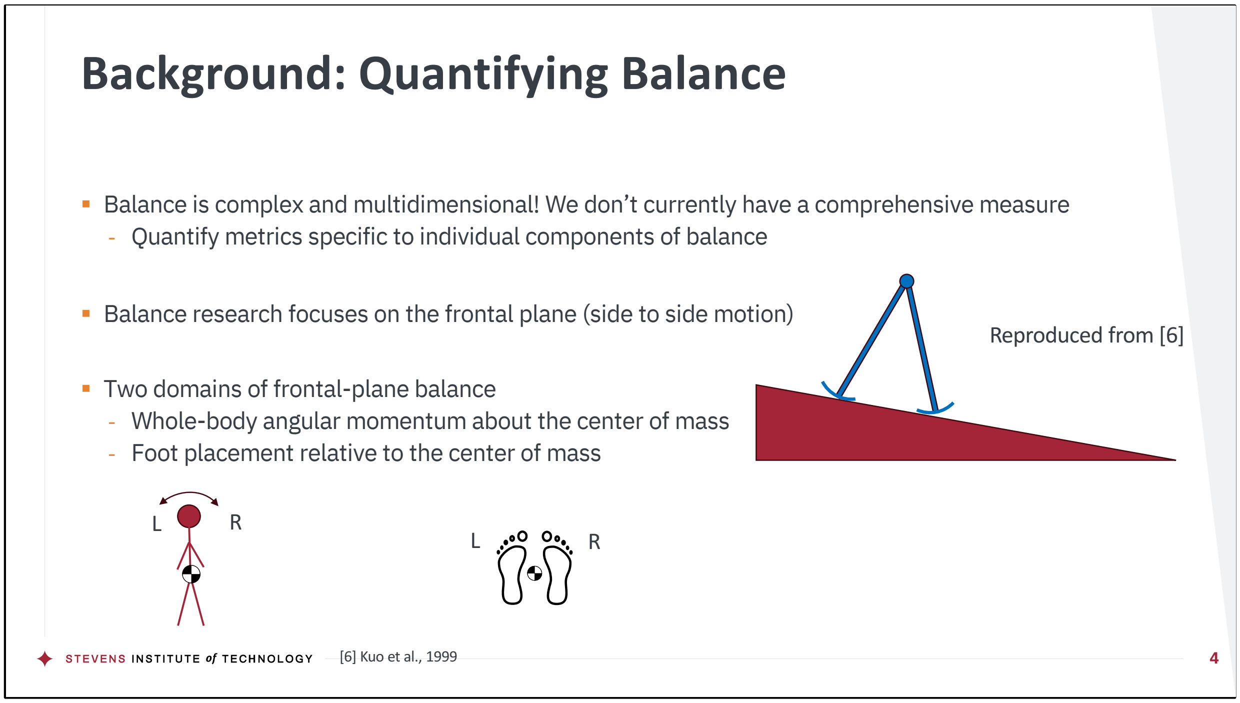

Unfortunately, balance is quite complex and multi-dimensional, and a comprehensive mechanics-based measure of a person's current balance state does not exist. Therefore, mechanics-based balance metrics quantify specific components of the balance state.

When we think about how someone could fall, a fall could occur either in the forward-backward direction, or sideways. Over the last few decades, research has focused on sideways balance (in the frontal plane). Experiments with unpowered legged robots in the late 1990's such as the one depicted here, showed that forward-backward (sagittal-plane) balance can potentially be maintained passively by regulating step length, and therefore is of less therapeutic interest.

Typically two domains of frontal-plane balance are motivated in the literature as the most directly mechanically related to loss of balance: whole-body angular momentum about the center of mass, and foot placement relative to the center of mass.

While much is known about balance control during straight-line gait, we are still developing our understanding of the mechanics of balance during turns. Next, I'll talk about what is already known about these two balance metrics during walking.

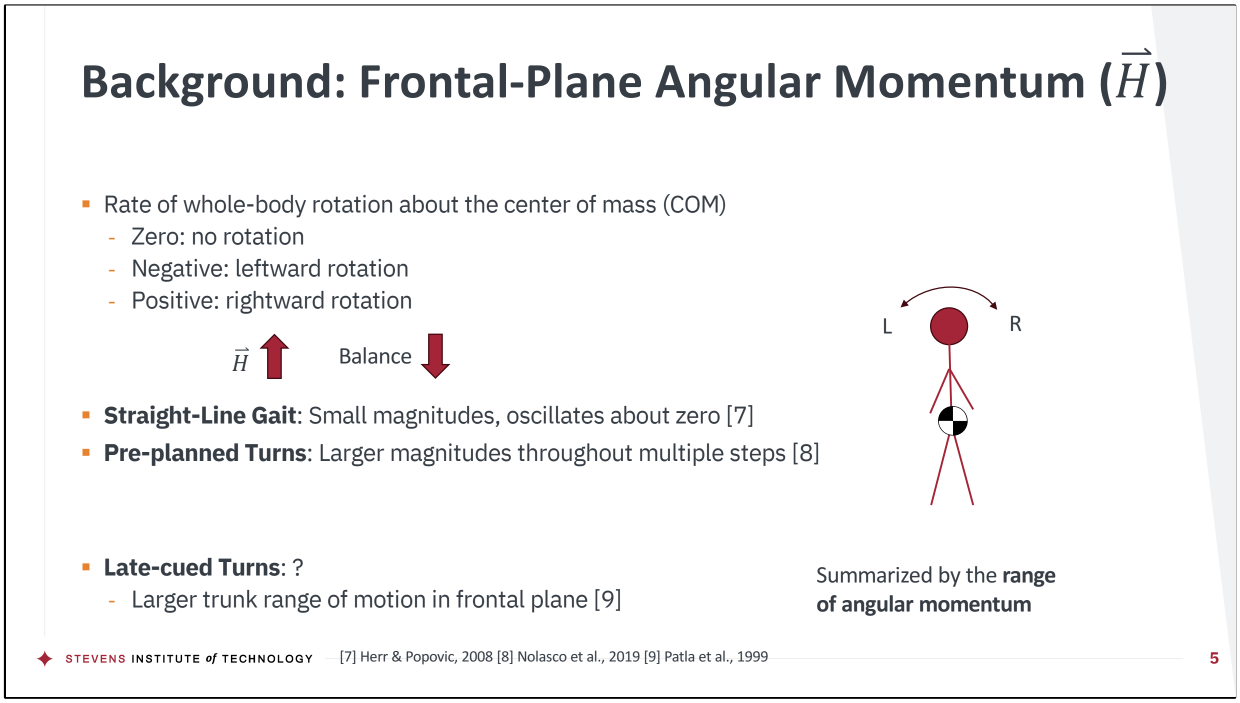

In lay terms, frontal-plane angular momentum, denoted by the letter H, can be thought of as the rate of whole-body rotation about the center of mass. In the frontal plane, you can rotate quickly, or more slowly. Angular momentum is defined such that zero means no rotation, and we've defined negative to be leftward rotation, and positive is rightward rotation.

Generally, the interpretation is that increasing angular momentum corresponds to a decrease in the balance state.

During straight-line gait, prior work has found H to oscillate about zero with small magnitudes. During pre-planned turns, angular momentum magnitude increases throughout multiple steps.

I'm not aware of any studies on frontal-plane angular momentum in late-cued turns, though prior work has shown larger frontal-plane trunk range of motion, leading us to believe that angular momentum will also increase.

Frontal-plane angular momentum is summarized by its range, as the max - min value is taken as a measure of stability.

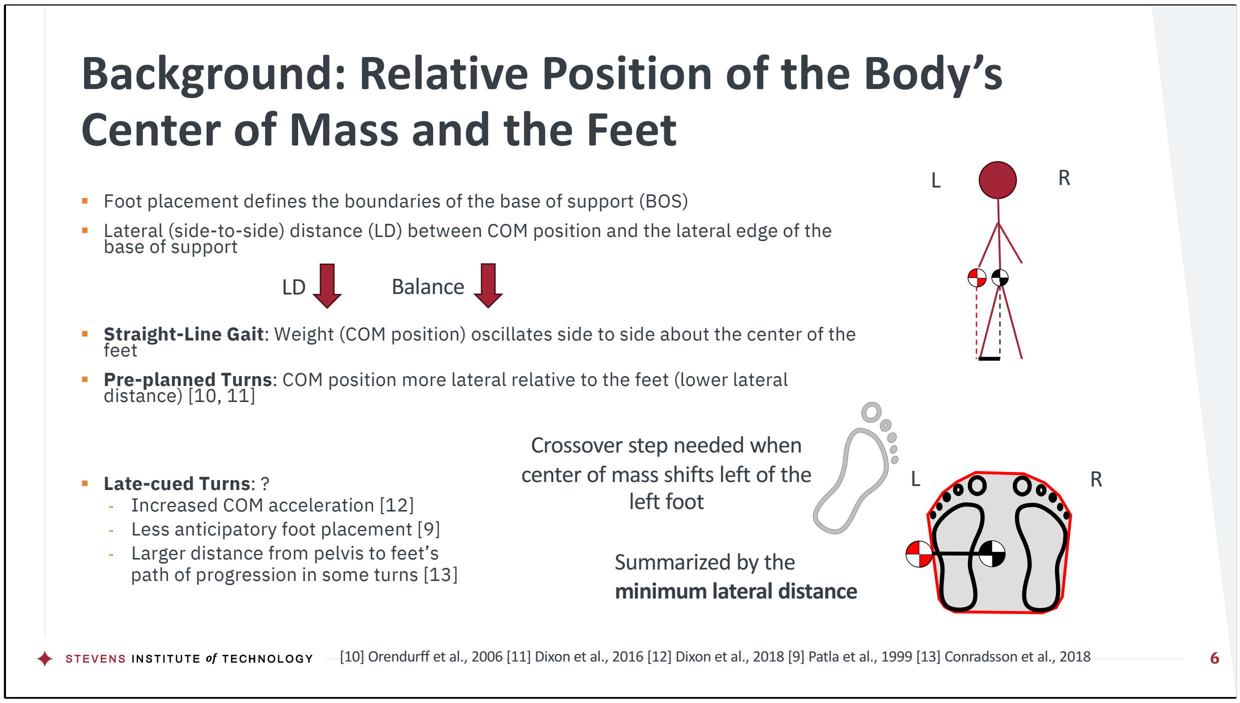

The second frontal-plane balance domain is foot placement relative to the body's center of mass. Foot placement defines the base of support. The lateral distance, or LD for short, is the lateral or side-to-side distance between the center of mass position and the lateral edge of the BOS.

Generally, decreasing lateral distance is viewed as a worse balance state, because the center of mass is nearer to the edge of the base of support, and therefore perhaps more likely to exit the base of support and cause a fall.

During straight-line gait, the person's weight, or COM position, oscillates side to side about the center line of the two feet. During pre-planned turns, prior work has shown that turns shift the COM position to be more lateral, nearer to the lateral edge of the BOS, meaning a lower LD.

I am not aware of any studies that have looked directly at the center of mass position relative to the feet during late-cued turns, although prior work does suggest that late-cued turns do affect the relative foot placement domain of balance. They've found that this domain of balance may be adversely affected during late-cued turns, due to less anticipatory foot placement, larger distance between the pelvis and the feet's path of progression, and increased center of mass acceleration.

Lateral distance is summarized by its minimum value, quantifying when the balance state is most at risk.

Background: Mechanical Objectives of Walking

- So far, discussed balance maintenance in the ***frontal*** plane
- The movement goals are accomplished in the ***transverse*** **(*horizontal*)** plane
  - Translation and rotation
  - Linear and angular momentum
- **Straight-Line Gait**: Maintain direction
  - Direction of travel & body-facing direction oscillate about a consistent direction

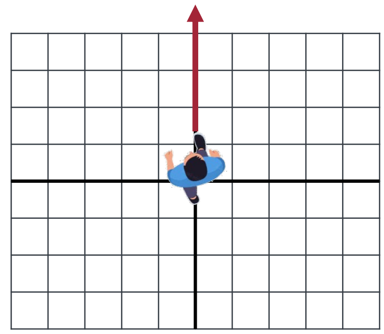

top-down view of a cartoon person walking

Up until now, I’ve been discussing metrics that quantify the balance state in the frontal plane. But the goals to accomplish locomotion are in the transverse, or horizontal, plane: control of translation and rotation about the vertical axis. These task goals are accomplished by generation and regulation of linear and angular momentum.

For example, during straight-line gait, the goal is to maintain the direction of walking. When you walk, your direction of travel and the direction that your body faces both rotate back and forth about the direction you’re walking in.

Background: Mechanical Objectives of Walking

- Balance is maintained in the ***frontal*** plane
- The movement goals are accomplished in the ***horizontal*** plane
  - Translation and rotation
  - Linear and angular momentum
- **Straight-Line Gait**: Maintain direction
  - Direction of travel & body-facing direction oscillate about a consistent direction
- **Turns**: Change of direction
  - Persistent change in linear momentum
  - Transient change in angular momentum

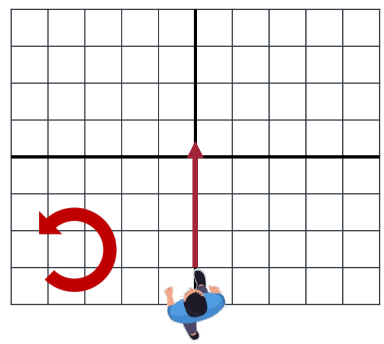

top-down view of a cartoon person walking

During turns, the goal is to change your direction of travel and body’s facing direction. [CLICK]

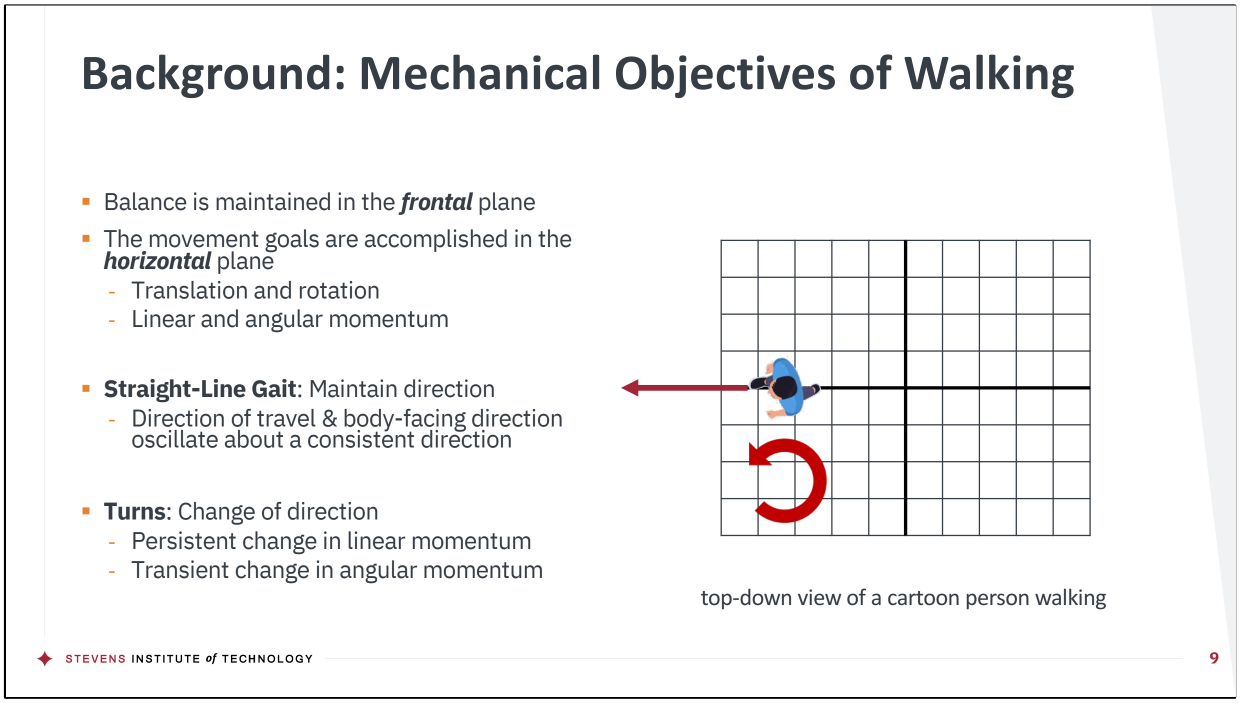

This is accomplished by a persistent change in linear momentum, shown by the direction of the arrow, and a transient change in angular momentum that disappears after the body is facing towards the new direction of travel.

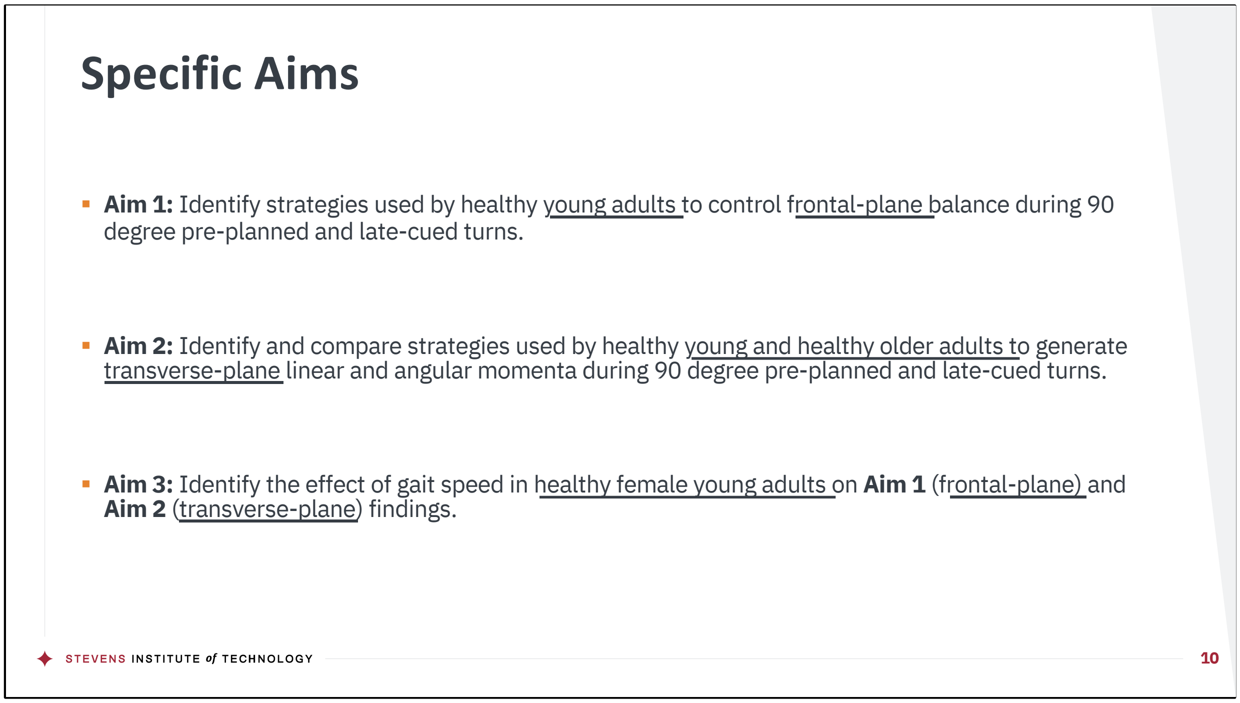

This leads to the specific aims of my dissertation research.
In Aim 1, the goal is to identify strategies used by healthy young adults to control frontal-plane balance during 90 degree pre-planned and late-cued turns.

In Aim 2, the goal is to identify and compare strategies used by healthy young and healthy older adults to generate transverse-plane linear and angular momenta during 90 degree pre-planned and late-cued turns.

In Aim 3, the goal is to identify the effect of gait speed in healthy female young adults on Aim 1 (frontal-plane) and Aim 2 (transverse-plane) findings.

STEVENS
INSTITUTE OF TECHNOLOGY
1870

Aim 1

Frontal-Plane Balance Metrics

Aim 1 Purpose

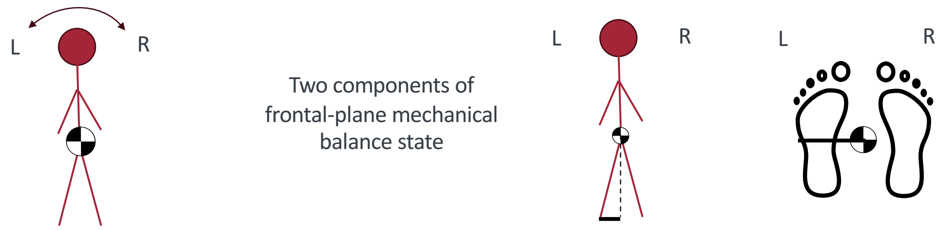

<u>Purpose:</u> Understand how healthy young adults modulate **rotation** (angular momentum) and **foot placement relative to the whole-body center of mass** (lateral distance) to maintain frontal-plane balance during straight-line gait and turns.

Now, in this aim, I'll talk about the frontal plane balance maintenance strategies during turns. So again, the goal of this aim is to look at the 2 domains of frontal plane balance, and that is the angular momentum about the center of mass and the lateral distance relative to the lateral edge of the base support.

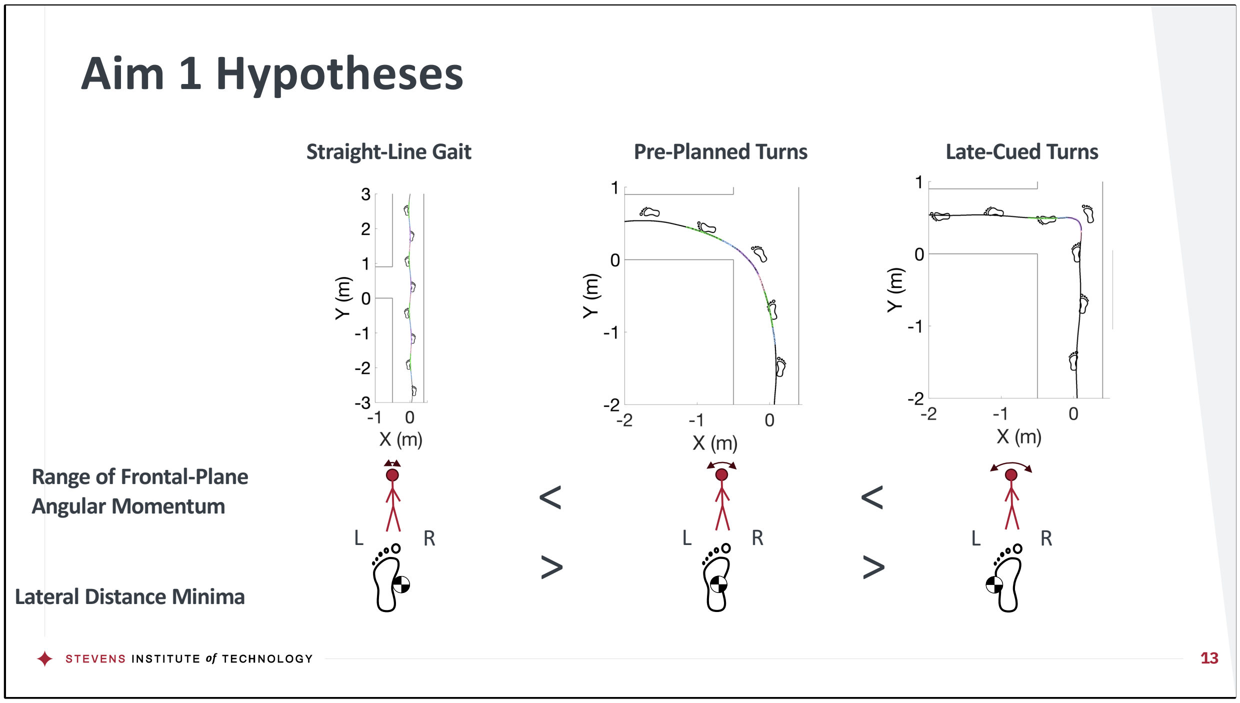

So we had hypotheses for each measures. We asked participants to come and perform 3 tasks: straight line gait, pre-planned turns, and late-cued turns. Building from the idea that straight line gait has the least demand for weight shifting and is the the lowest challenge to balance, we hypothesized that the range of frontal plane angular momentum would be smallest during straight line gait, and that the lateral distance minima would be largest, as the center of mass position is most centered relative to the feet.

During preplanned turns, as the goal now is to change our direction, due to the increased mechanical demand we hypothesize that the range of frontal plane angular momentum will be increased relative to straight line gait, and similarly, that the lateral distance minima will decrease. So the center of mass will shift nearer to the edge of the base of support.

Finally, for late-cued turns, owing to their sudden need to change direction, we hypothesize that they would show the largest range of frontal plane angular momentum, and generate an even smaller lateral distance, perhaps with the center mass, even outside of the base of support.

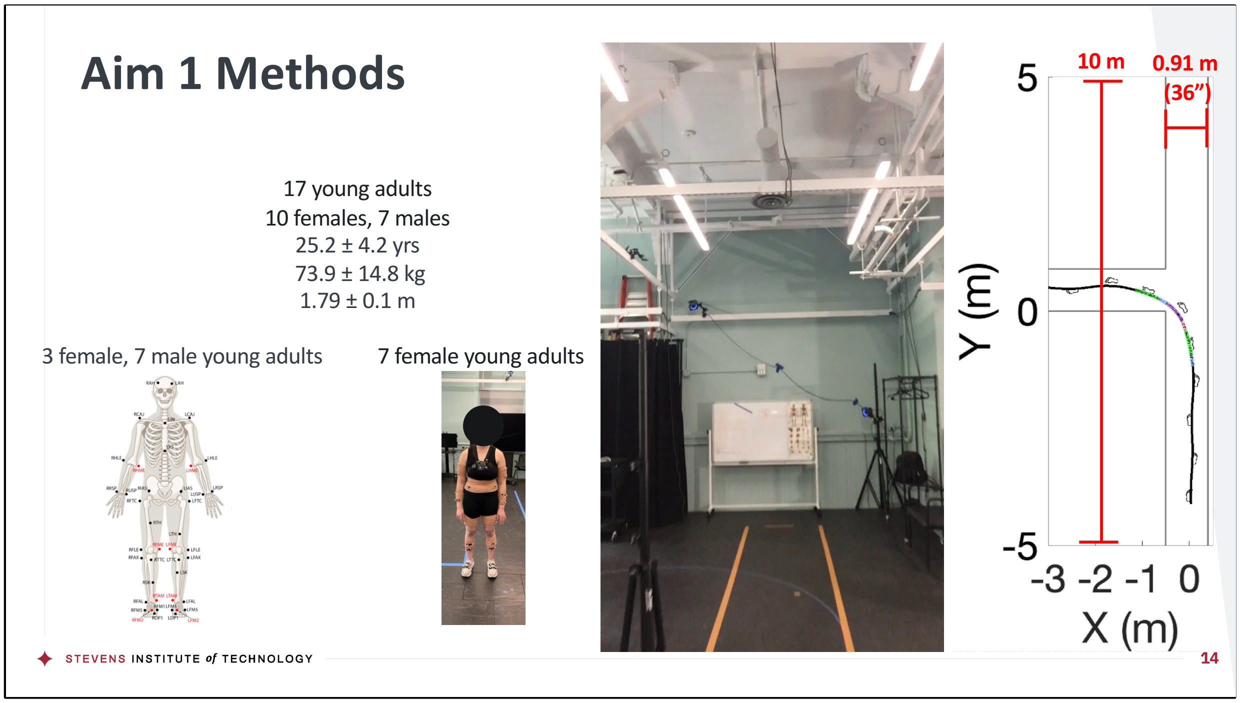

To test these hypotheses, we had 17 young adults come into the lab and perform these 3 tasks. So this video here is going to show from a 1st person view, preplanned turns first, where they simply knew that they needed to turn down the intersecting aisle. We told them they were looking for broccoli. And then next, the late-cued turns where they didn't know until they reached the intersection whether or not they needed to turn.

It's a 10 meter walkway, with the intersection about halfway down that 10 meter walkway, and it was a 36 inch width in accordance with ADA standards.

Note that for this cohort of 17 young adults, we actually had 2 different marker sets that we used. In the 1st marker set of 10 young adults we placed the markers directly onto their anatomic landmarks in order to record people's movements, and in the second cohort we placed the markers using rigid body clusters directly on each segment. And this change in data collection methods was simply due to changes in the way that our lab as a whole was collecting data improvements in our data collection methods.

Biomechanical Modelling

- Segment parameters from prior literature [14]
- For each segment:
  - Orientation
  - Moment of inertia
  - Center of mass position
  - Mass (kg)
- Whole body:
  - Whole-body center of mass position

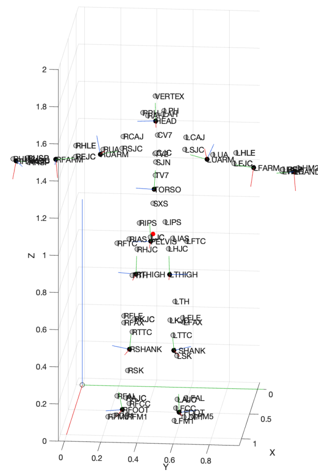

[14] Dumas et al., 2007

Using this movement data as well as segment parameters from prior literature we were able to obtain the orientation of each segment as well as their moment of inertia, center of mass position, and each segment's mass. And this is a person specific model. This allows us to generate or compute whole body measures such as the whole body center of mass position that then feeds into our 2 frontal plane balance measures.

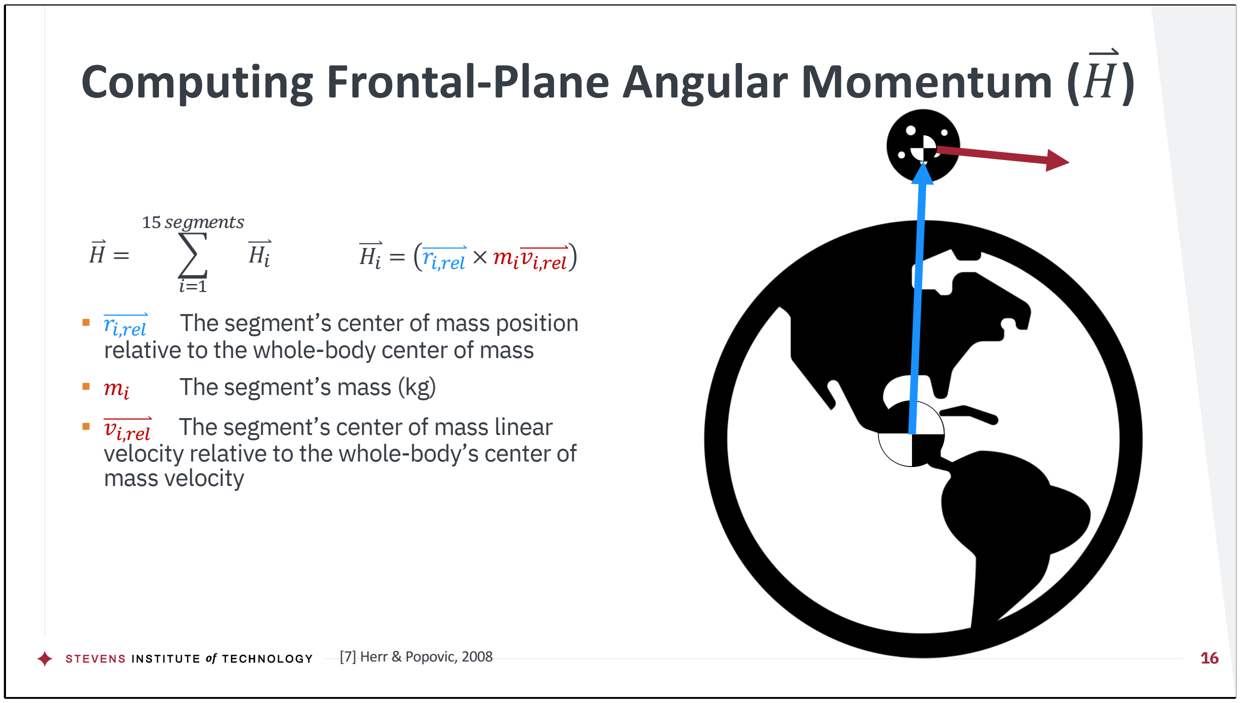

To compute this frontal plane angular momentum, or frontal H for the whole body, we compute the sum of each segment's angular momentum. Each segment's angular momentum consists of 2 terms. First, there's this remote term which I'll use an analogy of the earth and the moon to help illustrate what these terms are. So this remote term is the component of the angular momentum that is due simply to the moon's translation about the about the earth. So no rotation of the moon whatsoever. So that's its relative position and mass weighted velocity.

Computing Frontal-Plane Angular Momentum ($\vec{H}$)

$$\vec{H} = \sum_{i=1}^{15\ segments} \vec{H_i} \qquad \vec{H_i} = (\overrightarrow{r_{i,rel}} \times m_i \overrightarrow{v_{i,rel}})$$

- $\overrightarrow{r_{i,rel}}$ The segment's center of mass position relative to the whole-body center of mass
- m_i The segment's mass (kg)
- $\overrightarrow{v_{i,rel}}$ The segment's center of mass linear velocity relative to the whole-body's center of mass velocity

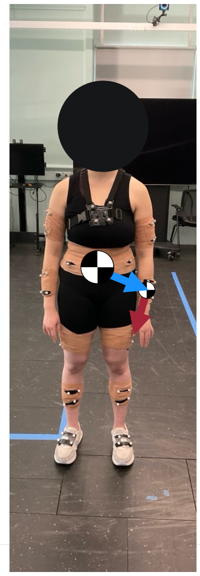

STEVENS INSTITUTE *of* TECHNOLOGY 17

And when we apply this to a person. Again, it's the relative position and mass weighted velocity of the segment relative to the whole body center of mass.

Computing Frontal-Plane Angular Momentum

$$\vec{H} = \sum_{i=1}^{15\ segments} \vec{H_i} \qquad \vec{H_i} = \left(\overrightarrow{r_{i,rel}} \times m_i \overrightarrow{v_{i,rel}}\right) + \vec{I_i}\overrightarrow{\omega_i}$$

- $\overrightarrow{r_{i,rel}}$ The segment's center of mass position relative to the whole-body center of mass
- m_i The segment's mass (kg)
- $\overrightarrow{v_{i,rel}}$ The segment's center of mass linear velocity relative to the whole-body's center of mass velocity
- $\vec{I_i}$ The segment's 3x3 moment of inertia in global coordinates
- $\overrightarrow{\omega_i}$ The segment's angular velocity about its own center of mass

The other component of frontal plane angular momentum is the local term. So this is the component of the angular momentum that is due just to the rotation of the segment about its own center of mass.

Computing Frontal-Plane Angular Momentum

$$\vec{H} = \sum_{i=1}^{15\ segments} \vec{H_i} \qquad \vec{H_i} = (\overrightarrow{r_{i,rel}} \times m_i \overrightarrow{v_{i,rel}}) + \vec{I_i}\vec{\omega_i}$$

- $\overrightarrow{r_{i,rel}}$ The segment's center of mass position relative to the whole-body center of mass
- m_i The segment's mass (kg)
- $\overrightarrow{v_{i,rel}}$ The segment's center of mass linear velocity relative to the whole-body's center of mass velocity
- $\vec{I_i}$ The segment's 3x3 moment of inertia in global coordinates
- $\vec{\omega_i}$ The segment's angular velocity about its own center of mass

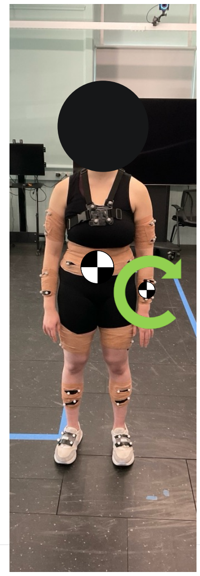

And when we apply it to a person right, this would be the rotation of a segment again, about its own center of mass. So both of these together give you the whole angular momentum term.

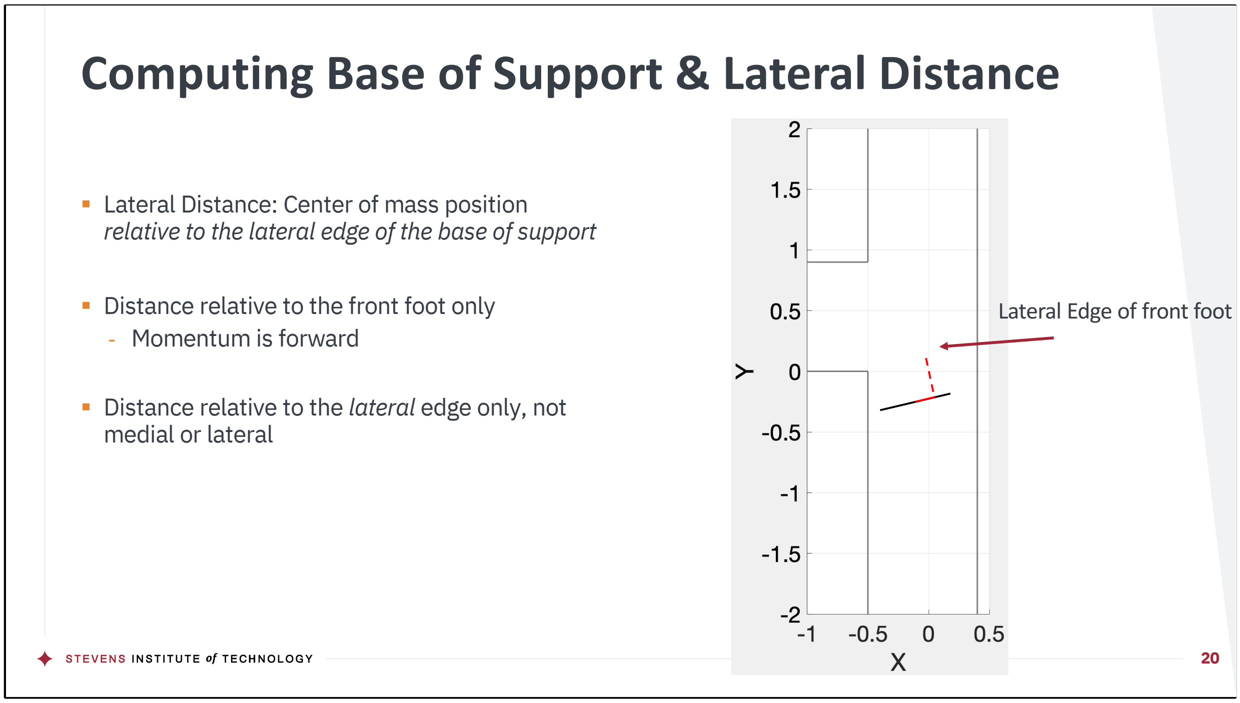

To compute the lateral distance, first we need to define where the feet are placed. We developed our own algorithm for base of support detection to attempt to more precisely map which parts of the feet are in contact with the ground at a given time. To define the base of support, for each point in time first we start with the markers that were placed on the feet. Then, we define a circle of best fit for the forefoot and rearfoot individually, to approximate the shape of the foot. Next, shown in green are the markers that we define as being in contact with the ground based on their heights being below their heights during quiet standing. Next, we compute the boundary of the base of support in red. Defining the lateral direction by the mediolateral axis of the pelvis, the lateral distance is the distance along that axis from the center of mass to the lateral edge of the front foot.

We use the front foot only because the momentum is oriented forward, so that is the direction in which a fall will occur, and using the front foot only simplifies the signal.

Computing Base of Support & Lateral Distance

- Lateral Distance: Center of mass position *relative to the lateral edge of the base of support*
- Distance relative to the front foot only
  - Momentum is forward
- Distance relative to the *lateral* edge only, not medial or lateral

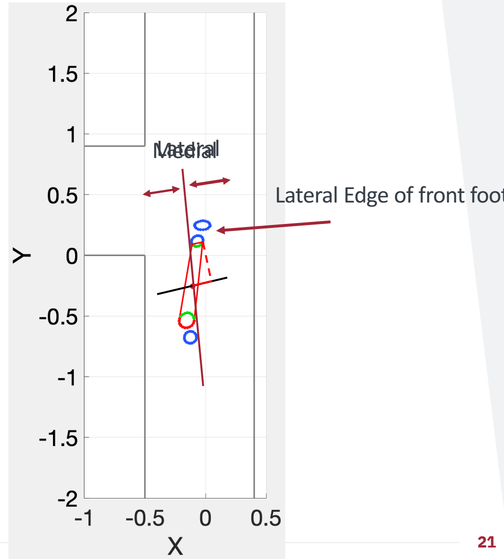

We're interested in the lateral edge only, not the medial or lateral edge, because when your center of mass shifts laterally to the lateral edge, that's where the crossover step comes into play, whereas if the center of mass shifts medially, then it's simply a large step. So this would result in a large, positive, lateral distance value. And this results in a negative lateral distance value. So again, this is the center line between the 2 feet, and so medial is directed towards the center line. Lateral is away, causing that crossover step with the lateral distance.

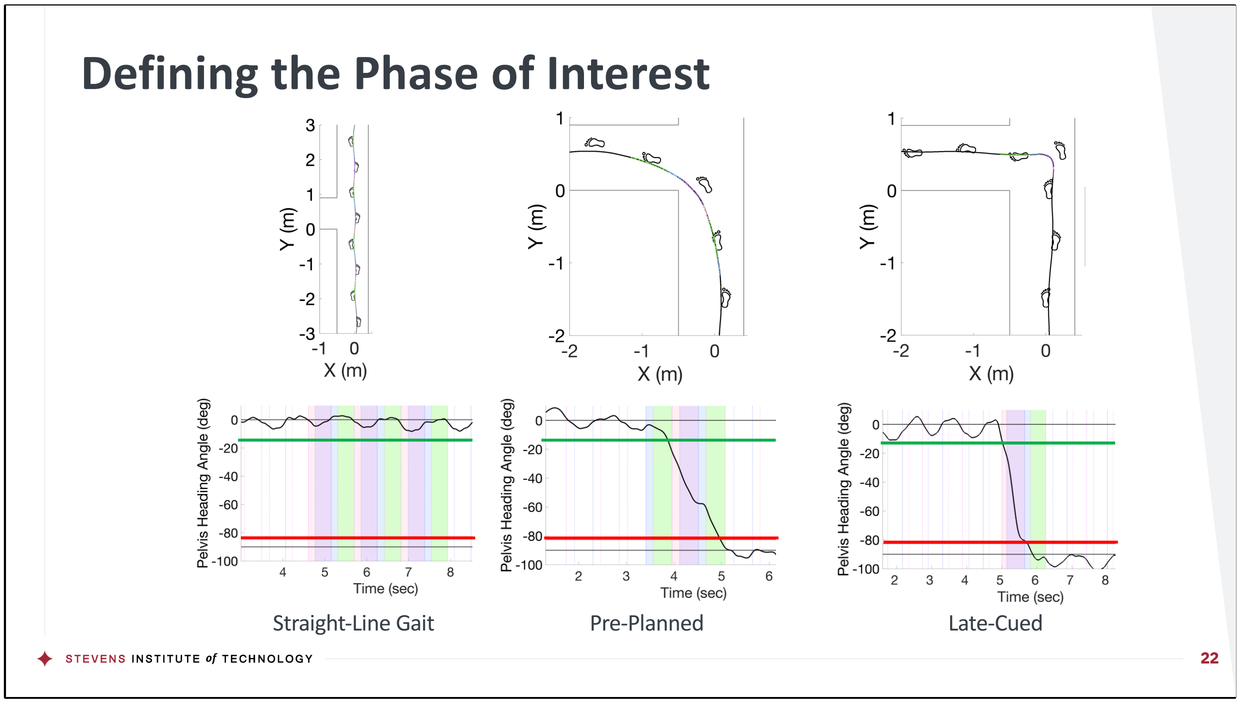

So next, now that we've defined our metrics, we need to only look at the phase of interest for each task. So during straight line gait, this is defined as the middle 6 meters of the walkway. Recall that while you're walking, your body rotates a little bit from side to side about the direction that you're walking. And so we quantified the heading angle the direction that your pelvis is facing, and use the standard deviation of those pelvis heading angles to help define the phase of interest for the turn.

3 times the standard deviation of the pelvis heading angles during straight line gait define this threshold value, and when the pelvis angle exceeded that threshold value, the turn was deemed to start, so that horizontal green line that just popped in is the start threshold.

And then, when that angle goes below that threshold relative to the new direction of travel, that is the red line, and that's when rotation is deemed to end. If you'll note that the green line is a little bit off of center, and this is to account for the offset of each person individually. People don't tend to oscillate directly about that 0 degrees. They're a little bit offset in a person specific fashion.

So then the turn phase. Now that we know when the pelvis begins and ends rotating,

we go backwards to the heel strike just before pelvis rotation began, and forward to the heel strike just after it, which defines the start and end of the turn phase so that 30
there's a consistent base of support context for the turn.

This of course was applied to both pre-planned and late-cued turns.

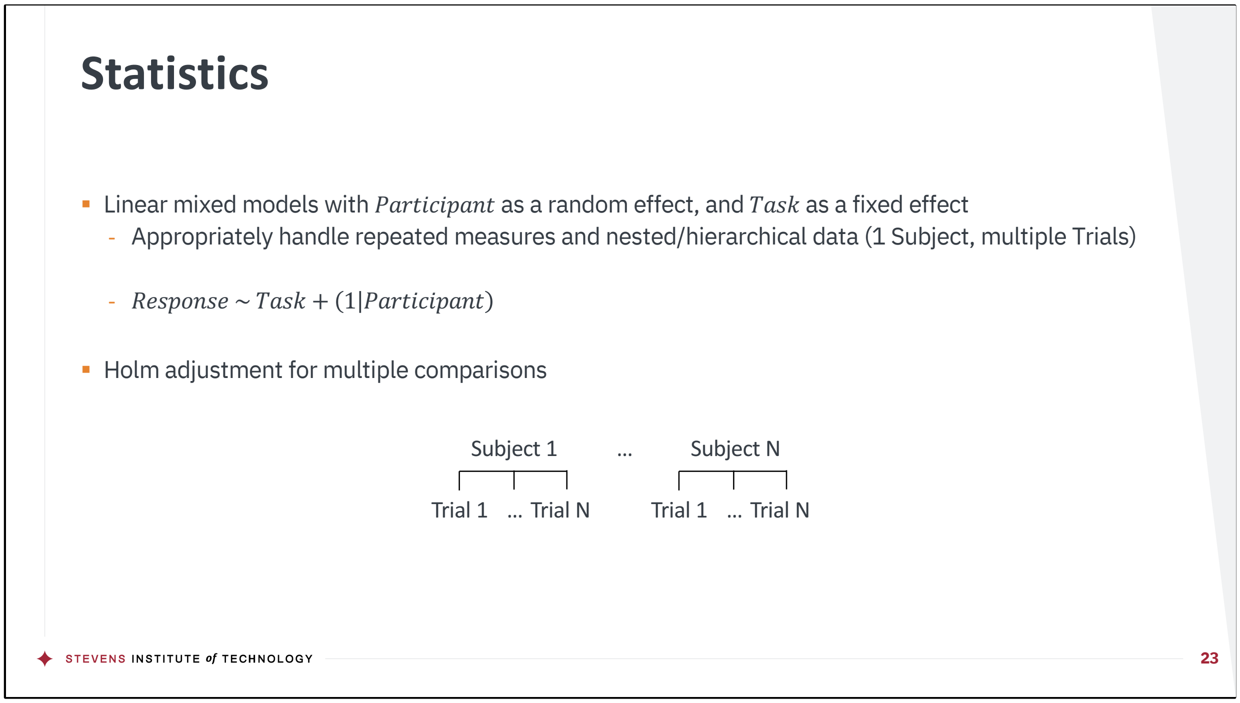

To summarize our findings, we use linear mixed models with participant as a random effect and task as a fixed effect. So task as a fixed effect means that we're only interested in the 3 tasks that we conducted in this study and participant as a random effect means that we want to be able to generalize these findings to participants other than those that were in this study.

We chose linear mixed models to appropriately handle the repeated measures and nested hierarchical data that we have in this data set. For example, where one subject does multiple conditions. And there are multiple trials within those conditions, right nested.

This is the the formula for this linear mixed model. And note that we also use the Holm adjustment for multiple comparisons.

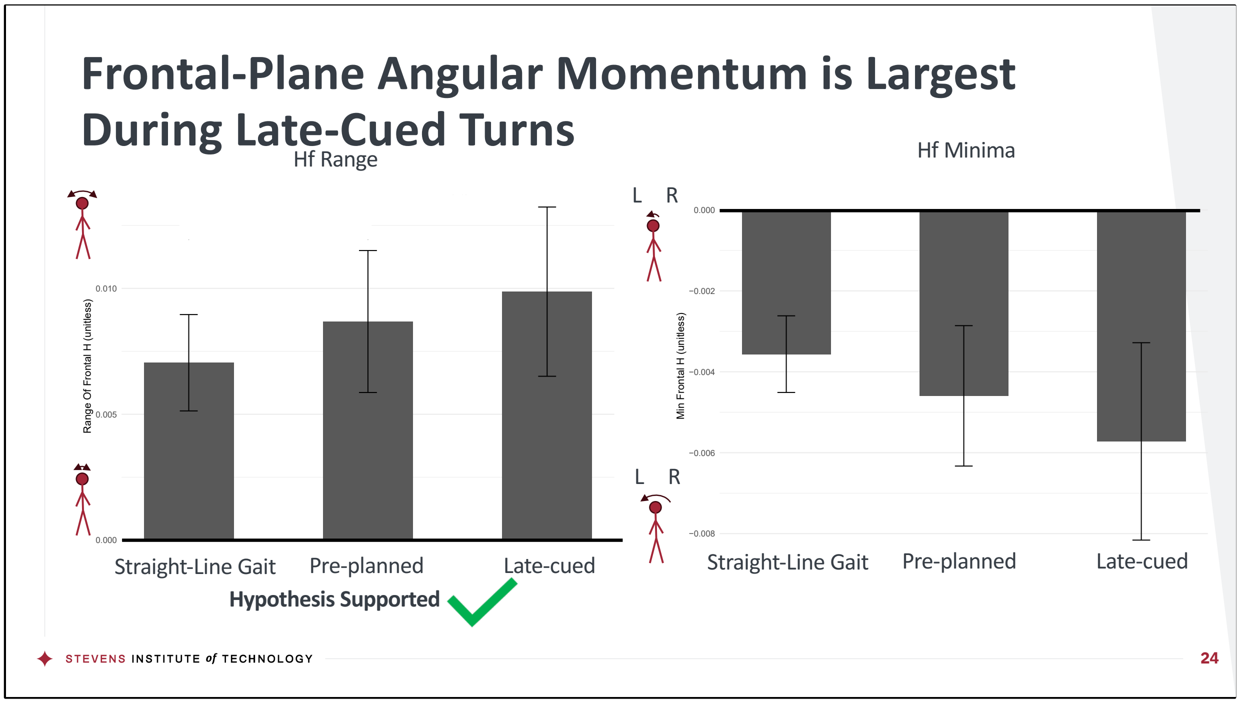

So what did we find? Firstly, at the group level, we found that there was a larger range of frontal plane. Angular momentum during both turns relative to straight line gait. In agreement with our hypothesis.

We also found that there's a larger range of frontal plane. Angular momentum during late cued versus preplanned turns, and this is again in agreement with our hypothesis, and this indicates that this angular momentum domain is sensitive to these late cued turns. And this again, remember that the range of frontal plane angular momentum is the maximum minus the minimum. So it's rightward minus leftward rotation, and we found that this range is generally driven by an increase in the magnitude of this leftward rotation, the angular momentum minimum. So each of these tasks are significantly different from one another, with late-cued showing the largest leftward angular momentum, preplanned smaller, and straight line gait even smaller.

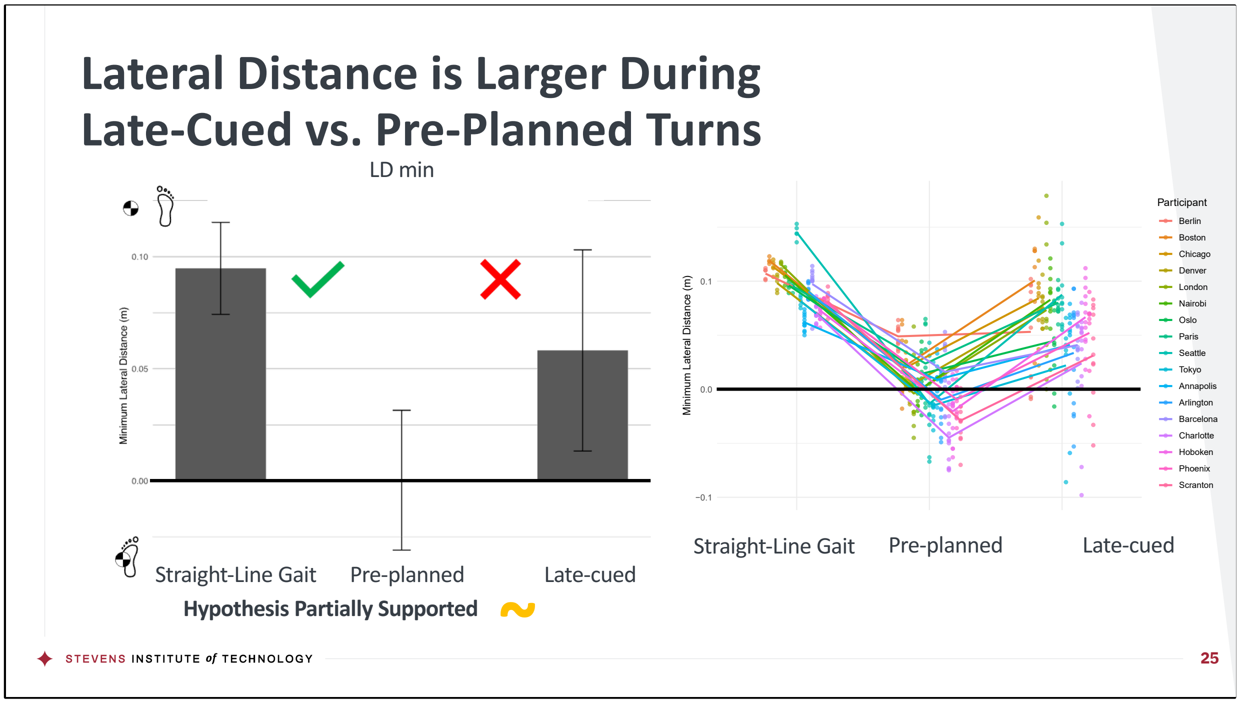

Next, for the other domain of frontal plane balance for lateral distance our hypotheses were partially supported. We did find that lateral distance minima were largest during straight line gait versus both turn types. However, in contrast to our hypothesis, we found that late-cued turns exhibited a larger lateral distance minima on average rather than preplanned turns.

So this was an interesting and unexpected finding. And so when we look at how people were actually performing these late-cued turns, we see that there's a much larger variability during late-cued turns than during preplanned turns. So on average, there's a larger lateral distance minima. But some of the trials actually exhibit lateral distance minima that are even smaller than preplanned turns.

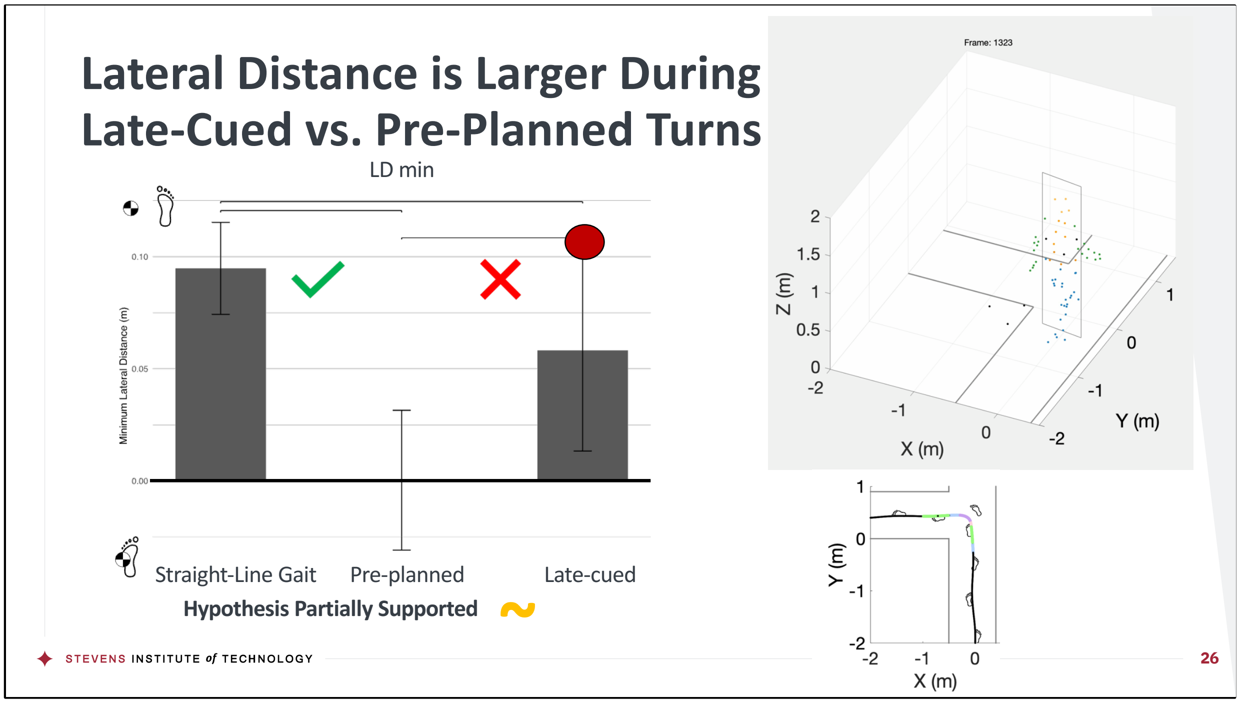

So here's an example of a trial where that red dot indicates for this particular trial that I'm showing now where the lateral distance minima is. So this is well above average. And we can see that this late-cued turn trial looks like 2 bouts of straight line gait, one coming into the turn and one coming out, and so, therefore, that right foot is really the the foot in this case that's used to conduct the turn. And so that maintains this large lateral distance throughout the turn.

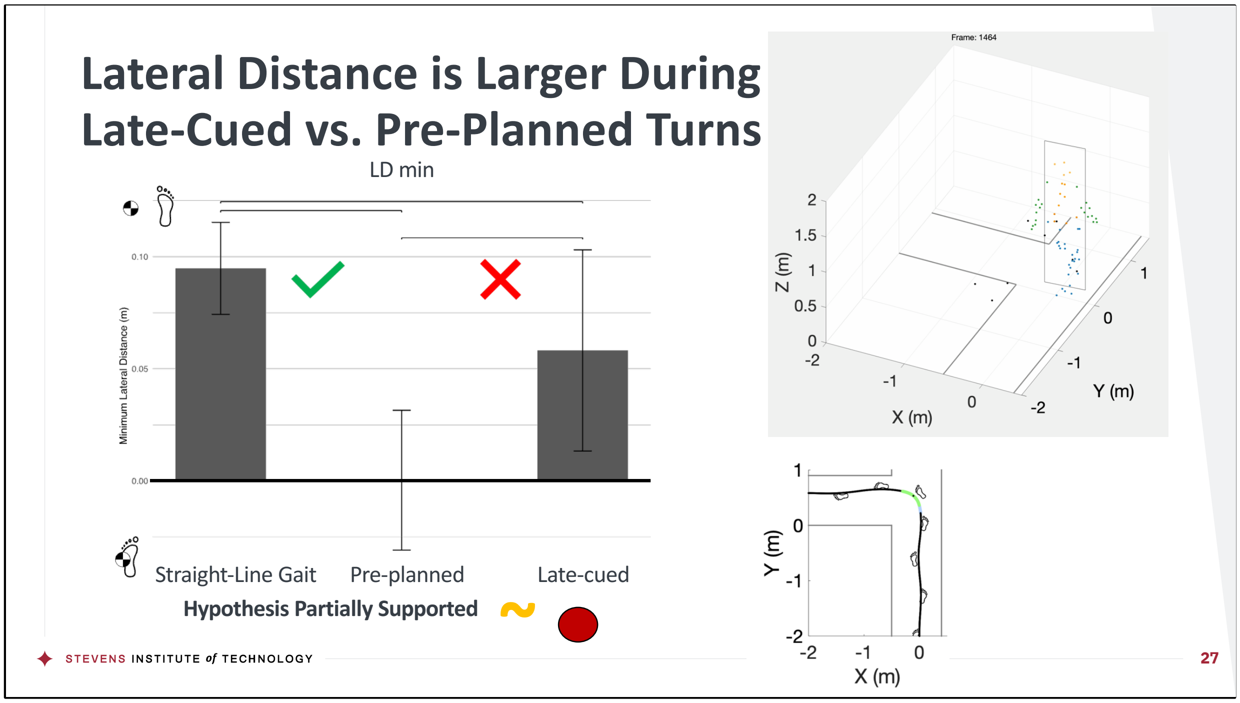

As I mentioned, some of the late-cued turns exhibit even lower lateral distance than did the preplanned turns. And so, for example, here's a trial where this red dot, way down at the bottom is the lateral distance minima for this particular trial, and in this case it seems that they found themselves with their left foot being the one that is in the intersection.

And so they had to make a very quick turn over this left foot. So as they're reaching the intersection, they determine that they need to turn. And so, therefore, they had to make this very late-cued turn, resulting in a lower lateral distance minimum.

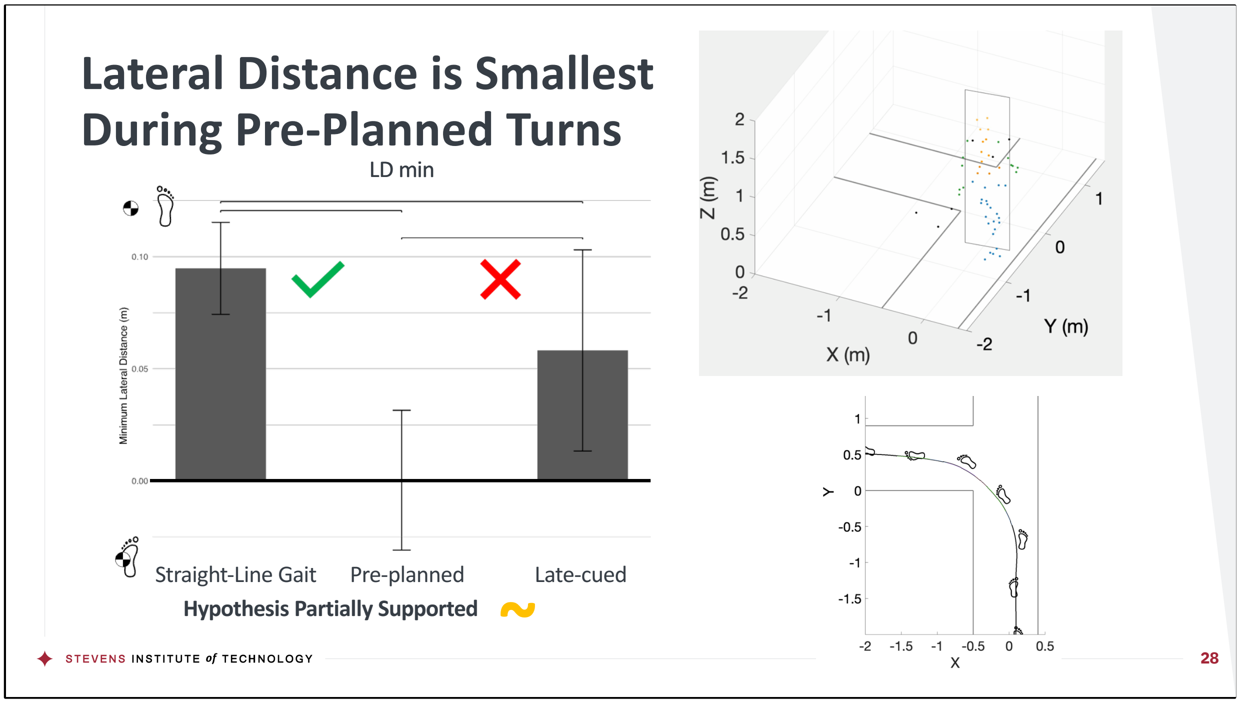

During preplanned turns, preplanned turns ended up looking like circular gait. So there's less variability on average during this task, and this finding is supported by prior research, that the center of mass shifts more laterally to the edge of the base of support. When, looking just at this domain of balance, you might think to yourself, Oh, well, then, preplanned turns are challenging balance more in the frontal plane in this metric.

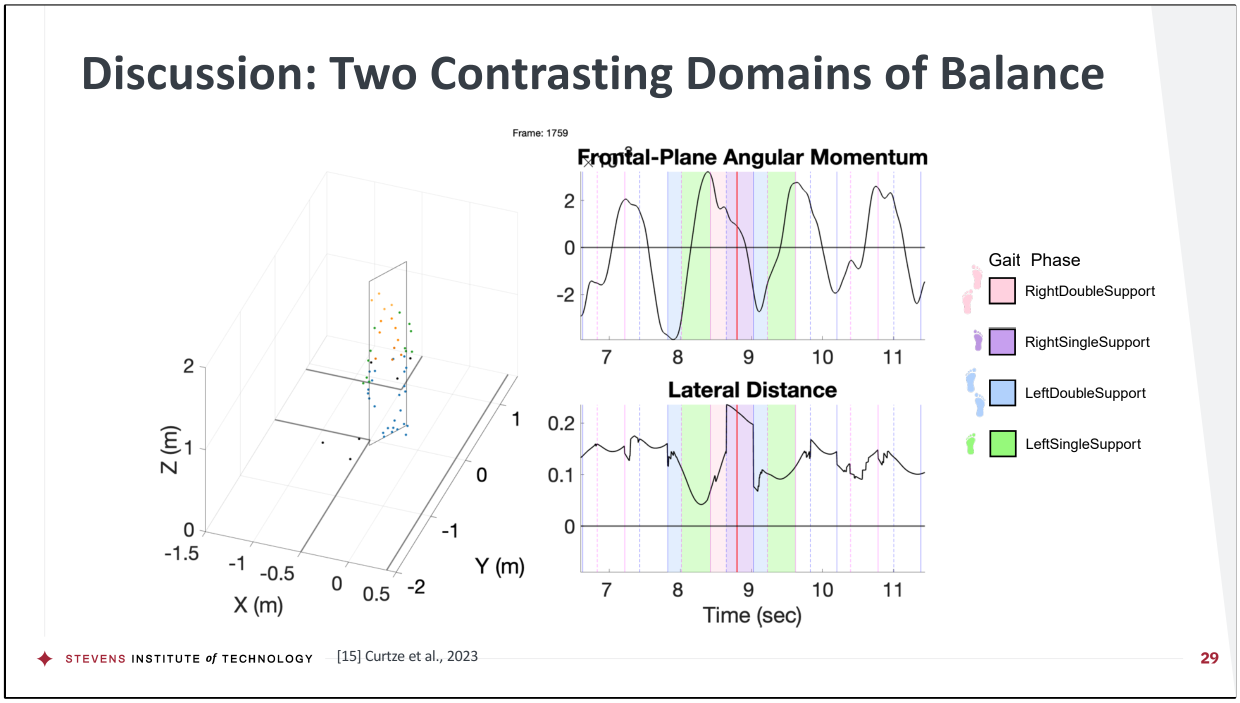

I want to make the point that these frontal plane metrics, angular momentum and lateral distance seem to kind of correct for one another. And so you can't look at one just in isolation. So, for example, here's a still image from one of our trials. If you see the red line around second 8 on both time series. There we note that at this point in time the frontal plane, angular momentum is actually quite large, and to the left.

But at the same time the lateral distance is large, so the center of mass is more centered between the feet. Whereas at a different point in time during this trial the lateral distance is at its minima, so the center of mass is nearest to that lateral or left edge of the base of support during this left turn. But at the same time the frontal plan. Angular momentum is quite large and to the right kind of correcting for that potential balance instability due to the lateral distance.

During a 3rd context, when the lateral distance is quite large, which again is a large leftward step the angular momentum is at a relatively small value, not contributing or perturbing to balance there. So again, these 2 domains interact.

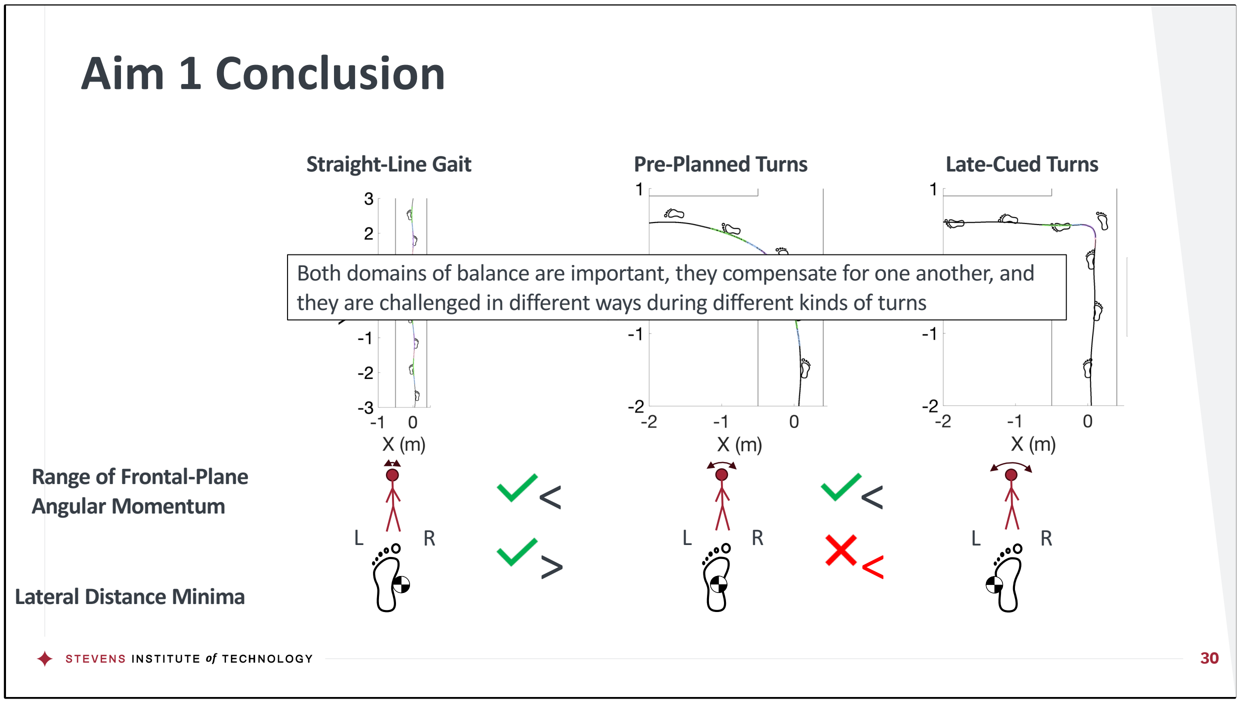

So to summarize the findings of this 1st aim. Our 1st hypothesis was supported that the range of frontal plane angular momentum was largest during late-cued turns, smaller during preplanned, and smallest during straight line gate. As the mechanical demand was increasing in late-cued versus preplanned versus straight line gait.

Our second hypothesis was partially supported. Preplanned turns and late-cued turns were both smaller than straight-line gait. However, late-cued turns actually exhibited on average larger lateral distance minimum.

The take home message here is that both domains of balance are important. They're challenged by late cued turns and preplanned turns, and they compensate for one another, and are challenged in different ways during different kinds of turns.

During my second aim, I'll talk about how the linear and angular momentum generation in the linear and angular momentum in the horizontal plane is generated to accomplish the straight line gait and turning movements

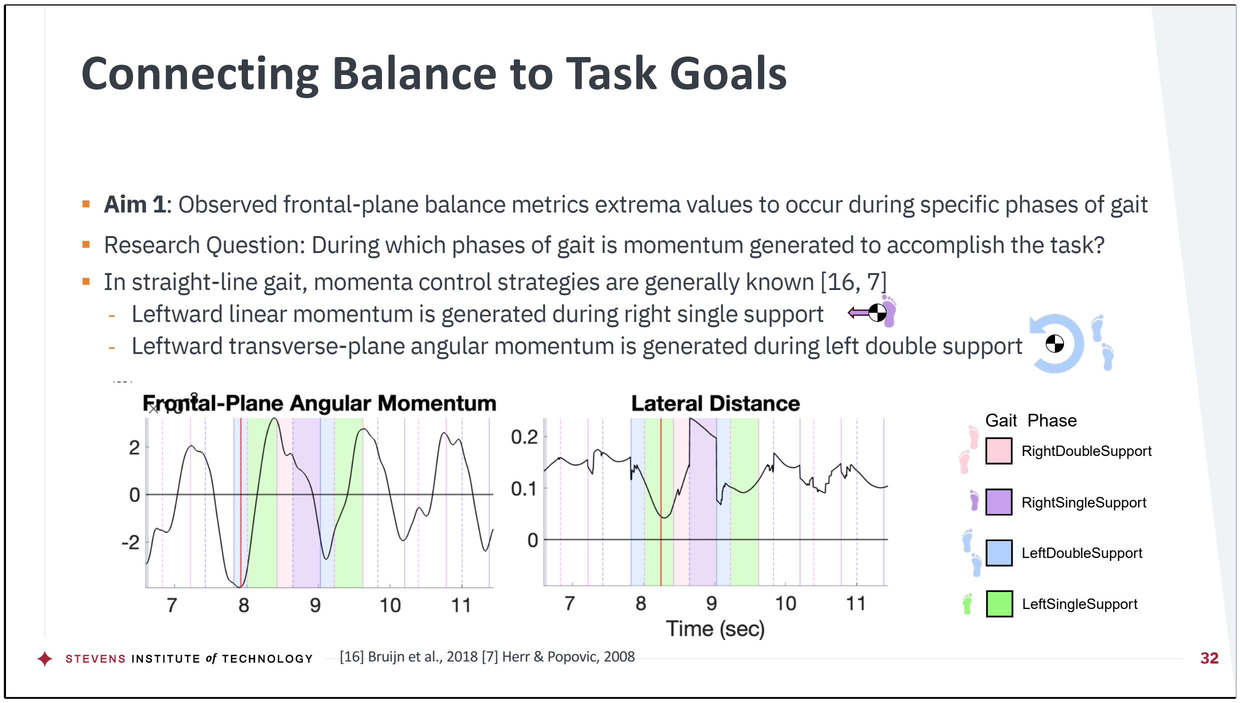

Recall that in aim one we observed that frontal plane balance metrics have their extrema values occur during specific phases of gait, so angular momentum tends to peak during double support, while lateral distance tends to reach its minimum value during single support.

This leads to the research question of during which phases of gait is the momentum actually generated in the horizontal plane to accomplish the goals of the task.

So during straight line gait, these momentum control strategies are relatively well known. So when we're looking at how leftward linear momentum is generated, it's known to occur during right single support as we're preparing for the left foot to come down so to act that out. If I'm just in right single support, with one foot on the ground, we push leftward to prepare for the left foot to come down.

In the transverse plane or horizontal plane, angular momentum is generated during left double support. So this is when the left foot is in front, but both feet are on the ground. This is when the rotation is generated. This change in angular momentum prepares for the right foot to step through, and double support is when this occurs, so that both the goals of translation and rotation can be simultaneously managed by both feet being in contact with the ground.

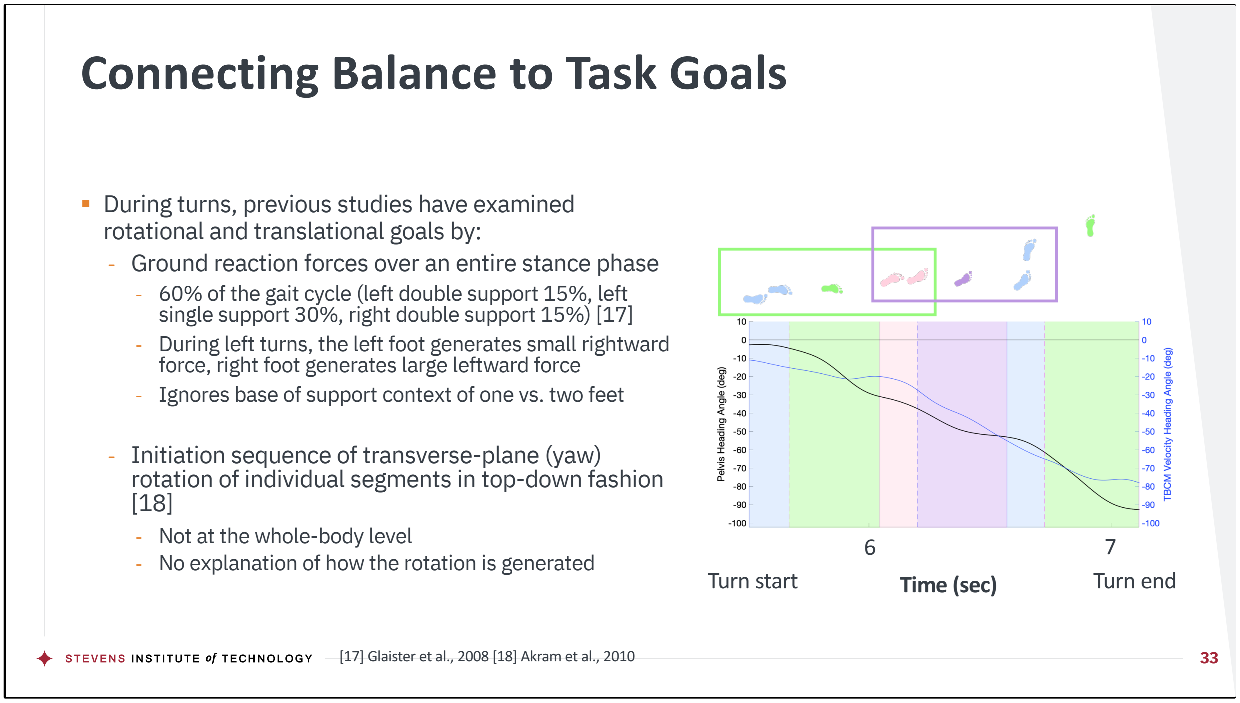

During turns, prior studies have examined these rotational and translational goals. For the translational component, they've looked at ground reaction forces over an entire stance phase. So an entire stance phase consists of about 60% of the gait cycle. This is 2 double support phases and one single support phase. So it's the entire time that one foot, let's say the left foot is in contact with the ground all the way through. This ignores the context of the base of support, again with 2 double support and one single support phase during that time.

They found that during left turns the left foot or the inside foot generates a bit of an outward or lateral force or medial force, whereas the outside foot, that right foot, generates a leftward or lateral force.

When looking at rotational goals, typically people focus on the sequence of initiation of each body segment in the transverse plane. And it's been found in prior research that turns are typically accomplished using a top down sequence of segmental rotation where 1st the head rotates, then the torso, then the pelvis, etc. And this is helpful, but it's not a whole body measure, and it also doesn't explain how the rotation is actually accomplished to perform this change of direction.

Mechanical Objectives to Turn

- **<u>Purpose:</u>** Determine which phase(s) of gait are responsible for generating leftward **linear & angular momentum** during straight-line gait and turns
  - Compare healthy young and older adults
- By identifying the specific phases of gait responsible for linear and angular momenta generation, we can better target therapies to address movement deficits.
  - Same phase(s) as frontal-plane balance extrema?

Healthy older adult participant

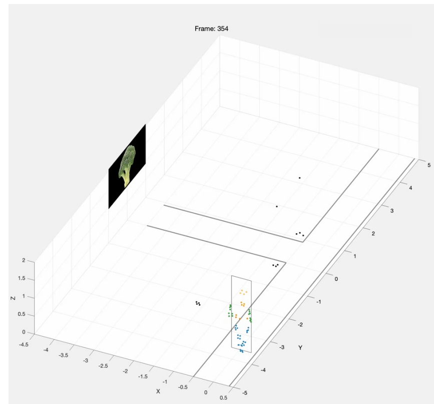

Therefore, the purpose of this study was to determine which phases of gait are responsible for generating leftward **linear & angular momentum** during straight-line gait and left turns in healthy young and older adults**.**

By identifying the specific phases of gait responsible for generating leftward linear and angular momenta, we can better target therapies to address movement deficits. For example, if the transverse plane momenta is being generated at the same time that frontal plane balance metrics are at an extrema value, that further suggests targeting those phases of gait to train turning gait.

Also, by looking within gait phase, this method can accommodate turns performed with any number of steps, avoiding the need to prescribe a certain number of steps during the turn as is commonly done.

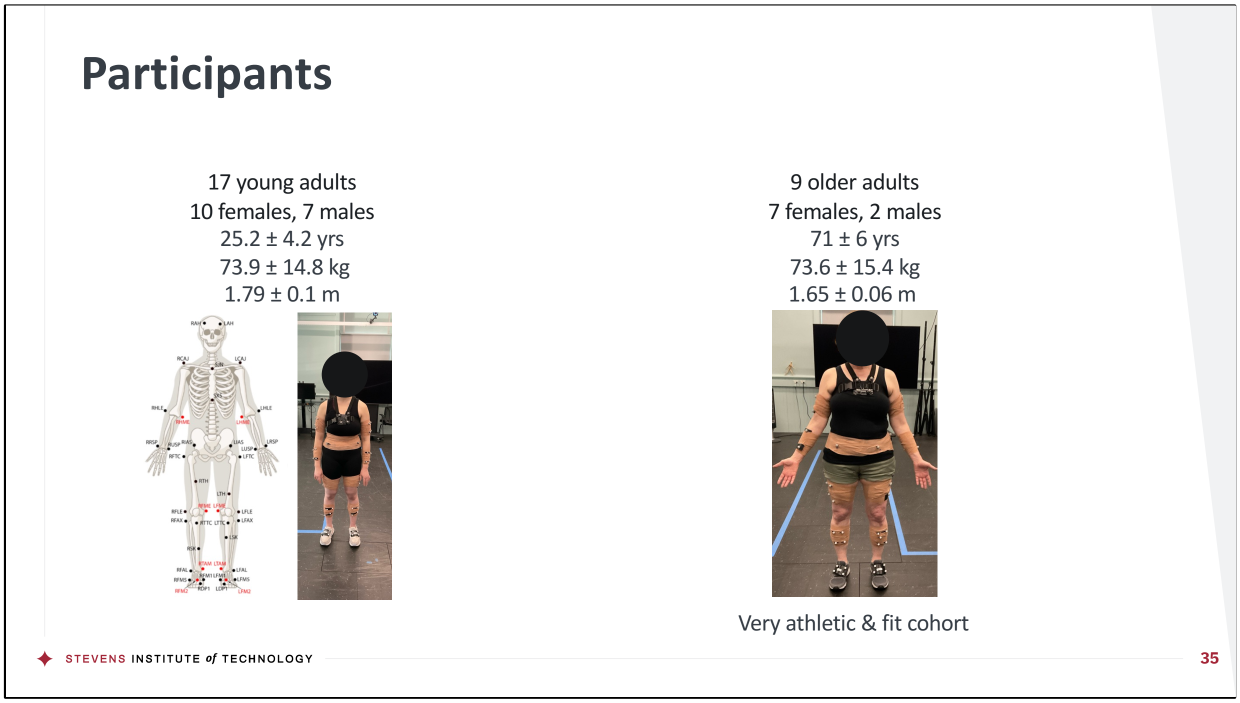

To accomplish these goals, we examined data from the same 17 young adults as in Aim 1, as well as a new cohort of 9 healthy older adults. Data on late-cued turns in older adults is not reported here, as their data collection sessions often ended before they could complete this task.

I want to make the point that this cohort was a relatively fit and athletic cohort average age only 71, and we found them at the senior center, where they were doing things like playing basketball, and reported walking a lot in Hoboken, going up and down stairs frequently, etc. So a relatively fit cohort of of older adults.

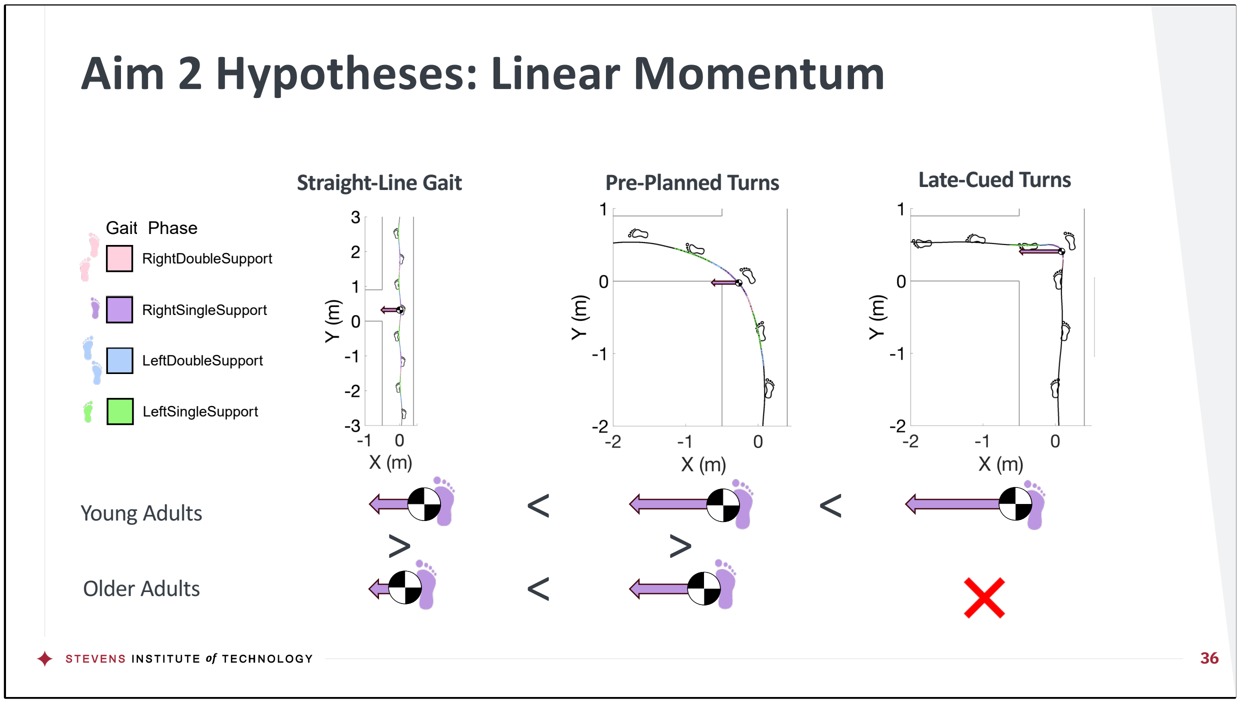

We asked each cohort to walk straight, walk and turn in a pre-planned fashion, and young adults also performed late-cued turns. We hypothesize that right single support will generate the largest change in leftward linear momentum in each of the three tasks, just like in straight-line gait. For both age groups, we hypothesize that more leftward linear momentum will be generated during turns vs. straight-line gait, and for young adults that late-cued turns will generate even more. We also hypothesize that young adults will generate larger linear momentum vs. older adults, due to their increased strength, and the suddenness of the movement.

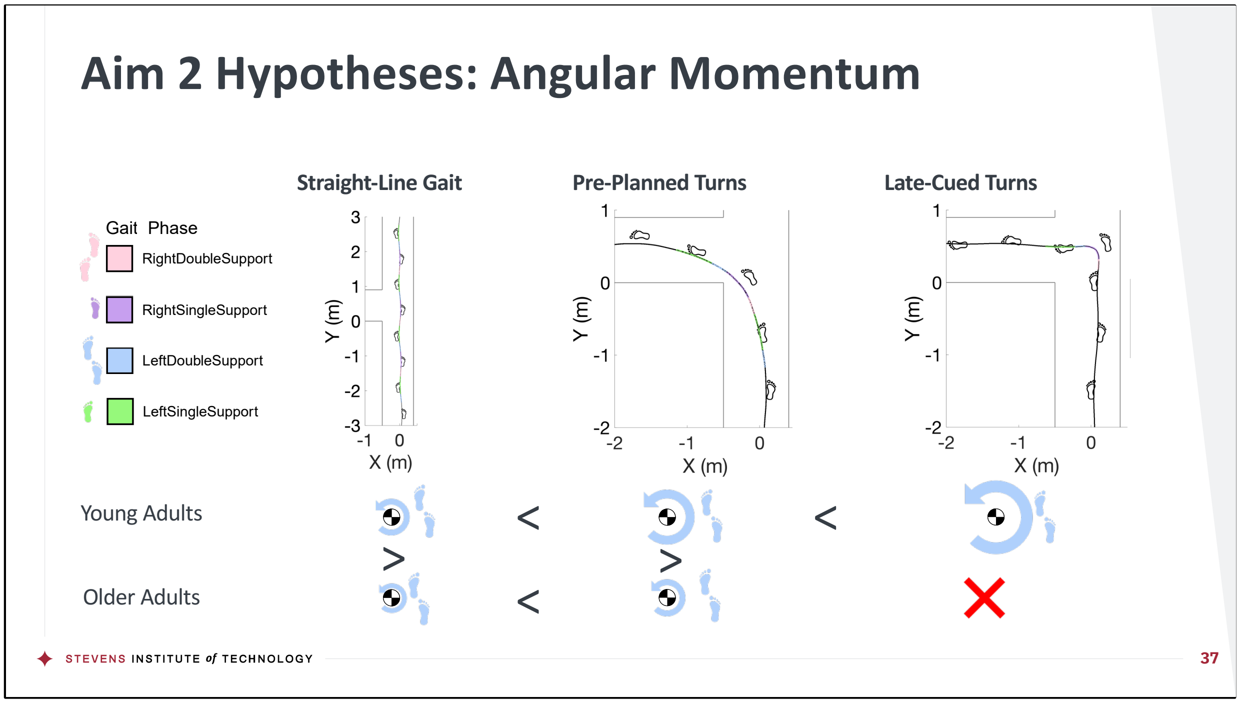

We anticipate essentially the same patterns to be true for leftward angular momentum generation. Largest in late-cued vs. pre-planned vs. straight-line gait for both age groups, and young adults generating more angular momentum than older adults.

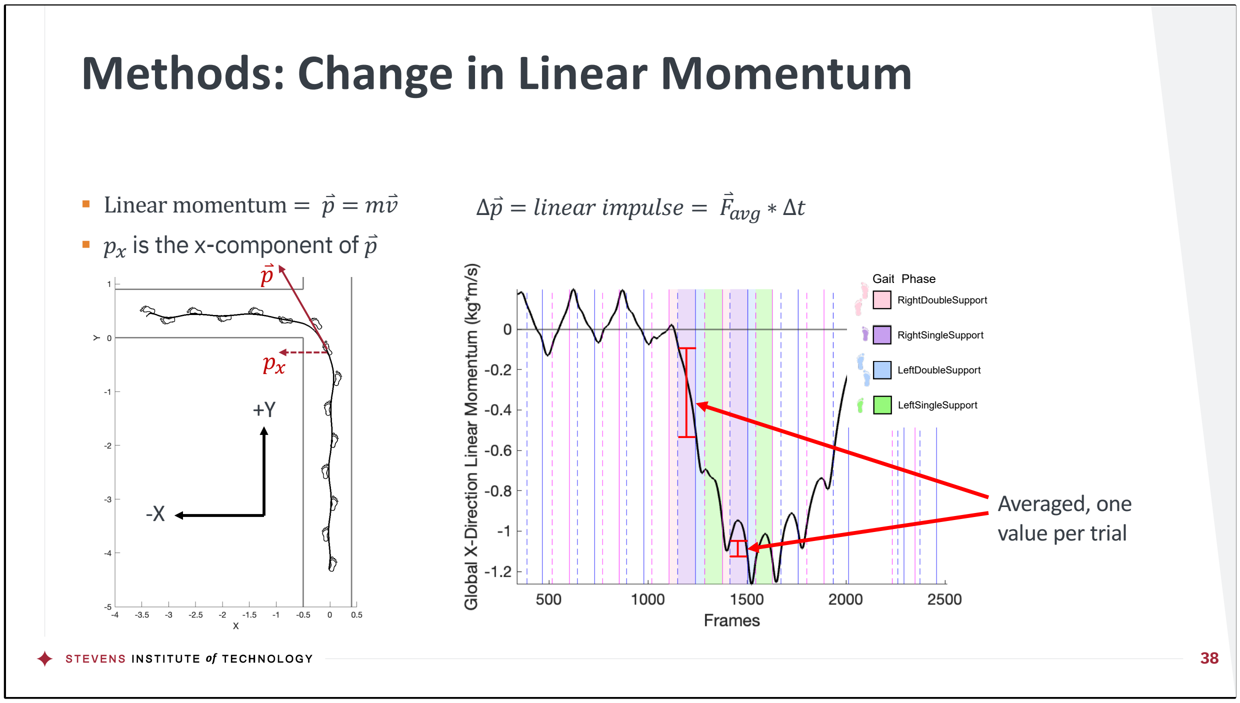

To compute the change in linear momentum, first, we need to compute linear momentum. So this is the linear velocity of the center of mass times the person's mass, and that gives us this P vector, that's the letter for linear momentum. And again, note that the goal for a left turn is to generate this linear momentum in the lab's Global Leftward axis. So that is this minus X axis on the figure there.

And we're interested in the change in linear momentum, because this is equivalent to the linear impulse and linear impulse is equal to the average force times the duration over which it's applied. So this is a fundamental variable that describes the change of momentum for the center of mass.

And again, we're only interested in this leftward generation. And so we take the X component in the global coordinate system.

And so here's an example of what that looks like. So note that during the turn is the shaded regions for the colored by gait phase. Before the turn you can see that the center mass is shifting, oscillating side to side. And then, during the turn, this leftward linear momentum is generated. So we see a larger negative value or more negative value, and then, at the end of the turn, they very quickly. Once they've completed the turn they run out of walkway, and so that's why you see the value going back towards 0, they have to stop.

So again, we're interested in this change in linear momentum or this linear impulse analog. And so these red bars are showing the the Delta final minus initial for the linear momentum value, and notice that there are 2 of them during this particular trial. And so, whenever we had more than one instance of a phase of gate, we would average them so that there's 1 value entered into our statistical analysis per trial.

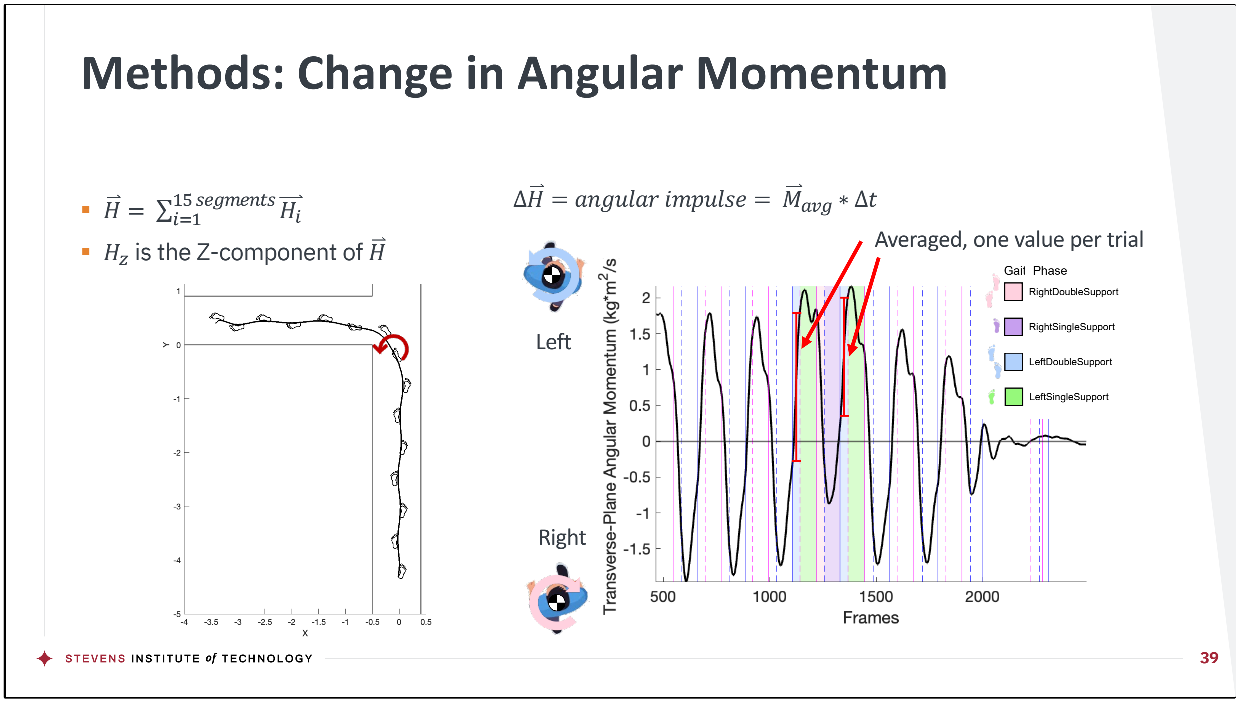

Very similar methods for the angular momentum. It's computed the same as it was during aim one, except now we're looking at the horizontal plane or transverse plane component. So we just take the z component of angular momentum. And again, this is equivalent. This change in angular momentum is equivalent to angular impulse, which is the average moment times the duration over which it's applied. And note that we're defining leftward as a positive value and rightward is a negative value.

So again, we're interested in the change. So there's red bars are showing the change in each instance of left double support. And again, when we have more than one instance of that gate phase. We average them so that there's 1 value per gait phase per trial

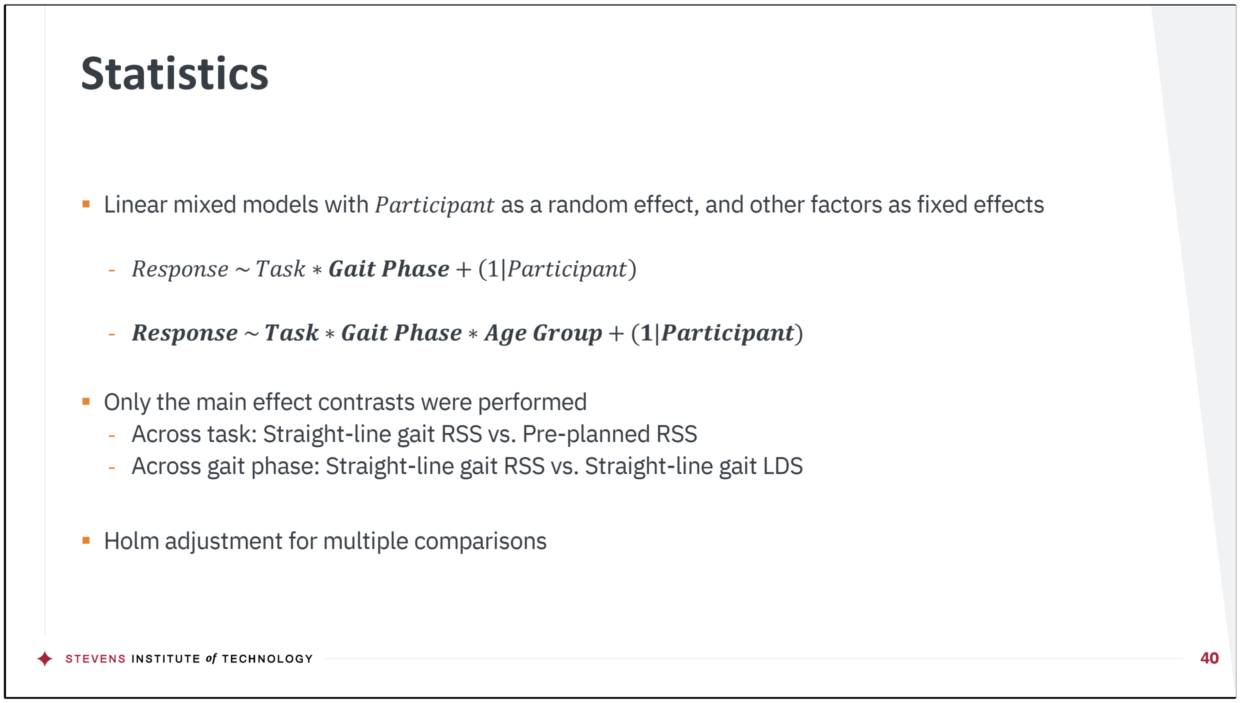

We again used linear mixed models with Participant as a random effect, and other factors as fixed effects. Now we add Gait Phase to the model to examine within each phase of gait. A second model with an Age Group term facilitates comparisons across age groups.

Note that only the main effect contrasts were performed. An across task main effect is one where only the task but not the gait phase changes, such as SLG RSS vs. PP RSS. An example of an across gait phase, within task, main effect is SLG RSS vs. SLG LDS.

I also applied the Holm adjustment for multiple comparisons.

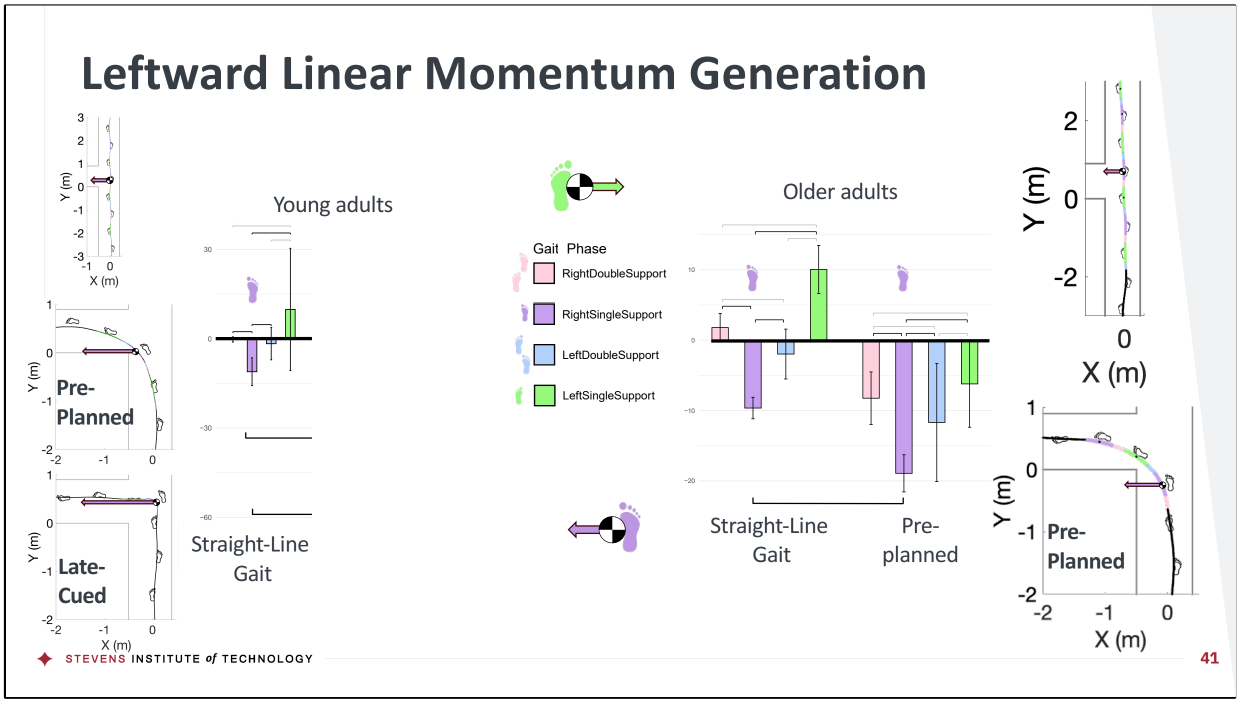

Next I'll show bar graphs of our findings at the group level. In the middle is the legend showing which tasks are which colors on the bar graphs, and the purple and green arrows indicate the leftward and rightward linear momentum generated by right and left single support, respectively. At the group level, our first hypothesis regarding the change in linear momentum was fully supported by the fact that RSS is the largest change in leftward linear momentum for all tasks in both age groups, and is larger in late-cued vs. pre-planned turns, and both turns vs. straight-line gait in both age groups.

[act out] Pushing leftward with the right foot facilitates the largest leftward step without shifting the center of mass position disadvantageously relative to the base of support. If this momentum were generated with the left foot instead, it would result in a crossover step over the lateral edge of the base of support. Knowing that the right single support phase is responsible for pushing leftward during left turns can help target rehabilitation protocols for patients with movement deficits. For example, these findings show that the right hip abductor should be targeted to generate this lateral movement, and even more so during late-cued turns.

Next, when comparing between age groups, the young adults generated more linear momentum during pre-planned turns than did the older adults. This makes sense along with older adults using more steps to complete the turn, they simply don't need to generate as much leftward linear momentum in an average right single support phase. This was a relatively fit cohort of young adults, and perhaps older adults with balance deficits who walk even slower during turns would generate even less linear momentum

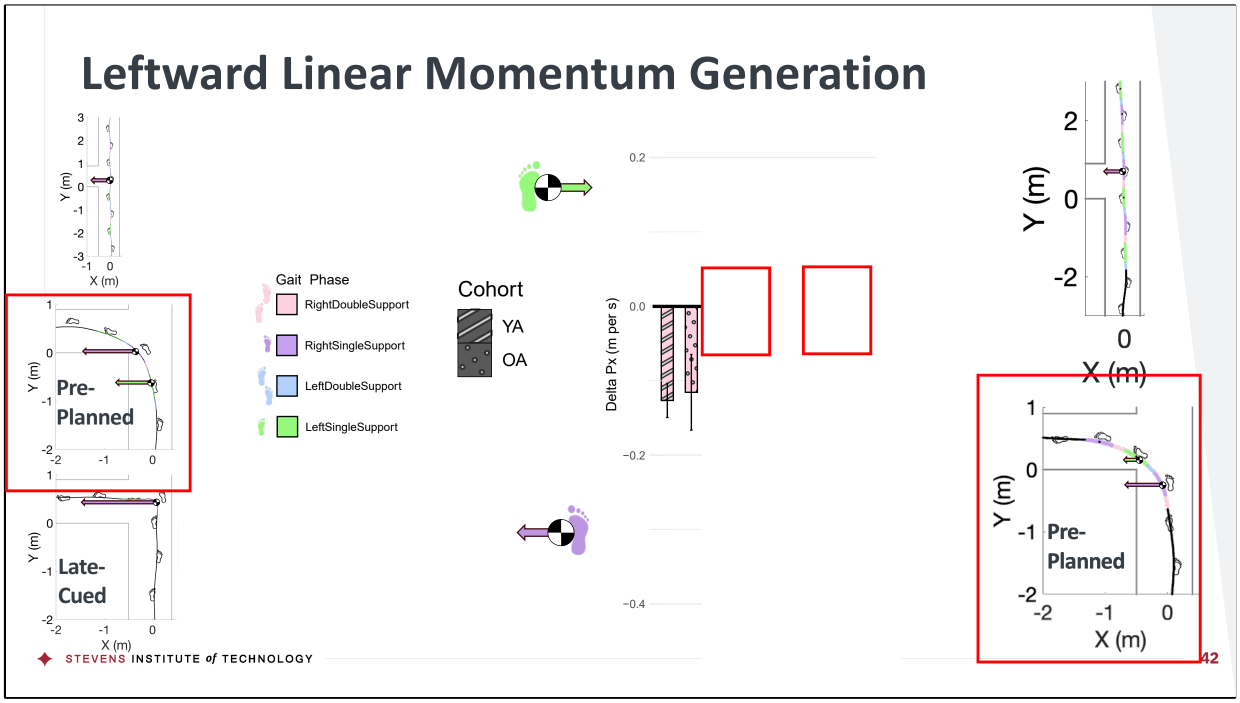

Next I'll show bar graphs of our findings at the group level. In the middle is the legend showing which tasks are which colors on the bar graphs, and the purple and green arrows indicate the leftward and rightward linear momentum generated by right and left single support, respectively. At the group level, our first hypothesis regarding the change in linear momentum was fully supported by the fact that RSS is the largest change in leftward linear momentum for all tasks in both age groups, and is larger in late-cued vs. pre-planned turns, and both turns vs. straight-line gait in both age groups.

[act out] Pushing leftward with the right foot facilitates the largest leftward step without shifting the center of mass position disadvantageously relative to the base of support. If this momentum were generated with the left foot instead, it would result in a crossover step over the lateral edge of the base of support. Knowing that the right single support phase is responsible for pushing leftward during left turns can help target rehabilitation protocols for patients with movement deficits. For example, these findings show that the right hip abductor should be targeted to generate this lateral movement, and even more so during late-cued turns.

Next, when comparing between age groups, the young adults generated more linear momentum during pre-planned turns than did the older adults. This makes sense along with older adults using more steps to complete the turn, they simply don't need to generate as much leftward linear momentum in an average right single support phase. This was a relatively fit cohort of young adults, and perhaps older adults with balance deficits who walk even slower during turns would generate even less linear momentum

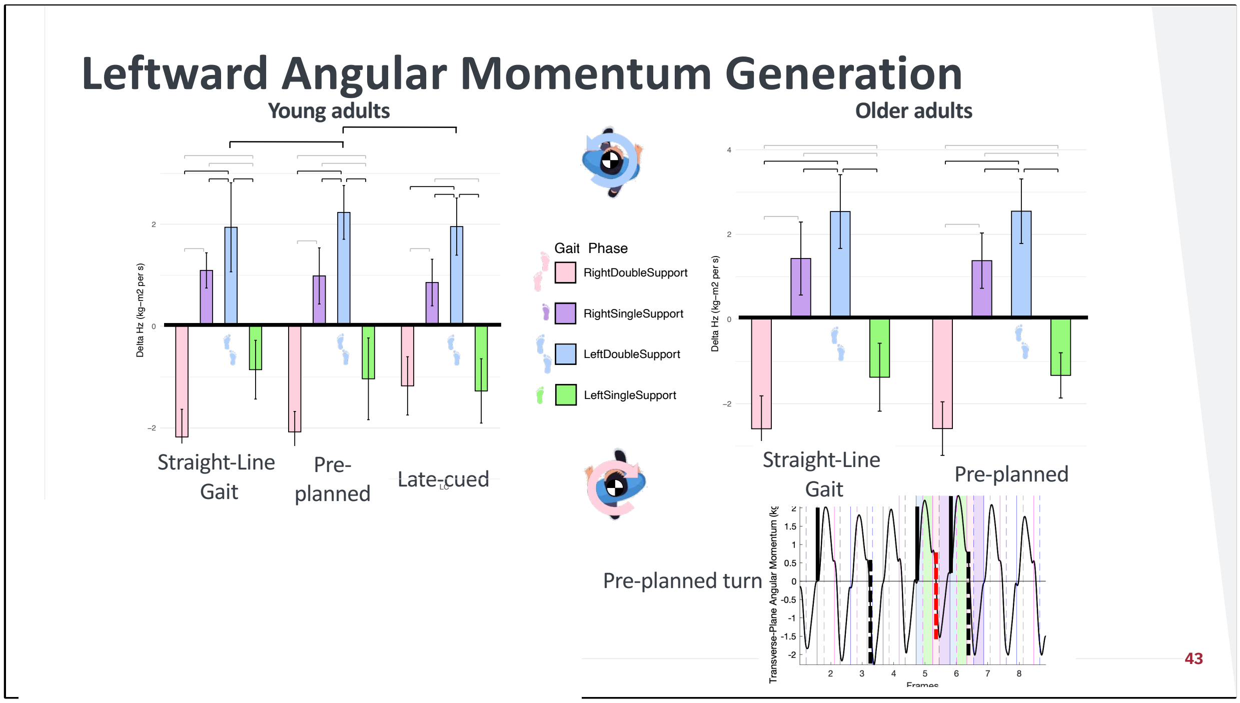

Our second hypothesis that leftward transverse-plane angular momentum is generated most during left double support phase was partially supported. The left double support phase did show the largest change in leftward angular momentum in both age groups. This makes sense to help facilitate the right foot to swing forward. Contrary to our hypothesis, in young adults the task with the largest change in transverse-plane angular momentum was pre-planned turns, while in older adults there was no difference between tasks. For the young adults, it makes sense that more rotation would be generated during pre-planned vs. straight-line gait, but I was surprised to see that pre-planned turns' change in angular momentum was larger than late-cued turns and straight-line gait. More transverse-plane rotation is certainly needed for late-cued turns relative to walking straight, yet late-cued turns' left double support value matches but does not exceed that of straight-line gait! Why doesn't the left turn generate more leftward angular momentum than walking straight? I think it is because it also generates less rightward angular momentum, so it doesn't need as much leftward angular momentum. The benefit of this strategy is not yet clear, but I hypothesize that it may help with fixating vision on the visual cue, especially because the head has to rotate quickly to look at the cue.

The older adult cohort did not show any change in angular momentum generation between straight-line gait and pre-planned turns, perhaps because they walk slower and so complete the turn over a longer period of time.

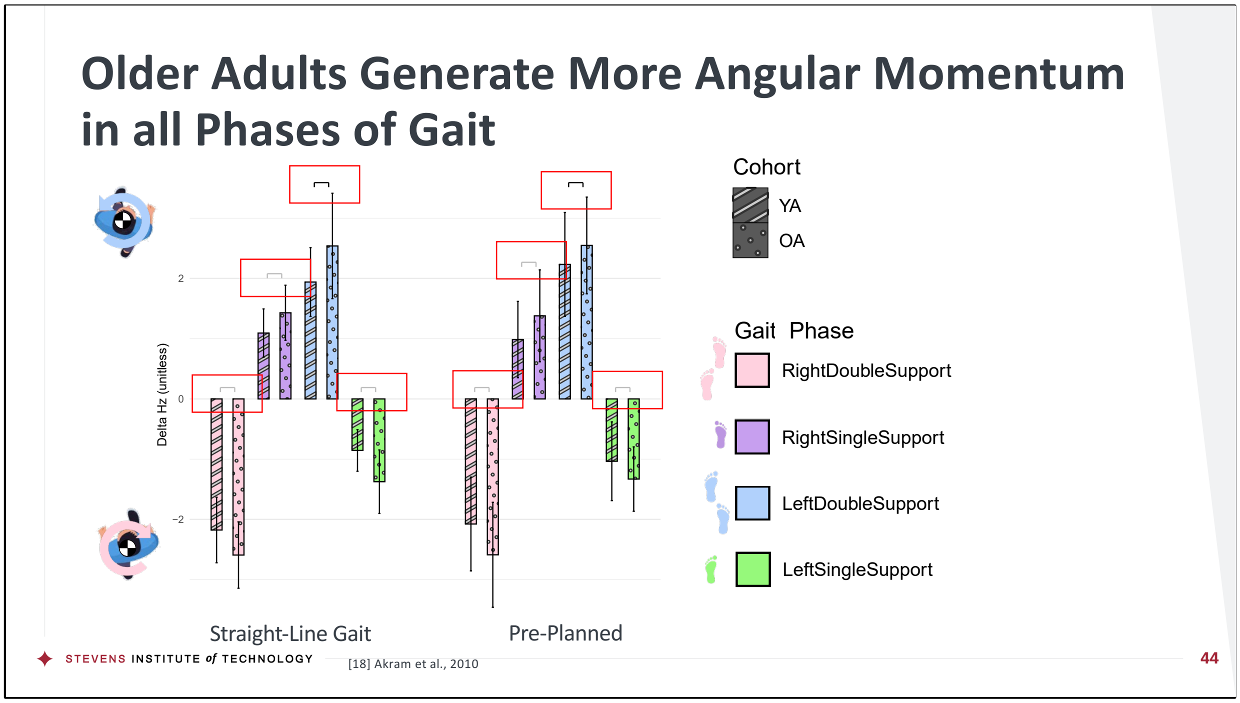

When comparing across age groups within straight-line gait and pre-planned turns only, we see that older adults in the polka dots generate more transverse-plane angular momentum in each phase of gait than do young adults in the striped bars. This also prompts future research questions to understand why older adults would generate more transverse-plane rotation than young adults. Perhaps it is due to a more en-bloc rotation, which older adults are known to exhibit during pre-planned turns? The theory would be supported if the amount of inter-segmental angular momentum cancellation decreases in older compared to young adults.

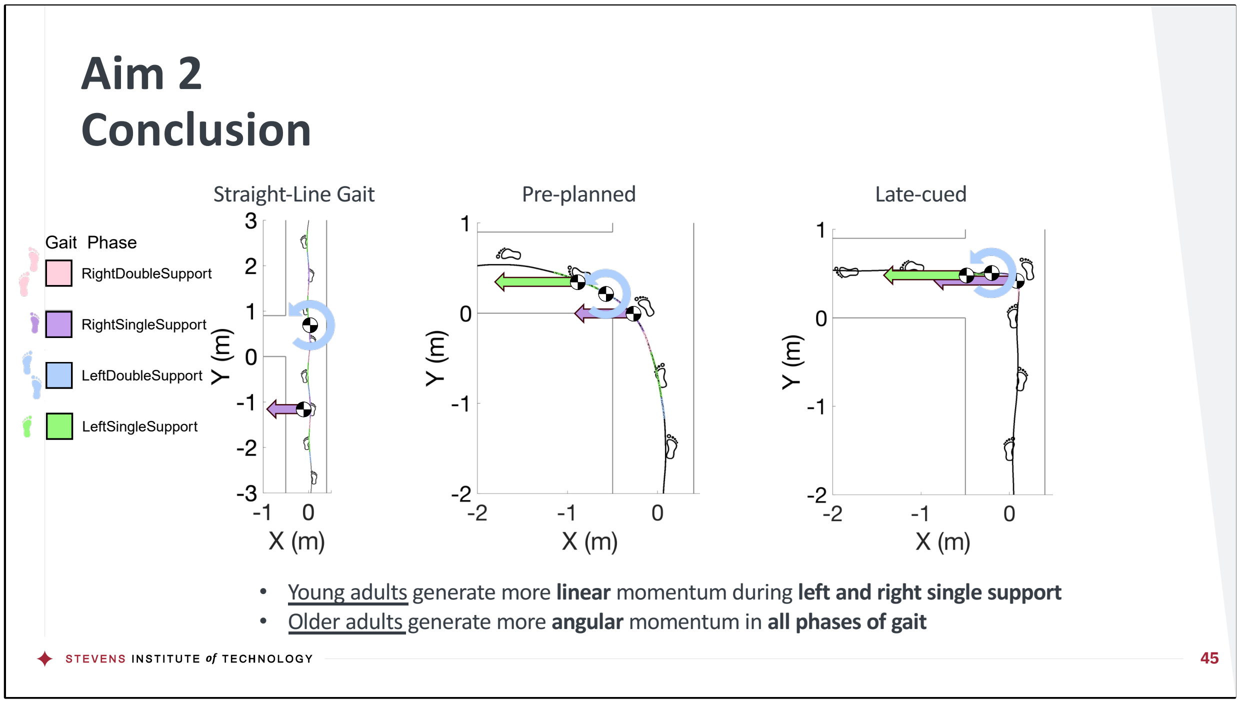

To summarize this Aim's findings, the right single support phase pushes leftward in straight-line gait and turns to facilitate COM translation without compromising COM position relative to the base of support by needing a crossover step. Second, the left double support phase generates the largest leftward change in rotation in straight-line gait and turns to facilitate the right foot swinging forward. These findings may help design rehabilitative protocols if a patient is observed to have deficits in generating momentum.

Note, these older adults are a relatively fit cohort, and the age-related differences may be different or more pronounced in an older cohort with advanced balance deficits.

And finally, the young adults' late-cued turns rotated less leftward and rightward, which may be an attempt at simplifying control to facilitate the head to turn and look at the visual cue.

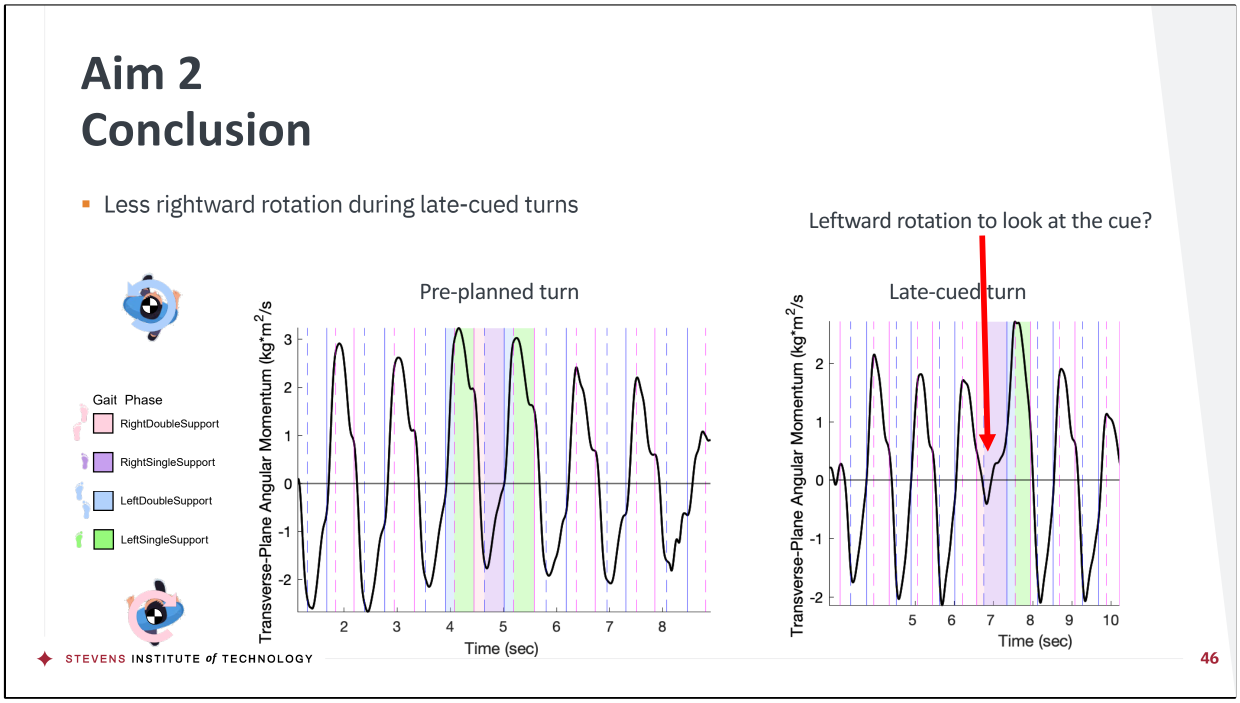

Finally, I want to highlight again that when evaluating these findings, we should remember that 10 of the 17 young adults had a different markerset and slightly different corner pole placement and shape that may have affected their turning behavior and our measurement accuracy. However, the 7 female young adults of the 17 young adult cohort that did have the same data collection methods as the older adults did also show the same trends as were reported here, so I don't think this issue substantially affects our findings.

To summarize this Aim's findings, the right single support phase pushes leftward in straight-line gait and turns to facilitate COM translation without compromising COM position relative to the base of support by needing a crossover step. Second, the left double support phase generates the largest leftward change in rotation in straight-line gait and turns to facilitate the right foot swinging forward. These findings may help design rehabilitative protocols if a patient is observed to have deficits in generating

And finally, the young adults' late-cued turns rotated less leftward and rightward compared to pre-planned turns. I hypothesize that this may be a mechanism to limit rotation, which may be an attempt at simplifying control to facilitate the head to turn and look at, and perceive, the visual cue. To test this theory, future research could examine angular momentum control in late-cued turns cued via auditory cue, which does not require visual fixation. If during that task, the change in angular momentum is larger, then we can infer that this lower change in angular momentum may assist with stabilizing the head during the turn and look movement.

STEVENS
INSTITUTE OF TECHNOLOGY
1870

Aim 3

Effect of Gait Speed

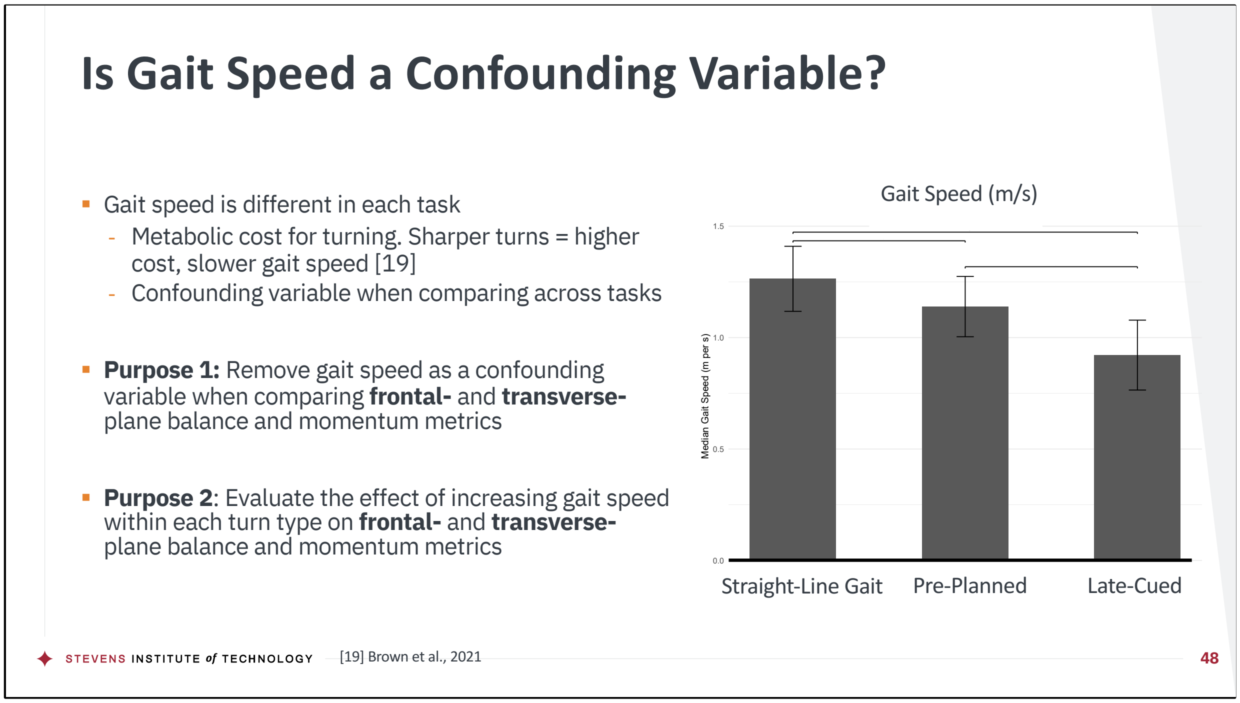

In Aims 1 and 2, parsing changing movement strategies from changes in momentum magnitude is difficult, as gait speed, and therefore "total momentum" is different between tasks. Therefore, the first goal of this aim is to remove gait speed as a confounding variable by asking participants to walk and turn faster than their preferred speed, at a speed that matches their straight-line gait speed. This will help isolate the changes in momentum that are due to varying gait speed vs. the different task goals.

The second goal of this study is to evaluate the effect of this increase in gait speed during turns on the frontal- and transverse-plane metrics reported in Aims 1 and 2. This helps understand how sensitive these frontal- and transverse-plane balance and momentum metrics are to increases in gait speed. If a metric is more sensitive to increasing gait speed, it may indicate that that metric can be trained just by increasing gait speed, or that during rehabilitation slower gait speeds should be used so as not to overly challenge the person.

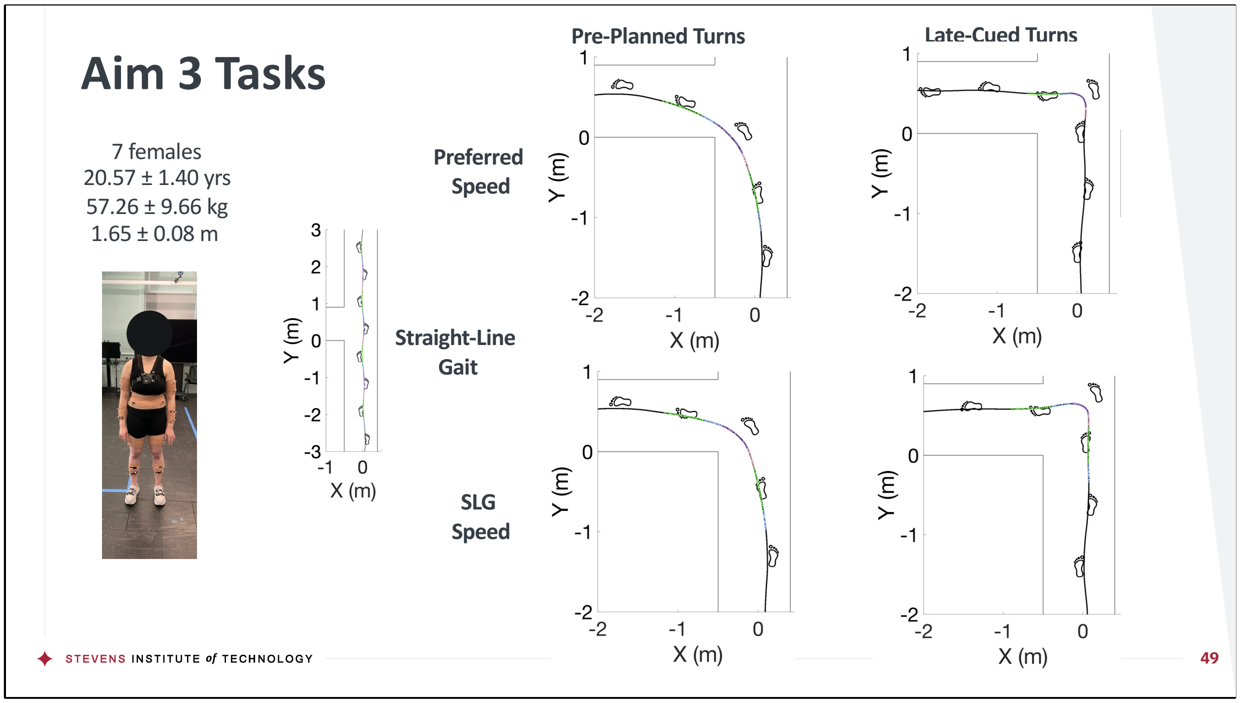

To accomplish these goals, we asked 7 young healthy adult females to perform the same three tasks as in Aims 1 and 2, as well as pre-planned and late-cued turns at a speed matching their straight-line gait speed, and were corrected and trials repeated if their speed did not match that of their straight-line gait.

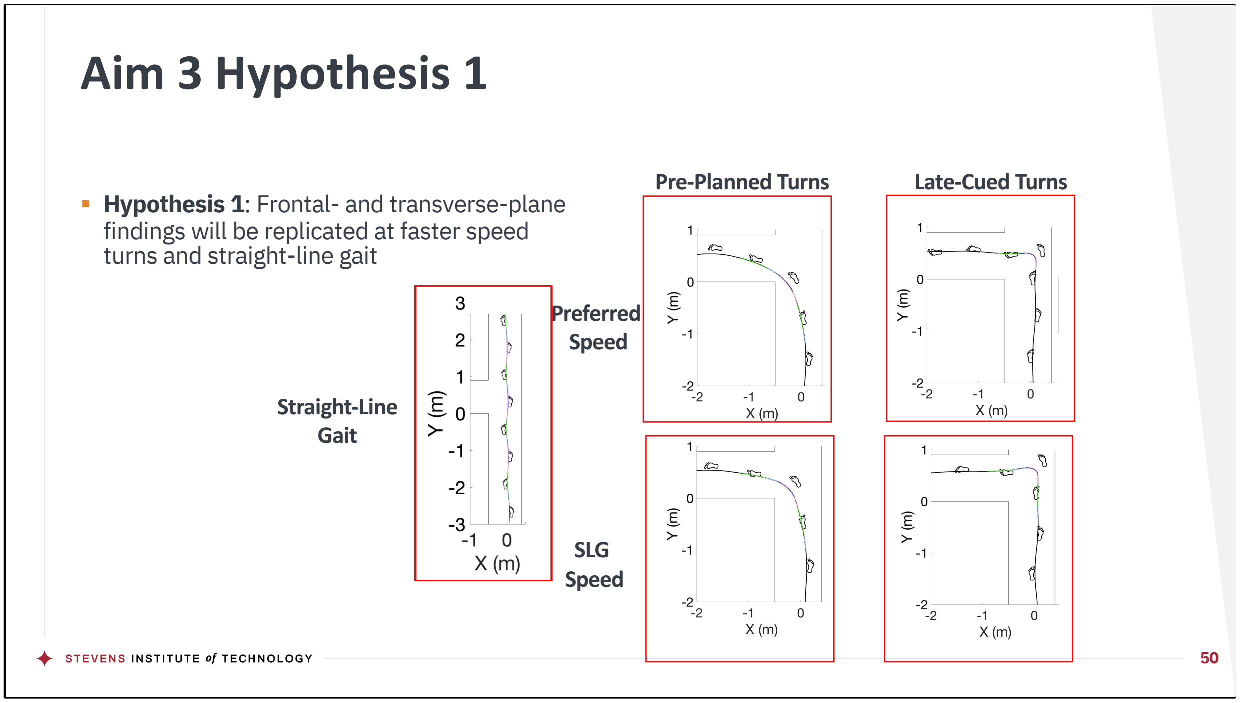

Previously we were looking at the preferred speed tasks. For our first hypothesis, we're asking the question of do we see the same patterns, the same findings at this faster speed that we did at the preferred speed?

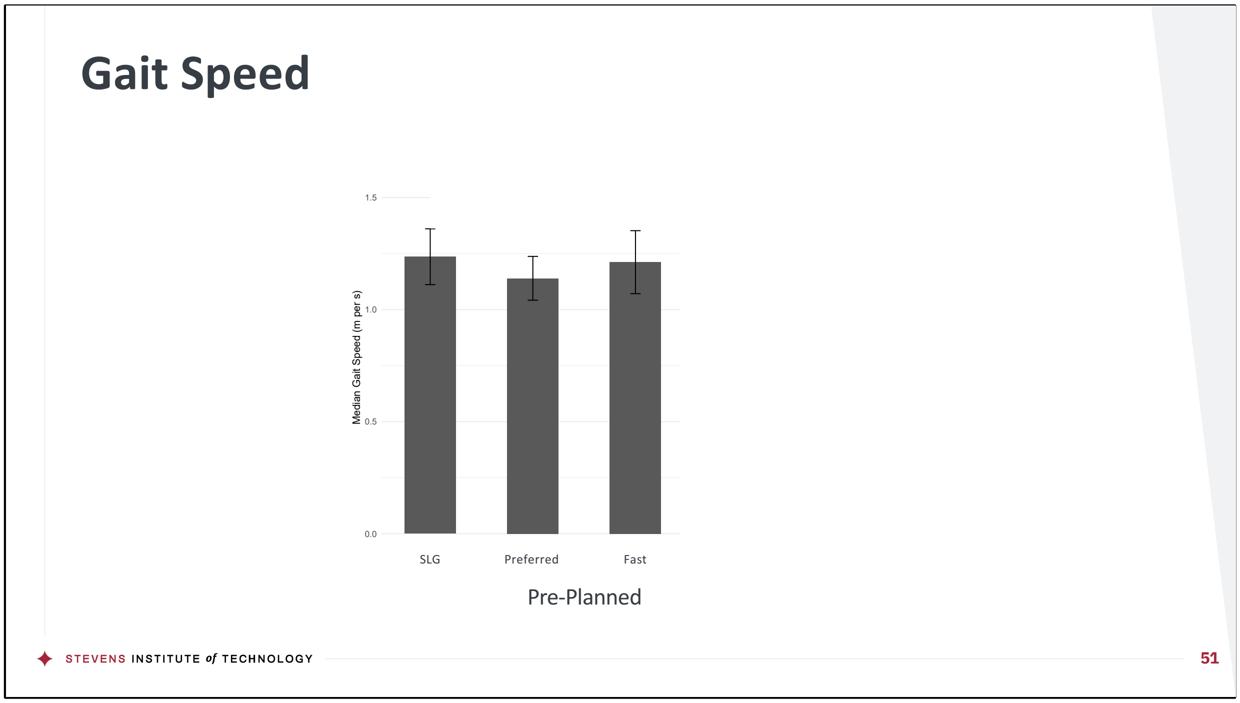

So the 1st question is, did we actually successfully induce this faster gate speed in our participants? And the short answer is, yes. During preplanned turns, so we can see that the faster preplanned turns down here were significantly faster than the preferred speed preplanned turns indicating we did statistically significantly increase their speed.

The lack of difference between the straight line gate bar and the fast preplanned turn speed bar indicates that this is not different from their straight line gate speed.

So we did, in fact, increase their gait speed to match straight line gait during preplanned turns. However, during late-cued turns, participants were unable to maintain their straight line gait speed during late-cued turns, and so they were performed at a slower speed.

We think that this is because you simply need more time to perceive the cue. When we asked them to walk faster, oftentimes they would almost overshoot the intersection. And so that was, we think, the limiting factor. But we did successfully induce an increase in gait speed between the 2 speeds of late-cued turns.

Pre-planned Turns at Different Speeds

Preferred speed pre-planned turn

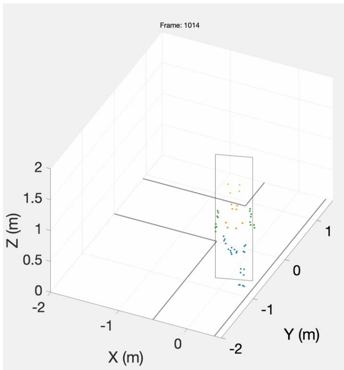

Faster speed pre-planned turn

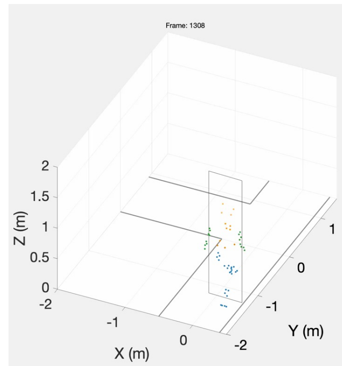

Okay, so this slide is to indicate that the preplanned turns actually was a relatively minor increase in gate speed only about 0.1 meters per second. So on the left you'll see a preplanned turn performed at their comfortable or preferred speed. It's only a couple seconds long. And then on the right we'll see the faster speed preplanned turn. It's a little bit faster, but it's not life changing faster.

Late-Cued Turns at Different Speeds

Preferred speed late-cued turn

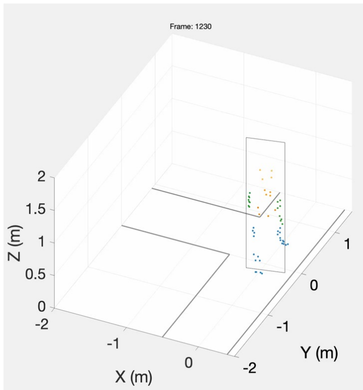

Faster speed late-cued turn

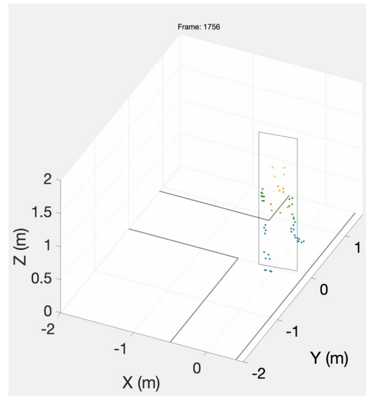

For the late-cued turns now, with preferred speed on the left and the faster speed on the right, you can kind of tell that there’s a bit of a speed increase on the right. You can tell that they're a little bit more surprised and and execute the turn just a bit more quickly, so slightly more difference between late-cued faster and preferred speed just visually before I get into the main results, despite a similar magnitude increase in in the gait speed.

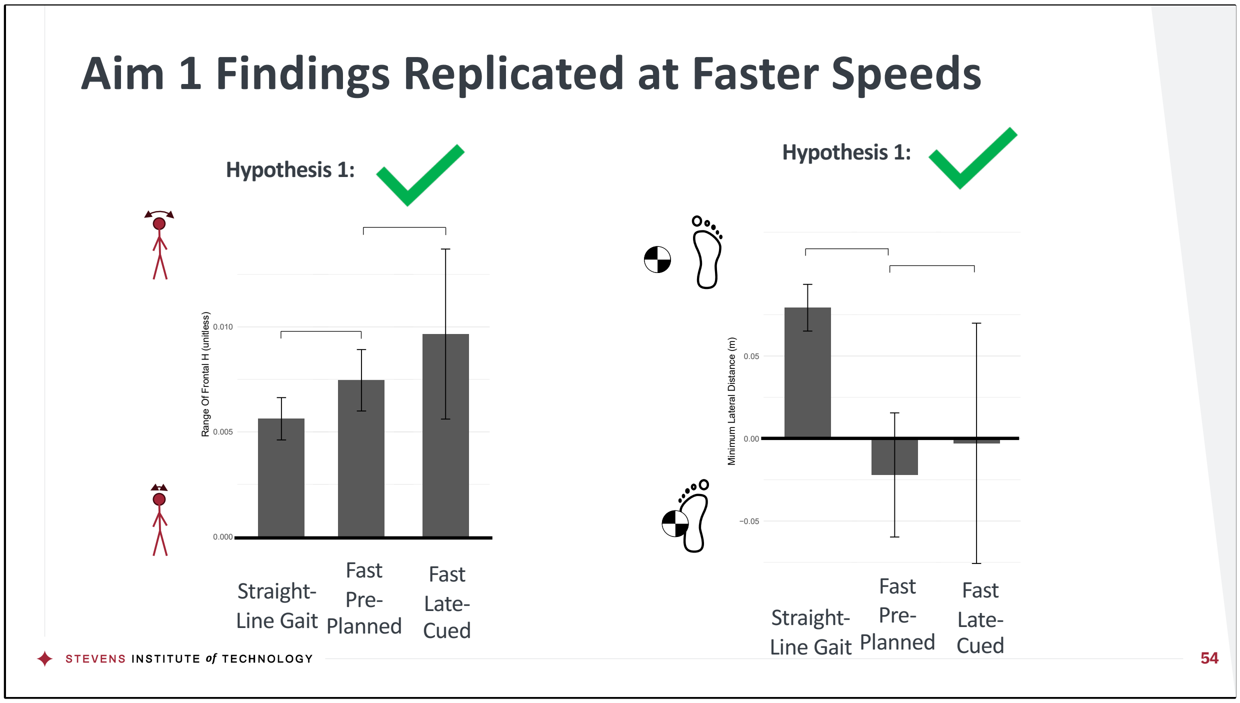

So to rip the Bandaid off, did we find at faster speeds that our findings at preferred speeds were replicated? Short answer, yes. We found that the range of frontal plane, angular momentum in the frontal plane was largest in late-cued turns, smaller in preplanned and smallest in straight line gait. This, of course, was expected, as the mechanical demand is still greatest in late cued turns, smaller in preplanned, etc.

And for the lateral distance we again found that we replicated our previous findings that the straight line gait had the largest lateral distance minima, smallest during preplanned turns and medium during the late-cued turns.

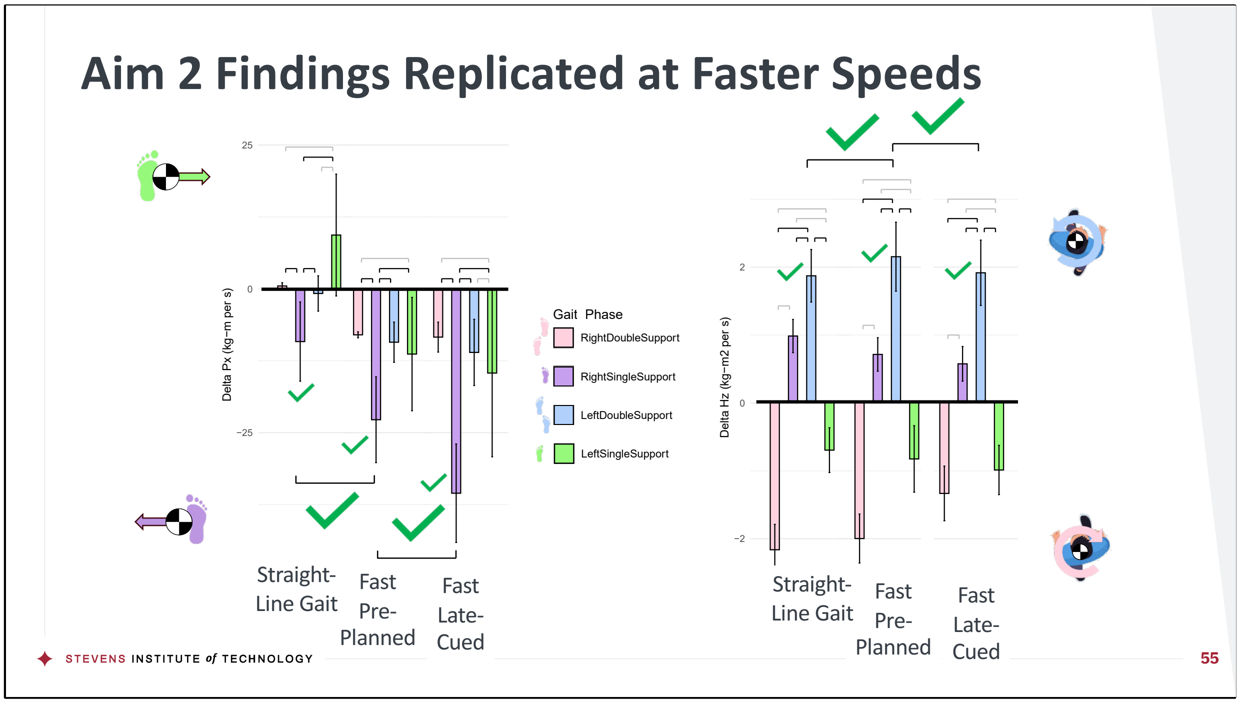

In the transverse plane we also managed to replicate our findings at preferred speed, so the right single support again generated the most leftward linear momentum during each task and leftward angular momentum was generated during left double support. Across tasks, we observed the same relationship at this faster speed between tasks, as we did at preferred speed. Late-cued being the largest leftward linear momentum generation, less so during preplanned and less during straight line gait. And we observed the largest leftward angular momentum generation again during preplanned turns and smaller during straight line gate and late cued.

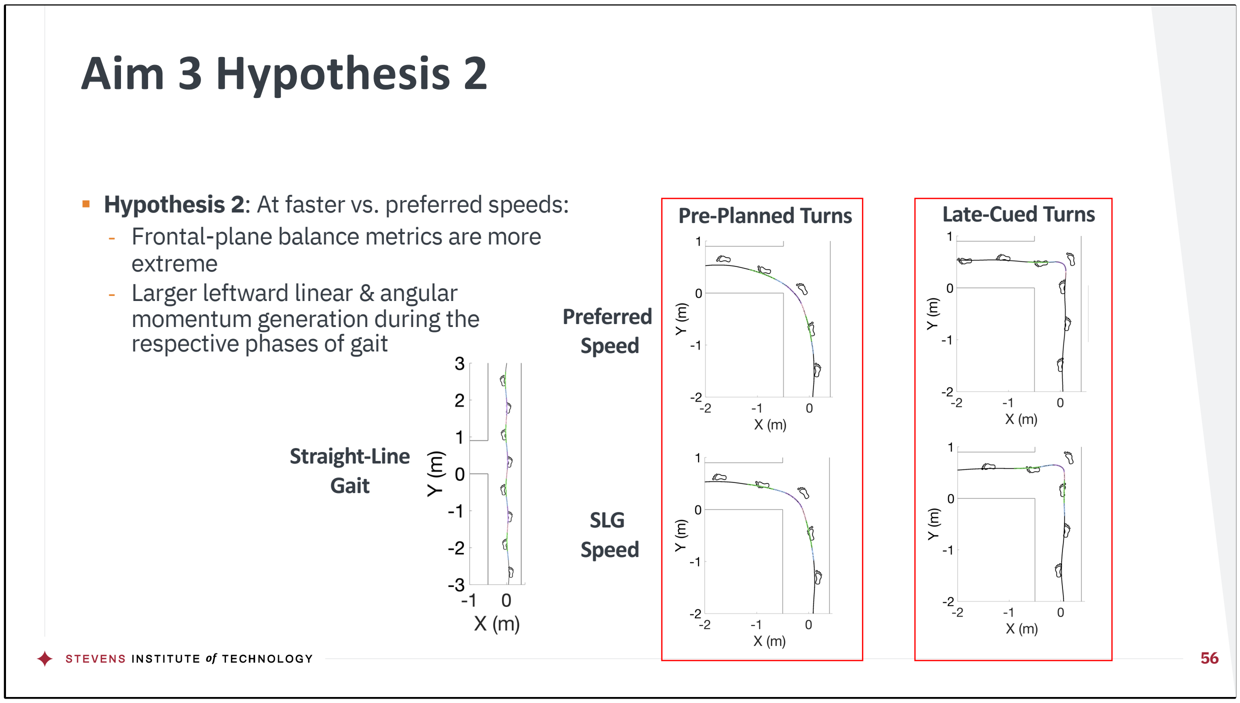

So next, our second goal of this aim was to identify the changes due to increasing gate speed within each task. So now we'll be looking at between speeds of pre-planned turns and late-cued turns and asking the question of whether the frontal plane balance measures and the transverse plane measures become more extreme.

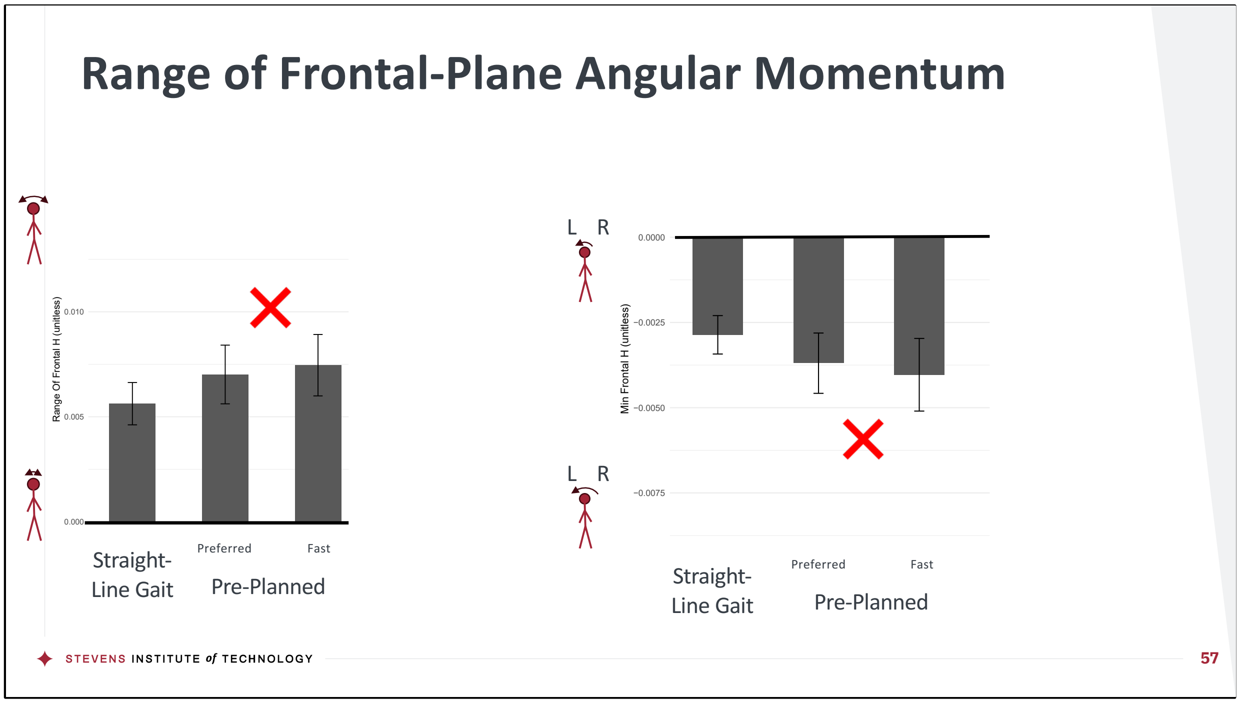

In contrast to the second hypothesis that increased gait speed would lead to more extreme frontal-plane angular momentum, there was no change between speeds of pre-planned turns, but the faster late-cued turns did show significantly larger range of angular momentum, supporting the hypothesis in late-cued turns. I interpret this as evidence that the relatively small increase in gait speed during pre-planned turns was insufficient to elicit increases in the range of frontal-plane angular momentum.

It is sufficient during late-cued turns, though, and this larger range of frontal-plane angular momentum was again driven a larger magnitude leftward angular momentum, towards the direction of the turn.

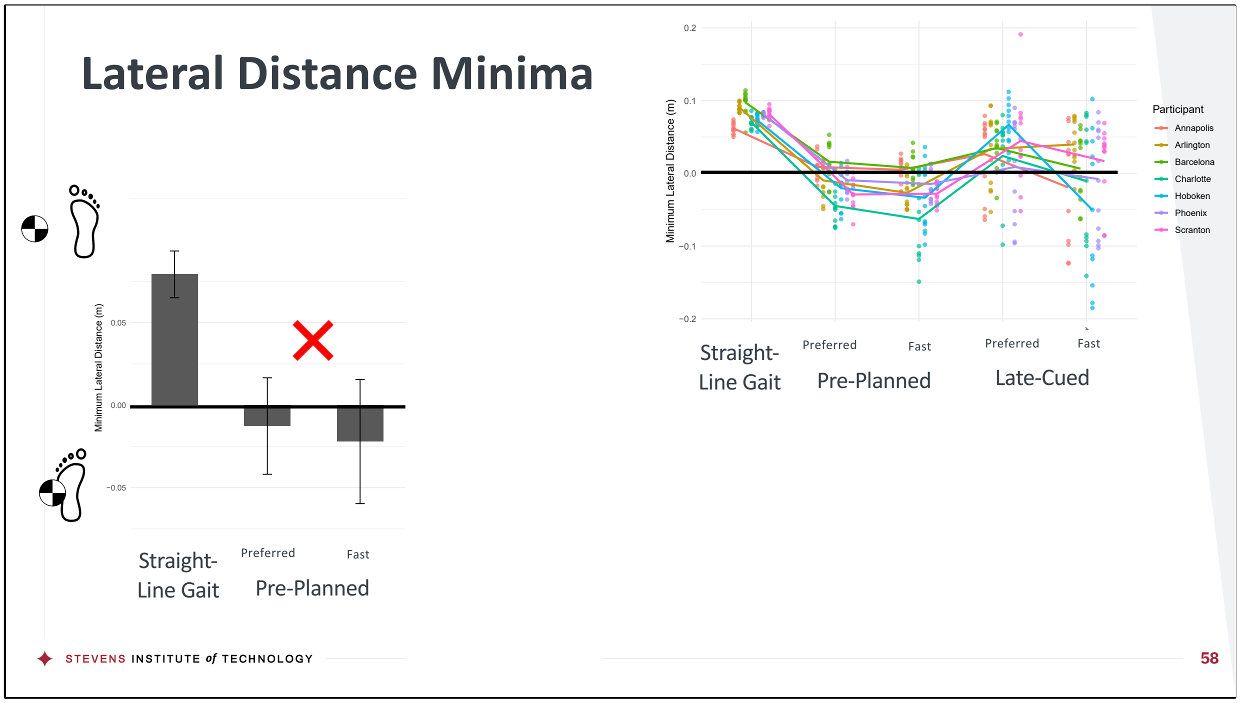

Our hypothesis that increasing gait speed would increase lateral distance minima was also partially supported. There was again no change between speeds of pre-planned turns, but late-cued turns showed a significantly smaller lateral distance value. Generally, prior work that looked at center of mass and foot placement in pre-planned turns has used gait speed increments of ~0.3 m/s, whereas in this study gait speed only changed by ~0.1m/s, apparently insufficient to change center of mass positioning relative to the feet during pre-planned turns.

However, in late-cued turns we do see a decrease in lateral distance minima. The lower lateral distance in faster late-cued turns occurs due to more spread in the data. During some trials, the lateral distance minima are similar values between preferred and faster speed late-cued turns. However, at faster speeds there are many more trials with lateral distance below zero, leading to a smaller overall mean lateral distance. Generally, it seems as though the trials with negative lateral distance were performed by spinning over the left foot, while the larger lateral distance trials were likely performed by pushing leftward with the right foot. Which turn strategy is used is likely determined by which foot is in stance phase when the intersection is reached.

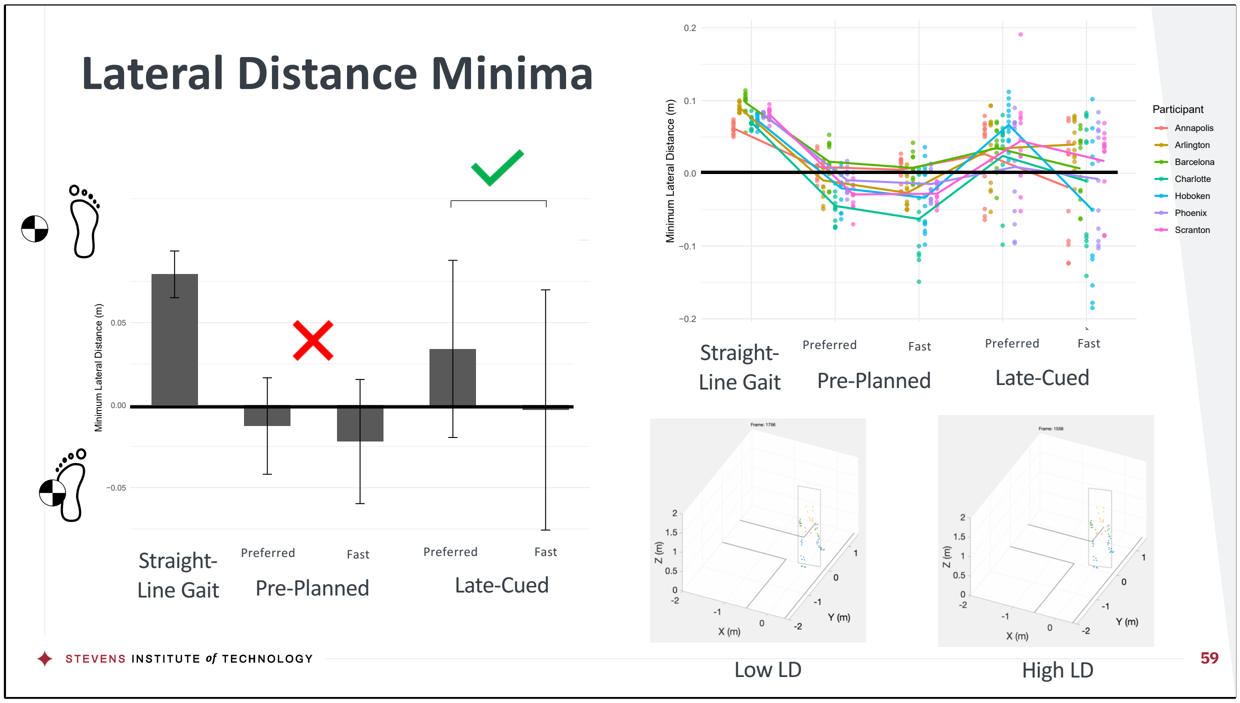

Our hypothesis that increasing gait speed would increase lateral distance minima was also partially supported. There was again no change between speeds of pre-planned turns, but late-cued turns showed a significantly smaller lateral distance value. Generally, prior work that looked at center of mass and foot placement in pre-planned turns has used gait speed increments of ~0.3 m/s, whereas in this study gait speed only changed by ~0.1m/s, apparently insufficient to change center of mass positioning relative to the feet during pre-planned turns.

However, in late-cued turns we do see a decrease in lateral distance minima. The lower lateral distance in faster late-cued turns occurs due to more spread in the data. During some trials, the lateral distance minima are similar values between preferred and faster speed late-cued turns. However, at faster speeds there are many more trials with lateral distance below zero, leading to a smaller overall mean lateral distance. Generally, it seems as though the trials with negative lateral distance were performed by spinning over the left foot, while the larger lateral distance trials were likely performed by pushing leftward with the right foot. Which turn strategy is used is likely determined by which foot is in stance phase when the intersection is reached.

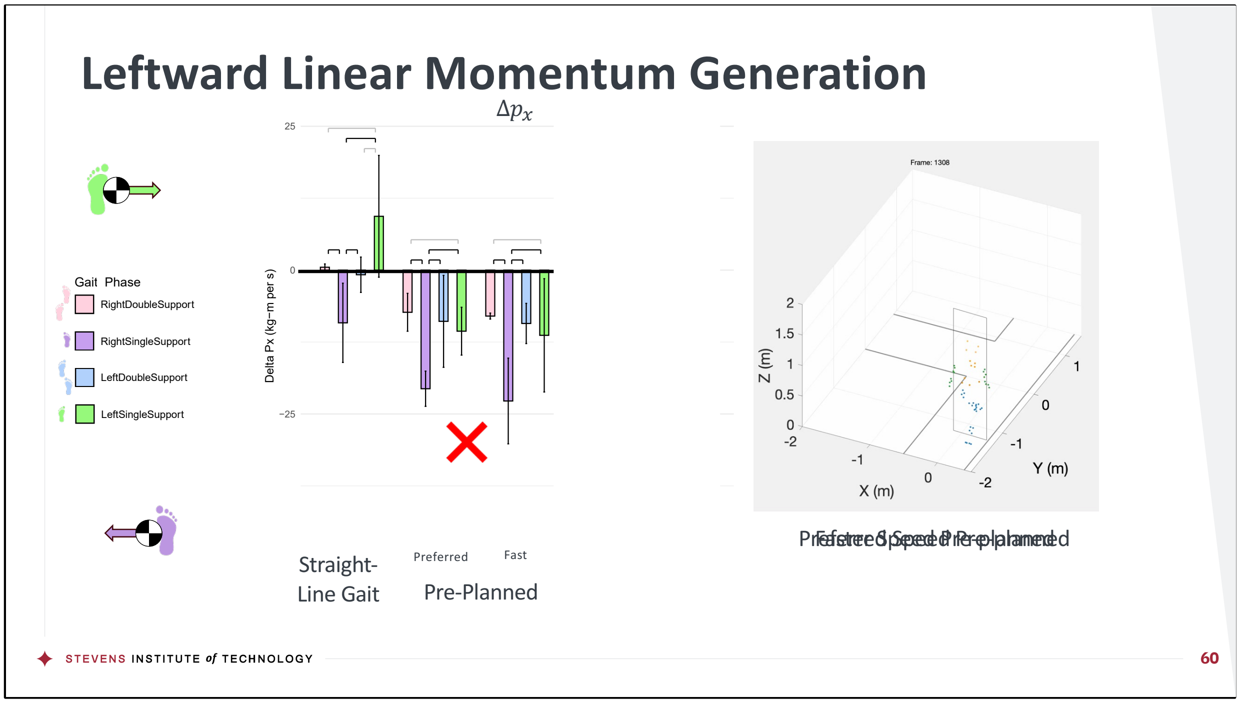

When looking at the transverse plane again, there was no difference between speeds of preplanned turns in terms of how much the magnitude of the leftward linear momentum that was generated. So just to put it into context, these are again the same example videos we saw before of the preplanned turns, so at preferred speed versus at faster speed. Again, a relatively small difference between these magnitudes of speed.

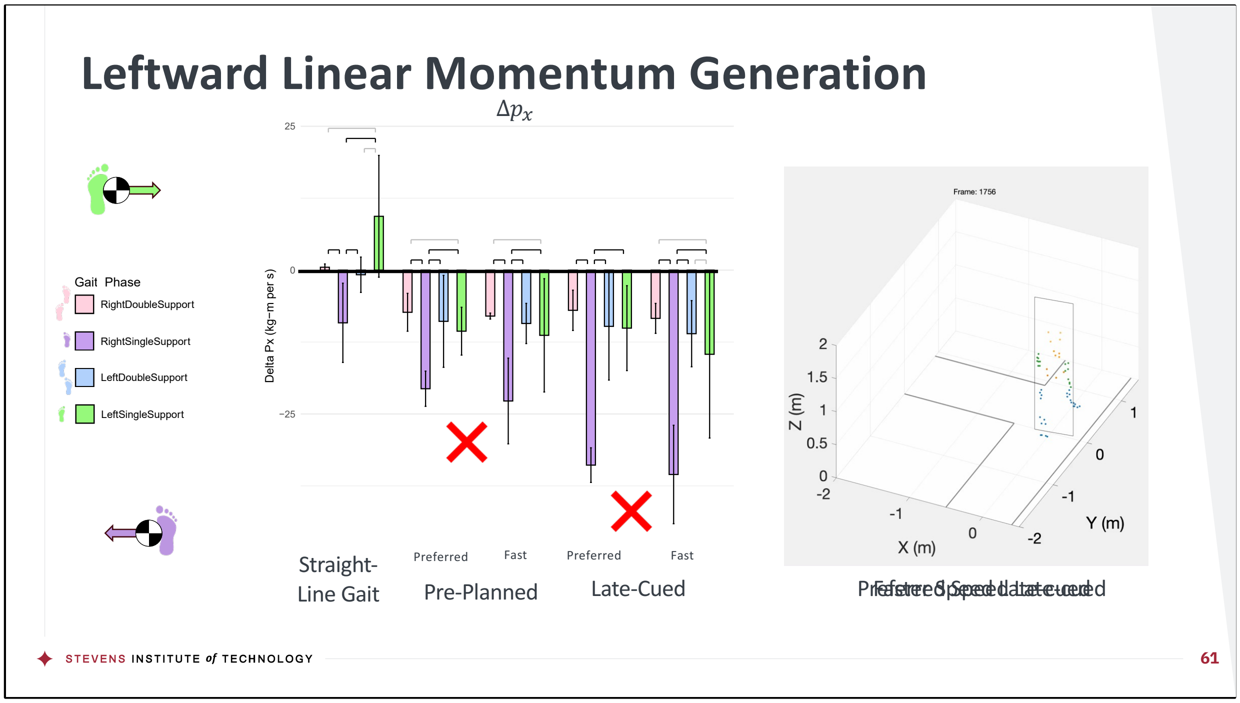

However, during late-cued turns, we expected to observe that the faster late-cued turns would generate more leftward linear momentum relative to preferred speed. However, that's not what we observed. We observed no statistically significant difference in the magnitude of this leftward linear momentum generation. And again, to put it into context, this is the preferred and faster speed late-cued turn videos.

The reason for this is still a bit unclear, and should be the subject of future research. Why the late-cued turns would be less sensitive to an increase in gait speed is an open research question.

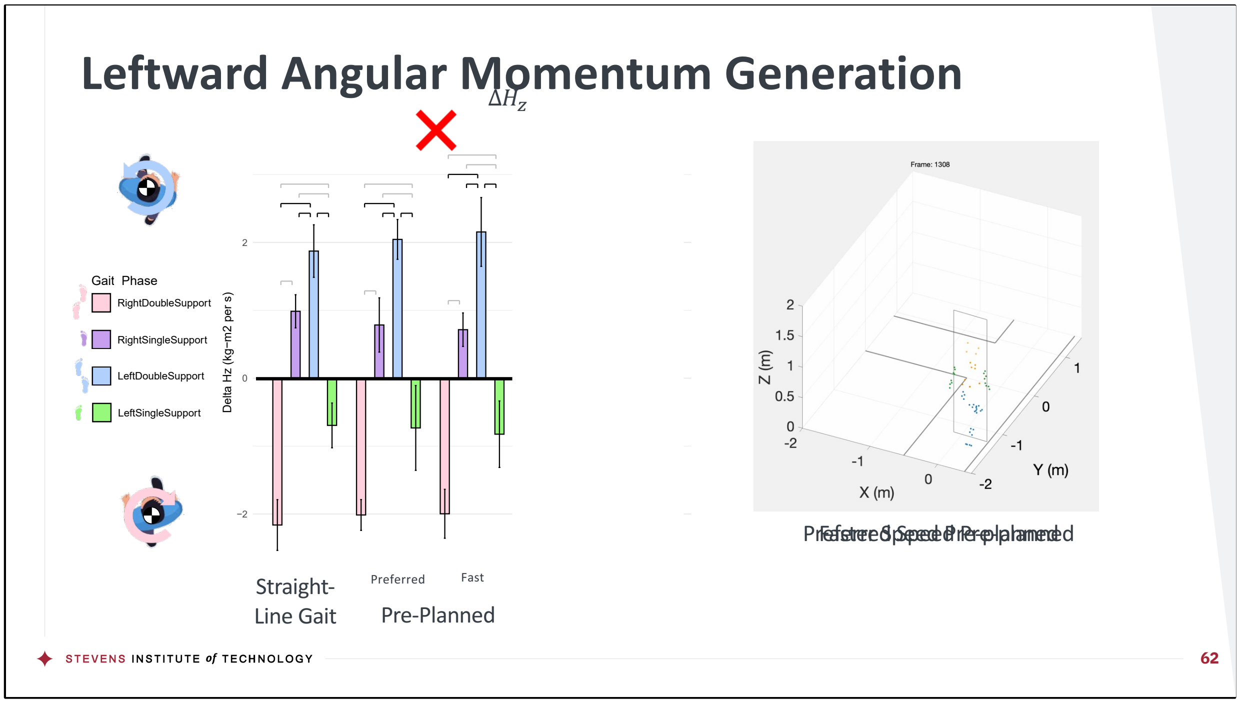

For angular momentum, during the preplanned turns we observed no difference between speeds, following the same the same pattern as linear momentum.

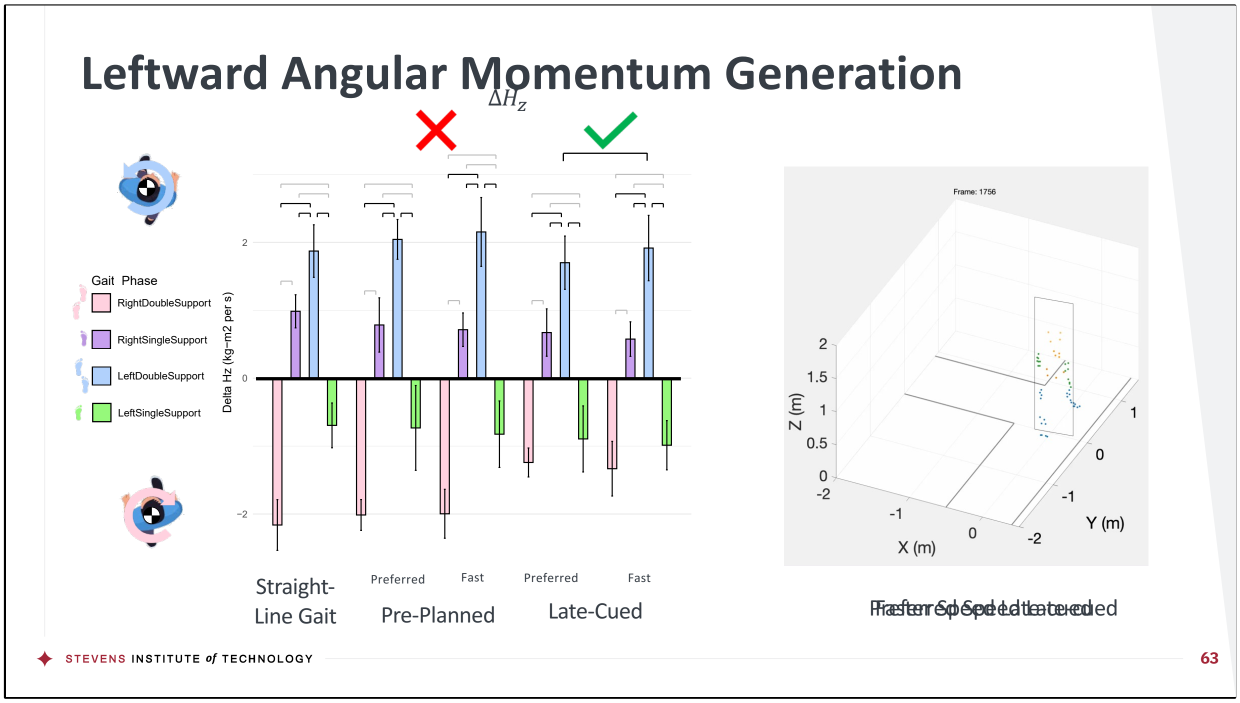

At different speeds of late-cued turns, we actually did see an increase in the transverse plane leftward angular momentum generation. So this metric is more sensitive to increases in speed during late-cued turns. The reason why the angular momentum would be more susceptible or more sensitive to increases in gait speed during late-cued turns and linear momentum generation showed no change is unclear, and should be the subject of future research.

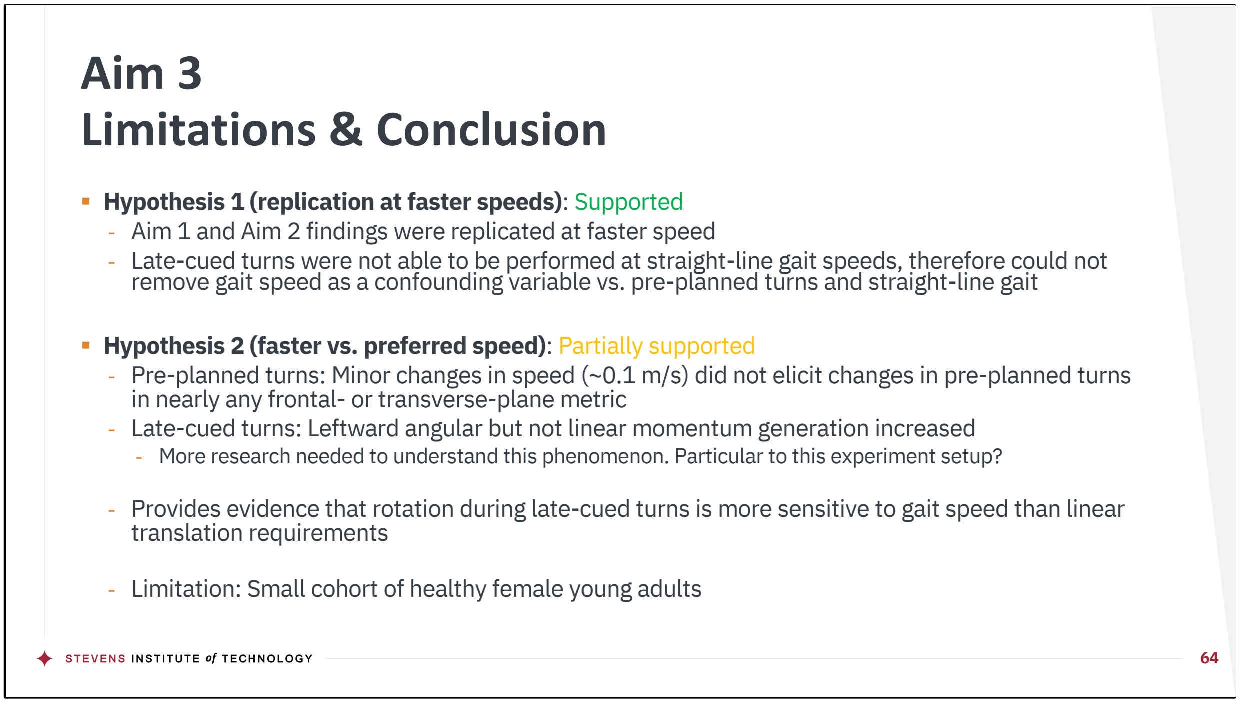

So, in conclusion, for this aim, our 1st hypothesis that we would replicate our preferred speed findings at faster speeds was supported. We replicated our 1st aims hypotheses. Our second hypothesis about whether the frontal and transverse plane extrema would increase during faster versus preferred speed was partially supported. We observed that during preplanned turns this relatively minor change in speed did not induce changes in the frontal or transverse plane. However, the late-cued turns did exhibit more extreme values in the frontal plane and in the transverse plane for angular momentum. Again, future research should attempt to understand why the linear momentum generation was not increased during late-cued turns. Perhaps it's particular to this experiment set up, something to do with having to turn their head to perceive the visual cue? I'm not sure.

And finally, this aim helps to provide evidence that rotation during late-cued turns is more sensitive to gait speed than than linear translation requirements. Again, recall that this is a relatively small cohort of healthy female young adults.

Overall Conclusion

- Clinical impact: Falls and mobility issues are a big obstacle for older adults
  - Developing an understanding of healthy movement can lead to better rehabilitation outcomes
  - This data may inform development of a global mechanics-based balance metric
- **Aim 1**
  - Late-cued and pre-planned turns challenge different aspects of balance control
  - These aspects often compensate for one another, and therefore they should not be examined in isolation
  - Future research: how frontal-plane angular momentum and lateral distance interact, especially during late-cued turns
- **Aim 2**
  - Linear and angular momentum generation occur primarily during specific phases of gait
  - Young adults generate more linear momentum, older adults generate more angular momentum
  - Future research: age-related changes in pre-planned and late-cued turns
- **Aim 3**
  - Late-cued turns are more sensitive to gait speed in the frontal and transverse plane
  - In young adults, pre-planned turns are not sensitive to small increases from preferred speed
  - Future research: why do faster late-cued turns generate more angular momentum, but not linear momentum?

STEVENS INSTITUTE *of* TECHNOLOGY 65

In conclusion, remember that falls and mobility issues are a big obstacle for older adults. And so these findings of my dissertation help to develop an understanding of healthy movement during turns which can help to lead to better rehabilitation outcomes for nonlinear gait and dynamic movements. And this data may help to inform as well the development of a global mechanics-based balance metric, so that we can have one number ideally in the future that represents comprehensively someone's mechanics based balance state.

And in the 1st aim we determined that late cued and preplanned turns challenge different aspects of balance control, and these aspects often compensate for one another or correct for one another, and therefore they should not be examined in isolation, and future research can focus on how frontal plane angular momentum and lateral distance interact, especially during late-cued turns.

In my second aim I discovered that linear and angular momentum generation occur primarily during specific phases of gait. Pushing yourself leftward occurs when just the right foot is in contact with the ground, and rotating yourself leftward occurs when both feet are in contact with the ground, with the left foot in front, so that both translation and rotational goals can be managed with both feet on the ground.

We also observed that young adults generate more linear momentum during both single support phases compared to older adults. But older adults generate more angular momentum, both leftward and rightward during straight line gait and preplanned turns, and again, perhaps they rotate more as a single unit, and have less agile movement of their segments relative to one another. So future research should investigate those age related changes.

And finally, in the 3rd aim, we uncovered that late-cued turns are more sensitive to this change in gait speed in the frontal and transverse plane rather than preplanned turns. So perhaps preplanned turns simply are not challenging enough of a movement to be susceptible to this increase in gait speed. Perhaps if we asked them to walk even faster, and then added another 0.1 meters per second, we would then see increases in gait speed, but 0.1 meters per second above their preferred speed was insufficient.

In conclusion, I'd like to thank everyone. Thank you, Dr. Zaferiou, for all of your support and guidance. Thank you to my committee for being here for your time and input. Thank you to my fellow graduate students, Sam Zahava and Erin. Thank you to my research participants for making this research possible by providing their data. Thank you to all of you for coming to Mom and family and everyone.

Thank you!

- Dr. Antonia Zaferiou
- My committee
  - Dr. Phil Dixon, Dr. George McConnell, Dr. Damiano Zanotto, Dr. Raviraj Nataraj
- My fellow graduate students
  - Sam Liu
  - Zahava Hirsch
  - Erin Kreis
- Research participants

References

1. B. C. Glaister, G. C. Bernatz, G. K. Klute, and M. S. Orendurff, “Video task analysis of turning during activities of daily living,” *Gait Posture*, vol. 25, no. 2, pp. 289–294, 2007, doi: 10.1016/j.gaitpost.2006.04.003.

2. B. Moreland, R. Kakara, and A. Henry, “Trends in Nonfatal Falls and Fall-Related Injuries Among Adults Aged ≥ 65 Years — United States, 2012–2018,” *MMWR Morb. Mortal. Wkly. Rep.*, vol. 69, no. 27, pp. 875–881, Jul. 2020, doi: 10.15585/mmwr.mm6927a5.

3. R. G. Cumming and R. J. Klineberg, “Fall Frequency and Characteristics and the Risk of Hip Fractures,” *J. Am. Geriatr. Soc.*, 1994, doi: 10.1111/j.1532-5415.1994.tb06540.x.

4. S. Mundi, B. Pindiprolu, N. Simunovic, and M. Bhandari, “Similar mortality rates in hip fracture patients over the past 31 years: A systematic review of RCTs,” *Acta Orthop.*, vol. 85, no. 1, pp. 54–59, Feb. 2014, doi: 10.3109/17453674.2013.878831.

5. S. N. Robinovitch *et al.*, “Video capture of the circumstances of falls in elderly people residing in long-term care: An observational study,” *The Lancet*, vol. 381, no. 9860, pp. 47–54, 2013, doi: 10.1016/S0140-6736(12)61263-X.

6. A. D. Kuo, “Stabilization of Lateral Motion in Passive Dynamic Walking,” *Int. J. Robot. Res.*, vol. 18, no. 9, pp. 917–930, Sep. 1999, doi: 10.1177/02783649922066655.

7. H. Herr and M. Popovic, “Angular momentum in human walking,” *J. Exp. Biol.*, vol. 211, no. 4, pp. 467–481, 2008, doi: 10.1242/jeb.008573.

8. L. A. Nolasco, A. K. Silverman, and D. H. Gates, “Whole-body and segment angular momentum during 90-degree turns,” *Gait Posture*, vol. 70, no. February, pp. 12–19, 2019, doi: 10.1016/j.gaitpost.2019.02.003.

9. A. E. Patla, A. Adkin, and T. Ballard, “Online steering : coordination and control of body center of mass , head and body reorientation,” *Exp. Brain Res.*, vol. 129, pp. 629–634, 1999.

10. M. S. Orendurff, A. D. Segal, J. S. Berge, K. C. Flick, D. Spanier, and G. K. Klute, “The kinematics and kinetics of turning: limb asymmetries associated with walking a circular path.,” *Gait Posture*, vol. 23, no. 1, pp. 106–11, Jan. 2006, doi: 10.1016/j.gaitpost.2004.12.008.

11. P. C. Dixon, J. Stebbins, T. Theologis, and A. B. Zavatsky, “The use of turning tasks in clinical gait analysis for children with cerebral palsy,” *Clin. Biomech.*, vol. 32, pp. 286–294, Feb. 2016, doi: 10.1016/j.clinbiomech.2015.10.010.

12. P. C. Dixon, J. V. Jacobs, J. T. Dennerlein, and J. M. Schiffman, “Late-cueing of gait tasks on an uneven brick surface impacts coordination and center of mass control in older adults,” *Gait Posture*, vol. 65, no. July 2018, pp. 143–148, Sep. 2018, doi: 10.1016/j.gaitpost.2018.07.168.

13. D. Conradsson, C. Paquette, and E. Franzén, “Medio-lateral stability during walking turns in older adults,” *PLoS ONE*, vol. 13, no. 6, pp. 1–12, Jun. 2018, doi: 10.1371/journal.pone.0198455.

14. R. Dumas, L. Chèze, and J. P. Verriest, “Adjustments to McConville et al. and Young et al. body segment inertial parameters,” *J. Biomech.*, vol. 40, no. 3, pp. 543–553, Jan. 2007, doi: 10.1016/j.jbiomech.2006.02.013.

15. C. Curtze, T. J. W. Buurke, and C. McCrum, “Notes on the margin of stability,” Open Science Framework, preprint, May 2023. doi: 10.31219/osf.io/nym5w.

15. B. C. Glaister, M. S. Orendurff, J. A. Schoen, G. C. Bernatz, and G. K. Klute, “Ground reaction forces and impulses during a transient turning maneuver,” *J. Biomech.*, no. 41, pp. 3090–3093, 2008, doi: 10.1016/j.jbiomech.2008.07.022.

16. S. M. Bruijn and J. H. Van Dieën, “Control of human gait stability through foot placement,” *J. R. Soc. Interface*, vol. 15, no. 143, 2018, doi: 10.1098/rsif.2017.0816.

17. S. B. Akram, J. S. Frank, and J. Fraser, “Effect of walking velocity on segment coordination during pre-planned turns in healthy older adults,” *Gait Posture*, vol. 32, no. 2, pp. 211–214, Jun. 2010, doi: 10.1016/j.gaitpost.2010.04.017.

18. G. L. Brown, N. Seethapathi, and M. Srinivasan, “A unified energy optimality criterion predicts human navigation paths and speeds,” *Proc. Natl. Acad. Sci.*, vol. 118, no. 29, p. e2020327118, Jul. 2021, doi: 10.1073/pnas.2020327118.

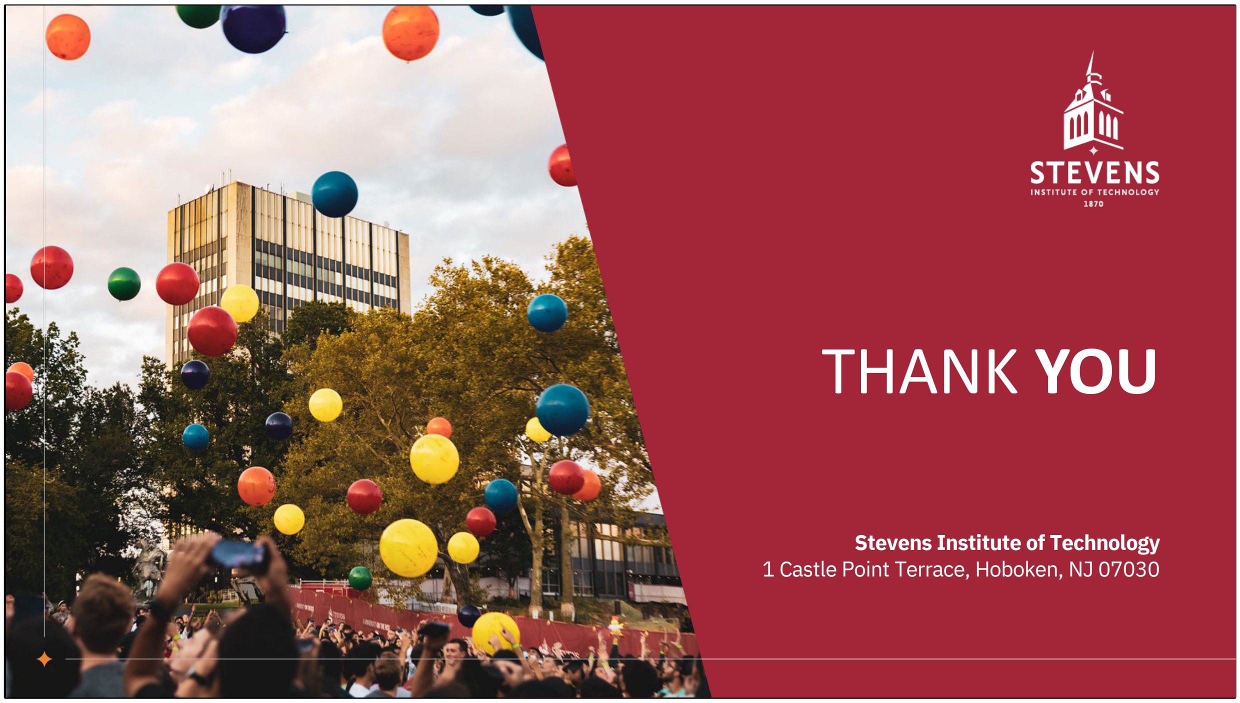
STEVENS
INSTITUTE OF TECHNOLOGY
1870
THANK YOU
Stevens Institute of Technology
1 Castle Point Terrace, Hoboken, NJ 07030

Bibliography

[1] C. S. Florence, G. Bergen, A. Atherly, E. Burns, J. Stevens, and C. Drake, "Medical Costs of Fatal and Nonfatal Falls in Older Adults," *Journal of the American Geriatrics Society*, vol. 66, no. 4, pp. 693–698, 2018, _eprint: https://onlinelibrary.wiley.com/doi/pdf/10.1111/jgs.15304. [Online]. Available: https://onlinelibrary.wiley.com/doi/abs/10.1111/jgs.15304

[2] M. J. H. Heijnen and S. Rietdyk, "Falls in young adults: Perceived causes and environmental factors assessed with a daily online survey," *Human Movement Science*, vol. 46, pp. 86–95, Apr. 2016, publisher: Elsevier B.V.

[3] S. K. Verma, J. L. Willetts, H. L. Corns, H. R. Marucci-Wellman, D. A. Lombardi, and T. K. Courtney, "Falls and Fall-Related Injuries among Community-Dwelling Adults in the United States," *PLOS ONE*, vol. 11, no. 3, p. e0150939, Mar. 2016, publisher: Public Library of Science. [Online]. Available: https://journals.plos.org/plosone/article?id=10.1371/journal.pone.0150939

[4] B. Moreland, R. Kakara, and A. Henry, "Trends in Nonfatal Falls and Fall-Related Injuries Among Adults Aged ≥ 65 Years — United States, 2012–2018," *MMWR. Morbidity and Mortality Weekly Report*, vol. 69, no. 27, pp. 875–881, Jul. 2020. [Online]. Available: http://www.cdc.gov/mmwr/volumes/69/wr/mm6927a5.htm?s_cid=mm6927a5_w

[5] S. N. Robinovitch, F. Feldman, Y. Yang, R. Schonnop, P. M. Leung, T. Sarraf, J. Sims-Gould, and M. Loughi, "Video capture of the circumstances of falls in elderly people residing in long-term care: An observational study," *The Lancet*, vol. 381, no. 9860, pp. 47–54, 2013, publisher: Elsevier Ltd. [Online]. Available: http://dx.doi.org/10.1016/S0140-6736(12)61263-X

[6] S. R. Cummings and M. C. Nevitt, "A hypothesis: The causes of hip fractures," *Journals of Gerontology*, vol. 44, no. 4, pp. 107–111, 1989.

[7] P.-A. Alffram, "An Epidemiologic Study of Cervical and Trochanteric Fractures of the Femur in an Urban Population Analysis of 1,664 Cases with Special Reference to Etiologic Factors," *Acta Orthopaedica Scandinavica*, vol. 35, no. sup65, pp. 1–109, Feb. 1964. [Online]. Available: http://www.tandfonline.com/doi/full/10.3109/ort.1964.35.suppl-65.01

[8] R. G. Cumming and R. J. Klineberg, "Fall Frequency and Characteristics and the Risk of Hip Fractures," *Journal of the American Geriatrics Society*, 1994.

[9] S. Mundi, B. Pindiprolu, N. Simunovic, and M. Bhandari, "Similar mortality rates in hip fracture patients over the past 31 years: A systematic review of RCTs," *Acta Orthopaedica*, vol. 85, no. 1, pp. 54–59, Feb. 2014. [Online]. Available: https://actaorthop.org/actao/article/view/10049

[10] J. M. Leach, S. Mellone, P. Palumbo, S. Bandinelli, and L. Chiari, "Natural turn measures predict recurrent falls in community-dwelling older adults: A longitudinal cohort study," *Scientific Reports*, vol. 8, no. 1, Dec. 2018, publisher:

Nature Publishing Group.
[11] B. C. Glaister, G. C. Bernatz, G. K. Klute, and M. S. Orendurff, "Video task analysis of turning during activities of daily living," *Gait and Posture*, vol. 25, no. 2, pp. 289–294, 2007.
[12] F. B. Horak, "Postural compensation for vestibular loss," in *Annals of the New York Academy of Sciences*, 2009, iSSN: 17496632.
[13] F. Franchignoni, F. Horak, M. Godi, A. Nardone, and A. Giordano, "Using psychometric techniques to improve the Balance Evaluation Systems Test: the mini-BESTest," *Journal of Rehabilitation Medicine*, vol. 42, no. 4, pp. 323–331, 2010. [Online]. Available: https://medicaljournals.se/jrm/content/abstract/10.2340/16501977-0537
[14] A. Shumway-Cook and M. H. Woollacott, *Motor control: Translating research into clinical practice: Fourth edition*, 2014, publication Title: Motor Control: Translating Research into Clinical Practice: Fourth Edition.
[15] S. Podsiadlo, D; Richardson, "The Timed Up and Go: A Test of Basic Functional Mobility for Frail Elderly Persons," *Journal of the American Geriatrics Society*, 1991.
[16] T. Herman, N. Inbar-Borovsky, M. Brozgol, N. Giladi, and J. M. Hausdorff, "The Dynamic Gait Index in healthy older adults: The role of stair climbing, fear of falling and gender," *Gait & Posture*, vol. 29, no. 2, pp. 237–241, Feb. 2009. [Online]. Available: https://www.sciencedirect.com/science/article/pii/S0966636208002592
[17] A. Vistamehr, S. A. Kautz, M. G. Bowden, and R. R. Neptune, "Correlations between Measures of Dynamic Balance in Individuals with Post-stroke Hemiparesis," *Physiology & behavior*, vol. 49, no. 3, pp. 396–400, 2016.
[18] J. K. Leestma, P. R. Golyski, C. R. Smith, G. S. Sawicki, and A. J. Young, "Linking whole-body angular momentum and step placement during perturbed walking," *The Journal of Experimental Biology*, p. jeb.244760, Feb. 2023.
[19] A. L. Hof, M. G. Gazendam, and W. E. Sinke, "The condition for dynamic stability," *Journal of Biomechanics*, vol. 38, no. 1, pp. 1–8, 2005.
[20] D. A. Winter, F. Prince, and A. Patla, "Validity of the inverted pendulum model of balance in quiet standing," *Gait & Posture*, 1997.
[21] S. M. Bruijn, O. G. Meijer, P. J. Beek, and J. H. Van Dieen, "Assessing the stability of human locomotion: A review of current measures," *Journal of the Royal Society Interface*, vol. 10, no. 83, Jun. 2013, publisher: Royal Society.
[22] P. C. Dixon, J. Stebbins, T. Theologis, and A. B. Zavatsky, "The use of turning tasks in clinical gait analysis for children with cerebral palsy," *Clinical Biomechanics*, vol. 32, pp. 286–294, Feb. 2016, publisher: Elsevier Ltd. [Online]. Available: http://linkinghub.elsevier.com/retrieve/pii/S0268003315002879
[23] C. Curtze, T. J. W. Buurke, and C. McCrum, "Notes on the margin of stability," Open Science Framework, preprint, May 2023. [Online]. Available: https://osf.io/nym5w

[24] J. A. Zeni, J. G. Richards, and J. S. Higginson, “Two simple methods for determining gait events during treadmill and overground walking using kinematic data,” *Gait and Posture*, vol. 27, no. 4, pp. 710–714, 2008.

[25] A. Kharb, V. Saini, Y. Jain, and S. Dhiman, “A review of gait cycle and its parameters,” *IJCEM Int J Comput Eng Manag*, vol. 13, no. July, pp. 78–83, 2011.

[26] H. Ohtsu, S. Yoshida, T. Minamisawa, T. Takahashi, S. i. Yomogida, and H. Kanzaki, “Investigation of balance strategy over gait cycle based on margin of stability,” *Journal of Biomechanics*, vol. 95, p. 109319, 2019, publisher: Elsevier Ltd. [Online]. Available: https://doi.org/10.1016/j.jbiomech.2019.109319

[27] K. Hase and R. B. Stein, “Turning strategies during human walking,” *Journal of Neurophysiology*, vol. 81, no. 6, pp. 2914–2922, 1999, publisher: American Physiological Society.

[28] A. D. Kuo, “Stabilization of Lateral Motion in Passive Dynamic Walking,” *The International Journal of Robotics Research*, vol. 18, no. 9, pp. 917–930, Sep. 1999, 647 citations (Semantic Scholar/DOI) [2023-02-17]. [Online]. Available: http://journals.sagepub.com/doi/10.1177/02783649922066655

[29] T. Mcgeer, “Passive Dynamic Walking,” *The International Journal of Robotics Research*, vol. 9, no. 2, pp. 62–82, Apr. 1990, publisher: Sage Publications, Inc. PUB1290 Thousand Oaks, CA, USA. [Online]. Available: http://journals.sagepub.com/doi/10.1177/027836499000900206

[30] M. A. Schrager, V. E. Kelly, R. Price, L. Ferrucci, and A. Shumway-Cook, “The effects of age on medio-lateral stability during normal and narrow base walking,” *Gait and Posture*, 2008.

[31] S.-U. Ko, K. B. Gunter, M. Costello, H. Aum, S. MacDonald, K. N. White, C. M. Snow, and W. C. Hayes, “Stride Width Discriminates Gait of Side-Fallers Compared to Other-Directed Fallers During Overground Walking,” *Journal of Aging and Health*, vol. 19, no. 2, pp. 200–212, Apr. 2007, publisher: SAGE Publications Inc. [Online]. Available: https://doi.org/10.1177/0898264307299308

[32] B. E. Maki, “Gait Changes in Older Adults: Predictors of Falls or Indicators of Fear?” *Journal of the American Geriatrics Society*, vol. 45, no. 3, pp. 313–320, Mar. 1997. [Online]. Available: https://agsjournals.onlinelibrary.wiley.com/doi/10.1111/j.1532-5415.1997.tb00946.x

[33] M. Arvin, M. Mazaheri, M. J. Hoozemans, M. Pijnappels, B. J. Burger, S. M. Verschueren, and J. H. van Dieën, “Effects of narrow base gait on mediolateral balance control in young and older adults,” *Journal of Biomechanics*, vol. 49, no. 7, pp. 1264–1267, May 2016, publisher: Elsevier Ltd.

[34] H. Herr and M. Popovic, “Angular momentum in human walking,” *Journal of Experimental Biology*, vol. 211, no. 4, pp. 467–481, 2008.

[35] G. G. Simoneau and D. E. Krebs, “Whole-body momentum during gait: A preliminary study of non-fallers and frequent fallers,” *Journal of Applied Biome-*

chanics, vol. 16, no. 1, pp. 1–13, 2000.

[36] J. W. Gu, "The Regulation of Angular Momentum During Human Walking," Bachelors, MIT, 2003. [Online]. Available: https://dspace.mit.edu/bitstream/handle/1721.1/28268/53102406-MIT.pdf?sequence=2

[37] C. E. Bauby and A. D. Kuo, "Active control of lateral balance in human walking," *Journal of Biomechanics*, vol. 33, no. 11, pp. 1433–1440, 2000.

[38] A. Vistamehr and R. R. Neptune, "Differences in Balance Control between Healthy Younger and Older Adults during Steady-State Walking," *Journal of Biomechanics*, p. 110717, Aug. 2021, publisher: Elsevier. [Online]. Available: https://linkinghub.elsevier.com/retrieve/pii/S0021929021004851

[39] D. Kim, C. L. Lewis, A. K. Silverman, and S. V. Gill, "Changes in dynamic balance control in adults with obesity across walking speeds," *Journal of Biomechanics*, vol. 144, p. 111308, Nov. 2022. [Online]. Available: https://www.sciencedirect.com/science/article/pii/S0021929022003499

[40] V. Thielemans, P. Meyns, and S. M. Bruijn, "Is angular momentum in the horizontal plane during gait a controlled variable?" *Human Movement Science*, vol. 34, no. 1, pp. 205–216, Apr. 2014, publisher: Elsevier.

[41] L. A. Nolasco, A. K. Silverman, and D. H. Gates, "Whole-body and segment angular momentum during 90-degree turns," *Gait and Posture*, vol. 70, no. February, pp. 12–19, 2019, publisher: Elsevier. [Online]. Available: https://doi.org/10.1016/j.gaitpost.2019.02.003

[42] B. C. Bennett, S. D. Russell, P. Sheth, and M. F. Abel, "Angular momentum of walking at different speeds," *Human Movement Science*, vol. 29, no. 1, pp. 114–124, Feb. 2010.

[43] J. Begue, N. Peyrot, G. Dalleau, and T. Caderby, "Effect of increasing speed on whole-body angular momentum during stepping in the elderly," *Journal of Biomechanics*, vol. 122, 2021.

[44] S. M. Bruijn, O. G. Meijer, J. H. van Dieën, I. Kingma, and C. J. Lamoth, "Coordination of leg swing, thorax rotations, and pelvis rotations during gait: The organisation of total body angular momentum," *Gait and Posture*, vol. 27, no. 3, pp. 455–462, Apr. 2008, publisher: Elsevier.

[45] S. M. Bruijn, P. Meyns, I. Jonkers, D. Kaat, and J. Duysens, "Control of angular momentum during walking in children with cerebral palsy," *Research in Developmental Disabilities*, vol. 32, no. 6, pp. 2860–2866, Nov. 2011, publisher: Pergamon.

[46] D. Kim, C. L. Lewis, and S. V. Gill, "The effect of obesity on whole-body angular momentum during steady-state walking," *Gait & Posture*, vol. 94, pp. 93–101, May 2022. [Online]. Available: https://www.sciencedirect.com/science/article/pii/S0966636222000637

[47] A. Goswami and V. Kallem, "Rate of change of angular momentum and balance maintenance of biped robots," in *IEEE International Conference on Robotics and Automation, 2004. Proceedings. ICRA '04. 2004*, vol. 4, Apr. 2004, pp.

3785–3790 Vol.4, 255 citations (Semantic Scholar/DOI) [2023-02-17] ISSN: 1050-4729.

[48] S. Kajita, F. Kanehiro, K. Kaneko, K. Fujiwara, K. Harada, K. Yokoi, and H. Hirukawa, "Resolved momentum control: humanoid motion planning based on the linear and angular momentum," in *Proceedings 2003 IEEE/RSJ International Conference on Intelligent Robots and Systems (IROS 2003) (Cat. No.03CH37453)*, vol. 2. Las Vegas, NV, USA: IEEE, 2003, pp. 1644–1650, 478 citations (Semantic Scholar/DOI) [2023-10-18]. [Online]. Available: http://ieeexplore.ieee.org/document/1248880/

[49] S. M. Bruijn and J. H. Van Dieën, "Control of human gait stability through foot placement," *Journal of the Royal Society Interface*, vol. 15, no. 143, 2018, publisher: Royal Society Publishing. [Online]. Available: /pmc/articles/PMC6030625/?report=abstract

[50] A. D. Kuo, "The six determinants of gait and the inverted pendulum analogy: A dynamic walking perspective," *Human Movement Science*, vol. 26, no. 4, pp. 617–656, Aug. 2007, 477 citations (Semantic Scholar/DOI) [2022-07-01]. [Online]. Available: https://linkinghub.elsevier.com/retrieve/pii/S0167945707000309

[51] D. A. Winter, *Biomechanics and motor control of human movement*, 4th ed. Hoboken, N.J: Wiley, 2009, oCLC: ocn318408191.

[52] D. A. Winter, A. E. Patla, F. Prince, M. Ishac, and K. Gielo-perczak, "Stiffness control of balance in quiet standing," *Journal of Neurophysiology*, 1998.

[53] A. L. Hof, "Comparison of three methods to estimate the center of mass during balance assessment [1]," *Journal of Biomechanics*, vol. 38, no. 10, pp. 2134–2135, Oct. 2005.

[54] A. L. Hof, R. M. van Bockel, T. Schoppen, and K. Postema, "Control of lateral balance in walking. Experimental findings in normal subjects and above-knee amputees," *Gait and Posture*, 2007.

[55] C. D. MacKinnon and D. A. Winter, "Control of whole body balance in the frontal plane during human walking," *Journal of Biomechanics*, vol. 26, no. 6, pp. 633–644, 1993.

[56] M. Vlutters, E. H. Van Asseldonk, and H. van der Kooij, "Foot placement modulation diminishes for perturbations near foot contact," *Frontiers in Bioengineering and Biotechnology*, vol. 6, no. MAY, May 2018, publisher: Frontiers Media S.A.

[57] A. L. Hof, S. M. Vermerris, and W. A. Gjaltema, "Balance responses to lateral perturbations in human treadmill walking," *Journal of Experimental Biology*, vol. 213, no. 15, pp. 2655–2664, Aug. 2010, publisher: The Company of Biologists. [Online]. Available: http://jeb.biologists.org/cgi/content/full/213/15/2655/DC1

[58] M. E. Kazanski, J. P. Cusumano, and J. B. Dingwell, "Rethinking margin of stability: Incorporating step-to-step regulation to resolve the paradox,"

Journal of Biomechanics, vol. 144, p. 111334, Nov. 2022. [Online]. Available: https://www.sciencedirect.com/science/article/pii/S002192902200375X

[59] P. M. McAndrew Young, J. M. Wilken, and J. B. Dingwell, "Dynamic margins of stability during human walking in destabilizing environments," *Journal of Biomechanics*, vol. 45, no. 6, pp. 1053–1059, Apr. 2012, publisher: Elsevier.

[60] S. Sivakumaran, A. Schinkel-Ivy, K. Masani, and A. Mansfield, "Relationship between margin of stability and deviations in spatiotemporal gait features in healthy young adults," *Human Movement Science*, vol. 57, pp. 366–373, Feb. 2018, publisher: Elsevier B.V.

[61] K. H. Stimpson, L. N. Heitkamp, J. S. Horne, and J. C. Dean, "Effects of walking speed on the step-by-step control of step width," *Journal of Biomechanics*, vol. 68, pp. 78–83, Feb. 2018. [Online]. Available: https://linkinghub.elsevier.com/retrieve/pii/S002192901730739X

[62] M. A. Bucklin, J. Deol, G. Brown, E. J. Perreault, and K. E. Gordon, "Optimism persists when walking in unpredictable environments," *Scientific Reports*, vol. 13, no. 1, p. 6853, Apr. 2023. [Online]. Available: https://www.nature.com/articles/s41598-023-33662-6

[63] F. Fallahtafti, A. Mohammadzadeh Gonabadi, K. Samson, and J. M. Yentes, "Margin of Stability May Be Larger and Less Variable during Treadmill Walking Versus Overground," *Biomechanics*, vol. 1, no. 1, pp. 118–130, May 2021, publisher: Multidisciplinary Digital Publishing Institute. [Online]. Available: https://www.mdpi.com/2673-7078/1/1/9

[64] N. J. Rosenblatt and M. D. Grabiner, "Measures of frontal plane stability during treadmill and overground walking," *Gait and Posture*, vol. 31, no. 3, pp. 380–384, 2010.

[65] H. Ohtsu, S. Yoshida, T. Minamisawa, N. Katagiri, T. Yamaguchi, T. Takahashi, S. i. Yomogida, and H. Kanzaki, "Does the balance strategy during walking in elderly persons show an association with fall risk assessment?" *Journal of Biomechanics*, vol. 103, no. xxxx, p. 109657, 2020, publisher: Elsevier Ltd. [Online]. Available: https://doi.org/10.1016/j.jbiomech.2020.109657

[66] F. Mersmann, S. Bohm, S. Bierbaum, R. Dietrich, and A. Arampatzis, "Young and old adults prioritize dynamic stability control following gait perturbations when performing a concurrent cognitive task," *Gait and Posture*, vol. 37, no. 3, pp. 373–377, 2013, publisher: Elsevier B.V. [Online]. Available: http://dx.doi.org/10.1016/j.gaitpost.2012.08.005

[67] R. R. Neptune and A. Vistamehr, "Dynamic Balance During Human Movement: Measurement and Control Mechanisms," 2019.

[68] L. Hak, H. Houdijk, P. Van Der Wurff, M. R. Prins, A. Mert, P. J. Beek, and J. H. Van Dieën, "Stepping strategies used by post-stroke individuals to maintain margins of stability during walking," *Clinical Biomechanics*, vol. 28, no. 9-10, pp. 1041–1048, Nov. 2013.

[69] T. Caderby, E. Yiou, N. Peyrot, M. Begon, and G. Dalleau, "Influence of gait

speed on the control of mediolateral dynamic stability during gait initiation," *Journal of Biomechanics*, vol. 47, no. 2, pp. 417–423, Jan. 2014.

[70] L. Hak, H. Houdijk, F. Steenbrink, A. Mert, P. van der Wurff, P. J. Beek, and J. H. van Dieën, "Speeding up or slowing down?: Gait adaptations to preserve gait stability in response to balance perturbations," *Gait & Posture*, vol. 36, no. 2, pp. 260–264, Jun. 2012. [Online]. Available: https://www.sciencedirect.com/science/article/pii/S0966636212000811

[71] G. L. Brown, N. Seethapathi, and M. Srinivasan, "A unified energy optimality criterion predicts human navigation paths and speeds," *Proceedings of the National Academy of Sciences*, vol. 118, no. 29, p. e2020327118, Jul. 2021, arXiv: 2001.02287. [Online]. Available: http://arxiv.org/abs/2001.02287

[72] M. Justine, H. Manaf, A. Sulaiman, S. Razi, and H. A. Alias, "Sharp turning and corner turning: Comparison of energy expenditure, gait parameters, and level of fatigue among community-dwelling elderly," *BioMed Research International*, 2014.

[73] G. Bruder, P. Lubas, and F. Steinicke, "Cognitive Resource Demands of Redirected Walking," *IEEE Transactions on Visualization and Computer Graphics*, vol. 21, no. 4, pp. 539–544, 2015, publisher: IEEE.

[74] M. Mancini, M. El-Gohary, S. Pearson, J. McNames, H. Schlueter, J. G. Nutt, L. A. King, and F. B. Horak, "Continuous monitoring of turning in Parkinson's disease: Rehabilitation potential." *NeuroRehabilitation*, vol. 37, no. 1, pp. 3–10, 2015, publisher: NIH Public Access. [Online]. Available: http://www.ncbi.nlm.nih.gov/pubmed/26409689

[75] M. Son, S.-M. Cheon, C. Youm, and J. W. Kim, "Turning reveals the characteristics of gait freezing better than walking forward and backward in Parkinson's disease," *Gait & Posture*, vol. 94, pp. 131–137, May 2022. [Online]. Available: https://www.sciencedirect.com/science/article/pii/S0966636222000807

[76] M. Bertoli, A. Cereatti, U. Della Croce, and M. Mancini, "An objective assessment to investigate the impact of turning angle on freezing of gait in Parkinson's disease," in *2017 IEEE Biomedical Circuits and Systems Conference, BioCAS 2017 - Proceedings*, vol. 2018-Janua, 2018, pp. 1–4.

[77] A. Salarian, C. Zampieri, F. B. Horak, P. Carlson-Kuhta, J. G. Nutt, and K. Aminian, "Analyzing 180° turns using an inertial system reveals early signs of progression of Parkinson's disease," in *Proceedings of the 31st Annual International Conference of the IEEE Engineering in Medicine and Biology Society: Engineering the Future of Biomedicine, EMBC 2009*, 2009, pp. 224–227.

[78] M. S. Orendurff, J. A. Schoen, G. C. Bernatz, A. D. Segal, and G. K. Klute, "How humans walk: Bout duration, steps per bout, and rest duration," vol. 45, no. 7, pp. 1077–1090, 2008.

[79] H. M. Maus and A. Seyfarth, "Walking in circles: a modelling approach," *Journal of The Royal Society Interface*, vol. 11, no. 99,

Oct. 2014, publisher: The Royal Society. [Online]. Available: https://royalsocietypublishing.org/doi/abs/10.1098/rsif.2014.0594

[80] J. L. Souman, I. Frissen, M. N. Sreenivasa, and M. O. Ernst, "Walking Straight into Circles," *Current Biology*, vol. 19, no. 18, pp. 1538–1542, 2009, publisher: Elsevier Ltd. [Online]. Available: http://dx.doi.org/10.1016/j.cub.2009.07.053

[81] M. Hollands, A. Patla, and J. Vickers, ""Look where you're going!": Gaze behaviour associated with maintaining and changing the direction of locomotion," *Experimental Brain Research*, 2002.

[82] D. Anastasopoulos, N. Ziavra, M. Hollands, and A. Bronstein, "Gaze displacement and inter-segmental coordination during large whole body voluntary rotations," *Experimental Brain Research*, 2009.

[83] L. A. Vallis, A. E. Patla, and A. L. Adkin, "Control of steering in the presence of unexpected head yaw movements: Influence on sequencing of subtasks," *Experimental Brain Research*, 2001.

[84] S. Akram, J. S. Frank, and M. Jog, "Parkinson's Disease and Segmental Coordination during Turning: I. Standing Turns," *Canadian Journal of Neurological Sciences*, vol. 40, no. 4, pp. 512–519, Jul. 2013, 17 citations (Semantic Scholar/DOI) [2023-03-23] Publisher: Cambridge University Press. [Online]. Available: https://www.cambridge.org/core/journals/canadian-journal-of-neurological-sciences/article/parkinsons-disease-and-segmental-coordination-during-turning-i-standing-turns/447457DDA32C2453DF47349609E4A772

[85] S. B. Akram, J. S. Frank, and J. Fraser, "Effect of walking velocity on segment coordination during pre-planned turns in healthy older adults," *Gait and Posture*, vol. 32, no. 2, pp. 211–214, Jun. 2010.

[86] J. R. Fuller, A. L. Adkin, and L. A. Vallis, "Strategies used by older adults to change travel direction," *Gait and Posture*, vol. 25, no. 3, pp. 393–400, Mar. 2007.

[87] C. Forsell, D. Conradsson, C. Paquette, and E. Franzén, "Reducing gait speed affects axial coordination of walking turns," *Gait and Posture*, vol. 54, pp. 71–75, May 2017, publisher: Elsevier B.V.

[88] J. B. Dingwell, A. C. Render, D. M. Desmet, and J. P. Cusumano, "Generalizing stepping concepts to non-straight walking," *Journal of Biomechanics*, vol. 161, p. 111840, Dec. 2023. [Online]. Available: https://www.sciencedirect.com/science/article/pii/S0021929023004116

[89] F. Huxham, J. Gong, R. Baker, M. Morris, and R. Iansek, "Defining spatial parameters for non-linear walking," *Gait and Posture*, vol. 23, no. 2, pp. 159–163, 2006.

[90] M. El-Gohary, S. Pearson, J. McNames, M. Mancini, F. Horak, S. Mellone, and L. Chiari, "Continuous monitoring of turning in patients with movement disability." *Sensors (Basel, Switzerland)*, vol. 14, no. 1, pp. 356–69, Dec. 2013, publisher: Multidisciplinary Digital Publishing Institute (MDPI). [Online].

Available: http://www.ncbi.nlm.nih.gov/pubmed/24379043

[91] B. C. Glaister, M. S. Orendurff, J. A. Schoen, G. C. Bernatz, and G. K. Klute, "Ground reaction forces and impulses during a transient turning maneuver," *Journal of Biomechanics*, no. 41, pp. 3090–3093, 2008.

[92] C. He, R. Xu, M. Zhao, Y. Guo, S. Jiang, F. He, and D. Ming, "Dynamic stability and spatiotemporal parameters during turning in healthy young adults," *BioMedical Engineering Online*, 2018.

[93] D. Conradsson, C. Paquette, J. Lökk, and E. Franzén, "Pre- and unplanned walking turns in Parkinson's disease – Effects of dopaminergic medication," *Neuroscience*, vol. 341, pp. 18–26, Jan. 2017. [Online]. Available: https://linkinghub.elsevier.com/retrieve/pii/S0306452216306376

[94] M. Mancini, H. Schlueter, M. El-Gohary, N. Mattek, C. Duncan, J. Kaye, and F. B. Horak, "Continuous Monitoring of Turning Mobility and Its Association to Falls and Cognitive Function: A Pilot Study," *Journals of Gerontology - Series A Biological Sciences and Medical Sciences*, vol. 71, no. 8, pp. 1102–1108, Aug. 2016, publisher: Oxford University Press.

[95] U. M. Fietzek, L. Stuhlinger, A. Plate, A. Ceballos-Baumann, and K. Bötzel, "Spatial constraints evoke increased number of steps during turning in Parkinson's disease," *Clinical Neurophysiology*, vol. 128, no. 10, pp. 1954–1960, Oct. 2017, publisher: Elsevier Ireland Ltd.

[96] M. Farrell and H. Herr, "Angular momentum primitives for human turning: Control implications for biped robots," in *Proceedings of the 2008 8th IEEE-RAS International Conference on Humanoid Robots, Humanoids 2008*, 2008, pp. 163–167.

[97] L. A. Nolasco, J. Livingston, A. K. Silverman, and D. H. Gates, "The ins and outs of dynamic balance during 90-degree turns in people with a unilateral transtibial amputation," *Journal of Biomechanics*, vol. 122, p. 110438, 2021, publisher: Elsevier Ltd. [Online]. Available: https://doi.org/10.1016/j.jbiomech.2021.110438

[98] M. Wu, J. H. Matsubara, and K. E. Gordon, "General and Specific Strategies Used to Facilitate Locomotor Maneuvers," *PLOS ONE*, vol. 10, no. 7, p. e0132707, Jul. 2015. [Online]. Available: http://dx.plos.org/10.1371/journal.pone.0132707

[99] M. S. Orendurff, A. D. Segal, J. S. Berge, K. C. Flick, D. Spanier, and G. K. Klute, "The kinematics and kinetics of turning: limb asymmetries associated with walking a circular path." *Gait and Posture*, vol. 23, no. 1, pp. 106–11, Jan. 2006. [Online]. Available: http://www.ncbi.nlm.nih.gov/pubmed/16311202

[100] M. Hollands, K. Sorensen, and A. Patla, "Effects of head immobilization on the coordination and control of head and body reorientation and translation during steering," *Experimental Brain Research*, 2001.

[101] J. R. Andrews, W. D. McLeod, T. Ward, and K. Howard, "The cutting mechanism," *The American Journal of Sports Medicine*, vol. 5, no. 3, pp.

111–121, May 1977. [Online]. Available: http://journals.sagepub.com/doi/10.1177/036354657700500303

[102] M. J. Taylor, P. Dabnichki, and S. C. Strike, "A three-dimensional biomechanical comparison between turning strategies during the stance phase of walking," *Human Movement Science*, vol. 24, no. 4, pp. 558–573, 2005, arXiv: 107 ISBN: 0167-9457.

[103] S. B. Akram, J. S. Frank, and J. Fraser, "Coordination of segments reorientation during on-the-spot turns in healthy older adults in eyes-open and eyes-closed conditions," *Gait and Posture*, vol. 32, no. 4, pp. 632–636, Oct. 2010, publisher: Elsevier B.V. [Online]. Available: http://dx.doi.org/10.1016/j.gaitpost.2010.09.006

[104] P. R. Golyski and B. D. Hendershot, "A computational algorithm for classifying step and spin turns using pelvic center of mass trajectory and foot position," *Journal of Biomechanics*, vol. 54, pp. 96–100, 2017. [Online]. Available: http://dx.doi.org/10.1016/j.jbiomech.2017.01.023

[105] P. C. Dixon, J. Stebbins, T. Theologis, and A. B. Zavatsky, "Spatio-temporal parameters and lower-limb kinematics of turning gait in typically developing children," *Gait and Posture*, vol. 38, no. 4, pp. 870–875, 2013, publisher: Elsevier B.V. ISBN: 1865227609. [Online]. Available: http://dx.doi.org/10.1016/j.gaitpost.2013.04.010

[106] A.-h. Olivier, "Analyse dans le plan courbure-vitesse d'un changement de direction lors de la marche," *Noûs*, no. December 2008, 2008.

[107] S. B. Akram, J. S. Frank, and S. Chenouri, "Turning behavior in healthy older adults: Is there a preference for step versus spin turns?" *Gait and Posture*, vol. 31, no. 1, pp. 23–26, 2010.

[108] A. E. Patla and G. E. Stelmach, "Visual control of human locomotion," *Adaptability of human gait: Implications for the control of locomotion*, vol. 78, 1991.

[109] P. Fino and T. E. Lockhart, "Required coefficient of friction during turning at self-selected slow, normal, and fast walking speeds," *Journal of Biomechanics*, vol. 47, no. 6, pp. 1395–1400, 2014, publisher: Elsevier.

[110] P. C. Dixon, T. Smith, M. J. Taylor, J. V. Jacobs, J. T. Dennerlein, and J. M. Schiffman, "Effect of walking surface, late-cueing, physiological characteristics of aging, and gait parameters on turn style preference in healthy, older adults," *Human Movement Science*, vol. 66, no. June, pp. 504–510, 2019.

[111] B. C. Glaister, M. S. Orendurff, J. A. Schoen, and G. K. Klute, "Rotating horizontal ground reaction forces to the body path of progression," *Journal of Biomechanics*, no. 40, pp. 3527–3532, 2007.

[112] P. C. Dixon, J. V. Jacobs, J. T. Dennerlein, and J. M. Schiffman, "Late-cueing of gait tasks on an uneven brick surface impacts coordination and center of mass control in older adults," *Gait and Posture*, vol. 65, no. July 2018, pp. 143–148, Sep. 2018, publisher: Elsevier B.V.

[113] A. E. Patla, A. Adkin, and T. Ballard, "Online steering : coordination and

control of body center of mass , head and body reorientation," *Experimental brain research*, vol. 129, pp. 629–634, 1999.

[114] A. Ashburn, C. Kampshoff, M. Burnett, E. Stack, R. M. Pickering, and G. Verheyden, "Sequence and onset of whole-body coordination when turning in response to a visual trigger: Comparing people with Parkinson's disease and healthy adults," *Gait and Posture*, vol. 39, no. 1, pp. 278–283, 2014, publisher: Elsevier B.V. [Online]. Available: http://dx.doi.org/10.1016/j.gaitpost.2013.07.128

[115] C. Cao, J. A. Ashton-Miller, A. B. Schultz, and N. B. Alexander, "Abilities to turn suddenly while walking: Effects of age, gender, and available response time," *Journals of Gerontology - Series A Biological Sciences and Medical Sciences*, vol. 52, no. 2, 1997, publisher: Oxford University Press.

[116] M. R. Paquette and L. A. Vallis, "Age-related kinematic changes in late visual-cueing during obstacle circumvention," *Experimental Brain Research*, 2010.

[117] M. Mak, A. Patla, and C. Hui-Chan, "Sudden turn during walking is impaired in people with Parkinson's disease," *Experimental Brain Research*, vol. 190, no. 1, pp. 43–51, 2008.

[118] K. Hase and R. B. Stein, "Analysis of rapid stopping during human walking," *Journal of Neurophysiology*, 1998.

[119] O. Tirosh and W. A. Sparrow, "Gait termination in young and older adults: Effects of stopping stimulus probability and stimulus delay," *Gait and Posture*, vol. 19, no. 3, pp. 243–251, Jun. 2004.

[120] R. D. Seidler, J. A. Bernard, T. B. Burutolu, B. W. Fling, M. T. Gordon, J. T. Gwin, Y. Kwak, and D. B. Lipps, "Motor control and aging: Links to age-related brain structural, functional, and biochemical effects," *Neuroscience and Biobehavioral Reviews*, vol. 34, no. 5, pp. 721–733, 2010, publisher: Elsevier Ltd. [Online]. Available: http://dx.doi.org/10.1016/j.neubiorev.2009.10.005

[121] P. Eichelberger, M. Ferraro, U. Minder, T. Denton, A. Blasimann, F. Krause, and H. Baur, "Analysis of accuracy in optical motion capture – A protocol for laboratory setup evaluation," *Journal of Biomechanics*, vol. 49, no. 10, pp. 2085–2088, Jul. 2016. [Online]. Available: https://www.sciencedirect.com/science/article/pii/S0021929016305681

[122] A. M. Aurand, J. S. Dufour, and W. S. Marras, "Accuracy map of an optical motion capture system with 42 or 21 cameras in a large measurement volume," *Journal of Biomechanics*, vol. 58, pp. 237–240, Jun. 2017. [Online]. Available: https://www.sciencedirect.com/science/article/pii/S0021929017302580

[123] R Core Team, "R: A Language and Environment for Statistical Computing," 2024.

[124] D. Bates, M. Mächler, B. Bolker, and S. Walker, "Fitting Linear Mixed-Effects Models Using **lme4**," *Journal of Statistical Software*, vol. 67, no. 1, 2015. [Online]. Available: http://www.jstatsoft.org/v67/i01/

[125] Department of Justice, "2010 ADA Standards for Accessible Design,"

2010, place: USA. [Online]. Available: https://www.ada.gov/regs2010/2010ADAStandards/2010ADAstandards.htm

[126] S. Kudo, M. Fujimoto, T. Sato, and A. Nagano, "Quantitative evaluation of linked rigid-body representations of the trunk," *Gait & Posture*, vol. 63, pp. 119–123, Jun. 2018. [Online]. Available: https://linkinghub.elsevier.com/retrieve/pii/S0966636218304697

[127] M. Tillman, J. Molino, and A. M. Zaferiou, "Frontal plane balance during pre-planned and late-cued 90 degree turns while walking," *Journal of Biomechanics*, vol. 141, p. 111206, Aug. 2022. [Online]. Available: https://www.sciencedirect.com/science/article/pii/S0021929022002494

[128] R. Dumas, L. Chèze, and J. P. Verriest, "Adjustments to McConville et al. and Young et al. body segment inertial parameters," *Journal of Biomechanics*, vol. 40, no. 3, pp. 543–553, Jan. 2007, publisher: Elsevier Ltd.

[129] P. De Leva, "Adjustments to Zatsiorsky-Seluyanov's segment inertia paremeters," *Journal of Biomechanics*, vol. 29, no. 9, pp. 1223–1230, 1996.

[130] W. T. Dempster, "The Anthropometry of Body Action," *Annals of the New York Academy of Sciences*, vol. 63, no. 4, pp. 559–585, Nov. 1955. [Online]. Available: https://nyaspubs.onlinelibrary.wiley.com/doi/10.1111/j.1749-6632.1955.tb32112.x

[131] J. T. McConville, T. D. Churchill, I. Kaleps, C. E. Clauser, and J. Cuzzi, "Anthropometric Measurement of Body and Body Segment Moments of Inertia," *AFAMRL Techical Report, Wright patterson Air Force Base, Ohio*, 1980.

[132] J. Young, R. Chandler, and C. Snow, "Anthropometric and Mass Distribution Characteristics of the Adult Female," 1983.

[133] T. Caderby, A. Lesport, N. A. Turpin, G. Dalleau, B. Watier, T. Robert, N. Peyrot, and J. Begue, "Influence of aging on the control of the whole-body angular momentum during volitional stepping: An UCM-based analysis," *Experimental Gerontology*, vol. 178, p. 112217, Jul. 2023. [Online]. Available: https://linkinghub.elsevier.com/retrieve/pii/S0531556523001389

[134] R. Tisserand, T. Robert, R. Dumas, and L. Chèze, "A simplified marker set to define the center of mass for stability analysis in dynamic situations," *Gait & Posture*, vol. 48, pp. 64–67, Jul. 2016. [Online]. Available: https://www.sciencedirect.com/science/article/pii/S0966636216300492

[135] J. Shippen and B. May, "A Kinematic Approach to Calculating Ground Reaction Forces in Dance," *Journal of Dance Medicine & Science*, vol. 16, no. 1, p. 5, 2012.

[136] M. S. Christensen, J. B. Tracy, and J. R. Crenshaw, "A pelvis-oriented margin of stability is robust against deviations in walking direction," *Journal of Biomechanics*, vol. 160, p. 111812, Nov. 2023, 0 citations (Semantic Scholar/DOI) [2023-10-11]. [Online]. Available: https://www.sciencedirect.com/science/article/pii/S0021929023003834

[137] B. Ulrich, A. N. Santos, B. M. Jolles, D. H. Benninger, and J. Favre, "Gait events

during turning can be detected using kinematic features originally proposed for the analysis of straight-line walking," *Journal of Biomechanics*, vol. 91, pp. 69–78, Jun. 2019, publisher: Elsevier Ltd.

[138] A. L. Hof and C. Curtze, "A stricter condition for standing balance after unexpected perturbations," *Journal of Biomechanics*, vol. 49, no. 4, pp. 580–585, Feb. 2016. [Online]. Available: https://www.sciencedirect.com/science/article/pii/S0021929016300318

[139] A. M. Zaferiou, R. R. Wilcox, and J. L. McNitt-Gray, "Modification of impulse generation during pirouette turns with increased rotational demands," *Journal of Applied Biomechanics*, vol. 32, no. 5, pp. 425–432, 2016.

[140] L. J. Dr. Melton, E. A. Chrischilles, C. Cooper, A. W. Lane, and B. L. Riggs, "Perspective how many women have osteoporosis?" *Journal of Bone and Mineral Research*, vol. 7, no. 9, pp. 1005–1010, Sep. 1992. [Online]. Available: https://academic.oup.com/jbmr/article/7/9/1005-1010/7500259

[141] J. R. Center, T. V. Nguyen, D. Schneider, P. N. Sambrook, and J. A. Eisman, "Mortality after all major types of osteoporotic fracture in men and women: an observational study," *The Lancet*, vol. 353, no. 9156, pp. 878–882, Mar. 1999. [Online]. Available: https://linkinghub.elsevier.com/retrieve/pii/S0140673698090758

[142] P. C. Dixon, K. H. Schütte, B. Vanwanseele, J. V. Jacobs, J. T. Dennerlein, and J. M. Schiffman, "Gait adaptations of older adults on an uneven brick surface can be predicted by age-related physiological changes in strength," *Gait and Posture*, vol. 61, no. January, pp. 257–262, 2018.

[143] A. K. Silverman, R. R. Neptune, E. H. Sinitski, and J. M. Wilken, "Whole-body angular momentum during stair ascent and descent," *Gait & Posture*, vol. 39, no. 4, pp. 1109–1114, Apr. 2014, publisher: Elsevier.

[144] L. Decker, F. Cignetti, N. Hunt, J. Potter, N. Stergiou, and S. Studenski, "Effects of aging on the relationship between cognitive demand and step variability during dual-task walking," *Age*, vol. 38, no. 4, pp. 363–375, 2016.

[145] S. Mellone, M. Mancini, L. A. King, F. B. Horak, and L. Chiari, "The quality of turning in Parkinson's disease: a compensatory strategy to prevent postural instability?" *Journal of NeuroEngineering and Rehabilitation*, vol. 13, no. 1, p. 39, Apr. 2016, publisher: Journal of NeuroEngineering and Rehabilitation. [Online]. Available: http://www.ncbi.nlm.nih.gov/pubmed/27094039

[146] R. Dumas, L. Chèze, and J. P. Verriest, "Corrigendum to "Adjustments to McConville et al. and Young et al. body segment inertial parameters" [J. Biomech. (2006) in press] (DOI:10.1016/j.jbiomech.2006.02.013)," *Journal of Biomechanics*, vol. 40, no. 7, pp. 1651–1652, 2007.

[147] M. P. Reed, M. A. Manary, and L. W. Schneider, "Methods for measuring and representing automobile occupant posture," in *SAE Technical Papers*, 1999, iSSN: 26883627.

[148] G. Rab, K. Petuskey, and A. Bagley, "A method for determination

of upper extremity kinematics," in *Gait and Posture*, vol. 15. Gait Posture, 2002, pp. 113–119, issue: 2 ISSN: 09666362. [Online]. Available: https://pubmed.ncbi.nlm.nih.gov/11869904/

[149] G. Courtine and M. Schieppati, "Human walking along a curved path. II. Gait features and EMG patterns," *European Journal of Neuroscience*, 2003.

[150] A. K. Silverman and R. R. Neptune, "Differences in whole-body angular momentum between below-knee amputees and non-amputees across walking speeds," *Journal of Biomechanics*, vol. 44, no. 3, pp. 379–385, Feb. 2011, 81 citations (Semantic Scholar/DOI) [2023-02-07] MAG ID: 2051878883 S2ID: 53fb6707e9af9770c2308a15f8c8f4c63e0db0c3.

[151] D. Conradsson, C. Paquette, and E. Franzén, "Medio-lateral stability during walking turns in older adults," *PLoS ONE*, vol. 13, no. 6, pp. 1–12, Jun. 2018, publisher: Public Library of Science ISBN: 1111111111.

[152] D. Xu, L. G. Carlton, and K. S. Rosengren, "Anticipatory postural adjustments for altering direction during walking." *Journal of motor behavior*, vol. 36, no. 3, pp. 316–26, 2004, iSBN: 0022-2895 (Print)\r0022-2895 (Linking). [Online]. Available: http://www.scopus.com/inward/record.url?eid=2-s2.0-3142609034&partnerID=tZOtx3y1

[153] T. Yamaguchi, A. Suzuki, and K. Hokkirigawa, "Required coefficient of friction in the anteroposterior and mediolateral direction during turning at different walking speeds," *PLoS ONE*, vol. 12, no. 6, pp. 1–16, 2017, iSBN: 1111111111.

[154] D. A. Bruening, R. E. Frimenko, C. D. Goodyear, D. R. Bowden, and A. M. Fullenkamp, "Sex differences in whole body gait kinematics at preferred speeds," *Gait & Posture*, vol. 41, no. 2, pp. 540–545, Feb. 2015. [Online]. Available: https://www.sciencedirect.com/science/article/pii/S0966636214007942

[155] D. A. Bruening, A. R. Baird, K. J. Weaver, and A. T. Rasmussen, "Whole body kinematic sex differences persist across non-dimensional gait speeds," *PLOS ONE*, vol. 15, no. 8, p. e0237449, Aug. 2020. [Online]. Available: https://dx.plos.org/10.1371/journal.pone.0237449

[156] C. Cao, A. Schultz, J. Ashton-Miller, and N. Alexander, "Age and gender differences in sudden stops and turns while walking," *American Society of Mechanical Engineers, Bioengineering Division (Publication) BED*, vol. 35, pp. 451–452, 1997.

[157] G. A. R. Zijlstra, J. C. M. van Haastregt, J. T. M. van Eijk, E. van Rossum, P. A. Stalenhoef, and G. I. J. M. Kempen, "Prevalence and correlates of fear of falling, and associated avoidance of activity in the general population of community-living older people," *Age and Ageing*, vol. 36, no. 3, pp. 304–309, May 2007. [Online]. Available: https://doi.org/10.1093/ageing/afm021

[158] M. T. Thigpen, K. E. Light, G. L. Creel, and S. M. Flynn, "Turning difficulty characteristics of adults aged 65 years or older," *Physical Therapy*, vol. 80, no. 12, pp. 1174–1187, 2000.

[159] Z. S. Nasreddine, N. A. Phillips, V. Bedirian, S. Charbonneau, V. Whitehead,

I. Collin, J. L. Cummings, and H. Chertkow, “The Montreal Cognitive Assessment, MoCA: A Brief Screening Tool For Mild Cognitive Impairment: MOCA: A BRIEF SCREENING TOOL FOR MCI,” *Journal of the American Geriatrics Society*, vol. 53, no. 4, pp. 695–699, Apr. 2005. [Online]. Available: http://doi.wiley.com/10.1111/j.1532-5415.2005.53221.x

[160] M. E. Harrington, A. B. Zavatsky, S. E. M. Lawson, Z. Yuan, and T. N. Theologis, “Prediction of the hip joint centre in adults, children, and patients with cerebral palsy based on magnetic resonance imaging,” *Journal of Biomechanics*, vol. 40, no. 3, pp. 595–602, Jan. 2007. [Online]. Available: https://www.sciencedirect.com/science/article/pii/S0021929006000583

[161] J. B. Dingwell and J. P. Cusumano, “Humans use multi-objective control to regulate lateral foot placement when walking,” *PLOS Computational Biology*, vol. 15, no. 3, p. e1006850, Mar. 2019, publisher: Public Library of Science. [Online]. Available: https://journals.plos.org/ploscompbiol/article?id=10.1371/journal.pcbi.1006850

[162] N. Veronese, B. Stubbs, S. Volpato, G. Zuliani, S. Maggi, M. Cesari, D. M. Lipnicki, L. Smith, P. Schofield, J. Firth, D. Vancampfort, A. Koyanagi, A. Pilotto, and E. Cereda, “Association Between Gait Speed With Mortality, Cardiovascular Disease and Cancer: A Systematic Review and Meta-analysis of Prospective Cohort Studies,” *Journal of the American Medical Directors Association*, vol. 19, no. 11, pp. 981–988.e7, Nov. 2018. [Online]. Available: https://www.sciencedirect.com/science/article/pii/S152586101830327X

[163] C. E. Adam, A. L. Fitzpatrick, C. S. Leary, A. Hajat, E. A. Phelan, C. Park, and E. O. Semmens, “The Association between Gait Speed and Falls in Community Dwelling Older Adults with and without Mild Cognitive Impairment,” *International Journal of Environmental Research and Public Health*, vol. 18, no. 7, p. 3712, Jan. 2021, number: 7 Publisher: Multidisciplinary Digital Publishing Institute. [Online]. Available: https://www.mdpi.com/1660-4601/18/7/3712

[164] R. W. Bohannon, “Comfortable and maximum walking speed of adults aged 20-79 years: Reference values and determinants,” *Age and Ageing*, 1997.

[165] N. G. Gomez, J. A. Dunn, M. A. Gomez, and K. Bo Foreman, “The effect of amplitude normalization technique, walking speed, and reporting metric on whole-body angular momentum and its interpretation during normal gait,” *Journal of Biomechanics*, vol. 168, p. 112075, May 2024. [Online]. Available: https://www.sciencedirect.com/science/article/pii/S0021929024001520

[166] I. Carpinella, P. Crenna, E. Calabrese, M. Rabuffetti, P. Mazzoleni, R. Nemni, and M. Ferrarin, “Locomotor function in the early stage of Parkinson’s disease,” *IEEE Transactions on Neural Systems and Rehabilitation Engineering*, vol. 15, no. 4, pp. 543–551, 2007.

[167] R. Grasso, P. Prévost, Y. P. Ivanenko, and A. Berthoz, “Eye-head coordination for the steering of locomotion in humans: An anticipatory synergy,” *Neuro-*

science Letters, 1998.

Vita

Mitchell Tillman

Place of birth Rota, Andalucia, Spain

Date of birth June 23, 1996

Education Stevens Institute of Technology, Hoboken, NJ
Doctoral Candidate in Biomedical Engineering
expected date of graduation, May 2024

Publications **Tillman, M.**, Molino, J., & Zaferiou, A. M. (2022). Frontal plane balance during pre-planned and late-cued 90 degree turns while walking. *Journal of Biomechanics*, 141, 111206. https://doi.org/10.1016/j.jbiomech.2022.111206

Tillman, M., Molino, J., & Zaferiou, A. M. (2023). Gait-phase specific transverse-plane momenta generation during pre-planned and late-cued 90 degree turns while walking. *Scientific Reports*, 13(1), Article 1. https://doi.org/10.1038/s41598-023-33667-1

Tillman, M., Liu, J. M., Hirsch, Z. M., Molino, J., & Zaferiou, A. M. (2024). Healthy older adults generate transverse-plane momenta required for 90° turns while walking during the same phases of gait as used in straight-line gait. *Journal of NeuroEngineering and Rehabilitation*, 21(1), p. 145. https://doi.org/10.1186/s12984-024-01437-3

Honors Doctoral Excellence Fellowship, 2023-24
Robert Crooks Stanley Fellowship, 2022-23